

THE POTENTIAL EFFECT AND MECHANISM OF CHINESE TRADITIONAL MEDICINE ON VASCULAR HOMEOSTASIS AND REMODELING

EDITED BY: Yuliang Wang, Zhang Yuefan, Tie-Jun Li, Ismail Laher and
Hongbin Wang

PUBLISHED IN: Frontiers in Pharmacology





frontiers

Frontiers eBook Copyright Statement

The copyright in the text of individual articles in this eBook is the property of their respective authors or their respective institutions or funders. The copyright in graphics and images within each article may be subject to copyright of other parties. In both cases this is subject to a license granted to Frontiers.

The compilation of articles constituting this eBook is the property of Frontiers.

Each article within this eBook, and the eBook itself, are published under the most recent version of the Creative Commons CC-BY licence.

The version current at the date of publication of this eBook is CC-BY 4.0. If the CC-BY licence is updated, the licence granted by Frontiers is automatically updated to the new version.

When exercising any right under the CC-BY licence, Frontiers must be attributed as the original publisher of the article or eBook, as applicable.

Authors have the responsibility of ensuring that any graphics or other materials which are the property of others may be included in the CC-BY licence, but this should be checked before relying on the CC-BY licence to reproduce those materials. Any copyright notices relating to those materials must be complied with.

Copyright and source acknowledgement notices may not be removed and must be displayed in any copy, derivative work or partial copy which includes the elements in question.

All copyright, and all rights therein, are protected by national and international copyright laws. The above represents a summary only. For further information please read Frontiers' Conditions for Website Use and Copyright Statement, and the applicable CC-BY licence.

ISSN 1664-8714

ISBN 978-2-88966-435-1

DOI 10.3389/978-2-88966-435-1

About Frontiers

Frontiers is more than just an open-access publisher of scholarly articles: it is a pioneering approach to the world of academia, radically improving the way scholarly research is managed. The grand vision of Frontiers is a world where all people have an equal opportunity to seek, share and generate knowledge. Frontiers provides immediate and permanent online open access to all its publications, but this alone is not enough to realize our grand goals.

Frontiers Journal Series

The Frontiers Journal Series is a multi-tier and interdisciplinary set of open-access, online journals, promising a paradigm shift from the current review, selection and dissemination processes in academic publishing. All Frontiers journals are driven by researchers for researchers; therefore, they constitute a service to the scholarly community. At the same time, the Frontiers Journal Series operates on a revolutionary invention, the tiered publishing system, initially addressing specific communities of scholars, and gradually climbing up to broader public understanding, thus serving the interests of the lay society, too.

Dedication to Quality

Each Frontiers article is a landmark of the highest quality, thanks to genuinely collaborative interactions between authors and review editors, who include some of the world's best academicians. Research must be certified by peers before entering a stream of knowledge that may eventually reach the public - and shape society; therefore, Frontiers only applies the most rigorous and unbiased reviews.

Frontiers revolutionizes research publishing by freely delivering the most outstanding research, evaluated with no bias from both the academic and social point of view. By applying the most advanced information technologies, Frontiers is catapulting scholarly publishing into a new generation.

What are Frontiers Research Topics?

Frontiers Research Topics are very popular trademarks of the Frontiers Journals Series: they are collections of at least ten articles, all centered on a particular subject. With their unique mix of varied contributions from Original Research to Review Articles, Frontiers Research Topics unify the most influential researchers, the latest key findings and historical advances in a hot research area! Find out more on how to host your own Frontiers Research Topic or contribute to one as an author by contacting the Frontiers Editorial Office: frontiersin.org/about/contact

THE POTENTIAL EFFECT AND MECHANISM OF CHINESE TRADITIONAL MEDICINE ON VASCULAR HOMEOSTASIS AND REMODELING

Topic Editors:

Yuliang Wang, Shanghai Jiao Tong University, China

Zhang Yuefan, Shanghai University, China

Tie-Jun Li, Second Military Medical University, China

Ismail Laher, University of British Columbia, Canada

Hongbin Wang, Texas A&M University, United States

Citation: Wang, Y., Yuefan, Z., Li, T.-J., Laher, I., Wang, H., eds. (2021). The Potential Effect and Mechanism of Chinese Traditional Medicine on Vascular Homeostasis and Remodeling. Lausanne: Frontiers Media SA.
doi: 10.3389/978-2-88966-435-1

Table of Contents

- 04 Editorial: The Potential Effect and Mechanism of Chinese Traditional Medicine on Vascular Homeostasis and Remodeling**
Yuliang Wang, Yuefan Zhang, Tie-Jun Li, Ismail Laher and Hongbin Wang
- 06 1-Deoxynojirimycin in Mulberry (*Morus indica* L.) Leaves Ameliorates Stable Angina Pectoris in Patients With Coronary Heart Disease by Improving Antioxidant and Anti-inflammatory Capacities**
Yan Ma, Wei Lv, Yan Gu and Shui Yu
- 15 Preclinical Absorption, Distribution, Metabolism, and Excretion of Sodium Danshensu, One of the Main Water-Soluble Ingredients in *Salvia miltiorrhiza*, in Rats**
Xiangguo Meng, Jingjing Jiang, Hui Pan, Shengyuan Wu, Shuowen Wang, Yuefen Lou and Guorong Fan
- 25 Dual Effects of Chinese Herbal Medicines on Angiogenesis in Cancer and Ischemic Stroke Treatments: Role of HIF-1 Network**
Ming Hong, Honglian Shi, Ning Wang, Hor-Yue Tan, Qi Wang and Yibin Feng
- 42 C-Phycocyanin Ameliorates Mitochondrial Fission and Fusion Dynamics in Ischemic Cardiomyocyte Damage**
Jinchao Gao, Lidong Zhao, Jinfeng Wang, Lihang Zhang, Dandan Zhou, Jinlong Qu, Hao Wang, Ming Yin, Jiang Hong and Wenjuan Zhao
- 55 Traditional Chinese Medicine for Coronary Heart Disease: Clinical Evidence and Possible Mechanisms**
Ke-Jian Zhang, Qun Zheng, Peng-Chong Zhu, Qiang Tong, Zhuang Zhuang, Jia-Zhen Zhu, Xiao-Yi Bao, Yue-Yue Huang, Guo-Qing Zheng and Yan Wang
- 77 Anisodamine Ameliorates Hyperkalemia During Crush Syndrome Through Estradiol-Induced Enhancement of Insulin Sensitivity**
Jian-Guang Yu, Bo-Shi Fan, Jin-Min Guo, Yun-Jie Shen, Ye-Yan Hu and Xia Liu
- 87 Edible Bird's Nest Protects Against Hyperglycemia-Induced Oxidative Stress and Endothelial Dysfunction**
Dharmani Devi Murugan, Zuhaida Md Zain, Ker Woon Choy, Nor Hisam Zamakshshari, Mel June Choong, Yang Mooi Lim and Mohd Rais Mustafa
- 98 Protective Effect of Stachydrine Against Cerebral Ischemia-Reperfusion Injury by Reducing Inflammation and Apoptosis Through P65 and JAK2/STAT3 Signaling Pathway**
Li Li, Lili Sun, Yan Qiu, Wenjun Zhu, Kangyuan Hu and Junqin Mao
- 112 Kaempferol Protects Against Cerebral Ischemia Reperfusion Injury Through Intervening Oxidative and Inflammatory Stress Induced Apoptosis**
Jing Wang, Junqin Mao, Rong Wang, Shengnan Li, Bin Wu and Yongfang Yuan
- 124 Caffeic Acid Phenethyl Ester Ameliorates Calcification by Inhibiting Activation of the AKT/NF- κ B/NLRP3 Inflammasome Pathway in Human Aortic Valve Interstitial Cells**
Ming Liu, Fei Li, Yuming Huang, Tingwen Zhou, Si Chen, Geng Li, Jiawei Shi, Nianguo Dong and Kang Xu



Editorial: The Potential Effect and Mechanism of Chinese Traditional Medicine on Vascular Homeostasis and Remodeling

Yuliang Wang^{1*}, Yuefan Zhang², Tie-Jun Li³, Ismail Laher⁴ and Hongbin Wang⁵

¹Joint International Research Laboratory of Metabolic and Developmental Sciences, Key Laboratory of Urban Agriculture (South) Ministry of Agriculture, Plant Biotechnology Research Center, Fudan-SJTU-Nottingham Plant Biotechnology R&D Center, School of Agriculture and Biology, Shanghai Jiao Tong University, Shanghai, China, ²Biomedical Innovation R&D Center, School of Medicine, Shanghai University, Shanghai, China, ³Department of Pharmacology, School of Pharmacy, Navy Medical University, Shanghai, China, ⁴Department of Pharmacology and Therapeutics, Faculty of Medicine, University of British Columbia, Vancouver, BC, Canada, ⁵Center for Biomedical Informatics, Texas A&M University Health Science University, Houston, TX, United States

Keywords: Chinese traditional medicine, vascular homeostasis and remodeling, clinical effect, mechanism, natural product

Editorial on the Research Topic

The Potential Effect and Mechanism of Chinese Traditional Medicine on Vascular Homeostasis and Remodeling

OPEN ACCESS

Edited and reviewed by:

Yung-Chi Cheng,
Yale University, United States

*Correspondence:

Yuliang Wang
wangyuliang@sjtu.edu.cn

Specialty section:

This article was submitted to
Ethnopharmacology,
a section of the journal
Frontiers in Pharmacology

Received: 28 August 2020

Accepted: 12 November 2020

Published: 17 December 2020

Citation:

Wang Y, Zhang Y, Li T-J, Laher I and
Wang H (2020) Editorial: The Potential
Effect and Mechanism of Chinese
Traditional Medicine on Vascular
Homeostasis and Remodeling.
Front. Pharmacol. 11:599766.
doi: 10.3389/fphar.2020.599766

Vascular diseases, such as coronary artery disease and stroke, are the leading cause of CVD deaths (Thomas et al., 2018) and mortality related to vascular diseases will continue to increase over the next 10 years (Liu et al., 2019). Cardiovascular diseases result from alterations in the homeostatic balance of vascular structure and function. Traditional Chinese Medicine (TCM) has long been proposed as an effective treatment for cardiovascular disease. Many formulae, herbs and natural products, such as Long-Dan-Xie-Gan Tang (formula), Danshen (herb) Bao et al., Huanglansu (natural product), have been investigated for their effects in the prevention and treatment of cardiovascular diseases by regulating the vascular homeostasis and remodeling, for example by scavenging free radicals, inhibiting inflammatory reaction, reducing oxidative stress and modulating apoptosis.

A study by Zhang et al. reviewed 27 high-quality randomized controlled trials (RCT) that evaluated the efficacy and safety of Chinese herbal medicines for coronary heart disease (CHD). The cardio-protection of TCM are likely related to its ability to inhibit inflammation, oxidative stress, apoptosis, improve circulatory function, and stimulate energy metabolism (Zhang et al.).

Ischemic stroke is another major cause of death and disability globally. The predominant risk factor in ischemic stroke is mitochondrial dysfunction caused by an imbalance of mitochondrial fusion and fission. A study by Gao et al. reports that C-phycocyanin (C-pc), an active component of *Spirulina platensis*, can affect mitochondrial fission and fusion dynamics and reduce apoptosis in cardiomyocytes, suggesting that C-pc may be used to protect the ischemic heart disease (Gao et al.).

Hypoxia-inducible factor-1 (HIF-1) has been suggested as a target when treating ischemic stroke. Levels of HIF-1 are increased under hypoxic conditions and regulate the adaptive responses to hypoxia-induced angiogenesis. Several preclinical studies report that TCM that target HIF-1 can be used either as anti-angiogenic agents (for example, to treat tumors) or as pro-angiogenic agents (for example, to treat stroke). The dual effects of TCM on the HIF-1 pathway make it suitable for the treatment of ischemic stroke and cancer (Hong et al.).

Danshensu is a water-soluble phenolic acid found in *Salvia miltiorrhiza*. Several studies reported that danshensu has unique bioactivity on acute myocardial ischemia injury. A report by Meng et al. described the pharmacokinetic profile (absorption, distribution, metabolism, and elimination profiles) of sodium danshensu in rats. Danshensu is poorly absorbed, widely distributed, bio-transformed via several metabolic pathways, and is excreted mainly in the urine (Meng et al.).

The majority (80%) of strokes are due to focal brain ischemia. Restoring blood flow is necessary to limit irreversible damage to brain tissue, but events related to cerebral ischemia reperfusion (I/R) can lead to an insufficient oxygen supply and restoration of blood flow, where the imbalance of brain energy levels causes further neuroinflammation, neuronal damage, and cerebral edema. A study by Li et al. demonstrates that stachydrine down-regulates inflammation, restores neurological function, reduces neuronal injury and cerebral infarction in a rat model of ischemic stroke. The antioxidant and anti-inflammatory effects of stachydrine could prevent reperfusion-induced injury in patients with stroke (Li et al.). Another study by Wang et al. indicates that kaempferol can protect against I/R induced brain damage *in vivo*. Kaempferol increases the activity of antioxidant pathways related to SOD and GSH, while also decreasing serum and brain tissue content of MDA by regulating the expression of proteins related to oxidative and inflammatory stress (Wang et al.).

Blood vessels are composed of multilayered cells with unique histological, biochemical, and functional characteristics. Each layer maintains vascular homeostasis and regulates vascular remodeling caused by hemodynamic stress or vascular injury. Alterations in vascular homeostasis are associated with a number of deleterious changes in the cardiovascular system, and many TCM can maintain vascular stability and prevent vascular dysfunction.

Bird's nest is formed by the saliva of swiftlets, and is used as both a medicine and as food in China. The aqueous extract of hydrolyzed edible bird nest (HBN) was examined on diabetic endothelial dysfunction *in vitro* and *in vivo*. HBN is able to protect against high-glucose induced endothelial dysfunction by restraining oxidative stress and increasing NO bioavailability (Murugan et al.). Caffeic acid phenethyl ester inhibits

activation of the AKT/NF- κ B pathway and NLRP3 inflammasome, and is a potential natural product for the prevention of calcific aortic valve disease (Liu et al.).

Traditional Chinese medicines can also be used to treat vascular diseases other than CHD and stroke. Patients with CHD and blood stasis syndrome often suffer from angina pectoris which is sometimes difficult to treat due to the lack of effective drugs. A study by Ma et al. used deoxyojirimycin, a unique polyhydroxy alkaloid found in mulberry leaves, to treat patients with stable angina pectoris in a clinic trial involving 144 patients. Deoxyojirimycin improved the clinical symptoms in patients with stable angina pectoris by increasing antioxidant and anti-inflammatory capacities (Ma et al.). Anisodamine, a belladonna alkaloid, decreased serum potassium and on-site mortality in crush syndrome through activation of $\alpha 7$ nAChR (Yu et al.).

The history and use of TCM go back thousands of years, and it is clear that TCM is a huge treasure trove awaiting research of new drug discovery. This *Research Topic* focuses on the effects and mechanisms of TCM in different vascular diseases, based on data from human and animal studies, and in isolated cells. These studies allowed for a description of the molecular mechanisms of action of many active compounds of TCM.

Traditional Chinese medicine is unique in its therapeutic approach in that it is often used as a combination with other herbs to treat a range of diseases, although it is still difficult to clarify the mechanisms of action of traditional TCM. The multi-target effects of TCM provides many therapeutic benefits and understanding the scale and nature of these effects will derive from a systems biology approach coupled with modern molecular techniques including proteomics (Li and Su, 2008; Gu and Pei 2017; Cai et al., 2018). A large scale evidence based approach using TCM candidates with therapeutic effects could reduce the global epidemic of cardiovascular health challenges.

AUTHOR CONTRIBUTIONS

Correspondence: YW, wangyuliang@sjtu.edu.cn YW wrote the article, IL edited the article and YZ revised the article.

REFERENCES

- Cai, X., Su, X., Wu, R., and Su, S.-B. (2018). Systems biology approaches in the study of Chinese herbal formulae. *Chin. Med.* 13, 65. doi:10.4324/9781315505855-5
- Gu, S. and Pei, J. (2017). Chinese herbal medicine meets biological networks of complex diseases: a computational perspective. *Evid. base Compl. Alternative Med.* 2017, 7198645. doi:10.1155/2017/7198645
- Li, Q.-y. and Su, S.-b. (2008). Application of systems biology in traditional Chinese medicine research. *World J. Sci. Technol.* 10 (4), 1–6. doi:10.1016/s1876-3553(09)60017-x
- Liu, S., Li, Y., Zeng, X., Wang, H., Yin, P., Wang, L., et al. (2019). Burden of cardiovascular diseases in China, 1990–2016: findings from the 2016 global burden of disease study. *JAMA Cardiol.* 4 (4), 342–352. doi:10.1001/jamacardio.2019.0295

- Thomas, H., Diamond, J., Vieco, A., Chaudhuri, S., Shinnar, E., Cromer, S., et al. (2018). Global atlas of cardiovascular disease 2000. *Global Heart* 13, 143–163. doi:10.1016/j.gheart.2018.09.511

Conflict of Interest: The authors declare that the research was conducted in the absence of any commercial or financial relationships that could be construed as a potential conflict of interest.

Copyright © 2020 Wang, Zhang, Li, Laher and Wang. This is an open-access article distributed under the terms of the Creative Commons Attribution License (CC BY). The use, distribution or reproduction in other forums is permitted, provided the original author(s) and the copyright owner(s) are credited and that the original publication in this journal is cited, in accordance with accepted academic practice. No use, distribution or reproduction is permitted which does not comply with these terms.



1-Deoxynojirimycin in Mulberry (*Morus indica* L.) Leaves Ameliorates Stable Angina Pectoris in Patients With Coronary Heart Disease by Improving Antioxidant and Anti-inflammatory Capacities

Yan Ma^{1†}, Wei Lv^{2†}, Yan Gu¹ and Shui Yu^{1*}

OPEN ACCESS

Edited by:

Yuliang Wang,
Shanghai Jiao Tong University, China

Reviewed by:

Ali H. Eid,
American University of Beirut,
Lebanon
Xin Hai Liang,
Second Military Medical University,
China

*Correspondence:

Shui Yu
yushuiji@126.com

[†] These authors have contributed
equally to this work

Specialty section:

This article was submitted to
Ethnopharmacology,
a section of the journal
Frontiers in Pharmacology

Received: 02 January 2019

Accepted: 06 May 2019

Published: 21 May 2019

Citation:

Ma Y, Lv W, Gu Y and Yu S (2019)
1-Deoxynojirimycin in Mulberry
(*Morus indica* L.) Leaves Ameliorates
Stable Angina Pectoris in Patients
With Coronary Heart Disease by
Improving Antioxidant
and Anti-inflammatory Capacities
Front. Pharmacol. 10:569.
doi: 10.3389/fphar.2019.00569

¹ Department of Cardiovascular, The First Hospital of Jilin University, Changchun, China, ² Department of Cadre Ward, Seven Therapy Area, The First Hospital of Jilin University, Changchun, China

Objective: Stable angina pectoris (SAP) in patients with coronary heart disease (CHD) and blood stasis syndrome (BSS) is a potentially serious threat to public health. NF- κ B signaling is associated with angina pectoris. 1-Deoxynojirimycin (DNJ), which is a unique polyhydroxy alkaloid, is the main active component in mulberry (*Morus indica* L.) leaves and may exhibit protective properties in the prevention of SAP in patients with CHD by affecting the NF- κ B pathway.

Methods: DNJ was purified from mulberry leaves by using a pretreated cation exchange chromatography column. A total of 144 SAP patients were randomly and evenly divided into experimental (DNJ treatment) and control (conventional treatment) groups. Echocardiography and ascending aortic elasticity were evaluated. The changes in inflammatory, oxidative, and antioxidant factors, including C-reactive protein (CRP), interleukin-6 (IL-6), tumor necrosis factor- α (TNF- α), superoxide dismutase (SOD), and malondialdehyde (MDA), were measured before and after a 4-week treatment. Self-Rating Anxiety Scale (SAS) and Hamilton Depression Scale (HAMD) scores were compared between the two groups. The improvement in SAP score, associated symptoms, and BSS was also investigated. The levels of I κ B kinase (IKK), nuclear factor-kappa B (NF- κ B), and inhibitor of kappa B α (I κ B α) were measured by Western blot.

Results: After the 4-week treatment, DNJ increased left ventricular ejection fraction and reduced left ventricular mass index, aortic distensibility, and atherosclerosis index ($p < 0.05$). DNJ intervention increased angina-free walking distance ($p < 0.05$). DNJ significantly reduced the levels of hs-CRP, IL-6, TNF- α , MDA, SAS, HAMD, AP, and BSS scores and increased SOD level ($p < 0.05$). The total effective rate was significantly increased ($p < 0.05$). The symptoms of angina attack frequency, nitroglycerin use, chest

pain and tightness, shortness of breath, and emotional upset were also improved. DNJ reduced IKK and NF- κ B levels and increased I κ B α level ($p < 0.05$).

Conclusion: The DNJ in mulberry leaves improved the SAP of patients with CHD and BSS by increasing their antioxidant and anti-inflammatory capacities.

Keywords: 1-deoxynojirimycin, mulberry leaves, coronary heart disease, angina pectoris, blood stasis syndrome

INTRODUCTION

Cardiovascular disease is a potentially serious threat to public health and has hindered social and economic development (Joseph et al., 2017; Pasquel et al., 2018). Coronary heart disease (CHD) is a common cardiovascular disease and is a main cause of disability and death (Awerbach et al., 2018; Dong et al., 2018).

Angina pectoris (AP), which is a common symptom in patients with CHD and blood stasis syndrome (BSS), is difficult to treat due to the lack of effective drugs (Qian et al., 2013). Traditional Chinese medicine plays an important role in improving the symptoms and life quality of patients with CHD (Zhang et al., 2017; Chen et al., 2018b). The effectiveness of traditional Chinese medicine helps to develop personalized medicine (Wang et al., 2010). Chinese herbal medicine has been increasingly used to treat AP due to its effectiveness and safety with few side effects (Chen et al., 2018a). Herbs have been widely used in the prevention of cardiovascular diseases. Plants contain many phytochemicals that exert protective function by reducing the risk of various disorders (Al Disi et al., 2016). Certain herbs and spices can control blood pressure in hypertensive and pre-hypertensive patients (Driscoll et al., 2019). Botanicals have also been used to prevent atherosclerosis (Al-Shehaby et al., 2016). Danshen, the dried root of *Salvia miltiorrhiza*, can regulate lipoprotein metabolism, oxidation, and inflammation and protect vascular endothelia by affecting related signaling pathways. The results reflected the multi-component and multi-target characteristics of danshen and its therapeutic potential in heart diseases (Zhang et al., 2018).

1-Deoxynojirimycin (DNJ) is a unique polyhydroxy alkaloid that is the main active component in mulberry leaves (Jiang et al., 2014). DNJ is a competitive inhibitor of α -glucosidase, inhibiting the digestion and glucose absorption of disaccharides and thereby lowering blood glucose levels (Cai et al., 2017). DNJ is a potent α -glucosidase inhibitor with strong affinity toward α -glucosidase. DNJ can competitively inhibit the binding of maltoseucose and other disaccharides to α -glucosidase and prevent the breakdown of disaccharides to form glucose. Thus, these disaccharides cannot be digested and absorbed and are passed into the large intestine and eventually excreted into feces. DNJ reduces glucose absorption and lowers blood sugar levels.

DNJ and its derivatives can effectively inhibit infection by HIV, HCV, and other viruses (Jacob et al., 2007; Onose et al., 2013). DNJ isolated from mulberry leaves exhibits strong inhibitory function on the oral pathogenic bacterium *Streptococcus mutans* (Hasan et al., 2014). DNJ protects against obesity-induced hepatic lipid abnormalities and mitochondrial dysfunction (Do et al., 2015). DNJ also promotes weight loss by increasing adiponectin

levels, which play an important role in energy intake and in the prevention of diet-induced obesity. Further work showed that DNJ reduces obesity by moderating feeding behavior and endoplasmic reticulum stress in the central nervous system (Kim et al., 2017). DNJ may show protective effect against stable AP (SAP) in BSS patients. However, the effects of DNJ on SAP and the molecular mechanism involved have never been reported. Therefore, this study explored the effects of DNJ on SAP in patients with CHD and BSS.

MATERIALS AND METHODS

DNJ Purification and HPLC Analysis

Mulberry (*Morus indica* L., voucher number HDIEC-2016198) leaves were purchased from Huzhou Daybreak Import & Export, Co., Ltd. (Zhejiang, China) and deposited in the Herbarium of Nanjing University (Nanjing, China). Approximately 1 kg of dried mulberry leaf powder was dissolved in a 5 L round bottom flask, and 5 L of 0.1 M citrate buffer (pH 4.0) was added. The mixture was sonicated at 500 W for 30 min and filtered, and residues were discarded. The crude extract of mulberry leaves was concentrated and slowly added to a pretreated D72 type cation-exchange resin chromatography column. The resin was rinsed with ddH₂O at a flow rate of 10 mL/min. DNJ was washed until the effluent solution was colorless then eluted with a 0.25 M aqueous ammonia solution at the same flow rate to collect the eluent at pH 9–12. The collected eluate was concentrated under reduced pressure to a volume, lyophilized, and stored for subsequent use. A total of 100 μ g of the sample was accurately weighed and dissolved in ddH₂O, and the volume was adjusted to 1 mL. The content and purity of DNJ were determined by HPLC pre-column derivatization.

A total of 10 mg of DNJ standard was dissolved in a 10 mL tube and diluted to 10 mL with distilled water to obtain a 1 mg/mL standard solution. The standard solutions were separately diluted to a standard solution series at concentrations of 5, 10, 20, 30, 40, and 50 μ g/mL. A total of 10 μ L of mulberry leaf extract was placed in a centrifuge tube and added with 10 μ L of 0.4 M borate solution pH 8.5, followed by 20 μ L of 5 mM FMOC-C1 acetonitrile solution. The solution was mixed and allowed to react in a 25°C water bath for 30 min. After the reaction, the mixture was added with 10 μ L of 0.1 M glycine solution and unreacted derivatization reagent diluted to 1 mL with 1% acetic acid. The mixture was then stirred and filtered with a 0.45 μ m filter. The following analysis conditions were used: column, Inertsil HPLC-NH2 analytical column (4.6 mm \times 250 mm, 5 μ m); mobile phase, acetonitrile:water (75:25, v/v); flow rate, 1.0 mL/min;

column temperature, 30°C; analysis time, 30 min; UV detector wavelength, 256 nm; and the injection volume, 10 µL.

Patients

Before the experiments were performed, all protocols were approved by the Human Research Committee of the First Hospital of Jilin University (Approval No. 20161201DY). Written informed consents were obtained from the participants of this study. A total of 144 patients with SAP and BSS were recruited from December 2016 to September 2017. The patients were diagnosed according to the diagnosis guidelines for SAP (Messerli et al., 2006) and ischemic heart disease (IHD) (Shah, 2018). A history or at least one case of myocardial infarction was confirmed by coronary angiography. The degree of stenosis of coronary artery was >50%. The diagnostic criteria for BSS were based on the “Diagnostic Criteria for Coronary Heart Disease and Blood Stasis Syndrome” (Fu et al., 2012; Li et al., 2014).

Inclusion Criteria

All patients satisfied the above criteria for SAP, BSS, and IHD. The patients were aged 35–80 years. The patients demonstrated SAP symptoms, including chest pain and tightness, shortness of breath, and emotional distress.

Exclusion Criteria

Patients with the following cases were excluded from the study: SAP caused by other heart diseases; history of trauma, surgical infection, and fever; undergone or planned to receive coronary intervention in the past 1 month; severe heart failure with an ejection fraction (EF) of < 35%; malignant tumors, infections, blood diseases, mental illness, and other serious diseases; pregnancy or lactation; and serious complications that limit their participation in the experiment.

Patient Grouping

A power test was used to calculate the population size with a power of 0.9 and an α of 0.5. The required population size was 140, with 70 patients in each group. A total of 144 patients were evenly divided into the control group (CG) and treatment group (EG) by using a computer-generated random number table. The patients in the CG and EG received conventional treatment and oral 10 mg of DNJ daily, respectively. The entire treatment duration was 4 weeks.

Outcome Measure

The echocardiography of each patient was examined by using a GE Vivid E9 Doppler diagnosis system (GE Healthcare, Princeton, NJ, United States) with M5S-d and 4V probes, and the image was captured with an Echo PAC workstation. The left side of the person was examined in a calm position. The M5S-d probe was used to collect 2-D gray-scale dynamic images of the patient's three cardiac cycles, including apical four-chamber heart, two-chamber heart, and left ventricular long axis. The 4V probe was placed on the apex position, and 3-D dynamic images were collected and analyzed. Echocardiographic analysis was performed using the following parameters: left

atrial diameter, end-diastolic interventricular septal thickness, left ventricular end-diastolic diameter, left ventricular end-systolic diameter, left ventricular mass index (LVMI), left ventricular EF (LVEF), E'/A' ratio (pulsed), left ventricular posterior wall thickness, and mean value of left ventricular outflow tract pressure gradient (LVOTPG, pulsed). Ascending aortic elasticity was evaluated by using the following indicators: aortic diastolic internal diameter (ADD) and aortic systolic inner diameter (ASD). The forward movement of the anterior wall of the ascending aorta was measured. The aortic elasticity index used was aortic distensibility. Aortic strain (AS) was calculated as follows: $AS = 100 \times [(ASD-ADD)/ADD]$, and aortic stiffness index was evaluated. The anterior wall systolic velocity of ascending aorta, early diastolic velocity, and late diastolic velocity were also measured. The patients recorded their walking distance in meters before experiencing angina during daily activity.

Changes in inflammatory factors and oxidative stress index, including high sensitivity C-reactive protein (hs-CRP, Cat. No. DEIA-BJ553, CD Creative-Diagnostics, Shirley, NY, United States), interleukin-6 (IL-6, Cat. No. ab47215, Abcam, Chicago, IL, United States), and tumor necrosis factor- α (TNF- α , Cat. No. ab181421), were compared before and after treatment by using corresponding ELISA kits. Superoxide dismutase (SOD) was measured by an automatic biochemical analyzer (Beckman Coulter, Inc., Brea, CA, United States). Malondialdehyde (MDA) was detected by a thiobarbituric acid reaction test (Baldi et al., 1993).

Zung's Self-Rating Anxiety Scale (SAS) (Samakouri et al., 2012) and Hamilton Depression Scale (HAMD) (Vindbjerg et al., 2018) scores were compared before and after treatment. The improvement of AP and BSS scores was also measured. The symptoms associated with SAP, including chest pain and tightness, shortness of breath, emotional distress, and other clinical symptoms, were measured.

Measurement of Therapeutic Effectiveness of SAP

Therapeutic effectiveness was defined as remarkably effective when the number of angina attacks or nitroglycerin decreased by >80%; effective when the number of angina attacks or nitroglycerin decreased by 50 to 80%, Invalid when the angina was unchanged or worsened and when the number of angina attacks or nitroglycerin was reduced by <50%.

Western Blot Analysis

Decreased transcriptional activity of the nuclear factor of transcription kappa B (NF- κ B) is associated with the improvement of angina (Yang et al., 2010). The effects of DNJ on NF- κ B pathway and related factors in SAP patients were investigated. Venous blood was collected on an empty stomach in the morning before and after treatment. The antibodies purchased included anti-IKK α (ab32041, Abcam, Chicago, IL, United States), anti-inhibitor of kappa B α (I κ B α , Santa Cruz Biotechnology, Santa Cruz, CA, United States), anti-NF- κ B p65 (Santa Cruz Biotechnology, Santa Cruz,

CA, United States, 1:1000), and HRP goat anti-mouse (IgG) secondary antibody (Ab205719, Abcam, 1:2000). Blood cells were lysed by SDS/proteinase K, and proteins were separated by 12% SDS-PAGE. After PAGE, the proteins were transferred to PVDF membranes and sealed with 5% skim milk at room temperature for 2 h. Primary antibodies were added (1:1000), incubated overnight at 4°C, and washed with TBST (10 mM Tris-HCl [pH 8.0], 150 mM NaCl, and 0.05% Tween 20). Goat anti-mouse HRP secondary antibody was added and incubated for 2 h at room temperature on a shaker. After the membrane was washed, the bands were scanned with a GE AI600 imager, and the results were analyzed by the Gel-ProAnalyzer 4.0 software (Media Cybernetics, Bethesda, MD, United States).

Statistical Method

SPSS19.0 was used for the analysis of data statistics. Count data were expressed as %, and the comparison between groups was performed by χ^2 test. The measurement data were tested for normality and conformed to the normal distribution. Comparison between the two groups was performed by a paired-sample *t*-test. The difference was considered statistically significant if $p < 0.05$.

RESULTS

DNJ Purification

DNJ is 1,5-dideoxy-1,5-imino-D-sorbitol (Figure 1A). After pre-column derivatization of DNJ standard and mulberry leaves, HPLC analysis was performed, and the results are shown in Figures 1B,C. Chromatographic peaks 1, 2, and 3 in the figure correspond to FMOC-DNJ, FMOC-GLY, and FMOC-OH, respectively. The DNJ in the mulberry leaf was well-separated from the adjacent components, and the derived reagent hydrolysates of FMOC-GLY and FMOC-OH did not interfere with measurement results.

Clinical Characterization

A total of 144 eligible patients with CHD and BSS were enrolled, all of whom were diagnosed with SAP. After 4 weeks of therapy, 8 and 4 patients were withdrawn from the EG and CG, respectively. Statistical analysis was performed among 132 patients who completed the present experiment. The mean age of the two groups was 67.68 ± 8.09 years. No significant statistical difference in age, gender, and related risk factors for CHD was observed ($p > 0.05$, Table 1).

DNJ Improved Conventional Echocardiographic Parameters

Before DNJ intervention, the statistical difference for all parameters was insignificant between the two groups (Table 2, $p > 0.05$). Compared with CG, EG showed increased LVEF and E'/A' values and significantly reduced LVMI and LVOTPG after DNJ intervention (Table 2, $p < 0.05$). The other parameters were only slightly reduced.

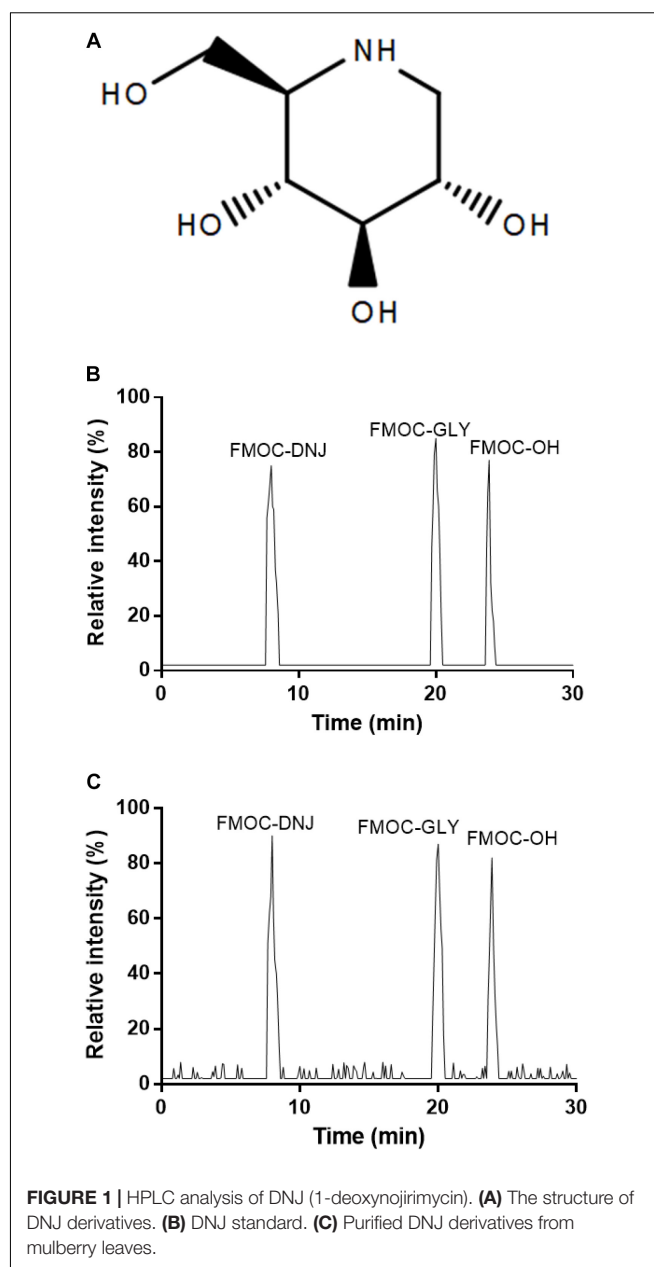


FIGURE 1 | HPLC analysis of DNJ (1-deoxynojirimycin). **(A)** The structure of DNJ derivatives. **(B)** DNJ standard. **(C)** Purified DNJ derivatives from mulberry leaves.

DNJ Improved Ascending Aortic Elasticity Parameters

Before DNJ intervention, the statistical difference for all parameters was insignificant between the two groups (Table 3, $p > 0.05$). After DNJ intervention, the aortic distensibility and atherosclerosis index in EG were lower than those in the CG (Table 3, $p < 0.05$). Early and late diastolic velocities in CG were also lower than those in EG (Table 3, $p < 0.05$).

DNJ Intervention Increased Angina-Free Walking Distance

Before DNJ intervention, angina-free walking distance was insignificant between two groups ($p > 0.05$). After the 4-week

TABLE 1 | Comparison of baseline clinical characters.

Parameters	Control group	Treatment group	p-values
Age (years)	68.16 ± 7.36	65.42 ± 8.48	0.15
Sex ratio (male/female)	42/26	44/20	0.552
Body mass index (kg/cm ²)	25.47 ± 3.61	25.67 ± 3.51	0.766
History of smoking (%)	18 (26.47)	28 (43.75)	0.141
Hypertension (%)	52 (76.47)	40 (62.5)	0.217
Diabetes (%)	28 (41.17)	20 (31.25)	0.402
Cholesterol (mM)	4.22 ± 1.10	4.39 ± 0.94	−0.495
Triglyceride (mM)	1.52 (1.12, 2.50)	1.99 (1.51, 2.34)	0.182
Low density lipoprotein (mM)	2.34 (1.78, 2.88)	2.31 (1.87, 2.74)	0.724
High density lipoprotein (mM)	1.19 (0.88, 1.42)	1.31 (1.13, 1.80)	0.095

The statistical difference was significant if $p < 0.05$ vs. the control group.

TABLE 2 | Conventional echocardiography.

Parameters	CG group	EG group
Before treatment		
Left atrial diameter/mm	41.80 ± 4.85	43.77 ± 4.94
Septal thickness/mm	17.13 ± 3.30	18.21 ± 3.86
Left ventricular end diastolic diameter/mm	43.51 ± 5.12	41.66 ± 4.71
Left ventricular end-systolic diameter/mm	28.15 ± 3.87	28.22 ± 3.86
Left ventricular posterior wall thickness/mm	10.65 ± 1.14	10.16 ± 0.81
Left ventricular ejection fraction/%	48.92 ± 7.95	49.51 ± 6.5
Left ventricular mass index/(g/m ²)	139.26 ± 31.98	129.50 ± 28.57
E'/A'/(cm/s)	0.56 ± 0.13	0.60 ± 0.15
After treatment		
Left atrial diameter/mm	41.44 ± 13.8	38.81 ± 11.42
Septal thickness/mm	15.8 ± 9.13	13.39 ± 9.82
Left ventricular end diastolic diameter/mm	39.74 ± 13.13	36.01 ± 12.01
Left ventricular end-systolic diameter/mm	27.91 ± 11.6	25.76 ± 10.42
Left ventricular posterior wall thickness/mm	10.31 ± 3.06	9.73 ± 2.89
Left ventricular ejection fraction/%	51.2 ± 7.86	57.95 ± 6.96*
Left ventricular mass index/(g/m ²)	134.79 ± 72.01	116.75 ± 51.65*
E'/A'/(cm/s)	0.58 ± 0.21	0.68 ± 0.28*
LVOTPG/mmHg	82.35 ± 37.19	70.06 ± 28.45*

LVOTPG, the mean value of the left ventricular outflow tract pressure gradient. E', peak early diastolic velocity of Tissue Doppler imaging (TDI) and A', peak late diastolic velocity of TDI. * $p < 0.05$ vs. the CG group.

treatment, DNJ intervention improved angina-free walking distance in EG ($p < 0.05$) but not in CG ($p > 0.05$, Table 4).

DNJ Treatment Increased Anti-inflammatory Properties

Before the treatment, the statistical difference for the serum levels of hs-CRP, IL-6, and TNF- α was insignificant between the two groups ($p > 0.05$, Table 5). After the 4-week treatment, the serum levels of inflammatory factors hs-CRP, IL-6, and TNF- α in EG were reduced compared with those in CG ($p < 0.05$, Table 5). The results suggest that DNJ treatment increased the anti-inflammatory features of the patients.

TABLE 3 | Ascending aortic elasticity.

Parameters	CG group	EG group
Before treatment		
The systolic velocity of the ascending aorta AWS'/(cm/s)	6.53 ± 2.05	6.01 ± 1.67
Early diastolic velocity, AWE'/(cm/s)	3.17 ± 0.85	3.24 ± 1.21
Late diastolic velocity, AWA'/(cm/s)	6.46 ± 2.07	6.17 ± 2.35
Aortic systolic inner diameter, ASD/mm	31.92 ± 5.41	31.58 ± 4.95
Aortic diastolic diameter, ADD/mm	30.72 ± 5.55	28.62 ± 3.91
Aortic distensibility, ADIS (cm ² /dyne × 10 ³)	0.19 ± 0.09	0.18 ± 0.07
Atherosclerosis index, ASI	3.79 ± 0.41	3.70 ± 0.38
The degree of stenosis of coronary artery, %	63.12 ± 10.86	65.56 ± 9.37
After treatment		
The systolic velocity of the ascending aorta AWS'/(cm/s)	6.22 ± 5.92	5.37 ± 4.13
Early diastolic velocity, AWE'/(cm/s)	3.89 ± 2.11	4.75 ± 2.52*
Late diastolic velocity, AWA'/(cm/s)	6.21 ± 4.51	6.94 ± 3.03*
Aortic systolic inner diameter, ASD/mm	31.2 ± 11.02	29.48 ± 10.37
Aortic diastolic diameter, ADD/mm	30.53 ± 12.13	28.61 ± 8.01
Aortic distensibility, ADIS (cm ² /dyne × 10 ³)	0.17 ± 0.05	0.13 ± 0.03*
Atherosclerosis index, ASI	3.69 ± 0.83	3.18 ± 0.69*
The degree of stenosis of coronary artery, %	72.56 ± 22.03	68.74 ± 18.89

* $p < 0.05$ vs. the CG group.

TABLE 4 | The comparison of angina-free walking distance between two groups.

Groups	Before treatment	After treatment	p-values
CG	542.6 ± 55.1	555.2 ± 63.9	0.523
EG	539.5 ± 52.1	621.2 ± 67.8	0.026
p-Values	0.632	0.021	

The statistical difference was significant if $p < 0.05$ vs. the control group.

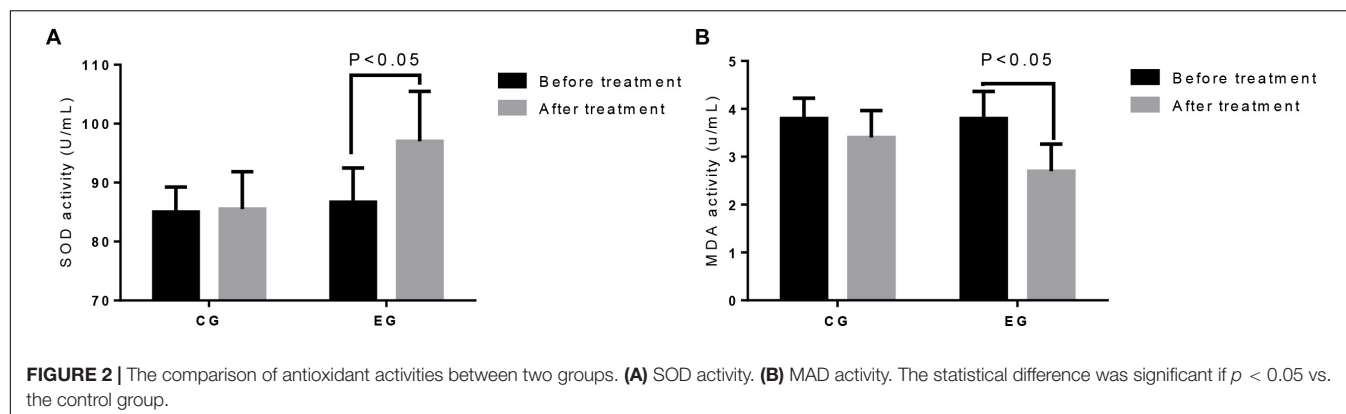
TABLE 5 | The comparison of serum levels of inflammatory cytokines before and after treatment.

Cytokines		Control group	Treatment group	p-values
CRP (μ g/mL)	Before	4.65 ± 0.86	4.79 ± 0.81	0.501
	After	3.96 ± 0.83	3.57 ± 0.75	0.042
IL-6 (pg/mL)	Before	150.12 ± 17.04	150.68 ± 16.26	0.892
	After	146.95 ± 14.27	139.65 ± 14.64	0.048
TNF (pg/mL)	Before	66.98 ± 7.08	66.29 ± 7.17	0.692
	After	65.34 ± 6.35	62.11 ± 6.63	0.047

The statistical difference was significant if $p < 0.05$ vs. the control group.

DNJ Treatment Increased Anti-antioxidant Activities

Before the treatment, the statistical difference for the serum levels of SOD (Figure 2A) and MAD (Figure 2B) was insignificant between the two groups ($p > 0.05$). After the 4-week treatment, the serum SOD levels (Figure 2A) were increased, whereas the MAD levels (Figure 2B) in EG were reduced compared with those in CG ($p < 0.05$). The results suggest that DNJ treatment increased the antioxidant capacities of the patients.



DNJ Treatment Improved the Anxiety and Depression of Patients With SAP

Before the treatment, the statistical difference for the scores of SAS and HAMD was insignificant between the two groups ($p > 0.05$, **Table 6**). After the 4-week treatment, the SAS and HAMD scores in EG were reduced relative to those in CG ($p < 0.05$, **Table 6**). The results suggest that DNJ treatment improved the anxiety and depression of patients with SAP.

DNJ Treatment Improved Therapeutic Results

After the 4-week treatment, the total effective rate in the EG (81.25%) was higher than that in the CG (47.06%, $p < 0.05$, **Table 7**). The findings suggest that DNJ treatment improved therapeutic results.

DNJ Treatment Improved SAP, BSS, and GIN Use

Before the treatment, the statistical difference for SAP scores, SAP frequency, BSS scores, and GIN use was insignificant between the two groups ($p > 0.05$, **Table 8**). After the 4-week treatment, SAP scores, SAP frequency, BSS scores, and GIN use were reduced in EG relative to those in CG ($p < 0.05$, **Table 8**). The results suggest that DNJ treatment improved SAP, BSS, and GIN use in patients with SAP.

DNJ Treatment Improved SAP Symptoms

Before the treatment, the statistical difference for SAP symptoms was insignificant (**Table 9**, $p < 0.05$). After the 4-week treatment,

the SAP symptoms, including chest pain, chest tightness, shortness of breath, and upset feeling, were evidently improved in the EG (**Table 9**, $p < 0.05$). The results suggest that DNJ treatment enhanced SAP symptoms.

DNJ Increased I κ B α Level and Reduced IKK and NF- κ B Levels

The statistical difference for the levels of I κ B α , IKK, and NF- κ B was insignificant between the two groups before treatment (**Figure 3A**, $p > 0.05$). The levels of IKK and NF- κ B in the EG were significantly lower than those in the CG, whereas the I κ B α level showed reverse results (**Figure 3B**, $p < 0.05$). These results suggest that DNJ reduced IKK and NF- κ B levels and increased I κ B α level.

DISCUSSION

Stable angina pectoris has become a global public health burden, and complementary treatment is often considered for patients with this disease. The key to complementary treatment is to find potential drugs for patients. As the main syndrome of CHD, SAP was reduced by DNJ treatment by affecting some parameters involved with conventional echocardiography and ascending aortic elasticity and by increasing angina-free walking distance. The present study showed that DNJ is a potential drug for SAP therapy in CHD patients with BSS.

Oxidative stress (Yan et al., 2009) and inflammatory responses (Militaru et al., 2013; Galon et al., 2015) are associated with SAP risks, whereas oxidative stress and inflammation can interact and promote each other (Herman et al., 2018; Zahran and Emam, 2018), possibly aggravating SAP. Oxidative stress and inflammation are associated with endothelial dysfunction (Zhenyukh et al., 2018), and impaired endothelial function results in blood flow decrease (Brunnekreef et al., 2012), vasospasm (Ganz et al., 1991), and embolus formation (Muci-Mendoza et al., 1980). Hs-CRP as a downstream inflammatory marker (Tayefi et al., 2017) and TNF- α and IL-6 (Zhou et al., 2013) as upstream inflammatory mediators are significant predictors of cardiovascular risk. The present study demonstrated that DNJ treatment reduced inflammatory responses (**Table 5**) and

TABLE 6 | The comparison of the scores of anxiety and depression between two groups.

Parameters		Control group	Treatment group	p -values
SAS	Before	51.18 \pm 7.06	53.72 \pm 9.73	0.227
	After	44.03 \pm 6.92	47.56 \pm 6.96	0.043
HAMD	Before	15.21 \pm 6.25	14.50 \pm 5.30	0.623
	After	13.06 \pm 7.27	9.16 \pm 5.15	0.014

SAS, Self-Rating Anxiety Scale. HAMD, Hamilton Depression Scale. The statistical difference was significant if $p < 0.05$ vs. the control group.

TABLE 7 | The comparison of therapeutic effectiveness between two groups [Cases (%)].

Groups	Cases	Significant effective	Effective	Invalid	Total effective	p-value
Control group	68	0	32 (47.06)	36 (52.94)	32 (47.06)	0.005
Treatment group	64	14 (21.88)	38 (59.37)	12 (18.75)	52 (81.25)	

The statistical difference was significant if $p < 0.05$ vs. the control group.

increased antioxidant activities (Table 6), contributing to the improvement of SAP symptoms.

Anxiety and depression are associated with the mortality of CHD and SAP patients (de Jager et al., 2018). The present findings suggested that DNJ treatment could ameliorate SAP by reducing SAS and HAMD scores and GIN use (Table 6). In clinical treatment, SAP symptoms could be alleviated by improving the anxiety and depression of patients (Table 8). The therapeutic results were improved, and SAP symptoms were reduced after treatment (Table 9). The total therapeutic results in EG were

TABLE 8 | The comparison of the outcome of SAP, BSS, and GIN use between two groups.

Parameters		Control group	Treatment group	p-values
SAP scores	Before	12 (10, 14)	12 (10, 16)	0.356
	After	10 (8, 15)	6 (6, 8)	< 0.01
SAP frequency	Before	4 (2, 4)	4 (2, 4)	0.879
	After	2 (2, 4)	2 (1, 3)	0.001
SAP duration	Before	3 (2, 4)	4 (2, 4)	0.711
	After	2 (2, 4)	2 (2, 2)	0.003
BSS scores	Before	25 (19, 27)	25 (17.25, 28)	0.892
	After	24 (18.5, 25)	17 (9.5, 17.75)	< 0.01
GIN tablets daily	Before	4 (2, 4)	4 (2, 4)	0.132
	After	4 (2, 5)	2 (0.5, 2)	0.017

SAP, stable angina pectoris; BSS, blood stasis syndrome. GIN, glyceryl trinitrate; the statistical difference was significant if $p < 0.05$ vs. the control group.

TABLE 9 | The comparison of SAP symptoms between two groups.

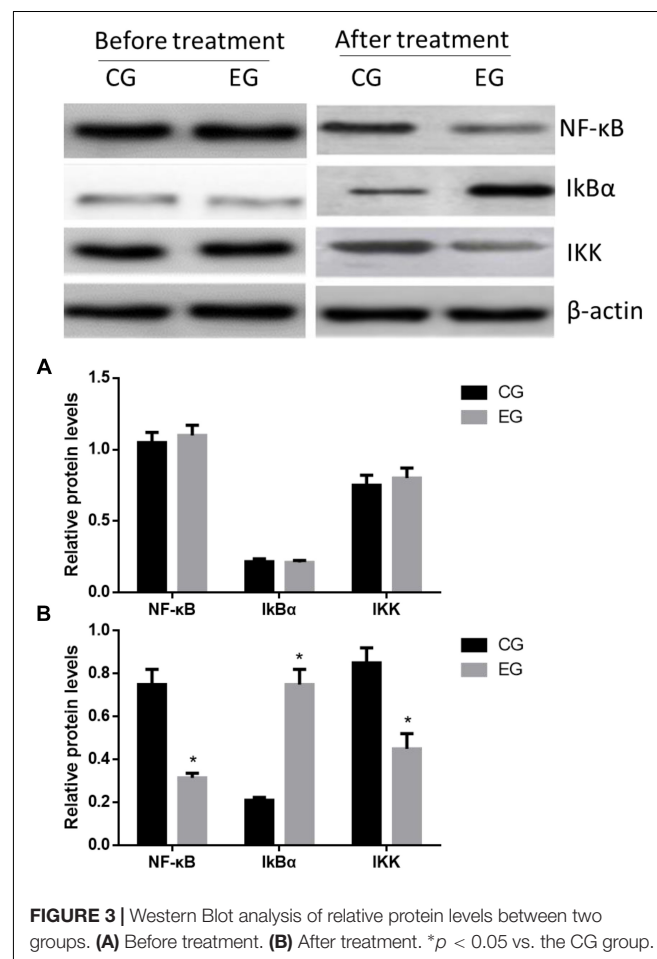
Parameters	Time	Control group	Treatment group	p-values
Chest pain	Before	3 (3, 6)	12 (6, 12)	0.296
	After	6 (6, 12)	6 (6, 6)	0.022
Chest tightness	Before	6 (6, 6)	6 (6, 12)	0.559
	After	6 (6, 12)	6 (6, 6)	0.004
Shortness of breath	Before	6 (6, 6)	4 (4, 8)	0.154
	After	6 (4, 8)	4 (1, 4)	0.003
Tired	Before	4 (4, 4)	6 (4, 8)	0.594
	After	4 (4, 8)	4 (4, 4)	0.061
Palpitate	Before	4 (4, 4)	4 (2, 4)	0.194
	After	2 (2, 4)	4 (2, 2)	0.063
Bitter	Before	2 (2, 2)	4 (2, 4)	0.358
	After	2 (2, 4)	2 (2, 2)	0.132
Upset	Before	2 (2, 2)	4 (2, 4)	0.407
	After	3 (2, 4)	2 (2, 2)	0.015
Total score	Before	19.41 ± 4.84	20.32 ± 4.54	0.392
	After	14.65 ± 2.65	11.22 ± 2.69	< 0.01

The statistical difference was significant if $p < 0.05$ the control group.

better than those in CG. DNJ treatment showed good clinical effect on the anxiety and depression of patients with SAP and BSS.

Exploring an effective therapeutic method of SAP is very important in its prevention. NF- κ B participates in various physiological functions, such as inflammation, immune response, and apoptosis, by regulating the expression of various genes associated with AP (Ritchie, 1998), whereas I κ B α is a key inhibitor of the NF- κ B pathway. The present results showed that DNJ inactivated the NF- κ B pathway by increasing I κ B α levels.

The present work suffered from some limitations. A small population size of 132 patients with SAP, CHD, and BSS were enrolled in this study. This study mainly focused on the anti-inflammatory and anti-oxidative properties and anxiety and depression of patients with SAP. The effects of DNJ on other



symptoms of SAP were not investigated. Further work must confirm the present conclusion in a large population.

CONCLUSION

DNJ intervention improved some parameters involved with conventional echocardiography and ascending aortic elasticity and increased angina-free walking distance. DNJ treatment reduced the serum levels of hs-CRP, IL-6, TNF- α , SOD, and MDA in the patients with SAP and BSS. Moreover, DNJ demonstrated anti-inflammatory and antioxidant properties. DNJ reduced SAS and HAMD scores in CHD patients, reflecting that DNJ regulated anxiety and depression in patients with SAP. DNJ treatment also decreased the SAP and BSS scores, suggesting that DNJ improved the curative effects in patients with SAP. Furthermore, DNJ improved the symptoms of chest pain, chest tightness, shortness

of breath, emotional upset, and other clinical symptoms, all of which are associated with SAP.

ETHICS STATEMENT

All procedures were approved by the human research ethical committee of The First Hospital of Jilin University (Changchun, China).

AUTHOR CONTRIBUTIONS

YM and SY conceived and designed the experiments and wrote the manuscript. WL and YG contributed to the evaluation of the results and corrected the manuscript.

REFERENCES

- Al Disi, S. S., Anwar, M. A., and Eid, A. H. (2016). Anti-hypertensive herbs and their mechanisms of action: part I. *Front. Pharmacol.* 6:323. doi: 10.3389/fphar.2015.00323
- Al-Shehaby, T. S., Itratni, R., and Eid, A. H. (2016). Anti-atherosclerotic plants which modulate the phenotype of vascular smooth muscle cells. *Phytomedicine* 23, 1068–1081. doi: 10.1016/j.phymed.2015.10.016
- Awerbach, J. D., Krasuski, R. A., and Camitta, M. G. W. (2018). Coronary disease and modifying cardiovascular risk in adult congenital heart disease patients: should general guidelines apply? *Prog. Cardiovasc. Dis.* 61, 300–307. doi: 10.1016/j.pcad.2018.07.018
- Baldi, E., Burra, P., Plebani, M., and Salvagnini, M. (1993). Serum malondialdehyde and mitochondrial aspartate aminotransferase activity as markers of chronic alcohol intake and alcoholic liver disease. *Ital. J. Gastroenterol.* 25, 429–432.
- Brunnekreef, J., Benda, N., Schreuder, T., Hopman, M., and Thijssen, D. (2012). Impaired endothelial function and blood flow in repetitive strain injury. *Int. J. Sports Med.* 33, 835–841. doi: 10.1055/s-0032-1306281
- Cai, D., Liu, M., Wei, X., Li, X., Wang, Q., Nomura, C. T., et al. (2017). Use of *Bacillus amyloliquefaciens* HZ-12 for high-level production of the blood glucose lowering compound, 1-deoxynojirimycin (DNJ), and nutraceutical enriched soybeans via fermentation. *Appl. Biochem. Biotechnol.* 181, 1108–1122. doi: 10.1007/s12010-016-2272-8
- Chen, M., Li, M., Ou, L., Kuang, R., Chen, Y., Li, T., et al. (2018a). Effectiveness and safety of Chinese herbal medicine formula Gualou Xiebai Banxia (GLXBBX) decoction for the treatment of stable angina pectoris: protocol for a systematic review. *Medicine* 97:e11680. doi: 10.1097/MD.00000000000011680
- Chen, R., Xiao, Y., Chen, M., He, J., Huang, M., Hong, X., et al. (2018b). A traditional Chinese medicine therapy for coronary heart disease after percutaneous coronary intervention: a meta-analysis of randomized, double-blind, placebo-controlled trials. *Biosci. Rep.* 38:BSR20180973. doi: 10.1042/BSR20180973
- de Jager, T. A. J., Dulfer, K., Radhoe, S., Bergmann, M. J., Daemen, J., van Domburg, R. T., et al. (2018). Predictive value of depression and anxiety for long-term mortality: differences in outcome between acute coronary syndrome and stable angina pectoris. *Int. J. Cardiol.* 250, 43–48. doi: 10.1016/j.ijcard.2017.10.005
- Do, H. J., Chung, J. H., Hwang, J. W., Kim, O. Y., Lee, J. Y., and Shin, M. J. (2015). 1-deoxynojirimycin isolated from *Bacillus subtilis* improves hepatic lipid metabolism and mitochondrial function in high-fat-fed mice. *Food Chem. Toxicol.* 75, 1–7. doi: 10.1016/j.fct.2014.11.001
- Dong, S. Y., Yan, S. T., Wang, M. L., Li, Z. B., Fang, L. Q., and Zeng, Q. (2018). Associations of body weight and weight change with cardiovascular events and mortality in patients with coronary heart disease. *Atherosclerosis* 274, 104–111. doi: 10.1016/j.atherosclerosis.2018.05.007
- Driscoll, K. S., Appathurai, A., Jois, M., and Radcliffe, J. E. (2019). Effects of herbs and spices on blood pressure: a systematic literature review of randomised controlled trials. *J. Hypertens* 37, 671–679. doi: 10.1097/HJH.0000000000001952
- Fu, C. G., Gao, Z. Y., and Wang, P. L. (2012). Study on the diagnostic criteria for coronary heart disease patients of blood stasis syndrome. *Zhongguo Zhong Xi Yi Jie He Za Zhi* 32, 1285–1286.
- Galon, M. Z., Wang, Z., Bezerra, H. G., Lemos, P. A., Schnell, A., Wilson, D. L., et al. (2015). Differences determined by optical coherence tomography volumetric analysis in non-culprit lesion morphology and inflammation in ST-segment elevation myocardial infarction and stable angina pectoris patients. *Catheter Cardiovasc. Interv.* 85, E108–E115. doi: 10.1002/ccd.25660
- Ganz, P., Weidinger, F. F., Yeung, A. C., Vekshtein, V. I., Vita, J. A., Ryan, T. J., et al. (1991). Coronary vasospasm in humans: the role of atherosclerosis and of impaired endothelial vasodilator function. *Basic Res. Cardiol.* 86(Suppl. 2), 215–222. doi: 10.1007/978-3-642-72461-9_21
- Hasan, S., Singh, K., Danisuddin, M., Verma, P. K., and Khan, A. U. (2014). Inhibition of major virulence pathways of *Streptococcus mutans* by quercitrin and deoxynojirimycin: a synergistic approach of infection control. *PLoS One* 9:e91736. doi: 10.1371/journal.pone.0091736
- Herman, F., Westfall, S., Brathwaite, J., and Pasinetti, G. M. (2018). Suppression of presymptomatic oxidative stress and inflammation in neurodegeneration by grape-derived polyphenols. *Front. Pharmacol.* 9:867. doi: 10.3389/fphar.2018.00867
- Jacob, J. R., Mansfield, K., You, J. E., Tennant, B. C., and Kim, Y. H. (2007). Natural iminosugar derivatives of 1-deoxynojirimycin inhibit glycosylation of hepatitis viral envelope proteins. *J. Microbiol.* 45, 431–440.
- Jiang, Y. G., Wang, C. Y., Jin, C., Jia, J. Q., Guo, X., Zhang, G. Z., et al. (2014). Improved 1-Deoxynojirimycin (DNJ) production in mulberry leaves fermented by microorganism. *Braz. J. Microbiol.* 45, 721–729. doi: 10.1590/s1517-83822014000200048
- Joseph, P., Leong, D., McKee, M., Anand, S. S., Schwalm, J. D., Teo, K., et al. (2017). Reducing the global burden of cardiovascular disease, Part 1: the epidemiology and risk factors. *Circ. Res.* 121, 677–694. doi: 10.1161/CIRCRESAHA.117.308903
- Kim, J., Yun, E. Y., Quan, F. S., Park, S. W., and Goo, T. W. (2017). Central administration of 1-deoxynojirimycin attenuates hypothalamic endoplasmic reticulum stress and regulates food intake and body weight in mice with high-fat diet-induced obesity. *Evid. Based Complement. Alternat. Med.* 2017:3607089. doi: 10.1155/2017/3607089
- Li, S. M., Xu, H., and Chen, K. J. (2014). The diagnostic criteria of blood-stasis syndrome: considerations for standardization of pattern identification. *Chin. J. Integr. Med.* 20, 483–489. doi: 10.1007/s11655-014-1803-9
- Messerli, F. H., Mancia, G., Conti, C. R., and Pepine, C. J. (2006). Guidelines on the management of stable angina pectoris: executive summary: the task force on the management of stable angina pectoris of the European society of cardiology. *Eur. Heart. J.* 27, 2902–2903. doi: 10.1093/eurheartj/ehl308

- Militaru, C., Donoiu, I., Craciun, A., Scorei, I. D., Bulearca, A. M., and Scorei, R. I. (2013). Oral resveratrol and calcium fructoborate supplementation in subjects with stable angina pectoris: effects on lipid profiles, inflammation markers, and quality of life. *Nutrition* 29, 178–183. doi: 10.1016/j.nut.2012.07.006
- Muci-Mendoza, R., Arruga, J., Edward, W. O., and Hoyt, W. F. (1980). Retinal fluorescein angiographic evidence for atheromatous microembolism. Demonstration of ophthalmoscopically occult emboli and post-embolic endothelial damage after attacks of amaurosis fugax. *Stroke* 11, 154–158. doi: 10.1161/01.str.11.2.154
- Onose, S., Ikeda, R., Nakagawa, K., Kimura, T., Yamagishi, K., Higuchi, O., et al. (2013). Production of the alpha-glycosidase inhibitor 1-deoxynojirimycin from *Bacillus* species. *Food Chem.* 138, 516–523. doi: 10.1016/j.foodchem.2012.11.012
- Pasquel, F. J., Gregg, E. W., and Ali, M. K. (2018). The evolving epidemiology of atherosclerotic cardiovascular disease in people with diabetes. *Endocrinol. Metab. Clin. North Am.* 47, 1–32. doi: 10.1016/j.ecl.2017.11.001
- Qian, W., Zhao, F. H., Shi, D. Z., Wu, W., and You, S. J. (2013). Association study between Chinese medicine blood stasis syndrome and TIMI risk stratification of patients with unstable angina pectoris. *Zhongguo Zhong Xi Yi Jie He Za Zhi* 33, 1042–1045.
- Ritchie, M. E. (1998). Nuclear factor- κ B is selectively and markedly activated in humans with unstable angina pectoris. *Circulation* 98, 1707–1713. doi: 10.1161/01.cir.98.17.1707
- Samakouri, M., Bouhos, G., Kadoglou, M., Giantzeli, A., Tsolaki, K., and Livaditis, M. (2012). Standardization of the Greek version of Zung's Self-rating Anxiety Scale (SAS). *Psychiatriki* 23, 212–220.
- Shah, R. (2018). Optimal guideline-directed medical therapy for patients with stable ischemic heart disease. *J. Am. Coll. Cardiol.* 71, 2861–2862. doi: 10.1016/j.jacc.2018.03.528
- Tayefi, M., Tajfard, M., Saffar, S., Hanachi, P., Amirabadizadeh, A. R., Esmaeili, H., et al. (2017). hs-CRP is strongly associated with coronary heart disease (CHD): a data mining approach using decision tree algorithm. *Comput. Methods Prog. Biomed.* 141, 105–109. doi: 10.1016/j.cmpb.2017.02.001
- Vindbjerg, E., Makransky, G., Mortensen, E. L., and Carlsson, J. (2018). Cross-cultural psychometric properties of the hamilton depression rating scale. *Can. J. Psychiatry* 64, 39–46. doi: 10.1177/0706743718772516
- Wang, C. C., Lin, J. D., and Chen, L. L. (2010). Personal health maintenance: the perspective of traditional Chinese medicine. *Hu Li Za Zhi* 57, 10–15.
- Yan, L. Y., Zhang, Y. Q., and Wang, X. M. (2009). Effect of buxu huayu qutan decoction on anti-oxidative capacity in aged patients with stable angina pectoris of coronary heart disease. *Zhongguo Zhong Xi Yi Jie He Za Zhi* 29, 695–697.
- Yang, X., Hu, W., Zhang, Q., Wang, Y., and Sun, L. (2010). Puerarin inhibits C-reactive protein expression via suppression of nuclear factor kappaB activation in lipopolysaccharide-induced peripheral blood mononuclear cells of patients with stable angina pectoris. *Basic Clin. Pharmacol. Toxicol.* 107, 637–642. doi: 10.1111/j.1742-7843.2010.00548.x
- Zahran, W. E., and Emam, M. A. (2018). Renoprotective effect of *Spirulina platensis* extract against nicotine-induced oxidative stress-mediated inflammation in rats. *Phytomedicine* 49, 106–110. doi: 10.1016/j.phymed.2018.06.042
- Zhang, G. X., Zhang, Y. Y., Zhang, X. X., Wang, P. Q., Liu, J., Liu, Q., et al. (2018). Different network pharmacology mechanisms of Danshen-based Fangjis in the treatment of stable angina. *Acta Pharmacol. Sin.* 39, 952–960. doi: 10.1038/aps.2017.191
- Zhang, J., Meng, H., Zhang, Y., Zhang, X., Shao, M., Li, C., et al. (2017). The therapeutic effect of chinese medicine for the treatment of atherosclerotic coronary heart disease. *Curr. Pharm. Des.* 23, 5086–5096. doi: 10.2174/1381612823666170803101602
- Zhenyukh, O., Gonzalez-Amor, M., Rodriguez-Diez, R. R., Esteban, V., Ruiz-Ortega, M., Salices, M., et al. (2018). Branched-chain amino acids promote endothelial dysfunction through increased reactive oxygen species generation and inflammation. *J. Cell. Mol. Med.* 22, 4948–4962. doi: 10.1111/jcmm.13759
- Zhou, S. Y., Duan, X. Q., Hu, R., and Ouyang, X. Y. (2013). Effect of non-surgical periodontal therapy on serum levels of TNF- α , IL-6 and C-reactive protein in periodontitis subjects with stable coronary heart disease. *Chin. J. Dent. Res.* 16, 145–151.

Conflict of Interest Statement: The authors declare that the research was conducted in the absence of any commercial or financial relationships that could be construed as a potential conflict of interest.

Copyright © 2019 Ma, Lv, Gu and Yu. This is an open-access article distributed under the terms of the Creative Commons Attribution License (CC BY). The use, distribution or reproduction in other forums is permitted, provided the original author(s) and the copyright owner(s) are credited and that the original publication in this journal is cited, in accordance with accepted academic practice. No use, distribution or reproduction is permitted which does not comply with these terms.



Preclinical Absorption, Distribution, Metabolism, and Excretion of Sodium Danshensu, One of the Main Water-Soluble Ingredients in *Salvia miltiorrhiza*, in Rats

Xiangguo Meng^{1†}, Jingjing Jiang^{2†}, Hui Pan³, Shengyuan Wu⁴, Shuowen Wang⁵, Yuefen Lou^{2*} and Guorong Fan^{3,4,5*}

OPEN ACCESS

Edited by:

Tie-Jun Li,
Second Military Medical
University, China

Reviewed by:

Zhi-Hong Jiang,
Macau University of Science and
Technology, Macau
Tai-jun Hang,
China Pharmaceutical
University, China
Xinhong Wang,
Shanghai University of Traditional
Chinese Medicine, China

*Correspondence:

Yuefen Lou
louyuefen@sina.cn
Guorong Fan
fanguorong@sjtu.edu.cn

[†]These authors have contributed
equally to this work

Specialty section:

This article was submitted to
Ethnopharmacology,
a section of the journal
Frontiers in Pharmacology

Received: 30 January 2019

Accepted: 02 May 2019

Published: 29 May 2019

Citation:

Meng X, Jiang J, Pan H, Wu S,
Wang S, Lou Y and Fan G (2019)
Preclinical Absorption, Distribution,
Metabolism, and Excretion of
Sodium Danshensu, One of the
Main Water-Soluble Ingredients in
Salvia miltiorrhiza, in Rats.
Front. Pharmacol. 10:554.
doi: 10.3389/fphar.2019.00554

¹Department of Pharmacy, Shanghai University of Medicine and Health Sciences, Shanghai, China, ²Department of Pharmacy, Shanghai Fourth People's Hospital, Shanghai, China, ³Department of Clinical Pharmacy, Shanghai General Hospital, School of Medicine, Shanghai Jiao Tong University, Shanghai, China, ⁴Laboratory of Drug Metabolism and Pharmacokinetics, School of Medicine, Tongji University, Shanghai, China, ⁵Shanghai Key Laboratory for Pharmaceutical Metabolite Research, School of Pharmacy, Second Military Medical University, Shanghai, China

In this study, the absorption, distribution, metabolism and excretion (ADME) of sodium danshensu (Sodium DL- β -(3, 4-dihydroxyphenyl)lactate), one of the main water-soluble active constituents in *Salvia miltiorrhiza*, were evaluated in rats. Pharmacokinetic study was evaluated in doses of 15, 30, and 60 mg/kg after intravenous administration of sodium danshensu. Bioavailability study was evaluated by comparing between 30 mg/kg (I.V.) and 180 mg/kg (P.O.) of sodium danshensu. Tissue distribution, metabolism, and excretion were evaluated at 30 mg/kg (I.V.) of sodium danshensu. Following intravenous administration, sodium danshensu exhibited linear pharmacokinetics in the dose range of 15–60 mg/kg. Sodium danshensu appeared to be poorly absorbed after oral administration, with an absolute bioavailability of 13.72%. The primary distribution tissue was kidney, but it was also distributed to lung, stomach, muscle, uterus, heart, etc. Within 96 h after intravenous administration, 46.99% was excreted *via* urine and 1.16% was excreted *via* feces as the parent drug. Biliary excretion of sodium danshensu was about 0.83% for 24 h. Metabolites in urine were identified as methylation, sulfation, both methylation and sulfation, and acetylation of danshensu. Sodium danshensu can be developed as an injection because of its poor oral bioavailability. In conclusion, sodium danshensu is widely distributed, mainly phase II metabolized and excreted primarily in urine as an unchanged drug in rats.

Keywords: sodium danshensu, pharmacokinetics, LC-MS/MS, ADME, bioavailability study

BACKGROUND

Salvia miltiorrhiza, named Danshen in Chinese, is one of the most versatile traditional Chinese medicinal herbs. It has been widely used to treat and prevent cardio vascular disease, hyperlipidemia and cerebro vascular disease throughout the world (Cheng 2007; Wang et al., 2017). Up to today, more than 70 compounds have been isolated and a wide spectrum of secondary metabolites

has been identified from *Salvia miltiorrhiza*, including diterpenoid quinines, hydrophilic phenolic acids and essential oil constituents (Li et al., 2009). It is generally known that lipophilic diterpenoid quinines and hydrophilic phenolic acids are the main bioactive components in *Salvia miltiorrhiza* (Su et al., 2015).

Danshensu, also named as salvianic acid, is the main water-soluble phenolic acids in *Salvia miltiorrhiza*. It has been reported that danshensu exhibited several pharmacological activities such as cardioprotective effect by inhibiting L-type calcium channels (Song et al., 2016), radioprotective effect by scavenging reactive oxygen species (Guo et al., 2013), protection of vascular endothelial cells by an antioxidative mechanism (Zhao et al., 2012), protection on liver injured by an antioxidative mechanism (Wang et al., 2007), etc.

Because danshensu is unstable in the nature, it was transformed into its sodium salt, sodium danshensu (sodium DL- β -(3,4-dihydroxyphenyl)lactate, **Figure 1**). Sodium danshensu has the same effectiveness as danshensu (Wang and Xu, 2005; Wang et al., 2007; Zhao et al., 2013; Jia et al., 2018). Due to its potential pharmacological activities, sodium danshensu has attracted more and more attention recently and is being investigated as a new drug (Zhou et al., 2009; Wei et al., 2018). In order to investigate the pharmacokinetics of sodium danshensu, several biological analytical methods have been reported (Li et al., 2008; Zhan et al., 2008; Liu et al., 2010, 2014; Fu et al., 2014; Zheng et al., 2015), and a high-throughput, simple, sensitive, selective and reliable LC-MS/MS method was developed and validated in our laboratory before (Jiang et al., 2017). Although many researchers published several articles about pharmacokinetic study of sodium danshensu in rats, detailed pharmacokinetic characteristics including absorption, distribution, metabolism, and elimination (ADME) of sodium danshensu have not been reported. In this study, we extensively investigated the preclinical ADME and bioavailability study of sodium danshensu in rats.

MATERIALS AND METHODS

Chemicals and Reagents

Sodium danshensu (purity 98.5%) was made and provided by the Prof. Chuan Zhang of School of Pharmacy, Second Military Medical University, Shanghai (Zhang et al., 2010). Ketoprofen (purity $\geq 95\%$), the internal standards (IS), was purchased from the National Institute for Food and Drug Control (Beijing, China). HPLC-grade methanol and acetonitrile were purchased from Merck (Darmstadt, Germany). Ethyl acetate was obtained

from Shanghai Sheng De Chemical Co., Ltd. (Shanghai, China). Formic acid was HPLC grade and purchased from TEDIA Company (Fairfield, CA, USA). Deionized water was prepared by using the Milli-Q Plus Ultrapure Water System (Millipore Corporation, Bedford, MA). All other chemicals used in this study were of the highest quality available.

Animals

Sprague–Dawley (SD) rats (male and female equally, 180–220 kg, 6–8 weeks) were purchased from the Shanghai Slack Experimental Animal co., LTD (Shanghai, China) and were acclimated in laboratory for at least 1 week prior to the study. The animal room was controlled to maintain a temperature of 18–25°C and relative humidity of 20–60%. The animals were housed under a 12-h light/dark cycles and allowed free access to food and water.

Pharmacokinetic Study

Rats were fasted overnight before dosing and 6 h after dosing. For the pharmacokinetic study and bioavailability study, 24 rats were randomly divided into four groups ($n = 24$, 6 per group) and were respectively designed as different dosages (15, 30, 60 mg/kg I.V., 180 mg/kg P.O.).

Blood samples were serially collected from orbital venous plexus into heparinized tubes pre-dose and at 0, 0.08, 0.17, 0.33, 0.67, 1.0, 1.5, 2.0, 3.0, 4.0, 6.0, 8.0, and 12.0 h after dosing for the three intravenous injection groups. For the oral administration group, blood samples were serially collected from orbital venous plexus into heparinized tubes pre-dose and at 0.08, 0.17, 0.25, 0.5, 0.75, 1.0, 1.5, 2.0, 3.0, 4.0, 6.0, 8.0, and 12.0 h after dosing. All rats were transfused normal saline after drawing blood. Plasma was then separated from blood by centrifuging at 3,500 rpm for 10 min immediately and transferred to another tubes and stored at -80°C before analysis.

Distribution

In tissue distribution study, rats ($n = 36$, 6 per group) were randomly divided into six groups and sex distribution equally per group, intravenously injected with a single dose of 30 mg/kg sodium danshensu. At 0.17, 0.67, 1, 2, 4, and 6 h after dosing, rats were anesthetized with diethyl ether and sacrificed. Tissues (heart, liver, spleen, lung, kidney, brain, stomach, intestinal, fat, muscle, testis, ovary, and uterus) were excised immediately, rinsed with saline, dried with filter paper, weighed, and homogenized in saline. Tissue homogenates were stored at -80°C before analysis.

Metabolism

Metabolites were analyzed in rat urine with intravenously injected with a single dose of 30 mg/kg sodium danshensu by LC-MS/MS. An aliquot of 500 μl of urine was acidified with 250 μl (3 mol/L) of HCl and vortexed. The mixture was then loaded to activate C18 SPE cartridges, washed with 1 ml of water, and eluted with 1 ml of 80% methanol. The eluant was then evaporated to dryness under a nitrogen gas stream

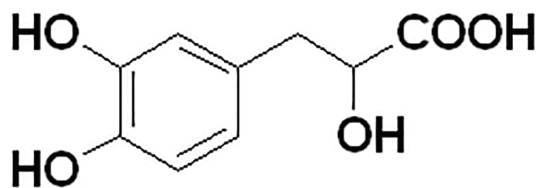


FIGURE 1 | Chemical structure of (D/L) sodium danshensu.

and reconstituted with 100 μ l of mobile phase, and centrifuged at 12,000 rpm for 10 min. The supernatant was then transferred and applied for LC-MS/MS detection.

Excretion

Urine and feces samples were obtained from rats ($n = 6$) intravenously administrated with intravenously injected with a single dose of 30 mg/kg sodium danshensu and housed individually in metabolic cages equipped with a urine and feces separator. The urine and fecal samples were collected pre-dose and at 0–2, 2–4, 4–6, 6–8, 8–12, 12–24, 24–36, 36–48, 48–60, 60–72, 72–84, and 84–96 h after doing. Urine and feces were stored at -80°C before analysis.

In biliary excretion study, SD rats ($n = 6$) were anesthetized with urethane (1.2 g/kg, ip) and the bile duct was cannulated. After intravenous administration with a single dose of 30 mg/kg sodium danshensu, bile was collected at 2 h intervals for the first 12 h and at 24 h. Bile samples were stored at -80°C before analysis.

Sample Preparation

In the present study, sodium danshensu and IS were extracted from rat plasma by using a liquid-liquid extraction method. A 25 μ l aliquot of IS solution containing 40.16 ng/ml of ketoprofen was added to a 50 μ l aliquot of rat plasma and then vortexed and acidified with 20 μ l of 3 mol/L HCl. The mixture was then extracted with 1 ml of ethyl acetate, vortexed, and centrifuged at 5,000 rpm for 10 min. A 800 μ l aliquot of the supernatant was then transferred to another tube and evaporated to dry. The residue was then reconstituted with 50 μ l of mobile phase and centrifuged at 12,000 rpm for 10 min. The supernatant was then transferred to LC-MS/MS detection.

In the tissue distribution study, 50 μ l IS solution (52.6 ng/ml) was added to 100 μ l tissue homogenates respectively. The mixed samples were vibrated 30 s and acidified with 50 μ l of 3 mol/L HCl. The rest of the experimental operation was same as the plasma samples' process.

In the excretion study, feces were prepared by ultrasonic extraction in 0.9%NS for 5 min and vortex for 3 min. After centrifuging at 3,500 rpm for 10 min, 100 μ l supernatant fecal extract was prepared immediately before analysis. The sample preparation for urine, bile and fecal extract were the same to plasma samples. Except that the concentrations of IS or the volumes of HCl were different. A 50 μ l aliquot of IS solutions at concentrations of 312, 103.2, and 103.2 ng/ml were added to a 100 μ l aliquot of urine, bile, or feces samples, respectively. And all were acidified with 50 μ l of 3 mol/L HCl by 30 s.

LC-MS/MS Conditions

The method combining liquid chromatography with electrospray ionization tandem mass spectrometry to determine the sodium danshensu in plasma was developed and validated as described previously (Yu et al., 2011). Analysis was performed using a VARIAN 1200L HPLC-MS system equipped with VARIAN ProStar 210 pump, VARIAN ProStar 410 autosampler, VARIAN

1200L Quadrupole MS/MS, and VARIAN MS 6.8 workstation. The analytes were separated by a Diamonsil C_{18} column (200 mm \times 4.6 mm, 5 μ m) at 25°C with a mobile phase consisting of methanol and 0.1% formic acid in water (80:20, v/v) at a flow rate of 0.8 ml/min, and 2/5 of flow was entered into mass spectrometer. Injection volume was set at 20 μ l and analysis time was set at 9 min. Electrospray ionization was operated in a negative ion mode. The optimized precursor-to-product ion transitions were monitored at m/z 197–135 and 253–209 for sodium danshensu and IS, respectively. Source-dependent parameters were set as follows: needle $-4,700$ V; shield -150 V; nebulizing gas flow 3.31 Mpa; drying gas 250°C , 1.38 MPa; capillary voltage -40 V; and collision energy 18.0 and 5.5 V for sodium danshensu and IS.

Data Analysis

Pharmacokinetic parameters of sodium danshensu were analyzed by using the BAPP software (version 3.1, Center of Drug Metabolism and Pharmacokinetics, China Pharmaceutical University, Nanjing, China) with a noncompartmental model. All data are presented as mean \pm SD. The absolute bioavailability (%F) of sodium danshensu was estimated *via* the ratio of $\text{AUC}_{0-\infty}$ after oral and intravenous administration.

RESULTS

Pharmacokinetic Results

The pharmacokinetic profiles of sodium danshensu in rats following intravenous administration of sodium danshensu at doses of 15, 30, and 60 mg/kg are shown in **Figure 2**, and relevant pharmacokinetic parameters obtained are listed in **Table 1**. Plasma concentrations of sodium danshensu decreased quickly with elimination half time ($t_{1/2}$) of 2.76 ± 0.72 , 3.00 ± 0.31 , and 2.64 ± 0.44 h, respectively. The AUC_{0-12} values were determined to be 12.67 ± 1.40 , 34.27 ± 2.49 , and

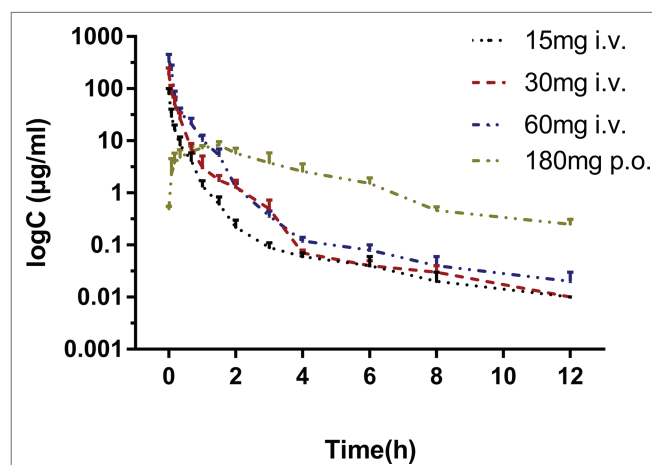


FIGURE 2 | Mean plasma concentration-time curves of sodium danshensu after intravenous administration of 15, 30, 60 mg/kg and oral administration 180 mg/kg in rats ($n = 6$).

TABLE 1 | Pharmacokinetic parameters of sodium danshensu in rats after intravenous administration of 15, 30, and 60 mg/kg and oral of 180 mg/kg ($n = 6$).

Parameters	Units	15 mg/kg (I.V.)	30 mg/kg (I.V.)	60 mg/kg (I.V.)	180 mg/kg (P.O.)
T_{\max}	h	–	–	–	1.40 ± 0.30
C_{\max}	$\mu\text{g/ml}$	81.18 ± 19.26	195.32 ± 53.15	349.32 ± 104.85	8.76 ± 0.85
$t_{1/2}$	h	2.76 ± 0.72	3.00 ± 0.31	2.64 ± 0.44	2.35 ± 0.25
AUC_{0-12}	$\mu\text{g h/ml}$	12.67 ± 1.40	34.27 ± 2.49	67.70 ± 11.71	27.40 ± 4.54
$\text{AUC}_{0-\infty}$	$\mu\text{g h/ml}$	12.73 ± 1.40	34.31 ± 2.49	67.76 ± 11.72	28.24 ± 4.57
MRT	h	0.46 ± 0.07	0.41 ± 0.04	0.39 ± 0.04	3.35 ± 0.23

$67.70 \pm 11.71 \mu\text{g h/ml}$. The results of the variance analysis showed that the $t_{1/2}$ and MRT had no significant differences among different groups ($p > 0.05$). It seems that exposure increases with dosages in the dose range of 15–60 mg/kg and the relationship between AUC_{0-12} and dose was reflected in the liner correlation coefficient ($r^2 = 0.9338$).

The absolute bioavailability was calculated by comparing between oral and intravenous administration of sodium danshensu in another study. The mean plasma concentration-time curves in rats following oral administration are also illustrated in **Figure 2**, and the pharmacokinetic parameters are listed in **Table 1**. T_{\max} after oral administration is 1.40 ± 0.30 h, indicating that the absorption of sodium danshensu from the gastrointestinal tract is in a moderate speed. The absolute oral bioavailability of sodium danshensu in rats was calculated to be 13.72%, indicating poor absorption following oral administration in rats.

Tissue Distribution

Following intravenous administration, sodium danshensu was distributed throughout the body. The concentration of sodium danshensu was detectable in all tissues studied, including heart, liver, spleen, lung, kidney, brain, stomach, intestinal, fat, muscle, testis, ovary, and uterus, as showed in **Figure 3**. Peak levels reached at 0.17 h in all tissues and decreased gradually in most of the tissues at 6 h post-dose. The primary distribution site was kidney, followed by uterus, lung, muscles, and stomach. Kidney distribution of sodium danshensu is 9-fold to 388-fold higher than other tissues at 0.17 h.

Metabolite Profiling in Rat Urine

Rat urine samples were collected from rats administrated with sodium danshensu and analyzed for metabolite profiling. Total ion chromatogram (TIC) of dosed rat urine was shown in **Figure 4**. There are seven metabolites speculated in rat urine, named as M1 to M7. Extracted ion chromatograms (EIC) of seven metabolites were displayed in **Figures 5–8**. M1–M3 were metabolites with molecular ions at m/z 211, 14 amu greater than that of danshensu (m/z 197). This additional evidence supported that M1–M3 were methylated metabolites of danshensu. Molecular ion of M4 was at m/z 277, 80 amu greater than that of danshensu, indicating that M4 was a sulfated metabolite of danshensu. M5 and M6 were metabolites with m/z 291, 94 amu greater than that of danshensu, presumed to be methylated and sulfated danshensu. Molecular ion of M7 was at m/z 239, 42 amu greater than that of danshensu,

indicating that M7 was an acetylated metabolite of danshensu. Possible metabolic pathways of sodium danshensu in rats were shown in **Figure 9**.

Excretion of Sodium Danshensu

Excretion of sodium danshensu into urine and feces after a single intravenous administration of sodium danshensu (30 mg/kg) to rats is presented in **Figure 10**. Urinary recovery of total sodium danshensu for the first 12 h period is about $46.57 \pm 19.25\%$ of the administrated dose, and the value for 96 h period was $46.99 \pm 19.37\%$. Compared with urinary excretion, feces excretion of sodium danshensu is very small, only about $1.16 \pm 0.26\%$ of the dose reclaimed in the feces within 96 h post-dose.

Biliary excretion of sodium danshensu after a single intravenous administration of sodium danshensu (30 mg/kg) is also shown in **Figure 10**. Total excretion into bile over 24 h is about $0.83 \pm 0.11\%$ of the administrated dose. In general, urine was the predominant route of elimination of the prototype drug, accounting for 46.99% of the administrated dose. Recovery of sodium danshensu in feces and bile were very small, with about 1.16 and 0.83% of the dose, respectively.

DISCUSSION

In this study, the preclinical absorption, distribution, metabolism, and excretion of sodium danshensu in rats was investigated. Sodium danshensu was poorly absorbed following a single oral administration, with an absolute bioavailability of 13.72%. It is generally known that many active compositions of Chinese Herbal Medicine have low bioavailability, which may be caused by reasons such as physical and chemical properties of drugs, damaged by intestinal environment, metabolized by intestinal microflora, metabolized by enzyme expressed in intestinal epithelial cell, efflux transported by transporters expressed in intestinal epithelial cell, and so on. Previous studies indicated that sodium danshensu was a substrate of P-gp (Yu et al., 2011). Besides, poor bioavailability, ranged from 11.09 to 28%, was also reported by other researchers (Zhou et al., 2009; Wang et al., 2015). In follow-up experiments, such as the tissue distribution, metabolites, and excretion study, sodium danshensu was given by intravenous administration.

Tissue distribution study indicated that sodium danshensu was highly distributed in the kidney. Wang reported that

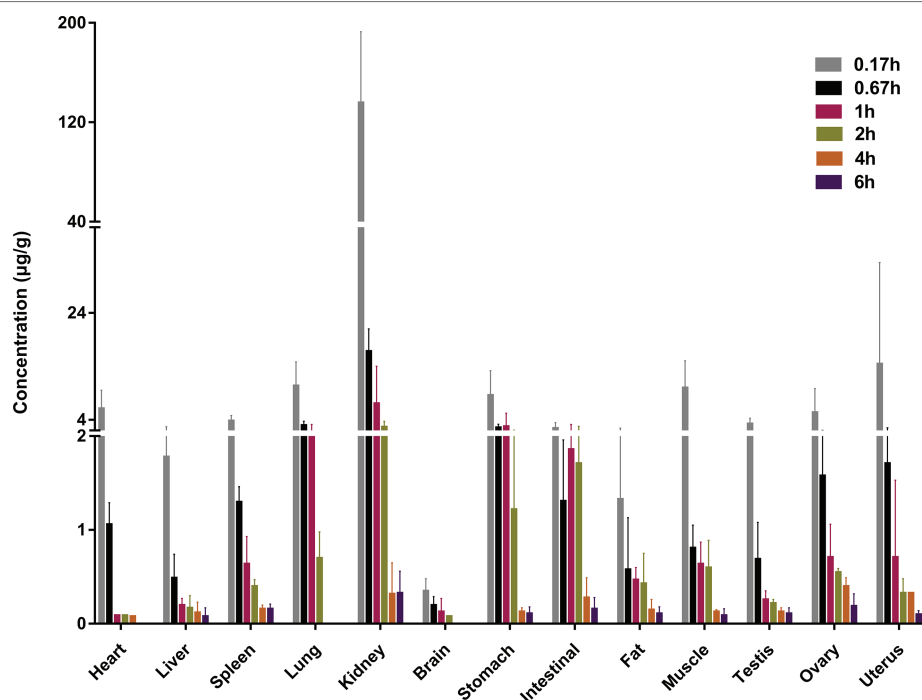


FIGURE 3 | Tissue concentration of sodium danshensu at different time points after intravenous administration of 30 mg/kg in rats.

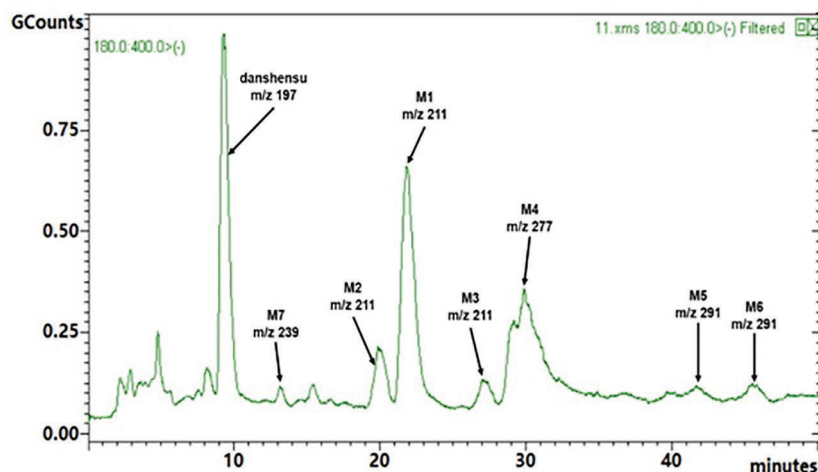


FIGURE 4 | TIC of rat urine sample after intravenous administration of 30 mg/kg sodium danshensu.

danshensu demonstrated a competitive inhibition towards organic anion transporters 1 and 3 (Wang and Sweet, 2013). However, no researcher has investigated whether danshensu is a substrate of organic anion transporter 1 or 3. Organic anion transporters 1 and 3 specifically expressed in the kidney mediated the renal accumulation of many drugs. Our study found that danshensu was highly accumulated in rat kidney. In addition, danshensu is an acidic compound, which is in accordance with substrate characteristics of organic anion transporter 1 or 3. It can be speculated that danshensu may be a substrate of organic anion transporter 1 or 3, which depends further

investigation. From the perspective of cardiovascular pharmacological, the tissue distribution study of sodium danshensu also indicated that kidney may be the important target organs exerting pharmacodynamic effects. Preliminary research demonstrated that Danshen has an anti-hypertensive effect through the inhibition of the renin angiotensin system (Kang et al., 2002). According to the theory of traditional Chinese medicine, Danshen could promote blood circulation and diuresis by regulation the AQP2 in kidney (Dong et al., 2014). So, this tissue distribution study could provide reference for further pharmacological research.

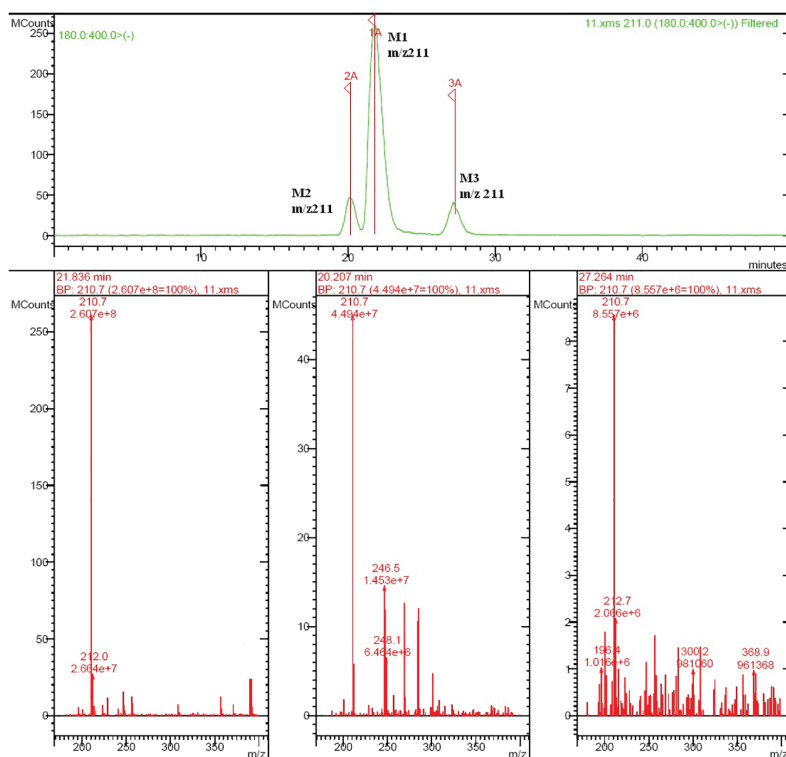


FIGURE 5 | EIC of rat urine sample at m/z 211.

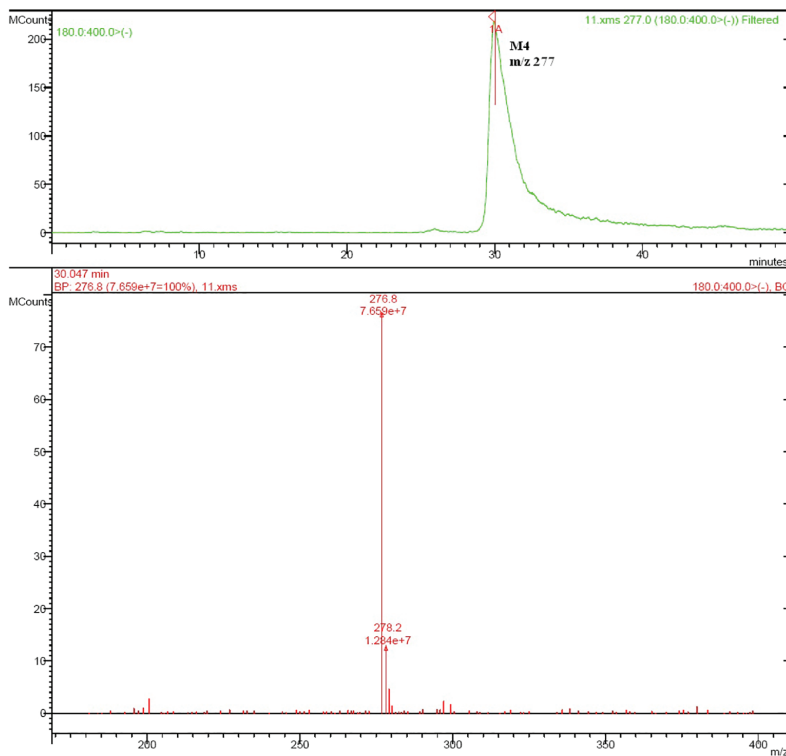


FIGURE 6 | EIC of rat urine sample at m/z 277.

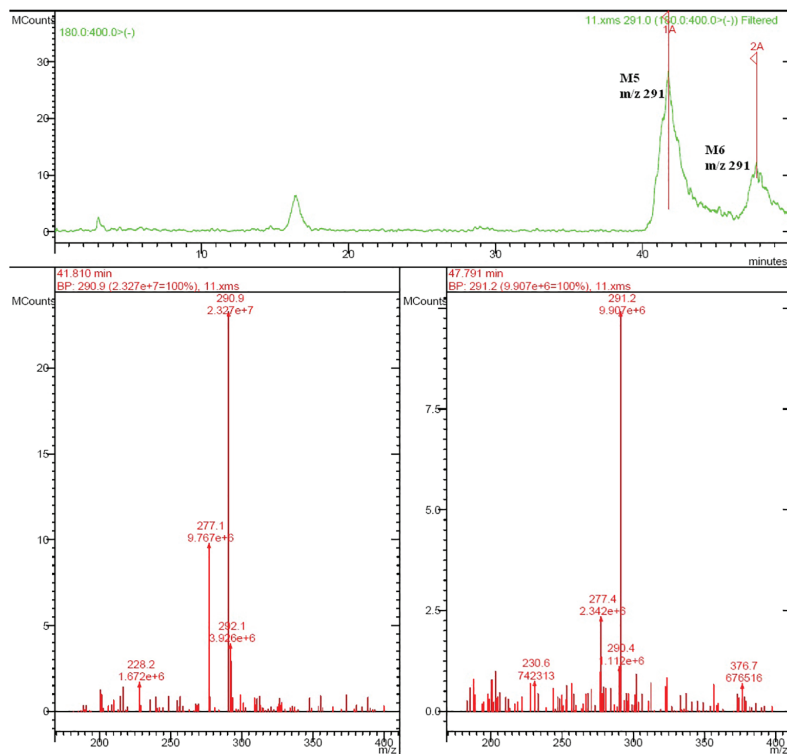


FIGURE 7 | EIC of rat urine sample at m/z 291.

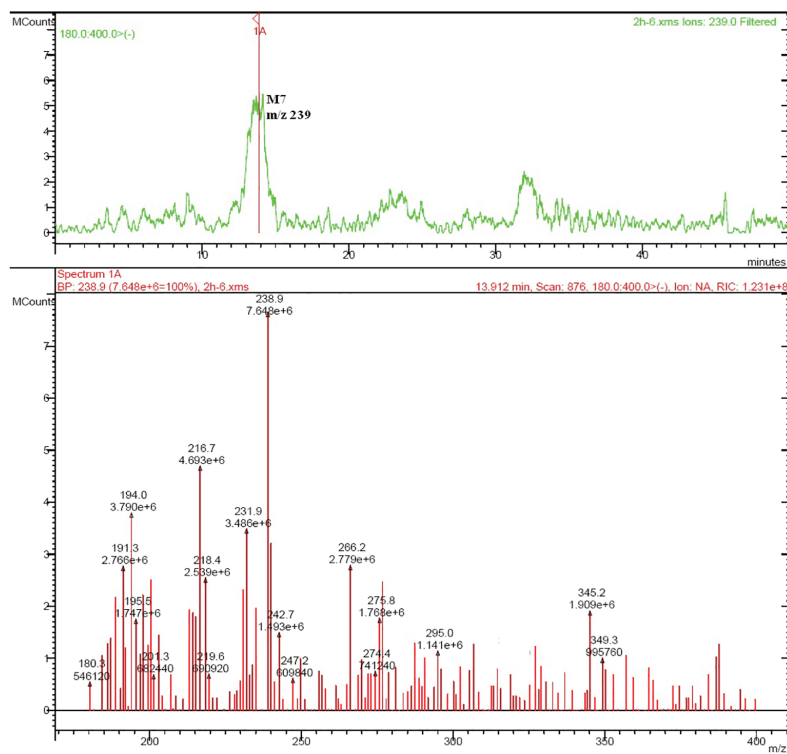


FIGURE 8 | EIC of rat urine sample at m/z 239.

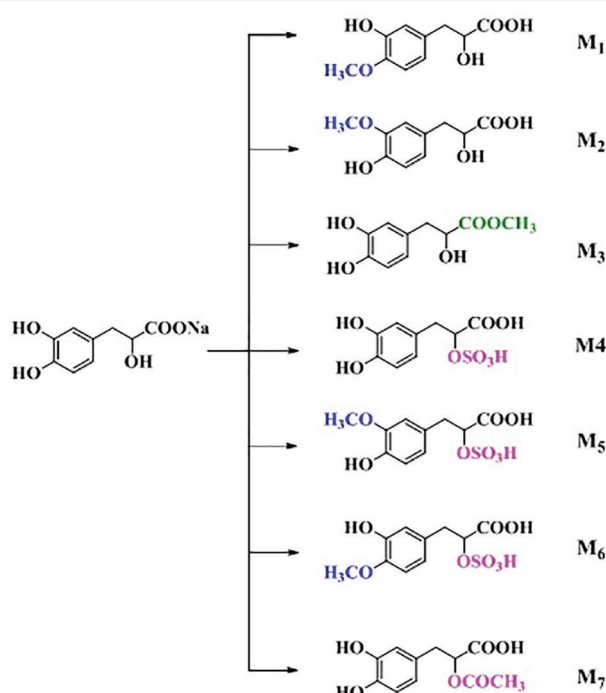


FIGURE 9 | Possible metabolic pathways of sodium danshensu in rats.

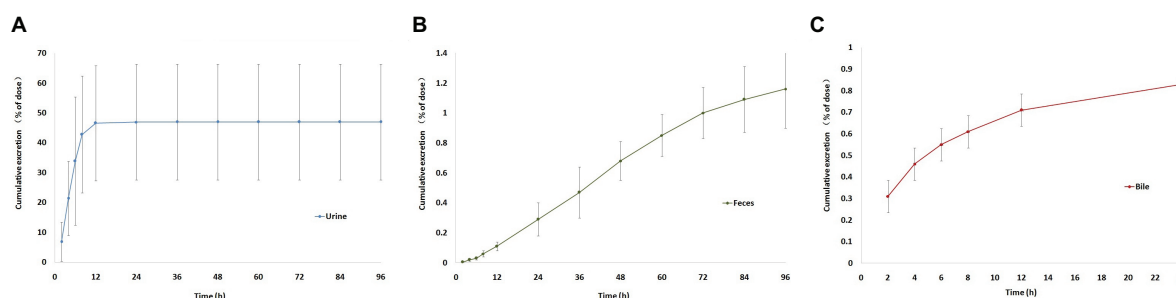


FIGURE 10 | Cumulative excretion of sodium danshensu in rat after intravenous administration of 30 mg/kg. **(A)** Cumulative excretion of sodium danshensu in rat urine. **(B)** Cumulative excretion of sodium danshensu in rat feces. **(C)** Cumulative excretion of sodium danshensu in rat bile.

There are seven sodium danshensu metabolites speculated in rat urine in this study, including three methyl-danshensu metabolites, one danshensu sulfate, one methyl-danshensu sulfate, and one acetyl-danshensu. Due to lack of reference substances, qualitative rather than quantitative analysis was conducted. All metabolites were deduced by their precursor ion and product ions (data not shown). Three hydroxyls exist in the structure of SAA, which may be served as methylation binding sites. Xu found that methylated metabolites of sodium danshensu displayed even higher antioxidant activity against lipid peroxidation in rat liver *in vitro*. Methylated metabolites may contribute to the pharmacological activities of SAA (Xu et al., 2014). Shen found five metabolites in rat plasma dosed with danshensu (20 mg/kg, IV), including danshensu mono-glucuronide, monomethyl-danshensu monoglucuronide,

mono-methyl-danshensu, dimethyl-danshensu, and dimethyl-danshensu-monoglucuronide (Shen et al., 2009). In another study, Gu JF found five metabolites in rat urine dosed with danshensu, including two danshensu sulfate, one methyl-danshensu sulfate, one danshensu mono-glucuronide, and one monomethyl-danshensu mono-glucuronide (Gu et al., 2014).

Urinary, fecal, and bile excretion of sodium danshensu in rats after intravenous administration of sodium danshensu have not been reported yet. In this study, the majority of sodium danshensu was found to be excreted in rat urine, with approximately 46.99% of administrated dose recovered in rat urine in 96 h. Furthermore, urinary excretion of sodium danshensu was concentrated in the first 12 h, with about 46.57% of sodium danshensu, and indicated that sodium danshensu can be excreted quickly and might not result in accumulation *in vivo*.

Excretion of sodium danshensu in rat feces and bile was relatively low, with about 1.16 and 0.83% of administrated dose. It means that feces and bile play minor role in the elimination of sodium danshensu.

CONCLUSIONS

In summary, this study provides a comprehensive delineation of sodium danshensu absorption, distribution, metabolism, and elimination profiles in rats. The data demonstrates that sodium danshensu is poorly absorbed, widely distributed, bio-transformed through several metabolic pathways, and excreted mainly in rat urine.

ETHICS STATEMENT

All pharmacokinetics studies that involved SD rats adhered to the International Guiding Principles for Biomedical Research Involving Animals, as revised by the International Council for

Laboratory Animal Science (ICLAS) and the Councils for International Organizations of Medical Sciences (CIOMS) in 2012.

AUTHOR CONTRIBUTIONS

XM and JJ preformed the bioanalysis and prepared the manuscript. HP established the analytical method and revised the manuscript. SWa performed the animal experiment. SWa analyzed data and calculated PK parameters. GF and YL designed the whole research and interpreted results of experiments. GF reviewed the final manuscript, and all the authors have read and approved the final version.

FUNDING

This work was supported by the Project Plan of Important Developing Discipline Construction, China (No. 2016ZB0302) and Funding scheme of young teachers in Shanghai universities (ZZJKYX16009).

REFERENCES

- Cheng, T. O. (2007). Cardiovascular effects of Danshen. *Int. J. Cardiol.* 121, 9–22. doi: 10.1016/j.ijcard.2007.01.004
- Dong, X. J., Guo, L. E., Yao, R., Xue, S. Y., and Li, F. (2014). Relationship between regulation effect of *Salvia miltiorrhiza* on AQP2 in kidney and promoting blood circulation and diuresis. *Zhongguo Zhong Yao Za Zhi* 39, 3162–3165. doi: 10.4268/cjcm20141631
- Fu, S., Li, L., Qiu, F., Wang, B., Du, W., and Feng, L. (2014). Application of a simple and rapid LC-MS/MS method for determination of danshensu in human plasma for an oral pharmacokinetic study of Danshen granules in chinese healthy subjects. *Anal. Methods* 6, 1956–1962. doi: 10.1039/C3AY42134A
- Gu, J. F., Feng, L., Zhang, M. H., Qin, D., Jiang, J., Cheng, X. D., et al. (2014). New metabolite profiles of Danshensu in rats by ultraperformance liquid chromatography/quadrupole-time-of-flight mass spectrometry. *J. Chromatogr. B Analyt. Technol. Biomed. Life Sci.* 955–956, 20–25. doi: 10.1016/j.jchromb.2014.02.010
- Guo, J., Zhang, Y., Zeng, L., Liu, J., Liang, J., and Guo, G. (2013). Salvianic acid a protects L-02 cells against gamma-irradiation-induced apoptosis via the scavenging of reactive oxygen species. *Environ. Toxicol. Pharmacol.* 35, 117–130. doi: 10.1016/j.etap.2012.11.010
- Jia, D., Li, T., Chen, X., and Ding, X. (2018). Salvianic acid a sodium protects HUVEC cells against tert-butyl hydroperoxide induced oxidative injury via mitochondria-dependent pathway. *Chem. Biol. Interact.* 279, 234–242. doi: 10.1016/j.cbi.2017.10.025
- Jiang, J. J., Zhao, X., Li, X. X., Wu, S. Y., Yu, S. D., Lou, Y. F., et al. (2017). High-throughput determination of sodium danshensu in beagle dogs by the LCMS/MS method, employing liquid-liquid extraction based on 96-well format plates. *Molecules* 22, 667–681. doi: 10.3390/molecules22050667
- Kang, D. G., Yun, Y. G., Ryoo, J. H., and Lee, H. S. (2002). Anti-hypertensive effect of water extract of danshen on renovascular hypertension through inhibition of the renin angiotensin system. *Am. J. Chin. Med.* 30, 87–93. doi: 10.1142/S0192415X02000107
- Li, W., Li, Z. W., Han, J. P., Li, X. X., Gao, J., and Liu, C. X. (2008). Determination and pharmacokinetics of danshensu in rat plasma after oral administration of danshen extract using liquid chromatography/tandem mass spectrometry. *Eur. J. Drug Metab. Pharmacokinet.* 33, 9–16. doi: 10.1007/BF03191013
- Li, Y. G., Song, L., Liu, M., Hu, Z. B., and Wang, Z. T. (2009). Advancement in analysis of *Salvia miltiorrhiza* radix et Rhizoma (Danshen). *J. Chromatogr. A* 1216, 1941–1953. doi: 10.1016/j.chroma.2008.12.032
- Liu, Y. Q., Cai, Q., Liu, C., Bao, F. W., and Zhang, Z. Q. (2014). Simultaneous determination and pharmacokinetic comparisons of multi-ingredients after oral administration of radix *salviae miltiorrhizae* extract, hawthorn extract, and a combination of both extracts to rats. *J. Anal. Methods Chem.* 2014:617367. doi: 10.1155/2014/617367
- Liu, Y., Li, X., Li, Y., Wang, L., and Xue, M. (2010). Simultaneous determination of danshensu, rosmarinic acid, cryptotanshinone, tanshinone I, and dihydrotanshinone I by liquid chromatographic-mass spectrometry and the application to pharmacokinetics in rats. *J. Pharm. Biomed. Anal.* 53, 698–704. doi: 10.1016/j.jpba.2010.03.041
- Shen, Y., Wang, X., Xu, L., Liu, X., and Chao, R. (2009). Characterization of metabolites in rat plasma after intravenous administration of salvianolic acid a by liquid chromatography/time-of-flight mass spectrometry and liquid chromatography/ion trap mass spectrometry. *Rapid Commun. Mass Spectrom.* 23, 1810–1816. doi: 10.1002/rcm.4078
- Song, Q., Chu, X., Zhang, X., Bao, Y., Zhang, Y., Guo, H., et al. (2016). Mechanisms underlying the cardioprotective effect of Salvianic acid a against isoproterenol-induced myocardial ischemia injury in rats: possible involvement of L-type calcium channels and myocardial contractility. *J. Ethnopharmacol.* 189, 157–164. doi: 10.1016/j.jep.2016.05.038
- Su, C. Y., Ming, Q. L., Rahman, K., Han, T., and Qin, L. P. (2015). *Salvia miltiorrhiza*: traditional medicinal uses, chemistry, and pharmacology. *Chin. J. Nat. Med.* 13, 163–182. doi: 10.1016/S1875-5364(15)30002-9
- Wang, X., Li, W., Ma, X., Yan, K., Chu, Y., Han, M., et al. (2015). Identification of a major metabolite of danshensu in rat urine and simultaneous determination of danshensu and its metabolite in plasma: application to a pharmacokinetic study in rats. *Drug Test. Anal.* 7, 727–736. doi: 10.1002/dta.1750
- Wang, L., Ma, R., Liu, C., Liu, H., Zhu, R., Guo, S., et al. (2017). *Salvia miltiorrhiza*: a potential red light to the development of cardiovascular diseases. *Curr. Pharm. Des.* 23, 1077–1097. doi: 10.2174/1381612822666161010105242
- Wang, C. Y., Ma, F. L., Liu, J. T., Tian, J. W., and Fu, F. H. (2007). Protective effect of salvianic acid a on acute liver injury induced by carbon tetrachloride in rats. *Biol. Pharm. Bull.* 30, 44–47. doi: 10.1248/bpb.30.44
- Wang, L., and Sweet, D. H. (2013). Competitive inhibition of human organic anion transporters 1 (SLC22A6), 3 (SLC22A8) and 4 (SLC22A11) by major components of the medicinal herb *Salvia miltiorrhiza* (Danshen). *Drug Metab. Pharmacokinet.* 28, 220–228. doi: 10.2133/dmpk.DMPK-12-RG-116
- Wang, X. J., and Xu, J. X. (2005). Salvianic acid a protects human neuroblastoma SH-SY5Y cells against MPP⁺-induced cytotoxicity. *Neurosci. Res.* 51, 129–138. doi: 10.1016/j.neures.2004.10.001
- Wei, Z. Z., Chen, D., Liu, L. P., Gu, X., Zhong, W., Zhang, Y. B., et al. (2018). Enhanced neurogenesis and collaterogenesis by sodium danshensu treatment

- after focal cerebral ischemia in mice. *Cell Transplant.* 27, 622–636. doi: 10.1177/0963689718771889
- Xu, H., Li, Y., Che, X., Tian, H., Fan, H., and Liu, K. (2014). Metabolism of salvianolic acid a and antioxidant activities of its methylated metabolites. *Drug Metab. Dispos.* 42, 274–281. doi: 10.1124/dmd.113.053694
- Yu, P. F., Wang, W. Y., Eerdun, G., Wang, T., Zhang, L. M., Li, C., et al. (2011). The role of P-glycoprotein in transport of Danshensu across the blood-brain barrier. *Evid. Based Complement. Alternat. Med.* 8, 1–5. doi: 10.1155/2011/713523
- Zhan, Y., Xu, J. P., Liang, J. B., Sheng, L. S., Xiang, B. R., Zou, Q. G., et al. (2008). Simultaneous LC–MS–MS analysis of danshensu, salvianolic acid B, and hydroxysafflor yellow a in beagle dog plasma, and application of the method to a pharmacokinetic study of Danhong lyophilized powder for injection. *Chromatographia* 68, 71–79. doi: 10.1365/s10337-008-0652-0
- Zhang, N., Zou, H., Jin, L., Wang, J., Zhong, M. F., Huang, P., et al. (2010). Biphasic effects of sodium danshensu on vessel function in isolated rat aorta. *Acta Pharmacol. Sin.* 31, 421–428. doi: 10.1038/aps.2010.24
- Zhao, Q. T., Guo, Q. M., Wang, P., and Wang, Q. (2012). Salvianic acid A inhibits lipopolysaccharide-induced apoptosis through regulating glutathione peroxidase activity and malondialdehyde level in vascular endothelial cells. *Chin. J. Nat. Med.* 10, 53–57. doi: 10.1016/S1875-5364(12)60012-0
- Zhao, D., Liu, H., Wang, F., Feng, Q., and Li, M. (2013). A simple, but highly sensitive, graphene-based voltammetric sensor for salvianic acid a sodium. *Anal. Sci.* 29, 625–630. doi: 10.2116/analsci.29.625
- Zheng, L., Gong, Z., Lu, Y., Xie, Y., Huang, Y., Liu, Y., et al. (2015). A UPLC–MS/MS method for simultaneous determination of danshensu, protocatechuic aldehyde, rosmarinic acid, and ligustrazine in rat plasma, and its application to pharmacokinetic studies of Shenxiong glucose injection in rats. *J. Chromatogr. B Analyt. Technol. Biomed. Life Sci.* 997, 210–217. doi: 10.1016/j.jchromb.2015.06.008
- Zhou, L., Chow, M. S., and Zuo, Z. (2009). Effect of sodium caprate on the oral absorptions of danshensu and salvianolic acid B. *Int. J. Pharm.* 379, 109–118. doi: 10.1016/j.ijpharm.2009.06.016

Conflict of Interest Statement: The handling editor declared a shared affiliation, though no other collaboration, with the authors, GF and SWa.

The remaining authors declare that the research was conducted in the absence of any commercial or financial relationships that could be construed as a potential conflict of interest.

Copyright © 2019 Meng, Jiang, Pan, Wu, Wang, Lou and Fan. This is an open-access article distributed under the terms of the Creative Commons Attribution License (CC BY). The use, distribution or reproduction in other forums is permitted, provided the original author(s) and the copyright owner(s) are credited and that the original publication in this journal is cited, in accordance with accepted academic practice. No use, distribution or reproduction is permitted which does not comply with these terms.



Dual Effects of Chinese Herbal Medicines on Angiogenesis in Cancer and Ischemic Stroke Treatments: Role of HIF-1 Network

Ming Hong^{1†}, Honglian Shi^{2†}, Ning Wang³, Hor-Yue Tan³, Qi Wang^{1*} and Yibin Feng^{3*}

¹ Institute of Clinical Pharmacology, Guangzhou University of Chinese Medicine, Guangzhou, China, ² Department of Pharmacology and Toxicology, University of Kansas, Lawrence, KS, United States, ³ School of Chinese Medicine, Li Ka Shing Faculty of Medicine, The University of Hong Kong, Hong Kong

OPEN ACCESS

Edited by:

Issy Laher,
University of British Columbia,
Canada

Reviewed by:

Wentzel Christoffel Gelderblom,
Cape Peninsula
University of Technology, South Africa
Maria Luisa Del Moral,
Universidad de Jaén, Spain

*Correspondence:

Yibin Feng
yfeng@hku.hk
Qi Wang
wangqi@gzucm.edu.cn

[†]These authors have contributed
equally to this work.

Specialty section:

This article was submitted to
Ethnopharmacology,
a section of the journal
Frontiers in Pharmacology

Received: 12 March 2019

Accepted: 29 May 2019

Published: 26 June 2019

Citation:

Hong M, Shi H, Wang N, Tan H-Y,
Wang Q and Feng Y (2019) Dual
Effects of Chinese Herbal Medicines
on Angiogenesis in Cancer
and Ischemic Stroke Treatments:
Role of HIF-1 Network.
Front. Pharmacol. 10:696.
doi: 10.3389/fphar.2019.00696

Hypoxia-inducible factor-1 (HIF-1)-induced angiogenesis has been involved in numerous pathological conditions, and it may be harmful or beneficial depending on the types of diseases. Exploration on angiogenesis has sparked hopes in providing novel therapeutic approaches on multiple diseases with high mortality rates, such as cancer and ischemic stroke. The HIF-1 pathway is considered to be a major regulator of angiogenesis. HIF-1 seems to be involved in the vascular formation process by synergistic correlations with other proangiogenic factors in cancer and cerebrovascular disease. The regulation of HIF-1-dependent angiogenesis is related to the modulation of HIF-1 bioactivity by regulating HIF-1 α transcription or protein translation, HIF-1 α DNA binding, HIF-1 α and HIF-1 α dimerization, and HIF-1 degradation. Traditional Chinese herbal medicines have a long history of clinical use in both cancer and stroke treatments in Asia. Growing evidence has demonstrated potential proangiogenic benefits of Chinese herbal medicines in ischemic stroke, whereas tumor angiogenesis could be inhibited by the active components in Chinese herbal medicines. The objective of this review is to provide comprehensive insight on the effects of Chinese herbal medicines on angiogenesis by regulating HIF-1 pathways in both cancer and ischemic stroke.

Keywords: angiogenesis, herbal medicine, hypoxia-inducible factor-1, cancer, ischemic stroke

INTRODUCTION

Angiogenesis is the formation and remodeling of new blood vessels and capillaries from the existing vasculature through interaction among cellular matrix, cytokines, and proteases. It plays a pivotal role in diffusion exchange of metabolites and nutrients in all the tissues and organs of the human body (Shi, 2009; Kusumbe et al., 2014), occurring throughout our lives in both diseased and healthy states. Changes in metabolism result in proportional changes in angiogenesis and, therefore, proportional changes in capillarity. Oxygen is crucial for this process. Hypoxia occurs when there is reduced oxygen supply and/or increased oxygen demand. It is the principal physiological stimulus for inducing angiogenesis, which provides a stimulus-response pathway that tries to maintain adequate oxygenation in pathological status, such as tumor growth and ischemic stroke (Mengozzi et al., 2012; Brown, 2016). There has been great interest during the past decades in regulating angiogenesis as a therapeutic target for cancer and ischemic stroke. The current clinical application based on the principle of angiogenesis

includes antiangiogenic therapy and proangiogenic therapy. Antiangiogenic therapy has been used for cancer treatment, which inhibits the delivery of oxygen and nutrients to cancer cells. On the other hand, proangiogenic therapies in ischemic stroke could be beneficial by increasing blood flow. Hypoxia-inducible factor-1 (HIF-1), a regulator of essential adaptive responses to hypoxia-induced angiogenesis, is highly expressed under hypoxic conditions, such as aggressive tumors and ischemic brains (Sendoel et al., 2010; Berlow et al., 2017). HIF-1 has been suggested to be an important target in treating cancer and ischemic stroke by regulating the transcriptional activity of its downstream genes. The activity and accumulation of HIF-1 α protein were found to be regulated at different levels, such as regulating HIF-1 α synthesis stability or transactivation throughout its life cycle inside the cells (Yeom et al., 2011; Soleymani Abyaneh et al., 2017).

Traditional Chinese herbal medicine has a long history of clinical use in both cancer and stroke treatments in Asia. Chinese herbal medicines often use a variety of herbs in different complex combinations to enhance their therapeutic effects or reduce their toxicity. Growing evidence has demonstrated potential proangiogenic benefits of Chinese herbal medicines in ischemic stroke whereas tumor angiogenesis could be inhibited by the active components in herbal medicines (Hong et al., 2015; Gandin et al., 2016; Hong et al., 2016; Guo et al., 2018). Thus, the objective of this review is to provide comprehensive insight on how Chinese herbal medicines impact angiogenesis by regulating HIF-1 pathways in both cancer and ischemic stroke. In this study, we tried to give a systematic and timely update about the effects and mechanisms of several Chinese herbal medicines targeting

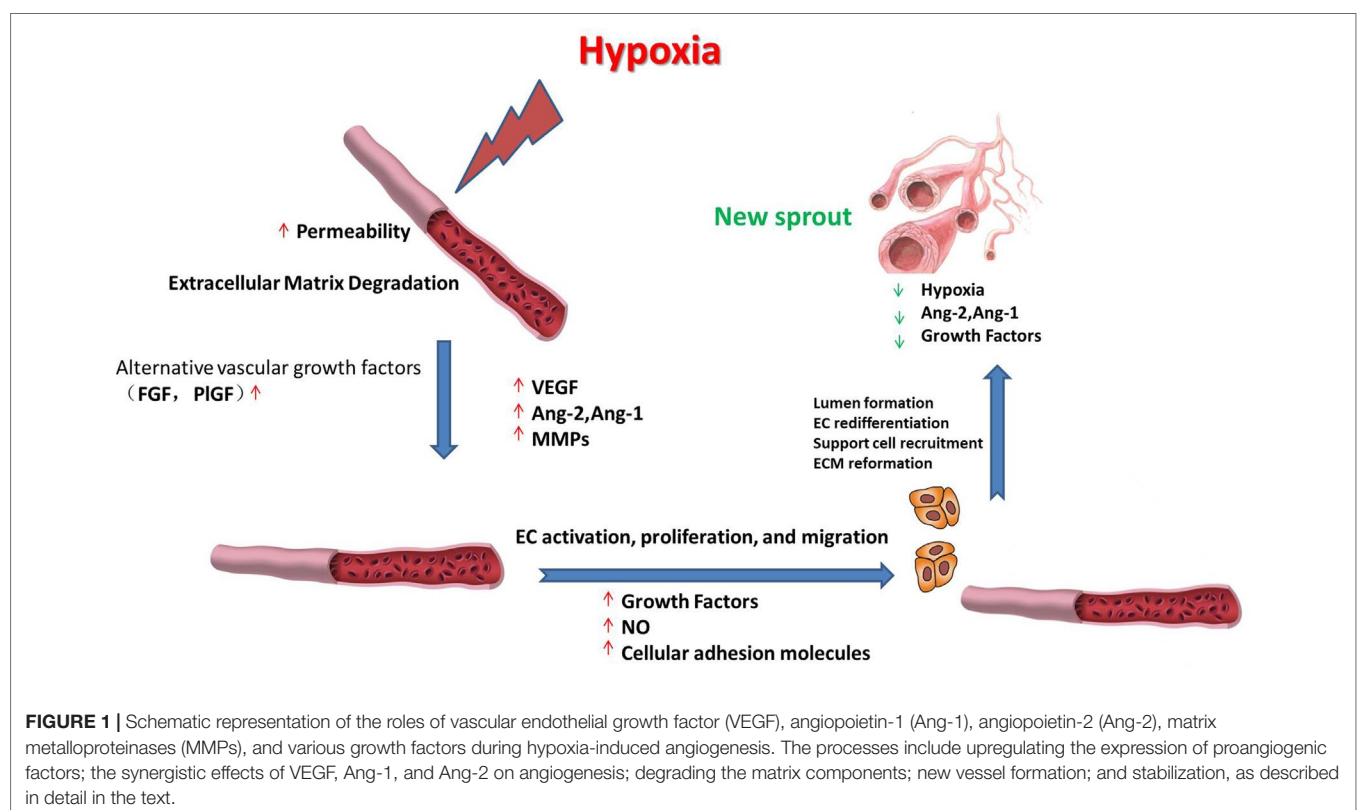
HIF-1 pathways in cancer or ischemic stroke, such as Xue-Fu-Zhu-Yu decoction, ginsenosides, Pien Tze Huang, Yi Ai Fang, baicalein, and curcumin. Their mechanisms of antiangiogenesis or proangiogenesis behaviors, potential toxicity, or side effects and future research directions were discussed.

METHOD

Both clinical trials and basic research on Chinese herbal medicines that target the HIF-1 pathway were included to assess their efficacy and underlying mechanisms. One Chinese database (China Journals Full-Text Database) and four English databases (AMED, MEDLINE, EMBASE, and The CENTRAL) were applied in our study to retrieve more recent publications on this topic. Chinese herbal medicines and their active compounds for ischemic stroke or cancer treatment will be included in this review paper if more than two research papers have described the *in vitro* and *in vivo* studies of the particular subject or of any paper describing clinical trials on the subject.

HYPOXIA-INDUCED ANGIOGENESIS

Hypoxia is the nonphysiological exposure to low oxygen tension of cells or tissues, which is associated with various pathological events, such as stroke, inflammation, and cancer. These pathological events induce the restoration of oxygen homeostasis by activating repair mechanisms such as angiogenesis. Hypoxia-induced angiogenesis includes several steps (Figure 1). 1) Exposure to



low oxygen tension upregulates the expression of proangiogenic growth factors that activate their receptors (Sendoel et al., 2010; Berlow et al., 2017). 2) Vascular permeability increases in response to vascular endothelial growth factor (VEGF), thereby inducing the exudation of plasma proteins that form a primitive scaffold for migrating endothelial cells. Angiopoietin-1 (Ang-1) and angiopoietin-2 (Ang-2) exhibit antagonistic properties during the development of the vessel. Ang-1 is critical for vessel maturation, adhesion, migration, and survival, whereas Ang-2 is involved in vessel destabilization and promoting cell death. Yet, when it is in conjunction with VEGFs, Ang-2 can promote neovascularization (Jain and Carmeliet, 2012). The matrix metalloproteinases (MMPs) such as MMP2 and MMP9 can further induce angiogenesis by degrading matrix components (Ota et al., 2009; Kang et al., 2012). 3) Proliferative endothelial cells assemble and form a lumen by migrating to a distant location (Nieuwenhuis et al., 2017). In this stage, several proteins can promote endothelial cell survival, adhesion, and migration, such as VE-cadherin and integrins $\alpha\beta$. After new vessels are formed, pericytes and smooth muscle cells will stabilize the walls and prevent leakage by surrounding the novel capillaries. Other factors including Ang-1 and platelet-derived growth factor receptor (PDGFR) also take part in the maturation of novel capillaries (Rivera and Bergers, 2014).

Hypoxia-induced angiogenesis shows significant differences in signal pathways compared with physiological angiogenesis. For example, physiological angiogenesis in embryonic development requires activating the VEGF pathway, whereas hypoxia-induced angiogenesis such as tumor angiogenesis can also induce angiogenesis by recruiting myeloid cells and upregulate alternative vascular growth factors in addition to VEGF, such as fibroblast growth factor (FGF) and placental growth factor (PlGF). Although postischemic tissue revascularization is crucial for recovery in brain tissues after ischemic stroke (Li Q. et al., 2018) or in the heart after myocardial infarction (Chen R. et al., 2018), the activation of angiogenesis is harmful in disorders such as macular degeneration and cancer (Pio et al., 2013). Therefore, there is great interest in regulating angiogenesis as a possible therapeutic method for different kinds of diseases. Elucidating the molecular mechanism of hypoxia-induced angiogenesis will help in the identification of potential therapeutic targets and improve therapeutic effects.

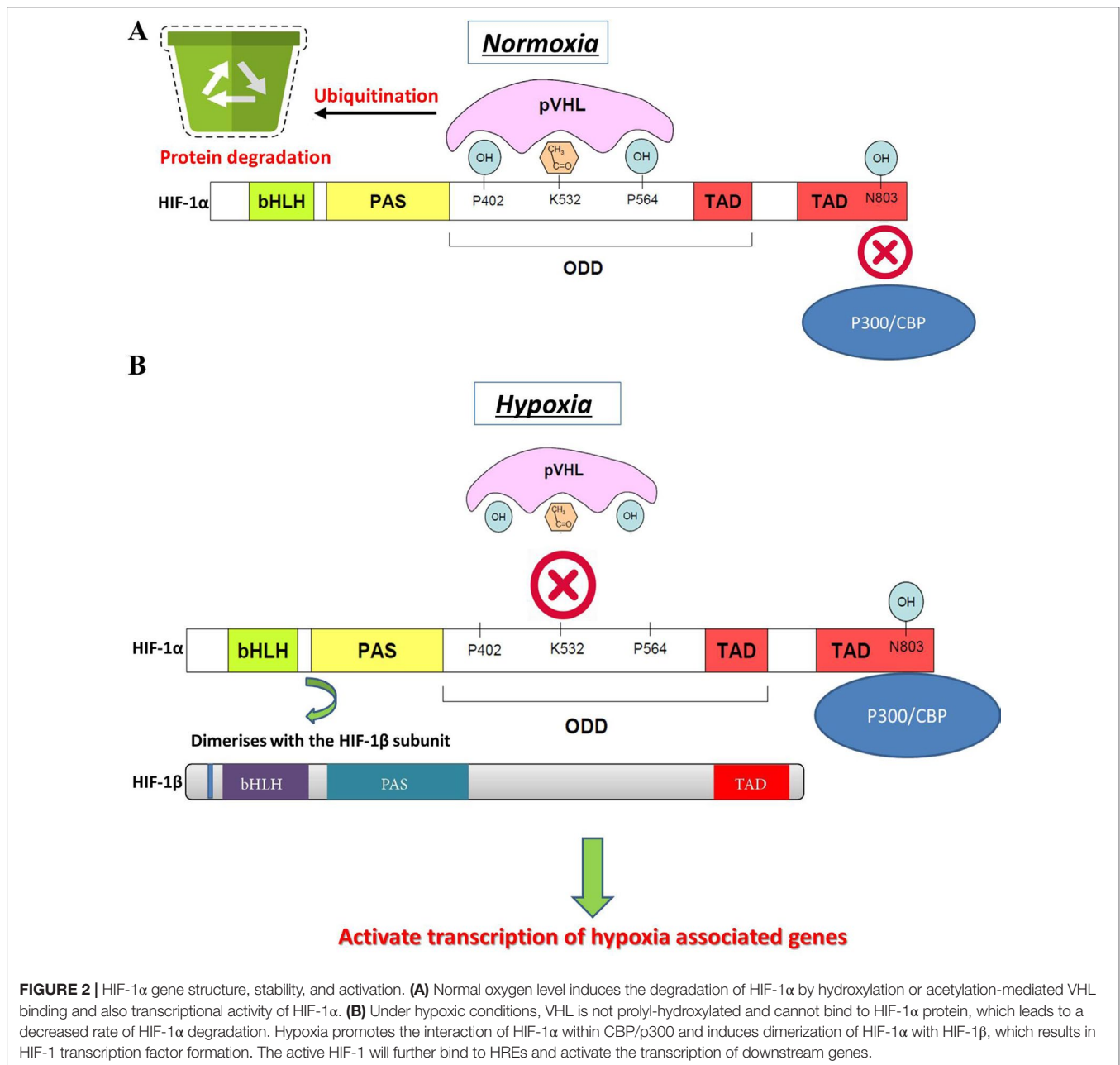
HYPOXIA-INDUCIBLE FACTOR-1

Changes in oxygen supply represent a pivotal physiological stimulus for all eukaryotic cells that require adequate oxygen consumption for intracellular metabolic reactions. In addition to its contribution to the maintenance of intracellular bioenergetics by producing mitochondrial ATP, O_2 also serves as a universal electron acceptor in various biochemical pathways. Therefore, genes involved in responding to hypoxia are highly conserved during evolution. HIF-1 is an oxygen-dependent transcriptional activator, which is composed of HIF-1 α , the alpha subunit, and the aryl hydrocarbon receptor nuclear translocator (Arnt), the beta subunit. Both subunits belong to the bHLH-PAS (Per/Arnt/Sim) family. HIF-1 is induced in hypoxic cells and binds to the cis-acting hypoxia

response element (HRE) of the human EPO gene, which is required for erythropoietin synthesis (Aldo and Elisabetta, 2018; Zhu and Zhang, 2018). Intracellular oxygen concentration levels can affect the subcellular localization and protein activity of the HIF-1 α subunit, whereas the expression of HIF-1 β is not regulated by the oxygen level (Wang et al., 2018). The HIF-1 α and HIF-1 β subunits are similar in structure, and both contain two PAS domains. The bHLH and PAS domains are critical for the heterodimer formation of HIF-1 α and HIF-1 β and for DNA binding. The HIF-1 α subunit contains N-terminal transactivation domains (TAD-N) and C-terminal transactivation domains (TAD-C) concatenated by an inhibitory domain (**Figure 2**). The TAD-N is continuous with protein stability that overlaps with the oxygen-dependent degradation (ODD) domain. The TAD-C is independent of protein stability that interacts with p300/CBP and is critical for transcription activity. The HIF-1 α protein is unstable (half-life = 5 min) and is modified by various posttranscriptional regulations, including phosphorylation, hydroxylation, ubiquitination, acetylation, and nitrosation. Factor inhibiting HIF-1 (FIH-1) hydroxylates asparagine-803 of HIF-1 α within the TAD-C under normoxic conditions, which inhibits the interaction of HIF-1 α with transcriptional coactivators. The molecular mechanisms of the pivotal role of HIF-1 in the regulation of angiogenesis have been revealed in recent years. Recent studies have demonstrated that HIF-1 activity in human tissues can induce angiogenesis in the following ways: 1) by activating the transcription of various angiogenic genes or their receptors such as ANGPT1, ANGPT2, VEGF, PlGF, and PDGFB (Chen et al., 2017); 2) by modulating proangiogenic chemokines and receptors (SDF-1 α , sphingosine-1-phosphate, stromal cell-derived factor 1 α , receptor CXCR4, sphingosine-1-phosphate receptors, and C-X-C chemokine receptor type 4), thus promoting the recruitment of endothelial progenitor cells to the hypoxic site (Soni and Padwad, 2017); and 3) by facilitating cell cycle progression and DNA replication in endothelial cells (Toth and Warfel, 2017). Through the phosphoinositide 3-kinase (PI3K) or Ras/MAPK pathway, several growth factors and their cognate receptors can influence cellular responses to hypoxia and regulate the expression of HIF-1 α . Previous studies have shown that inhibition of PI3K pathway downregulates both basal and mitogen-induced HIF-1 α expression (Cheng et al., 2018). In general, the modifications of HIF-1 are rapidly and precisely regulated according to the cellular oxygen concentration by multiple signaling. The hypoxia-induced angiogenesis is a highly complex and orchestrated process in human disease. HIF-1 was found to be a major modulator of hypoxia-induced angiogenesis by synergistic correlations with various proangiogenic factors and regulates many genes that play important roles in angiogenesis (**Table 1**). Thus, HIF-1 modulation could offer therapeutic benefits for various hypoxia pathologies, including diseases with high mortality and morbidity rates, such as cancer and ischemic stroke.

HYPOXIA-INDUCED ANGIOGENESIS IN CANCER AND THE ROLE OF HIF-1

Because of the expansive growth activities within malignant tumor, cancer cells are highly metabolic. However, the poorly



vascularized original tissue structure leads to inadequate oxygen supply for tumor progression. Hypoxia is commonly observed in the microenvironment of cancer, which arises in cancer *via* the uncontrolled proliferation driven by the oncogene of cancer cells in the absence of an efficient vascular bed. As a result of rapid cell proliferation, the cancer cell quickly exhausts the oxygen supply and nutrient from the normal vasculature, which leads to hypoxia. In previous studies, the relationship between hypoxia and tumor progression has been proven by O_2 -sensitive microsensors (Semenza, 2003; Bohonowych et al., 2011). Clinical studies have shown that patients with hypoxic cervical tumors, head and neck cancer, and sarcoma of soft tissue may have worse disease-free survival than that of patients with normally aerated tumors. The

inadequate oxygen supply at the tumor tissue may induce tumor progression through selective pressure by the mutation of cancer suppressor genes, which may reduce tumor cells' apoptotic capacity and promote tumor growth. Another key characteristic of the hypoxic response in tumor is the modulation of multiple genes that promote angiogenesis to fortify oxygen supply (Zagzag et al., 2000).

Cancer growth and metastasis depend on lymphangiogenesis and neovascularization triggered by hypoxia signals from cancer cells. Cancer cells under hypoxic conditions will upregulate the expression of PDGF, Ang-2, stromal-derived factor 1 (SDF-1), and VEGF, which are crucial in endothelial cell activation and promoting neoangiogenesis. Activated HIF-1 plays a crucial role in hypoxia-adaptive responses of the tumor cells through transcriptional

TABLE 1 | Angiogenesis-Related Genes That Are Transcriptionally Activated by HIF-1.

Target Gene	Protein Name	Roles in Angiogenesis	Reference
c-MET	c-mesenchymal-epithelial transition	Promotes endotheliocyte motility and vascular formation	(Matteucci et al., 2003)
LRP1	Low-density lipoprotein receptor-related protein 1	Regulates vascular integrity	(Woodley et al., 2009; Li et al., 2014)
HO-1	Heme oxygenase-1	Regulates vascular tone and blood pressure	(Sato et al., 2012; Mathew and Sarada, 2018)
GPI	Glucose-6-phosphate isomerase	Tumor-secreted cytokine that stimulates vascular endothelial cell motility	(Zdrazil et al., 2018)
MIC2	CD99 antigen	Inhibits cell-extracellular matrix adhesion and promotes vascular remodeling	(Ohradanova et al., 2008; Liurba et al., 2014)
VEGF	Vascular endothelial growth factor	Stimulates the formation of blood vessels	(Al-Anazi et al., 2018; Fortenberry et al., 2018; Prangsaengtong et al., 2018)
EG-VEGF	Endocrine gland-derived vascular endothelial growth factor	Angiogenic growth factor specifically expressed in the ovaries	(Su et al., 2014; Mi et al., 2018)
ENG	Endoglin	Regulates transforming growth factor- β -dependent vascular remodeling and angiogenesis	(Bluff et al., 2009; Tal et al., 2010)
ET1	Endothelin 1	Regulates vascular tone and blood pressure	(Kaul et al., 2013; Ambrosini et al., 2015; Belaidi et al., 2016)
LEP	Leptin	Has mitogenic activity on vascular endothelial cells and plays a role in matrix remodeling by regulating the expression of matrix metalloproteinases (MMPs) and tissue inhibitors of metalloproteinases (TIMPs)	(Al-Anazi et al., 2018; Rausch et al., 2018)
TGF- β 3	Transforming growth factor beta 3	Regulates angiogenesis in the developing brain via paracrine signaling to vascular epithelial cells	(Taheem et al., 2018; Tsai et al., 2018)
$\alpha_{1\beta}$ -AR	$\alpha_{1\beta}$ -adrenergic receptor	Activates vascular epithelial cell proliferation	(Park et al., 2011; Forbes et al., 2016)
ADM	Adrenomedullin	Regulates vascular tone and blood pressure	(Sena et al., 2014; Matsumoto et al., 2018)
NOS2	Nitric oxide synthase 2	Regulates vascular tone and blood pressure	(Magierowski et al., 2018; Pena-Mercado et al., 2018; Suvanish Kumar et al., 2018)
TFF	Intestinal trefoil factor	Regulates vascular epithelial restitution	(Miki et al., 2004; Manresa and Taylor, 2017)
MMP2	Matrix metalloproteinase 2	Regulates vascular patterning and branching	(Sharma et al., 2018; Tyska-Czochara et al., 2018)
PDGF β	platelet-derived growth factor receptor- β	Maintains vascular stability	(Beppu et al., 2005; Gramley et al., 2010; Hsu et al., 2014)
FN1	Fibronectin 1	Promotes vascular remodeling	(Kondisetty et al., 2018; Zeinali et al., 2018)
PAI-1	plasminogen activator inhibitor-1	Promotes vascular remodeling	(Kabei et al., 2018; Peterle et al., 2018; Toullec et al., 2018)
UPAR	Urokinase-type plasminogen activator receptor	Regulates growth factor activation; promotes ECM and vascular remodeling	(Carroll and Ashcroft, 2006; Laurenzana et al., 2017)
P4H (I)	prolyl-4-hydroxylase (I)	Regulates vascular collagen production	(Trollmann et al., 2018)
ANGPT2	Angiopoietin-Tie2	Regulates vascular remodeling	(Yamakawa et al., 2004; Trollmann et al., 2018)
KRT19	keratin-19	responsible for the structural integrity of vascular ECs	(Copple, 2010)
KRT14	keratin-14	Responsible for the structural integrity of vascular ECs	(Pahlman et al., 2015)
KRT18	keratin-18	Responsible for the structural integrity of vascular ECs	(Muller et al., 2018)

activation of these proangiogenesis genes. As shown in previous studies, HIF-1 can mediate acute hypoxia-induced VEGF expression in neuroblastoma, whereas HIF-2 modulates VEGF expression during prolonged hypoxia (Maxwell et al., 1999). Furthermore, VEGF expression under hypoxia may increase the activity of other proangiogenic factors and their receptors; thus, vessel outgrowth was stimulated through multiple factors. This so-called “angiogenic switching” induces tumor angiogenesis and stimulates tumor growth by supplying nutrients and oxygen by newly formed vessels (Singh et al., 2017). During the cellular adaptation to hypoxic stress, PI3K/AKT/mTOR and MAPK signaling pathways are involved in hypoxia-induced tumor angiogenesis by various growth factors that bind to toll-like receptors (TLRs), alarmin receptors, receptor tyrosine kinases, and G protein-coupled receptors on cell surface, which may also activate HIF-1 (De Francesco et al., 2018). The

mitogen-activated protein kinase (MAPK) and PI3K pathways are activated by the combination of growth factor with its cognate receptor tyrosine kinase. PI3K promotes the activation of the downstream mammalian target of rapamycin (mTOR) and serine/threonine kinase AKT. mTOR further induces p70 S6 kinase (S6K) and its substrate phosphorylation then induces HIF-1 α protein synthesis. In the MAPK pathway, the extracellular signal-regulated kinase (ERK) is activated by the upstream signal cascade (RAS/RAF/MEK). Activated ERK promotes the phosphorylation of eukaryotic translation initiation factor 4E (eIF-4E) binding protein (4E-BP1) and MAP kinase interacting kinase (MNK). MNK can also phosphorylate eukaryotic translation initiation factor 4E (eIF-4E) directly. Then, the HIF-1 α mRNA translation is activated (Rius et al., 2008; Ban et al., 2017; Aldo and Elisabetta, 2018). Key cellular responses to the hypoxic tumor microenvironment

triggered by HIF-1 and its downstream targets increase the vascular formation, cancer invasiveness, and resistance to treatment (Liu H. et al., 2018).

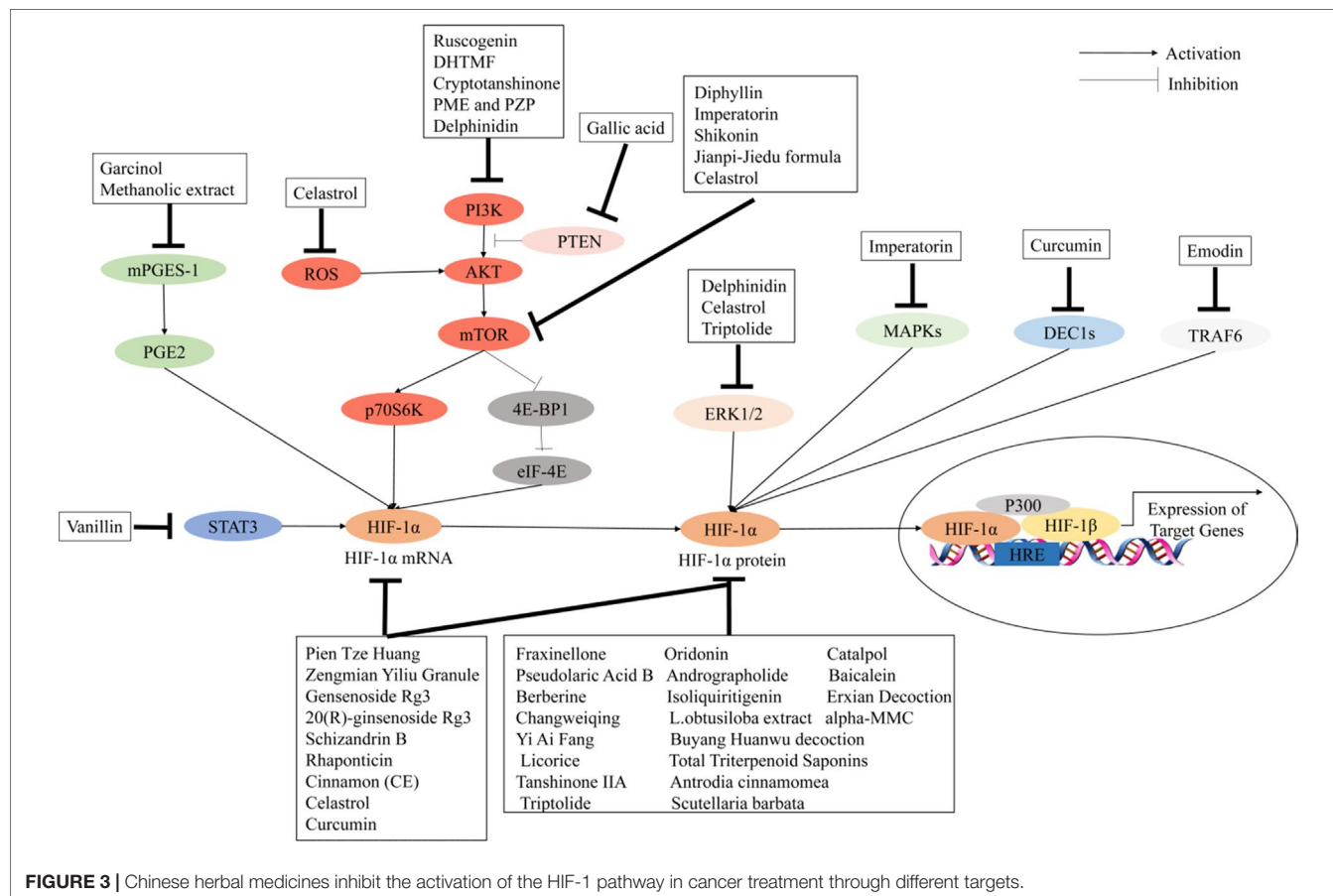
Hypoxia-induced tumor angiogenesis is stimulated and regulated by both activator and inhibitor molecules. However, simple upregulation of the activity of proangiogenesis factors is not sufficient for neovascularization of the tumor. Negative regulators or endogenous inhibitors of vessel growth also need to be downregulated, such as the thrombospondin-1 and thrombospondin-2. In recent years, various anticancer agents have been developed by targeting these angiogenic activator or inhibitor molecules in malignant tumor. A number of antiangiogenesis drugs have been approved by the U.S. Food and Drug Administration (FDA) for treating progressive cancer. So far, most of these drugs are molecular targeted agents that were developed specifically to target VEGF or its receptors, such as bevacizumab (Avastin) and vandetanib (Caprelsa) (Li et al., 2018a). During the last two decades, interest in the role of HIF-1 in tumor angiogenesis has grown exponentially since its identification and molecular characterization in human cancer. Much progress has been made recently about the cellular and molecular mechanism of HIF-1 and its involvement in cancer growth and metastasis based on the analysis of experimental animal models and human cancer biopsies.

In brief, activation of HIF-1 in cancer cells is one of the key masters orchestrating their adaptation mechanism to the hypoxic conditions. Considering the pivotal roles of HIF-1 in tumor

angiogenesis, there has been great interest in developing novel anticancer agents inhibiting the related pathway. As we know, HIF-1 modulation in cancer cells is a complex network including various signal cascades and overlapping mechanisms, each of which might act as a potential target to selectively intervene cancer.

CHINESE HERBAL MEDICINES MEDIATE ANTIANGIOGENIC FACTORS BY REGULATING HIF-1 PATHWAYS IN CANCER TREATMENT

The use of Chinese herbal medicines to treat cancer dates back centuries in ancient traditional folklore in China and Asian countries (Qin et al., 2018; Oyenihni and Smith, 2019). Many herbal extracts and herbal soups have been reported that could relieve clinical symptoms, improve quality of life, and reduce side effects in cancer therapy (Dong et al., 2010; Xu et al., 2014; Tian et al., 2010). In view of the importance of HIF-1 in tumor angiogenesis, the development of herbal medicine inhibitors for this pathway has attracted wide interest. It is clear that the regulation of HIF-1 is a highly complex network cascade and overlapping mechanisms involving multiple targets and signaling pathways, such as HIF-1 α mRNA expression, HIF-1 α protein expression, and HIF-1 transcriptional activity. As shown in **Figures 2 and 3**, we have concluded that Chinese herbal



medicines can regulate HIF-1 by targeting different targets that exert antiangiogenic effects in cancer therapy.

Inhibitors of HIF-1 α mRNA and/or Protein Expression

Numerous herbal medicines that inhibit HIF-1 α mRNA and/or protein expression have significant antiangiogenic effects. Berberine, the main active ingredient isolated from *Coptis chinensis*, has been shown to decrease the expression of HIF-1 α and VEGF in esophageal cancer, hepatocellular carcinoma, prostate cancer, nasopharyngeal carcinoma, and lung cancer (Fu et al., 2013; Yang et al., 2013; Tsang et al., 2015; Zhang et al., 2014a; Zhang C. et al., 2014). Isoliquiritigenin, a natural product derived from liquorice, could significantly decrease VEGF expression by promoting HIF-1 α degradation in breast cancer cells (Wang et al., 2013). Ginsenoside Rg3 is one of the active ingredients in ginseng. Chen et al. (2010) reported that ginsenoside Rg3 could inhibit VEGF expression through downregulation of HIF-1 α protein in various human cancers. Wang et al. (2009) reported that ginsenoside Rg3 could inhibit HIF-1 α and VEGF expression during hypoxia and inhibit hep-2 cell growth by affecting cell cycle progression. Another report has shown that 20(R)-ginsenoside Rg3 could inhibit tumor angiogenesis by suppressing the expression of VEGF, MMP9, and HIF-1 α in a mouse model of Lewis lung cancer (Geng et al., 2016). Schisandrin B (Sch B) is the most abundant

dibenzocyclooctadiene lignan in *Schisandra chinensis*. Lv et al. (2015) found that Sch B could inhibit the migration and invasion of A549 cells by decreasing the expressions of HIF-1, VEGF, MMP-2, and MMP-9 *in vitro*. *Scutellaria barbata* is widely used in the treatment of cancer in traditional Chinese medicine. Shiao et al. (2014) found that *S. barbata* could play an antiangiogenic role by targeting the HIF-1 α signaling pathway and reducing the expression of VEGF. Hu et al. (2012) used a mouse model of ovarian carcinoma xenograft to study the underlying anticancer mechanisms of Zengmian Yiliu granule (ZMYLG), a traditional Chinese formula. ZMYLG could downregulate the protein expression and mRNA of HIF-1 α and VEGF and exert antiangiogenic effects on ovarian carcinoma xenografts. Triptolide (TPL) is an active ingredient extracted from triptolide and widely used in cancer treatment. Li et al. (2018b) found that TPL could inhibit angiogenesis by reducing the expression of HIF-1 α and VEGF in a dose-dependent manner. Protein alpha-momorcharin (alpha-MMC) is isolated from seeds of the bitter melon *Momordica charantia*. Pan et al. (2014) showed that alpha-MMC has significant inhibitory effects on normal and hypoxic nasal-pharyngeal cancer cells by blocking HIF-1 α signaling such as the expression of VEGF and UPR. Baicalein, a type of flavonoid isolated from the roots of *Scutellaria baicalensis*, could suppress tumor growth, which is associated with a reduction of HIF-1 α and VEGF in an orthotopic glioma mouse model (Wang and Jiang, 2015) (Figure 4). Table 2 lists important Chinese herbal medicines that act on HIF-1 mRNA and/or protein expression.

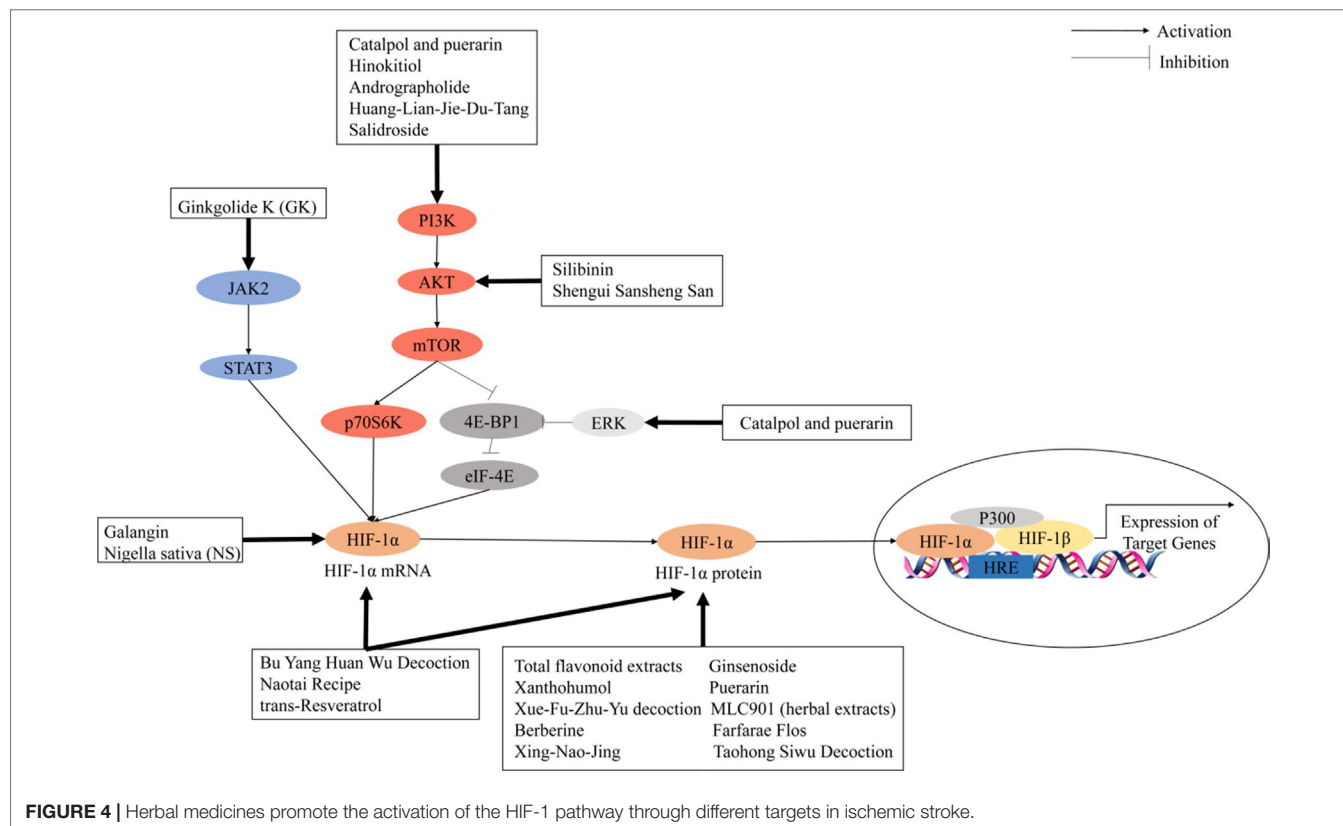


FIGURE 4 | Herbal medicines promote the activation of the HIF-1 pathway through different targets in ischemic stroke.

TABLE 2 | Chinese Herbal Medicines and Their Molecular Targets That Are Regulated by the HIF-1 Pathway in Cancer.

Herb Medicine	Molecular Target	Reference
Inhibitors of HIF-1 mRNA and/or protein expression		
Scutellaria barbata	HIF-1 α protein expression	(Shiau et al., 2014)
Antrodia cinnamomea	HIF-1 α protein expression	(Liu et al., 2013)
<i>L. obtusiloba</i> extract	HIF-1 α protein expression	(Freise et al., 2011)
Pien Tze Huang	HIF-1 α mRNA and protein expression	(Chen et al., 2015)
Yi Ai Fang	HIF-1 α protein expression	(Hou et al., 2016)
Changweiqing	HIF-1 α protein expression	(Li et al., 2011)
Erxian decoction	HIF-1 α protein expression	(Yu et al., 2012)
Zengmian Yiliu granule	HIF-1 α mRNA and protein expression	(Hu et al., 2012)
Buyang Huanwu decoction	HIF-1 α protein expression	(Min et al., 2016)
Fraxinellone	HIF-1 α protein expression	(Xing et al., 2018)
Oridonin	HIF-1 α protein expression	(Li C. et al., 2018)
Catalpol	HIF-1 α protein expression	(Zhu et al., 2017)
Pseudolaric acid B	HIF-1 α protein expression	(Wang et al., 2017)
Andrographolide	HIF-1 α protein expression	(Shi et al., 2017)
Baicalein	HIF-1 α protein expression	(Wang and Jiang, 2015)
Berberine	HIF-1 α protein expression	(Fu et al., 2013; Yang et al., 2013; Zhang et al., 2014a; Zhang C. et al., 2014; Tsang et al., 2015)
Isoliquiritigenin	HIF-1 α protein expression	(Wang et al., 2013)
alpha-MMC	HIF-1 α protein expression	(Pan et al., 2014)
Total triterpenoid saponins	HIF-1 α protein expression	(Jia et al., 2017)
Licorice	HIF-1 α protein expression	(Park et al., 2016)
Tanshinone IIA	HIF-1 α protein expression	(Fu et al., 2014; Sui et al., 2017)
Triptolide	HIF-1 α protein expression	(Li et al., 2018b)
Ginsenoside Rg3	HIF-1 α mRNA and protein expression	(Wang et al., 2009; Chen et al., 2010)
20(R)-ginsenoside Rg3	HIF-1 α mRNA and protein expression	(Geng et al., 2016)
Schizandrin B	HIF-1 α mRNA and protein expression	(Lv et al., 2015)
Rhaponticin	HIF-1 α mRNA and protein expression	(Kim and Ma, 2018)
Cinnamon (CE)	HIF-1 α mRNA and protein expression	(Zhang et al., 2017)
Celastral	HIF-1 α mRNA and protein expression	(Huang et al., 2011)
Curcumin	HIF-1 α mRNA and protein expression	(Bae et al., 2006; Das and Vinayak, 2014; Li et al., 2018a)
Inhibitors of HIF-1 transcriptional activity		
Triptolide	HIF-1 α transcriptional activity	(Zhou et al., 2010)
Scutellaria barbata	HIF-1 α transcriptional activity	(Shiau et al., 2014)
Inhibitors of signal transduction pathways		
Methanolic extract	mPGES-1-PGE2-HIF-1 α	(Ranjbarnejad et al., 2017a)
Jianpi-Jiedu formula	mTOR-HIF-1 α -VEGF	(Mao et al., 2016)
Vanillin	STAT3-HIF-1 α	(Park et al., 2017)
Garcinol	mPGES-1-PGE2-HIF-1 α	(Ranjbarnejad et al., 2017b)
Diphyllin	mTORC1-HIF-1 α -VEGF	(Chen H. et al., 2018)
Imperatorin	mTOR-p70S6K-4E-BP1, MAPK	(Mi et al., 2017)
Shikonin	mTOR-p70S6K-4E-BP1	(Li M. et al., 2017)
Tanshinone IIA	mTOR-p70S6K-4E-BP1	(Wang X. et al., 2017)
Celastral	mTOR-p70S6K-eIF4E, ERK1/2	(Ma et al., 2014)
5,3'-Dihydroxy-6,7,4'-trimethoxyflavone (DHTMF)	PI3K-Akt-mTOR	(Kim et al., 2015)
Ruscogenin	PI3K-Akt-mTOR	(Hua et al., 2018)
Cryptotanshinone	PI3K-Akt-mTOR	(Zhang et al., 2018)
PME and PZP	PI3K-Akt	(Sathya et al., 2010)
Delphinidin	PI3K-Akt-mTOR-p70S6K, ERK	(Kim et al., 2017)
Gallic acid	PTEN-AKT-HIF-1 α	(He et al., 2016)
Emodin	TRAF6-HIF-1 α -VEGF	(Shi and Zhou, 2018)
Celastral	ROS-Akt-p70S6K	(Han et al., 2014)
Triptolide	ERK1/2-HIF-1 α	(Liu H. et al., 2018)
Curcumin	DEC1-HIF-1 α	(Wang X. et al., 2017)

Inhibitors of HIF-1 Transcriptional Activity

So far, several herbal medicines have been shown to inhibit tumor angiogenesis through downregulating HIF-1 activation by inhibiting its transcriptional activity. Shiau et al. explored the underlying mechanisms of *S. barbata* on regulating HIF-1-dependent

expression of VEGF. Hypoxia induces angiogenesis by upregulating VEGF expression. However, after treatment with *S. barbata*, the expression of VEGF was downregulated in lung cancer cells. In addition, *S. barbata* inhibited the proliferation and migration of endothelial cells under a hypoxic environment. *S. barbata*

suppressed the transcriptional activity of HIF-1 α and promoted the phosphorylation of the upstream signal molecule AKT (Shiau et al., 2014). Triptolide is the major active compound in traditional Chinese medicine (TCM) herb *Tripterygium wilfordii* Hook F. Triptolide exhibits significant chemotherapeutic effects against cancer based on its antiangiogenesis and drug resistance circumvention activities. Various biological molecules suppressed by triptolide have been identified as its potential targets. Triptolide could downregulate the transcriptional activity of HIF-1 α and further decrease the transcriptional activity of its target genes including VEGF (Zhou et al., 2010).

Inhibitors of Signal Transduction Pathways

Several Chinese herbal medicines have been reported to act on different signaling pathways to indirectly regulate HIF-1 activation and exert antiangiogenic effects in cancer treatment. Imperatorin is an active natural furocoumarin ingredient from *Angelica dahurica*. Mi et al. (2017) reported that imperatorin administration could inhibit tumor growth and tumor angiogenesis *in vivo* and *in vitro* and downregulate HIF-1 α activation by targeting the mTOR/p70S6K/4E-BP1 and MAPK pathways. 5,3'-Dihydroxy-6,7,4'-trimethoxyflavone (DHTMF) is one of the main ingredients of *Vitex rotundifolia*. Kim et al. (2015) showed that DHTMF could inhibit angiogenesis and induce apoptosis by decreasing the expression levels of HIF-1 α and VEGF *via* the Akt/mTOR pathway in cancer cells. Kim et al. (2017) reported that diphyllin, a natural component of traditional Chinese medicine, could regulate the mTORC1/HIF-1 α /VEGF pathway in the treatment of esophageal cancer (Kim et al.,

2017). Curcumin is an active molecule isolated from the dried rhizome of *Curcuma longa*. Wang D. et al. (2017) found that curcumin could downregulate the HIF-1 α , VEGF, DEC1, and STAT3 signal transduction pathways in the treatment of gastric cancer. Garcinol (camboginol) is a natural polyisoprenylated benzophenone isolated from dried rind of the *Garcinia indica*. Ranjbarnejad et al. (2017a) found that garcinol could inhibit VEGF, MMP2/9, and CXCR4 expression by targeting the mPGES-1/PGE2/HIF-1 α pathway. Herbal medicines targeting signal transduction pathways are reported in Table 2.

ACTIVATION OF HIF-1-DEPENDENT ANGIOGENESIS IN ISCHEMIC STROKE

Stroke is one of the major causes of death and long-term disability worldwide. About 50% of patients who have suffered from a stroke live less than 1 year (Zhang and Chopp, 2009). There are two main types of stroke: ischemic and hemorrhagic. Ischemic strokes account for about 85% of all strokes, which is caused by a sudden halt of blood supply to the brain tissue because of ischemia and can result in permanent brain injury (Senior, 2001). The thrombotic or embolic occlusion of a cerebral artery will lead to irreversible neuronal cell death and further induce serious brain injury at the core of the infarct immediately. In addition, the secondary injury will result in the expansion of the area of brain injury, which can continue for an extended period after the first ischemic attack (Chopp and Li, 2002). Thus, reestablishment of the functional cerebral microvasculature network will improve regional blood supply and promote stroke recovery.

TABLE 3 | Herbal Medicines and Their Molecular Targets Regulated by the HIF-1 Pathway in Ischemic Stroke.

Herb Medicines	Molecular Targets	Reference
Activators of HIF-1 mRNA and/or protein expression		
Total flavonoid extracts	HIF-1 α protein expression	(He et al., 2018)
MLC901 (herbal extracts)	HIF-1 α protein expression	(Gandin et al., 2016)
<i>Nigella sativa</i> (NS)	HIF-1 α mRNA expression	(Soleimannejad et al., 2017)
Flos Farfarae	HIF-1 α protein expression	(Hwang et al., 2018)
Xue-Fu-Zhu-Yu decoction	HIF-1 α protein expression	(Lee et al., 2011)
Bu Yang Huan Wu decoction	HIF-1 α mRNA and protein expression	(Chen Z. et al., 2018)
Taohong Siwu decoction	HIF-1 α protein expression	(Yen et al., 2014)
Xing-Nao-Jing	HIF-1 α protein expression	(Chen Y. et al., 2018)
Naotai recipe	HIF-1 α mRNA and protein expression	(Chen et al., 2014)
Berberine	HIF-1 α protein expression	(Zhang et al., 2012)
trans-Resveratrol	HIF-1 α mRNA and protein expression	(Agrawal et al., 2013)
Ginsenoside	HIF-1 α protein expression	(Gao et al., 2018)
Xanthohumol	HIF-1 α protein expression	(Yen et al., 2012)
Puerarin	HIF-1 α protein expression	(Chang et al., 2009)
Galangin	HIF-1 α mRNA expression	(Wu et al., 2015)
Activators of signal transduction pathways		
Catalpol and puerarin	PI3K-AKT-mTOR, ERK	(Liu et al., 2017)
Hinokitiol	PI3K-AKT	(Jayakumar et al., 2013)
Salidroside	PI3K-AKT	(Wei et al., 2017)
Silibinin	AKT-mTOR	(Wang et al., 2012)
Andrographolide	PI3K-AKT	(Chen et al., 2011)
Ginkgolide K (GK)	JAK2-STAT3	(Chen M. et al., 2018)
Shengui Sansheng San (SSS)	AKT-mTOR	(Liu B. et al., 2018)
Huang-Lian-Jie-Du-Tang	PI3K-AKT	(Zhang et al., 2014b)

Angiogenesis is a fundamental pathological process in malignant tumor growth and development. However, it may also occur as an advantageous defense response against hypoxia in ischemic stroke by improving blood supply to the brain tissue. Previous research has shown that angiogenesis is positively correlated to the survival rate of ischemic stroke patients, indicating that regulation of the neovascular growth in the ischemic brain could be a pivotal target for ischemic stroke treatment. Numerous studies have shown that the HIF-1 signaling pathway is likely involved in promoting angiogenesis after ischemic stroke in the brain (Zhang et al., 2011). As a transcription factor in response to hypoxia, HIF-1 activity is increased in brains after ischemic attacks. In 1996, it was first reported that both subunit mRNAs of HIF-1 were upregulated in the brains of mice or rats when they were exposed to a hypoxic environment for 30 to 60 min (Jiang et al., 1996). Another study showed that HIF-1 α expression was dramatically increased in the cerebral cortex of a rat after 60 min of recovery from cardiac arrest and remained boosted for more than 10 h. In addition, HIF-1 α mRNA expression was fortified after focal ischemia in rat brain tissue. The increase was detected 8 h after the onset of ischemia and further elevated at 20 and 25 h (Zaman et al., 1999). These results demonstrate that the activity of HIF-1 is increased in ischemic brains and that the level of HIF-1 α expression is heterogeneous. It has been reported that the HIF-1-mediated VEGF/Notch1 signaling pathway plays a crucial role in the development of angiogenesis in the ischemic brain. Apart from VEGF signaling, other complex mechanisms may also take part in HIF-1-mediated angiogenesis regulation after ischemic stroke. The expressions of angiogenesis-related genes such as the endothelin-1 (ET1), adrenomedullin (ADM), α 1B-adrenergic receptor, nitric oxide synthase, Ang-2, stromal-derived growth factor-1 (SDF-1), PDGF-B, PIGF, and heme oxygenase-1 (HO-1) are also modulated by HIF-1 (Weih et al., 1999; Zhang et al., 2007; Yeh et al., 2008). In addition, HIF-1 mediated the regulation of collagen prolyl hydroxylase, MMPs, and plasminogen activator receptor and inhibitor (PAI) expression, which further modulates matrix metabolism and vascular maturation in the ischemic brain (Zou et al., 2018).

Because of the potentially pivotal roles in promoting angiogenesis by HIF-1 after ischemic stroke, it has been recommended that upregulation of HIF-1 activity is a highly promising therapeutic strategy for ischemic brain injury. Thus, the mechanism of HIF-1-induced angiogenesis in ischemic cerebral tissue has drawn much attention and is under extensive exploration. Currently, the only FDA-approved therapy for focal occlusive ischemia in the brain is the administration of the thrombolytic agent tissue plasminogen activator (tPA), which may have the risk of bleeding complications (Ohsawa et al., 2005). Thus, it is imperative to develop additional approaches to enhance therapeutic safety in ischemic stroke treatment. In recent years, several studies have raised great interest on the role of HIF-1 activation in the prognosis of ischemic stroke and whether upregulation of HIF-1 could benefit this disease. Therapeutic activation of HIF-1 applied before the ischemic stress or in the peri-ischemic period may theoretically enhance the natural response of angiogenesis in ischemic stroke patients. Some strategies have been used successfully on experimental

activation of HIF-1 in ischemic disease animal models. For example, knocking out the central ODD domain will promote the activity of HIF-1 α . The expression of such an HIF-1 α transgenic protein in mouse models leads to significant activation of HIF-1 transcriptional targets and angiogenesis (Lin-Holderer et al., 2016). In addition, those neovessels are not leaky, and the intensive vascularity will not induce edema. This result contrasts with that of another study of VEGF therapy wherein edema is frequently detected and demonstrates that HIF-1 activation might keep away from this potential side effect in ischemic disease treatment (Ryou et al., 2015). Other studies have tried to use genetic therapy targeting to activate HIF-1 in the rabbit hind limb ischemia model and rat myocardial infarction model; these therapies improved angiogenesis and increased blood flow to the ischemic area (Li et al., 2016). Another focus on improving HIF-1-induced angiogenesis is suppressing the degradation of HIF-1 α . For example, a macrophage-derived peptide called PR39 can interact with the proteasome and inhibit HIF degradation. Animal experiments have confirmed that PR39 treatment can improve peri-infarct angiogenesis in ischemic cardiac tissue (Hao et al., 2009). Besides using proteasome inhibitors, overexpression of peptides corresponding to the VHL-binding prolyl hydroxylation sites in HIF-1 also inhibits the degradation process of HIF-1 α and further enhances angiogenesis in ischemic tissue. Another combined treatment with transgenic stem cells was applied in ischemic stroke rats. Rat bone marrow-derived mesenchymal stem cells were transfected with adenovirus containing HIF-1 α genes with mutations at Asn 803 and Pro 564 sites, which prevent HIF-1 degradation. The cells with transgenic genes were injected into the cerebral artery occlusion of rats. After a week, improved angiogenesis and reduced infarction in brain tissue were observed; the rats' ischemic stroke symptoms were also relieved (Li C. et al., 2017). HIF prolyl 4-hydroxylase domain proteins (PHD) are among the most pivotal inhibitors of the HIF-1 pathway. Suppression of the HIF-1 PHD by small molecular agents or genetic therapy may also inhibit HIF-1 degradation and activate the downstream gene's transcriptional activity (Liu Y. et al., 2018). One study verified that PHD ablation in neurons improved ischemic stroke recovery in mice through endogenous adaptive angiogenesis by activation of the HIF-VEGF signaling (Mi et al., 2018). In general, the activation of HIF-1-dependent angiogenesis may provide therapeutic potential in ischemic and hypoxic cerebrovascular diseases. The central role of HIF-1 in the modulation of the hypoxia-correlated pathway has provided a promising approach for the development of novel therapeutic agents for ischemic stroke.

CHINESE MEDICINES MEDIATE ANGIOGENIC FACTORS TO PROMOTE ANGIOGENESIS BY REGULATING THE HIF-1 PATHWAY AFTER ISCHEMIC STROKE

Herbal medicines, including herbal formulas, herbal extract, and chemical ingredients, have been widely used in the treatment

of cardiovascular and cerebrovascular diseases for centuries because of reduced side effects (Fan et al., 2017). Previous studies indicated that herbal medicines are often used as an alternative therapy for prevention, treatment, and rehabilitation interventions of ischemic stroke (Table 3). As an important component of cerebral angiogenesis in patients with ischemic stroke, there has been great attention in developing activators targeting the HIF-1 pathway. HIF-1 activation can be induced by regulation of one of the following pathways: HIF-1 mRNA expression, HIF-1 protein expression, or signal transduction pathways. Figure 3 summarizes the treatment of ischemic stroke by herbal medicines that regulate HIF-1 α to promote angiogenesis through the different mechanisms.

Activators of HIF-1 mRNA and/or Protein Expression

Several Chinese herbal medicines that target upregulating HIF-1 mRNA and/or protein expression have proangiogenic effects in ischemic stroke treatment. Ginsenoside, a major active ingredient of ginseng, has been demonstrated to be effective in the treatment of acute ischemic stroke. Gao et al. (2018) found that ginsenoside has therapeutic effects on cerebral ischemia and hypoxic injury through the HIF-1 α -VEGF pathway in an oxygen-glucose deprivation/reperfusion (OGD/R) model of neural stem cells (NSCs). Xanthohumol, an ingredient of beer, is the principal prenylated flavonoid in hops (*Humulus lupulus* L). Yen et al. reported that xanthohumol-induced neuroprotection is associated with many factors such as HIF-1 α , iNOS, and TNF- α . He et al. established a rat model of transient middle cerebral artery occlusion (tMCAO), followed by 24 h of reperfusion (Yen et al., 2012). Administration of total flavonoid extracts (TFC) could improve neurological deficits, reduce infarct volume, and promote angiogenesis by increasing the expression of HIF-1 α , VEGF, Ang-1, DLL4, Notch1, and CD31 (He et al., 2018). MLC901, an herbal extract preparation modified from the TCM herbal formula, has been proven to have neuroprotective and neurorestorative properties in preclinical models of stroke, traumatic brain injury, and global cerebral ischemia. Gandin et al. (2016) found that 5-week pretreatment with MLC901 in MCAO-induced cerebral ischemia mouse models could regulate the expression of HIF-1 α and its downstream targets, such as VEGF, Ang-1, and Ang-2. Chen et al. showed that administration of TCM formula Bu Yang Huan Wu (BYHW) decoction decreased cerebral edema, the neurological deficit score, and brain infarct volume in a rat model of cerebral ischemia/reperfusion (I/R) injury. Furthermore, BYHW treatment markedly decreased the mRNA and protein levels of HIF-1 α and VEGF compared with those of the model treatment (Chen Z. et al., 2018). *Nigella arvensis* (NS) is one of the widely used herbs from the family ranunculaceae. Soleimannejad et al. (2017) found that the *N. arvensis* extract was associated with increased expression of VEGF and HIF-1 α , markers of brain angiogenesis after total cerebral ischemia in rats. Puerarin, a major isoflavonoid isolated from the Chinese medicinal herb *Radix puerariae* (kudzu root), is widely used for treating cardiovascular disease in clinics. Chang et al. (2009) used a tMCAO rat model to study the effects of puerarin.

Administration of puerarin inhibited the expression of HIF-1 α , TNF- α , iNOS, caspase-3, and many factors, and it may be an ideal therapeutic measure after ischemia-reperfusion brain injury. Xue-Fu-Zhu-Yu decoction (XFZYD) is a traditional Chinese medicine formula widely used in cardiovascular diseases. Lee et al. found that XFZYD administration slightly reduced infarct volume compared with that of solvent-treated rats. However, the combination of XFZYD and recombinant tissue plasminogen activator (rt-PA) significantly reduced the infarct volume in cerebral ischemic areas. In addition, rt-PA administration significantly reduced the expression of TNF- α and iNOS but did not decrease the expression of HIF-1 α or caspase-3, whereas XFZYD administration significantly reduced the expression of all these proteins in the ischemic region. In addition, XFZYD administration significantly enhanced the reduction of rt-PA-mediated TNF- α , iNOS, HIF-1 α , and active caspase-3 expression (Lee et al., 2011). Galangin, a commonly used antioxidant, is a natural flavonoid derived from the rhizome of *Alpinia officinarum* Hance. Wu et al. (2015) showed that galangin could promote angiogenesis and vascular remodeling to improve neurological function scores and the cerebral infarct area by upregulating the Wnt/ β -catenin and HIF-1 α /VEGF signaling pathway in a MCAO rat model. Herbal medicines targeting HIF-1 mRNA and/or protein expression are provided in Table 2.

Activators of Signal Transduction Pathways

Several studies have shown that Chinese herbal medicines can also target different signal transduction pathways to upregulate HIF-1-induced angiogenesis. Huang-Lian-Jie-Du-Tang (HLJDT) is a classical heat-clearing and detoxicating formula of traditional Chinese medicine. Zhang et al. found that HLJDT preconditioning in the MCAO rat model could decrease the cerebral infarction volume, neurological deficit score, and cerebral water content. In addition, HLJDT preconditioning in cerebral cortical neurons *in vitro* under oxygen and glucose deprivation (OGD) could increase HIF-1 α , VEGF, and erythropoietin (EPO) expression levels and activation of the PI3K/AKT signaling pathway (Zhang et al., 2014b). Shengui Sansheng San (SSS), a traditional Chinese herbal formula, has been used for stroke for more than 300 years. B. Liu et al. (2018) showed that SSS could activate AKT/mTOR/HIF-1 α and ERK1/2 signals to facilitate VEGF production, resulting in angiogenesis after stroke in the rat MCAO model. Ginkgolide K (GK) is an extract isolated from the leaves of *Ginkgo biloba*. Chen et al. have used a tMCAO mouse model to verify the pharmacological properties of GK. GK treatment could significantly increase the expressions of HIF-1 α and VEGF in the tMCAO model. In the OGD/R model of bEnd.3 cells, GK-induced upregulation of HIF-1 α and VEGF could be eliminated by JAK2/STAT3 inhibitor AG490 (Chen et al., 2018). Andrographolide is a bicyclic diterpenoid lactone from the leaves of *Andrographis paniculata* (Acanthaceae). Chen et al. suggested that andrographolide could ameliorate brain injury in ischemic stroke by PI3K/AKT-dependent activation of the NF- κ B and further activation of HIF-1 α pathways *in vivo* and *in vitro* (Chern et al., 2011). As a conclusion, the herbal medicines

targeting HIF-1 signal transduction pathways are provided in Table 2.

CONCLUSIONS AND FUTURE DIRECTIONS

HIF-1-induced angiogenesis has been involved in numerous pathological conditions, and it may be harmful or beneficial depending on the types of specific disease. Since the 1970s, the exploration on angiogenesis has sparked hopes in providing novel therapeutic approaches in multiple diseases with high mortality rates, such as cancers and ischemic stroke. Depending on different types of diseases and the expected treatment effects, angiogenesis-targeted therapies have different approaches. Generally, the clinical application of angiogenesis can be classified into two different strategies: antiangiogenesis (cancer) and proangiogenesis (ischemic stroke). The induction of angiogenesis for therapeutic purposes in ischemic stroke can be directly stimulated by various angiogenic factors, such as PlGF, VEGF, PDGF, and FGF, some of which have been applied in preclinical and clinical studies. However, treatments only using proangiogenic factors to induce angiogenesis were proven to be insufficient in ischemic disease; thus, novel treatments that can stabilize neovascularization with high-efficiency are required for better therapeutic effects. Therefore, HIF-1-induced angiogenesis may be a promising strategy for ischemic cerebrovascular disease. HIF-1 activation in ischemic cerebrovascular disease leads to a more mature and stable vascular formation compared with that of traditional proangiogenic factor therapy, wherein neovascularization tends to be leaky. Instead of proangiogenesis in ischemic stroke therapy, cancer treatments are based on suppression of angiogenesis for inhibiting tumor growth and metastasis. Current therapies are focused on suppressing VEGF activity, such as sunitinib (VEGFR2 inhibitor) and bevacizumab (VEGF inhibitor) target therapy. Because of the pivotal role of the HIF-1 pathway in modulating the activation of various proangiogenic factors in cancers, HIF-1 has been considered as a promising target for developing novel anticancer agents. Suppression of HIF-1-dependent angiogenesis involves the modulation of HIF-1 activity by regulating HIF-1 α transcription and protein translation, HIF-1 α DNA binding, HIF-1 α and HIF-1 β dimerization, and HIF-1 degradation. Considering the profound impact of HIF-1 on cancer progression and the unsatisfactory efficacy of current treatment protocols, several clinical trials are being conducted with potential antiangiogenesis agents that involve protein degradation, downregulation, or inactivation of HIF-1. It is noteworthy that, within a single herb concoction, sometimes we can find both inhibitors and activators of HIF-1, which will complicate the use of herbal medicines under clinical conditions. For example, ginsenoside Rg3 and ginsenoside Rg1 are both natural triterpenoid saponins extracted from red ginseng. Previous studies showed that ginsenoside Rg3 could inhibit tumor angiogenesis by decreasing the expression of

HIF-1 in various cancers, whereas ginsenoside Rg1 might inhibit myocardial ischemia and reperfusion injury by activating HIF-1 (Chen et al., 2010; Yuan et al., 2019).

With a long history of more than 2,000 years of clinical use, Chinese herbal medicine is emerging as a complementary and alternative choice for its multitargeted, multileveled, and coordinated intervention effects against complex disorders, such as cancer and ischemic stroke. Research results from many *in vitro* and *in vivo* studies have demonstrated that several Chinese herbal formulations, herbs, or herbal compounds can induce or inhibit angiogenesis through multiple cellular mechanisms. Numerous preclinical studies have provided supportive evidence for using Chinese herbal medicines as a novel antiangiogenesis therapy for cancer or proangiogenesis therapy for ischemic stroke by targeting the HIF-1 pathway. However, the overall scientific evidence to back the application of Chinese herbal medicines for the management of cancer and ischemic stroke remains limited, and the results of these researches are sometimes contradictory and inconclusive. The underlying reasons for these inconsistencies include the complex chemical and pharmacological properties of Chinese herbal medicines and the interactions between the multiple bioactive ingredients of Chinese herbal medicines. More researches are needed to gain a better understanding of the dual effects of Chinese herbal medicines on angiogenesis in cancer and ischemic stroke treatment. In addition, despite the long history of Chinese herbal medicines in the treatment of cancer and ischemic stroke, well-controlled clinical studies with herbal medicinal products used for treating these diseases are still limited. More rigorously designed, controlled, randomized, international, multicenter clinical trials are urgently required for further validating Chinese herbal medicine efficacy in cancer and ischemic stroke treatment. Finally, as a double-edged sword, the important role of HIF-1 in angiogenesis should be considered as a promising target for treating cancer or ischemic stroke. The possible side effects and potential risk of angiogenesis-related complications by Chinese herbal medicines should also be considered when applying the HIF-1 target strategy for management of ischemic stroke and cancer.

AUTHOR CONTRIBUTIONS

MH and HS wrote the manuscript. NW, H-YT, QW, and YF revised the manuscript.

FUNDING

This work was supported by the National Natural Science Foundation of China (No. 81673627), Guangzhou Science Technology and Innovation Commission Research Projects (201805010005), Research Grant Council, HKSAR (Project code: RGC GRF 17152116), and Commissioner for Innovation Technology, HKSAR (Project code: ITS/091/16FX).

REFERENCES

- Agrawal, M., Kumar, V., Singh, A. K., Kashyap, M. P., Khanna, V. K., Siddiqui, M. A., et al. (2013). trans-Resveratrol protects ischemic PC12 Cells by inhibiting the hypoxia associated transcription factors and increasing the levels of antioxidant defense enzymes. *ACS Chem. Neurosci.* 4 (2), 285–294. doi: 10.1021/cn300143m
- Al-Anazi, A., Parhar, R., Saleh, S., Al-Hijailan, R., Inglis, A., Al-Jufan, M., et al. (2018). Intracellular calcium and NF- κ B regulate hypoxia-induced leptin, VEGF, IL-6 and adiponectin secretion in human adipocytes. *Life Sci.* 212, 275–284. doi: 10.1016/j.lfs.2018.10.014
- Aldo, P., and Elisabetta, C. (2018). Role of HIF-1 in cancer progression: novel insights. A review. *Curr. Mol. Med.* 18 (6), 343–351. doi: 10.2174/1566524018666181109121849.
- Ambrosini, S., Sarchielli, E., Comeglio, P., Porfiro, B., Gallina, P., Morelli, A., et al. (2015). Fibroblast growth factor and endothelin-1 receptors mediate the response of human striatal precursor cells to hypoxia. *Neuroscience* 289, 123–133. doi: 10.1016/j.neuroscience.2014.12.073
- Bae, M. K., Kim, S. H., Jeong, J. W., Lee, Y. M., Kim, H. S., Kim, S. R., et al. (2006). Curcumin inhibits hypoxia-induced angiogenesis via down-regulation of HIF-1. *Oncol. Rep.* 15 (6), 1557–62. doi: 10.3892/or.15.6.1557
- Ban, H. S., Kim, B. K., Lee, H., Kim, H. M., Harmalkar, D., Nam, M., et al. (2017). The novel hypoxia-inducible factor-1 α inhibitor IDF-11774 regulates cancer metabolism, thereby suppressing tumor growth. *Cell Death Dis.* 8 (6), e2843. doi: 10.1038/cddis.2017.235
- Belaidi, E., Morand, J., Gras, E., Pepin, J. L., and Godin-Ribuot, D. (2016). Targeting the ROS-HIF-1-endothelin axis as a therapeutic approach for the treatment of obstructive sleep apnea-related cardiovascular complications. *Pharmacol. Ther.* 168, 1–11. doi: 10.1016/j.pharmthera.2016.07.010
- Beppu, K., Nakamura, K., Linehan, W. M., Rapisarda, A., and Thiele, C. J. (2005). Topotecan blocks hypoxia-inducible factor-1 α and vascular endothelial growth factor expression induced by insulin-like growth factor-I in neuroblastoma cells. *Cancer Res.* 65 (11), 4775–4781. doi: 10.1158/0008-5472.CAN-04-3332
- Berlow, R. B., Dyson, H. J., and Wright, P. E. (2017). Hypersensitive termination of the hypoxic response by a disordered protein switch. *Nature* 543 (7645), 447–451. doi: 10.1038/nature21705
- Bluff, J. E., Menakuru, S. R., Cross, S. S., Higham, S. E., Balasubramanian, S. P., Brown, N. J., et al. (2009). Angiogenesis is associated with the onset of hyperplasia in human ductal breast disease. *Br. J. Cancer* 101 (4), 666–672. doi: 10.1038/sj.bjc.6605196
- Bohonowych, J. E., Peng, S., Gopal, U., Hance, M. W., Wing, S. B., Argraves, K. M., et al. (2011). Comparative analysis of novel and conventional Hsp90 inhibitors on HIF activity and angiogenic potential in clear cell renal cell carcinoma: implications for clinical evaluation. *BMC Cancer* 11, 520. doi: 10.1186/1471-2407-11-520
- Brown, C. (2016). Targeted therapy: an elusive cancer target. *Nature* 537 (7620), S106–108. doi: 10.1038/537S106a
- Carroll, V. A., and Ashcroft, M. (2006). Role of hypoxia-inducible factor (HIF)-1 α versus HIF-2 α in the regulation of HIF target genes in response to hypoxia, insulin-like growth factor-I, or loss of von Hippel-Lindau function: implications for targeting the HIF pathway. *Cancer Res.* 66 (12), 6264–6270. doi: 10.1158/0008-5472.CAN-05-2519
- Chang, Y., Hsieh, C. Y., Peng, Z. A., Yen, T. L., Hsiao, G., Chou, D. S., et al. (2009). Neuroprotective mechanisms of puerarin in middle cerebral artery occlusion-induced brain infarction in rats. *J. Biomed. Sci.* 16, 9. doi: 10.1186/1423-0127-16-9
- Chen, Q. J., Zhang, M. Z., and Wang, L. X. (2010). Gensenoside Rg3 inhibits hypoxia-induced VEGF expression in human cancer cells. *Cell Physiol. Biochem.* 26 (6), 849–858. doi: 10.1159/000323994
- Chen, Y., Zhu, H. B., Liao, J., Yi, Y. Q., Wang, G. Z., Tong, L., et al. (2014). [Regulation of naotai recipe on the expression of HIF-1 α /VEGF signaling pathway in cerebral ischemia/reperfusion rats]. *Zhongguo. Zhong. Xi. Yi. Jie. He. Za. Zhi.* 34 (10), 1225–1230.
- Chen, H., Feng, J., Zhang, Y., Shen, A., Chen, Y., Lin, J., et al. (2015). Pien Tze Huang inhibits hypoxia-induced angiogenesis via HIF-1 α /VEGF-A pathway in colorectal cancer. *Evid. Based Complement. Alternat. Med.* 2015, 454279. doi: 10.1155/2015/454279
- Chen, C., Tang, Q., Zhang, Y., Dai, M., Jiang, Y., Wang, H., et al. (2017). Metabolic reprogramming by HIF-1 activation enhances survivability of human adipose-derived stem cells in ischaemic microenvironments. *Cell Prolif.* 50 (5). doi: 10.1111/cpr.12363
- Chen, H., Liu, P., Zhang, T., Gao, Y., Zhang, Y., Shen, X., et al. (2018). Effects of diphyllin as a novel V-ATPase inhibitor on TE-1 and ECA-109 cells. *Oncol. Rep.* 39 (3), 921–928. doi: 10.3892/or.2018.6191
- Chen, M., Zou, W., Chen, M., Cao, L., Ding, J., Xiao, W., et al. (2018). Ginkgolide K promotes angiogenesis in a middle cerebral artery occlusion mouse model via activating JAK2/STAT3 pathway. *Eur. J. Pharmacol.* 833, 221–229. doi: 10.1016/j.ejphar.2018.06.012
- Chen, R., Cai, X., Liu, J., Bai, B., and Li, X. (2018). Sphingosine 1-phosphate promotes mesenchymal stem cell-mediated cardioprotection against myocardial infarction via ERK1/2-MMP-9 and Akt signaling axis. *Life Sci.* 215, 31–42. doi: 10.1016/j.lfs.2018.10.047
- Chen, Y., Sun, Y., Li, W., Wei, H., Long, T., Li, H., et al. (2018). Systems pharmacology dissection of the anti-stroke mechanism for the Chinese traditional medicine Xing-Nao-Jing. *J. Pharmacol. Sci.* 136 (1), 16–25. doi: 10.1016/j.jphs.2017.11.005
- Chen, Z. Z., Gong, X., Guo, Q., Zhao, H., and Wang, L. (2018). Bu Yang Huan Wu decoction prevents reperfusion injury following ischemic stroke in rats via inhibition of HIF-1 α , VEGF and promotion beta-ENaC expression. *J. Ethnopharmacol.* 228, 70–81. doi: 10.1016/j.jep.2018.09.017
- Cheng, Z., Fu, J., Liu, G., Zhang, L., Xu, Q., and Wang, S. Y. (2018). Angiogenesis in JAK2 V617F positive myeloproliferative neoplasms and ruxolitinib decrease VEGF, HIF-1 α and JAK2 V617F positive cells. *Leuk. Lymphoma.* 59 (1), 196–203. doi: 10.1080/10428194.2017.1324155
- Chern, C. M., Liou, K. T., Wang, Y. H., Liao, J. F., Yen, J. C., and Shen, Y. C. (2011). Andrographolide inhibits PI3K/AKT-dependent NOX2 and iNOS expression protecting mice against hypoxia/ischemia-induced oxidative brain injury. *Planta. Med.* 77 (15), 1669–1679. doi: 10.1055/s-0030-1271019
- Chopp, M., and Li, Y. (2002). Treatment of neural injury with marrow stromal cells. *Lancet Neurol.* 1 (2), 92–100. doi: 10.1016/S1474-4422(02)00040-6
- Copple, B. L. (2010). Hypoxia stimulates hepatocyte epithelial to mesenchymal transition by hypoxia-inducible factor and transforming growth factor-beta-dependent mechanisms. *Liver Int.* 30 (5), 669–682. doi: 10.1111/j.1478-3231.2010.02205.x
- Das, L., and Vinayak, M. (2014). Long term effect of curcumin in regulation of glycolytic pathway and angiogenesis via modulation of stress activated genes in prevention of cancer. *PLoS One* 9 (6), e99583. doi: 10.1371/journal.pone.0099583
- De Francesco, E. M., Maggiolini, M., and Musti, A. M. (2018). Crosstalk between Notch, HIF-1 α and GPER in Breast Cancer EMT. *Int. J. Mol. Sci.* 19 (7), 2011. doi: 10.3390/ijms19072011
- Dong, H., Lin, W., Wu, J., and Chen, T. (2010). Flavonoids activate pregnane x receptor-mediated CYP3A4 gene expression by inhibiting cyclin-dependent kinases in HepG2 liver carcinoma cells. *BMC Biochem.* 11, 23. doi: 10.1186/1471-2091-11-23
- Fan, X. X., Li, F., Lv, Y. N., Zhang, Y., Kou, J. P., and Yu, B. Y. (2017). An integrated shotgun proteomics and bioinformatics approach for analysis of brain proteins from MCAO model using serial affinity chromatograph with four active ingredients from Shengmai preparations as ligands. *Neurochem. Int.* 103, 45–56. doi: 10.1016/j.neuint.2016.12.017
- Forbes, A., Anoopkumar-Dukie, S., Chess-Williams, R., and McDermott, C. (2016). Relative cytotoxic potencies and cell death mechanisms of alpha1-adrenoceptor antagonists in prostate cancer cell lines. *Prostate* 76 (8), 757–766. doi: 10.1002/pros.23167
- Fortenberry, G. W., Sarathy, B., Carraway, K. R., and Mansfield, K. D. (2018). Hypoxic stabilization of mRNA is HIF-independent but requires mtROS. *Cell Mol. Biol. Lett.* 23, 48. doi: 10.1186/s11658-018-0112-2
- Freise, C., Ruehl, M., Erben, U., Neumann, U., Seehofer, D., Kim, K. Y., et al. (2011). A hepatoprotective *Lindera obtusiloba* extract suppresses growth and attenuates insulin like growth factor-1 receptor signaling and NF- κ B activity in human liver cancer cell lines. *BMC Complement. Alternat. Med.* 11, 39. doi: 10.1186/1472-6882-11-39
- Fu, L., Chen, W., Guo, W., Wang, J., Tian, Y., Shi, D., et al. (2013). Berberine targets AP-2/hTERT, NF- κ B/COX-2, HIF-1 α /VEGF and cytochrome-c/caspase signaling to suppress human cancer cell growth. *PLoS One* 8 (7), e69240. doi: 10.1371/journal.pone.0069240
- Fu, P., Du, F., Chen, W., Yao, M., Lv, K., and Liu, Y. (2014). Tanshinone IIA blocks epithelial-mesenchymal transition through HIF-1 α downregulation, reversing hypoxia-induced chemotherapy resistance in breast cancer cell lines. *Oncol. Rep.* 31 (6), 2561–2568. doi: 10.3892/or.2014.3140

- Gandin, C., Widmann, C., Lazdunski, M., and Heurteaux, C. (2016). MLC901 favors angiogenesis and associated recovery after ischemic stroke in mice. *Cerebrovasc. Dis.* 42 (1–2), 139–154. doi: 10.1159/000444810
- Gao, J., Bai, H., Li, Q., Li, J., Wan, F., Tian, M., et al. (2018). *In vitro* investigation of the mechanism underlying the effect of ginsenoside on the proliferation and differentiation of neural stem cells subjected to oxygen-glucose deprivation/reperfusion. *Int. J. Mol. Med.* 41 (1), 353–363. doi: 10.3892/ijmm.2017.3253
- Geng, L., Fan, J., Gao, Q. L., Yu, J., and Hua, B. J. (2016). Preliminary study for the roles and mechanisms of 20(R)-ginsenoside Rg3 and PEG-PLGA-Rg3 nanoparticles in the Lewis lung cancer mice. *Beijing Da. Xue. Xue. Bao. Yi. Xue. Ban.* 48 (3), 496–501.
- Gramley, F., Lorenzen, J., Jedamzik, B., Gatter, K., Koellensperger, E., Munzel, T., et al. (2010). Atrial fibrillation is associated with cardiac hypoxia. *Cardiovasc. Pathol.* 19 (2), 102–111. doi: 10.1016/j.carpath.2008.11.001
- Guo, D., Murdoch, C. E., Liu, T., Qu, J., Jiao, S., Wang, Y., et al. (2018). Therapeutic angiogenesis of Chinese herbal medicines in ischemic heart disease: a review. *Front. Pharmacol.* 9, 428. doi: 10.3389/fphar.2018.00428
- Han, X., Sun, S., Zhao, M., Cheng, X., Chen, G., Lin, S., et al. (2014). Celastrol stimulates hypoxia-inducible factor-1 activity in tumor cells by initiating the ROS/Akt/p70S6K signaling pathway and enhancing hypoxia-inducible factor-1alpha protein synthesis. *PLoS One* 9 (11), e112470. doi: 10.1371/journal.pone.0112470
- Hao, Y. W., Sun, L. J., Liu, Y., Wang, Q. Y., and Yang, G. X. (2009). [Secretory expression of PR39 following adeno-associated viral-encoding fusion gene transfer induces angiogenesis in hypoxia chick embryo]. *Zhonghua. Xin. Xue. Guan. Bing. Za. Zhi.* 37 (8), 746–749.
- He, Z., Chen, A. Y., Rojanasakul, Y., Rankin, G. O., and Chen, Y. C. (2016). Gallic acid, a phenolic compound, exerts anti-angiogenic effects via the PTEN/AKT/HIF-1alpha/VEGF signaling pathway in ovarian cancer cells. *Oncol. Rep.* 35 (1), 291–297. doi: 10.3892/or.2015.4354
- He, Q., Li, S., Li, L., Hu, F., Weng, N., Fan, X., et al. (2018). Total Flavonoids in Caragana (TFC) promotes angiogenesis and enhances cerebral perfusion in a rat model of ischemic stroke. *Front. Neurosci.* 12, 635. doi: 10.3389/fnins.2018.00635
- Hong, M., Wang, N., Tan, H. Y., Tsao, S. W., and Feng, Y. (2015). MicroRNAs and Chinese medicinal herbs: new possibilities in cancer therapy. *Cancers (Basel)* 7 (3), 1643–1657. doi: 10.3390/cancers7030855
- Hong, M., Tan, H. Y., Li, S., Cheung, F., Wang, N., Nagamatsu, T., et al. (2016). Cancer stem cells: the potential targets of Chinese medicines and their active compounds. *Int. J. Mol. Sci.* 17 (6), 893. doi: 10.3390/ijms17060893
- Hou, F., Li, W., Shi, Q., Li, H., Liu, S., Zong, S., et al. (2016). Yi Ai Fang, a traditional Chinese herbal formula, impacts the vasculogenic mimicry formation of human colorectal cancer through HIF-1alpha and epithelial mesenchymal transition. *BMC Complement. Altern. Med.* 16 (1), 428. doi: 10.1186/s12906-016-1419-z
- Hsu, H. W., Wall, N. R., Hsueh, C. T., Kim, S., Ferris, R. L., Chen, C. S., et al. (2014). Combination antiangiogenic therapy and radiation in head and neck cancers. *Oral Oncol.* 50 (1), 19–26. doi: 10.1016/j.oraloncology.2013.10.003
- Hu, X. X., Zhang, Q. H., and Qi, C. (2012). Anti-angiogenic effects of zengmian Yiliu granule on ovarian carcinoma xenograft. *Zhongguo. Zhong. Xi. Yi. Jie. He. Za. Zhi.* 32 (7), 970–974.
- Hua, H., Zhu, Y., and Song, Y. H. (2018). Ruscogenin suppressed the hepatocellular carcinoma metastasis via PI3K/Akt/mTOR signaling pathway. *Biomed. Pharmacother.* 101, 115–122. doi: 10.1016/j.biopha.2018.02.031
- Huang, L., Zhang, Z., Zhang, S., Ren, J., Zhang, R., Zeng, H. et al. (2011). Inhibitory action of Celastrol on hypoxia-mediated angiogenesis and metastasis via the HIF-1alpha pathway. *Int. J. Mol. Med.* 27 (3), 407–415. doi: 10.3892/ijmm.2011.600
- Hwang, J. H., Kumar, V. R., Kang, S. Y., Jung, H. W., and Park, Y. K. (2018). Effects of flower buds extract of *Tussilago farfara* on focal cerebral ischemia in rats and inflammatory response in BV2 microglia. *Chin. J. Integr. Med.* 24 (11), 844–852. doi: 10.1007/s11655-018-2936-4
- Jain, R. K., and Carmeliet, P. (2012). SnapShot: tumor angiogenesis. *Cell* 149 (6), 1408–1408 e1. doi: 10.1016/j.cell.2012.05.025
- Jayakumar, T., Hsu, W. H., Yen, T. L., Luo, J. Y., Kuo, Y. C., Fong, T. H., et al. (2013). Hinokitiol, a natural tropolone derivative, offers neuroprotection from thromboembolic stroke *in vivo*. *Evid. Based Complement. Alternat. Med.* 2013, 840487. doi: 10.1155/2013/840487
- Jia, L. Y., Wu, X. J., Gao, Y., Rankin, G. O., Pigliacampi, A., Bucur, H., et al. (2017). Inhibitory effects of total triterpenoid saponins isolated from the seeds of the tea plant (*Camellia sinensis*) on human ovarian cancer cells. *Molecules* 22 (10), 1649. doi: 10.3390/molecules22101649
- Jiang, B. H., Semenza, G. L., Bauer, C., and Marti, H. H. (1996). Hypoxia-inducible factor 1 levels vary exponentially over a physiologically relevant range of O₂ tension. *Am. J. Physiol.* 271 (4 Pt 1), C1172–1180. doi: 10.1152/ajpcell.1996.271.4.C1172
- Kabei, K., Tateishi, Y., Nozaki, M., Tanaka, M., Shiota, M., Osada-Oka, M., et al. (2018). Role of hypoxia-inducible factor-1 in the development of renal fibrosis in mouse obstructed kidney: special references to HIF-1 dependent gene expression of profibrogenic molecules. *J. Pharmacol. Sci.* 136 (1), 31–38. doi: 10.1016/j.jphs.2017.12.004
- Kang, S. G., Zhou, G., Yang, P., Liu, Y., Sun, B., Huynh, T., et al. (2012). Molecular mechanism of pancreatic tumor metastasis inhibition by Gd@C82(OH)₂₂ and its implication for de novo design of nanomedicine. *Proc. Natl. Acad. Sci. U.S.A.* 109 (38), 15431–15436. doi: 10.1073/pnas.1204600109
- Kaul, D. K., Fabry, M. E., Suzuka, S. M., and Zhang, X. (2013). Antisickling fetal hemoglobin reduces hypoxia-inducible factor-1alpha expression in normoxic sickle mice: microvascular implications. *Am. J. Physiol. Heart Circ. Physiol.* 304 (1), H42–50. doi: 10.1152/ajpheart.00296.2012
- Kim, A., and Ma, J. Y. (2018). Rhaponticin decreases the metastatic and angiogenic abilities of cancer cells via suppression of the HIF1alpha pathway. *Int. J. Oncol.* 53 (3), 1160–1170. doi: 10.3892/ijo.2018.4479
- Kim, K. M., Heo, D. R., Lee, J., Park, J. S., Baek, M. G., Yi, J. M., et al. (2015). 5,3'-Dihydroxy-6,7,4'-trimethoxyflavanone exerts its anticancer and antiangiogenesis effects through regulation of the Akt/mTOR signaling pathway in human lung cancer cells. *Chem. Biol. Interact.* 225, 32–9. doi: 10.1016/j.cbi.2014.10.033
- Kim, M. H., Jeong, Y. J., Cho, H. J., Hoe, H. S., Park, K. K., Park, Y. Y., et al. (2017). Delphinidin inhibits angiogenesis through the suppression of HIF-1alpha and VEGF expression in A549 lung cancer cells. *Oncol. Rep.* 37 (2), 777–784. doi: 10.3892/or.2016.5296
- Kondisetty, S., Menon, K. N., and Pooleri, G. K. (2018). Fibronectin protein expression in renal cell carcinoma in correlation with clinical stage of tumour. *Biomark Res.* 6, 23. doi: 10.1186/s40364-018-0137-8
- Kusumbe, A. P., Ramasamy, S. K., and Adams, R. H. (2014). Coupling of angiogenesis and osteogenesis by a specific vessel subtype in bone. *Nature* 507 (7492), 323–328. doi: 10.1038/nature13145
- Laurenzana, A., Chilla, A., Luciani, C., Peppicelli, S., Biagioni, A., Bianchini, F., et al. (2017). uPA/uPAR system activation drives a glycolytic phenotype in melanoma cells. *Int. J. Cancer* 141 (6), 1190–1200. doi: 10.1002/ijc.30817
- Lee, J. J., Hsu, W. H., Yen, T. L., Chang, N. C., Luo, Y. J., Hsiao, G., et al. (2011). Traditional Chinese medicine, Xue-Fu-Zhu-Yu decoction, potentiates tissue plasminogen activator against thromboembolic stroke in rats. *J. Ethnopharmacol.* 134 (3), 824–830. doi: 10.1016/j.jep.2011.01.033
- Li, J., Fan, Z. Z., Sun, J., and Xu, J. H. (2011). *In vitro* antimetastatic effect of Changweiqing through antiinvasion of hypoxic colorectal carcinoma LoVo cells. *Chin. J. Integr. Med.* 17 (7), 517–24. doi: 10.1007/s11655-011-0785-0
- Li, Y., Liu, X., Zhou, T., Kelley, M. R., Edwards, P., Gao, H., et al. (2014). Inhibition of APE1/Ref-1 redox activity rescues human retinal pigment epithelial cells from oxidative stress and reduces choroidal neovascularization. *Redox. Biol.* 2, 485–494. doi: 10.1016/j.redox.2014.01.023
- Li, G., Shan, C., Liu, L., Zhou, T., Zhou, J., Hu, X., et al. (2015). Tanshinone IIA inhibits HIF-1alpha and VEGF expression in breast cancer cells via mTOR/p70S6K/RPS6/4E-BP1 signaling pathway. *PLoS One* 10 (2), e0117440. doi: 10.1371/journal.pone.0117440
- Li, L., Saliba, P., Reischl, S., Marti, H. H., and Kunze, R. (2016). Neuronal deficiency of HIF prolyl 4-hydroxylase 2 in mice improves ischemic stroke recovery in an HIF dependent manner. *Neurobiol. Dis.* 91, 221–235. doi: 10.1016/j.nbd.2016.03.018
- Li, C., Zhang, B., Zhu, Y., Li, Y., Liu, P., Gao, B., et al. (2017). Post-stroke constraint-induced movement therapy increases functional recovery, angiogenesis, and neurogenesis with enhanced expression of HIF-1alpha and VEGF. *Curr. Neurovasc. Res.* 14 (4), 368–377. doi: 10.2174/1567202614666171128120558
- Li, M. Y., Mi, C., Wang, K. S., Wang, Z., Zuo, H. X., Piao, L. X., et al. (2017). Shikonin suppresses proliferation and induces cell cycle arrest through the inhibition of hypoxia-inducible factor-1alpha signaling. *Chem. Biol. Interact.* 274, 58–67. doi: 10.1016/j.cbi.2017.06.029
- Li, C., Wang, Q., Shen, S., Wei, X., and Li, G. (2018). Oridonin inhibits VEGF-A-associated angiogenesis and epithelial-mesenchymal transition of breast cancer *in vitro* and *in vivo*. *Oncol. Lett.* 16 (2), 2289–2298. doi: 10.3892/ol.2018.8943
- Li, Q. F., Decker-Rockefeller, B., Bajaj, A., and Pumiglia, K. (2018). Activation of ras in the vascular endothelium induces brain vascular malformations and hemorrhagic stroke. *Cell Rep.* 24 (11), 2869–2882. doi: 10.1016/j.celrep.2018.08.025

- Li, X., Ma, S., Yang, P., Sun, B., Zhang, Y., Sun, Y., et al. (2018). Anticancer effects of curcumin on nude mice bearing lung cancer A549 cell subsets SP and NSP cells. *Oncol. Lett.* 16 (5), 6756–6762. doi: 10.3892/ol.2018.9488
- Li, X., Lu, Q., Xie, W., Wang, Y., and Wang, G. (2018). Anti-tumor effects of triptolide on angiogenesis and cell apoptosis in osteosarcoma cells by inducing autophagy via repressing Wnt/beta-Catenin signaling. *Biochem. Biophys. Res. Commun.* 496 (2), 443–449. doi: 10.1016/j.bbrc.2018.01.052
- Lin-Holderer, J., Li, L., Gruneberg, D., Marti, H. H., and Kunze, R. (2016). Fumaric acid esters promote neuronal survival upon ischemic stress through activation of the Nrf2 but not HIF-1 signaling pathway. *Neuropharmacology* 105, 228–240. doi: 10.1016/j.neuropharm.2016.01.023
- Liu, Y. M., Liu, Y. K., Lan, K. L., Lee, Y. W., Tsai, T. H., and Chen, Y. J. (2013). Medicinal fungus *antrodia cinnamomea* inhibits growth and cancer stem cell characteristics of hepatocellular carcinoma. *Evid. Based Complement. Alternat. Med.* 2013, 569737. doi: 10.1155/2013/569737
- Liu, Y., Tang, Q., Shao, S., Chen, Y., Chen, W., and Xu, X. (2017). Lyophilized powder of catalpol and puerarin protected cerebral vessels from ischemia by its anti-apoptosis on endothelial cells. *Int. J. Biol. Sci.* 13 (3), 327–338. doi: 10.7150/ijbs.17751
- Liu, B., Luo, C., Zheng, Z., Xia, Z., Zhang, Q., Ke, C., et al. (2018). Shengui Sansheng San extraction is an angiogenic switch via regulations of AKT/mTOR, ERK1/2 and Notch1 signal pathways after ischemic stroke. *Phytomedicine* 44, 20–31. doi: 10.1016/j.phymed.2018.04.025
- Liu, H., Tang, L., Li, X., and Li, H. (2018). Triptolide inhibits vascular endothelial growth factor-mediated angiogenesis in human breast cancer cells. *Exp. Ther. Med.* 16 (2), 830–836. doi: 10.3892/etm.2018.6200
- Liu, Y., Ran, H., Xiao, Y., Wang, H., Chen, Y., Chen, W., et al. (2018). Knockdown of HIF-1 α impairs post-ischemic vascular reconstruction in the brain via deficient homing and sprouting bmEPCs. *Brain Pathol.* 28 (6). doi: 10.1111/bpa.12628
- Llurba, E., Sanchez, O., Ferrer, Q., Nicolaides, K. H., Ruiz, A., Dominguez, C., et al. (2014). Maternal and foetal angiogenic imbalance in congenital heart defects. *Eur. Heart. J.* 35 (11), 701–707. doi: 10.1093/eurheartj/ehs389
- Lv, X. J., Zhao, L. J., Hao, Y. Q., Su, Z. Z., Li, J. Y., Du, Y. W., et al. (2015). Schisandrin B inhibits the proliferation of human lung adenocarcinoma A549 cells by inducing cycle arrest and apoptosis. *Int. J. Clin. Exp. Med.* 8 (5), 6926–6936.
- Ma, J., Han, L. Z., Liang, H., Mi, C., Shi, H., Lee, J. J., et al. (2014). Celastrol inhibits the HIF-1 α pathway by inhibition of mTOR/p70S6K/eIF4E and ERK1/2 phosphorylation in human hepatoma cells. *Oncol. Rep.* 32 (1), 235–42. doi: 10.3892/or.2014.3211
- Magierowski, M., Magierowska, K., Hubalewska-Mazgaj, M., Surmiak, M., Sliwowski, Z., Wierdak, M., et al. (2018). Cross-talk between hydrogen sulfide and carbon monoxide in the mechanism of experimental gastric ulcers healing, regulation of gastric blood flow and accompanying inflammation. *Biochem. Pharmacol.* 149, 131–142. doi: 10.1016/j.bcp.2017.11.020
- Manresa, M. C., and Taylor, C. T. (2017). Hypoxia inducible factor (HIF) hydroxylases as regulators of intestinal epithelial barrier function. *Cell Mol. Gastroenterol. Hepatol.* 3 (3), 303–315. doi: 10.1016/j.jcmgh.2017.02.004
- Mao, D., Lei, S., Ma, J., Shi, L., Zhang, S., Huang, J., et al. (2016). [Effect of jianpi-jiedu formula on tumor angiogenesis-relevant genes expression in colorectal cancer]. *Zhong. Nan. Da. Xue. Xue. Bao. Yi. Xue. Ban.* 41 (12), 1297–1304.
- Mathew, T., and Sarada, S. K. S. (2018). Intonation of Nrf2 and Hif1- α pathway by curcumin prophylaxis: a potential strategy to augment survival signaling under hypoxia. *Respir. Physiol. Neurobiol.* 258, 12–24. doi: 10.1016/j.resp.2018.09.008
- Matsumoto, L., Hirota, Y., Saito-Fujita, T., Takeda, N., Tanaka, T., Hiraoka, T., et al. (2018). HIF2 α in the uterine stroma permits embryo invasion and luminal epithelium detachment. *J. Clin. Invest.* 128 (7), 3186–3197. doi: 10.1172/JCI98931
- Matteucci, E., Modora, S., Simone, M., and Desiderio, M. A. (2003). Hepatocyte growth factor induces apoptosis through the extrinsic pathway in hepatoma cells: favouring role of hypoxia-inducible factor-1 deficiency. *Oncogene* 22 (26), 4062–4073. doi: 10.1038/sj.onc.1206519
- Maxwell, P. H., Wiesener, M. S., Chang, G. W., Clifford, S. C., Vaux, E. C., Cockman, M. E., et al. (1999). The tumour suppressor protein VHL targets hypoxia-inducible factors for oxygen-dependent proteolysis. *Nature* 399 (6733), 271–275. doi: 10.1038/20459
- Mengozzi, M., Cervellini, I., Villa, P., Erbayraktar, Z., Gokmen, N., Yilmaz, O., et al. (2012). Erythropoietin-induced changes in brain gene expression reveal induction of synaptic plasticity genes in experimental stroke. *Proc. Natl. Acad. Sci. U.S.A.* 109 (24), 9617–9622. doi: 10.1073/pnas.1200554109
- Mi, C., Ma, J., Wang, K. S., Zuo, H. X., Wang, Z., Li, M. Y., et al. (2017). Imperatorin suppresses proliferation and angiogenesis of human colon cancer cell by targeting HIF-1 α via the mTOR/p70S6K/4E-BP1 and MAPK pathways. *J. Ethnopharmacol.* 203, 27–38. doi: 10.1016/j.jep.2017.03.033
- Mi, D. H., Fang, H. J., Zheng, G. H., Liang, X. H., Ding, Y. R., Liu, X., et al. (2018). DPP-4 inhibitors promote proliferation and migration of rat brain microvascular endothelial cells under hypoxic/high-glucose conditions, potentially through the SIRT1/HIF-1/VEGF pathway. *CNS Neurosci. Ther.* 25 (3). doi: 10.1111/cns.13042
- Miki, K., Unno, N., Nagata, T., Uchijima, M., Konno, H., Koide, Y., et al. (2004). Butyrate suppresses hypoxia-inducible factor-1 activity in intestinal epithelial cells under hypoxic conditions. *Shock* 22 (5), 446–452. doi: 10.1097/01.shk.0000140664.80530.bd
- Min, L., Ling, W., Hua, R., Qi, H., Chen, S., Wang, H., et al. (2016). Antiangiogenic therapy for normalization of tumor vasculature: a potential effect of Buyang Huanwu decoction on nude mice bearing human hepatocellular carcinoma xenografts with high metastatic potential. *Mol. Med. Rep.* 13 (3), 2518–2526. doi: 10.3892/mmr.2016.4854
- Muller, S., Djurdjaj, S., Lange, J., Iacovescu, M., Goppelt-Strube, M., and Boor, P. (2018). HIF stabilization inhibits renal epithelial cell migration and is associated with cytoskeletal alterations. *Sci. Rep.* 8 (1), 9497. doi: 10.1038/s41598-018-27918-9
- Nieuwenhuis, J., Adamopoulos, A., Bleijerveld, O. B., Mazouzi, A., Stickel, E., Celie, P., et al. (2017). Vasohibins encode tubulin detyrrosinating activity. *Science* 358 (6369), 1453–1456. doi: 10.1126/science.aao5676
- Ohradanova, A., Gradin, K., Barathova, M., Zatovicova, M., Holotnakova, T., Kopacek, J., et al. (2008). Hypoxia upregulates expression of human endosialin gene via hypoxia-inducible factor 2. *Br. J. Cancer* 99 (8), 1348–1356. doi: 10.1038/sj.bjc.6604685
- Ohsawa, S., Hamada, S., Kakinuma, Y., Yagi, T., and Miura, M. (2005). Novel function of neuronal PAS domain protein 1 in erythropoietin expression in neuronal cells. *J. Neurosci. Res.* 79 (4), 451–458. doi: 10.1002/jnr.20365
- Ota, I., Li, X. Y., Hu, Y., and Weiss, S. J. (2009). Induction of a MT1-MMP and MT2-MMP-dependent basement membrane transmigration program in cancer cells by Snail1. *Proc. Natl. Acad. Sci. U.S.A.* 106 (48), 20318–20323. doi: 10.1073/pnas.0910962106
- Oyenihi, A. B., and Smith, C. (2019). Are polyphenol antioxidants at the root of medicinal plant anti-cancer success? *J. Ethnopharmacol.* 229, 54–72. doi: 10.1016/j.jep.2018.09.037
- Pahlman, S., Lund, L. R., and Jogi, A. (2015). Differential HIF-1 α and HIF-2 α expression in mammary epithelial cells during fat pad invasion, lactation, and involution. *PLoS One* 10 (5), e0125771. doi: 10.1371/journal.pone.0125771
- Pan, W. L., Wong, J. H., Fang, E. F., Chan, Y. S., Ng, T. B., and Cheung, R. C. (2014). Preferential cytotoxicity of the type I ribosome inactivating protein alaphomomorpharin on human nasopharyngeal carcinoma cells under normoxia and hypoxia. *Biochem. Pharmacol.* 89 (3), 329–339. doi: 10.1016/j.bcp.2014.03.004
- Park, S. Y., Kang, J. H., Jeong, K. J., Lee, J., Han, J. W., Choi, W. S., et al. (2011). Norepinephrine induces VEGF expression and angiogenesis by a hypoxia-inducible factor-1 α protein-dependent mechanism. *Int. J. Cancer* 128 (10), 2306–2316. doi: 10.1002/ijc.25589
- Park, S. Y., Kwon, S. J., Lim, S. S., Kim, J. K., Lee, K. W., and Park, J. H. (2016). Licoricidin, an active compound in the hexane/ethanol extract of *Glycyrrhiza uralensis*, inhibits lung metastasis of 4T1 murine mammary carcinoma cells. *Int. J. Mol. Sci.* 17 (6), 934. doi: 10.3390/ijms17060934
- Park, E. J., Lee, Y. M., Oh, T. I., Kim, B. M., Lim, B. O., and Lim, J. H. (2017). Vanillin suppresses cell motility by inhibiting STAT3-Mediated HIF-1 α mRNA expression in malignant melanoma cells. *Int. J. Mol. Sci.* 18 (3), 532. doi: 10.3390/ijms18030532
- Pena-Mercado, E., Garcia-Lorenzana, M., Arechaga-Ocampo, E., Gonzalez-De la Rosa, C. H., and Beltran, N. E. (2018). Evaluation of HIF-1 α and iNOS in ischemia/reperfusion gastric model: bioimpedance, histological and immunohistochemical analyses. *Histol. Histopathol.* 33 (8), 815–823.
- Peterle, G. T., Maia, L. L., Trivilin, L. O., de Oliveira, M. M., Dos Santos, J. G., Mendes, S. O., et al. (2018). PAI-1, CAIX, and VEGFA expressions as prognosis markers in oral squamous cell carcinoma. *J. Oral Pathol. Med.* 47 (6), 566–574. doi: 10.1111/jop.12721
- Pio, R., Ajona, D., and Lambris, J. D. (2013). Complement inhibition in cancer therapy. *Semin. Immunol.* 25 (1), 54–64. doi: 10.1016/j.smim.2013.04.001

- Prangsaengtong, O., Jantaree, P., Lirdprapamongkol, K., Svasti, J., and Koizumi, K. (2018). Shikonin suppresses lymphangiogenesis via NF-kappaB/HIF-1alpha axis inhibition. *Biol. Pharm. Bull.* 41 (11), 1659–1666. doi: 10.1248/bpb.b18-00329
- Qin, J. J., Li, X., Hunt, C., Wang, W., Wang, H., and Zhang, R. (2018). Natural products targeting the p53-MDM2 pathway and mutant p53: recent advances and implications in cancer medicine. *Genes. Dis.* 5 (3), 204–219. doi: 10.1016/j.gendis.2018.07.002
- Ranjbarnejad, T., Saidijam, M., Moradkhani, S., and Najafi, R. (2017a). Methanolic extract of *Boswellia serrata* exhibits anti-cancer activities by targeting microsomal prostaglandin E synthase-1 in human colon cancer cells. *Prostaglandins Other Lipid Mediat.* 131, 1–8. doi: 10.1016/j.prostaglandins.2017.05.003
- Ranjbarnejad, T., Saidijam, M., Tafakh, M. S., Pourjafar, M., Talebzadeh, F., and Najafi, R. (2017b). Garcinol exhibits anti-proliferative activities by targeting microsomal prostaglandin E synthase-1 in human colon cancer cells. *Hum. Exp. Toxicol.* 36 (7), 692–700. doi: 10.1177/0960327116660865
- Rausch, L. K., Hofer, M., Pramschler, S., Kaser, S., Ebenbichler, C., Haacke, S., et al. (2018). Adiponectin, leptin and visfatin in hypoxia and its effect for weight loss in obesity. *Front. Endocrinol. (Lausanne)* 9, 615. doi: 10.3389/fendo.2018.00615
- Rius, J., Guma, M., Schachtrup, C., Akassoglou, K., Zinkernagel, A. S., Nizet, V., et al. (2008). NF-kappaB links innate immunity to the hypoxic response through transcriptional regulation of HIF-1alpha. *Nature* 453 (7196), 807–811. doi: 10.1038/nature06905
- Rivera, L. B., and Bergers, G. (2014). Angiogenesis. Targeting vascular sprouts. *Science* 344 (6191), 1449–1450. doi: 10.1126/science.1257071
- Ryou, M. G., Choudhury, G. R., Li, W., Winters, A., Yuan, F., Liu, R., et al. (2015). Methylene blue-induced neuronal protective mechanism against hypoxia-reoxygenation stress. *Neuroscience* 301, 193–203. doi: 10.1016/j.neuroscience.2015.05.064
- Sathya, S., Sudhagar, S., Vidhya Priya, M., Bharathi Raja, R., Muthusamy, V. S., Niranjali Devaraj, S., et al. (2010). 3beta-hydroxylup-20(29)-ene-27,28-dioic acid dimethyl ester, a novel natural product from *Plumbago zeylanica* inhibits the proliferation and migration of MDA-MB-231 cells. *Chem. Biol. Interact.* 188 (3), 412–420. doi: 10.1016/j.cbi.2010.07.019
- Sato, K., Morimoto, N., Kurata, T., Mimoto, T., Miyazaki, K., Ikeda, Y., et al. (2012). Impaired response of hypoxic sensor protein HIF-1alpha and its downstream proteins in the spinal motor neurons of ALS model mice. *Brain Res.* 1473, 55–62. doi: 10.1016/j.brainres.2012.07.040
- Semenza, G. L. (2003). Targeting HIF-1 for cancer therapy. *Nat. Rev. Cancer* 3 (10), 721–732. doi: 10.1038/nrc1187
- Sena, J. A., Wang, L., Pawlus, M. R., and Hu, C. J. (2014). HIFs enhance the transcriptional activation and splicing of adrenomedullin. *Mol. Cancer Res.* 12 (5), 728–741. doi: 10.1158/1541-7786.MCR-13-0607
- Sendoel, A., Kohler, I., Fellmann, C., Lowe, S. W., and Hengartner, M. O. (2010). HIF-1 antagonizes p53-mediated apoptosis through a secreted neuronal tyrosinase. *Nature* 465 (7298), 577–583. doi: 10.1038/nature09141
- Senior, K. (2001). Angiogenesis and functional recovery demonstrated after minor stroke. *Lancet* 358 (9284), 817. doi: 10.1016/S0140-6736(01)06014-7
- Sharma, D., Singh, P., and Singh, S. S. (2018). beta-N-oxalyl-L-alpha,beta-diaminopropionic acid induces wound healing by stabilizing HIF-1alpha and modulating associated protein expression. *Phytomedicine* 44, 9–19. doi: 10.1016/j.phymed.2018.04.024
- Shi, H. (2009). Hypoxia inducible factor 1 as a therapeutic target in ischemic stroke. *Curr. Med. Chem.* 16 (34), 4593–600. doi: 10.2174/092986709789760779
- Shi, G. H., and Zhou, L. (2018). Emodin suppresses angiogenesis and metastasis in anaplastic thyroid cancer by affecting TRAF6-mediated pathways in vivo and in vitro. *Mol. Med. Rep.* 5191–5197. doi: 10.3892/mmr.2018.9510
- Shi, L., Zhang, G., Zheng, Z., Lu, B., and Ji, L. (2017). Andrographolide reduced VEGFA expression in hepatoma cancer cells by inactivating HIF-1alpha: the involvement of JNK and MTA1/HDCA. *Chem. Biol. Interact.* 273, 228–236. doi: 10.1016/j.cbi.2017.06.024
- Shiau, A. L., Shen, Y. T., Hsieh, J. L., Wu, C. L., and Lee, C. H. (2014). *Scutellaria barbata* inhibits angiogenesis through downregulation of HIF-1 alpha in lung tumor. *Environ. Toxicol.* 29 (4), 363–70. doi: 10.1002/tox.21763
- Singh, D., Arora, R., Kaur, P., Singh, B., Mannan, R., and Arora, S. (2017). Overexpression of hypoxia-inducible factor and metabolic pathways: possible targets of cancer. *Cell Biosci.* 7, 62. doi: 10.1186/s13578-017-0190-2
- Soleimannejad, K., Rahmani, A., Hatefi, M., Khataminia, M., Hafezi Ahmadi, M. R., and Asadollahi, K. (2017). Effects of nigella sativa extract on markers of cerebral angiogenesis after global ischemia of brain in rats. *J. Stroke Cerebrovasc. Dis.* 26 (7), 1514–1520. doi: 10.1016/j.jstrokecerebrovasdis.2017.02.040
- Soleymani Abyaneh, H., Gupta, N., Radziwon-Balicka, A., Jurasz, P., Seubert, J., Lai, R., et al. (2017). STAT3 but not HIF-1alpha is important in mediating hypoxia-induced chemoresistance in MDA-MB-231, a triple negative breast cancer cell line. *Cancers (Basel)* 9 (10), 137. doi: 10.3390/cancers9100137
- Soni, S., and Padwad, Y. S. (2017). HIF-1 in cancer therapy: two decade long story of a transcription factor. *Acta. Oncol.* 56 (4), 503–515. doi: 10.1080/0284186X.2017.1301680
- Su, M. T., Lin, S. H., Chen, Y. C., and Kuo, P. L. (2014). Gene-gene interactions and gene polymorphisms of VEGFA and EG-VEGF gene systems in recurrent pregnancy loss. *J. Assist. Reprod. Genet.* 31 (6), 699–705. doi: 10.1007/s10815-014-0223-2
- Sui, H., Zhao, J., Zhou, L., Wen, H., Deng, W., Li, C., et al. (2017). Tanshinone IIA inhibits beta-catenin/VEGF-mediated angiogenesis by targeting TGF-beta1 in normoxic and HIF-1alpha in hypoxic microenvironments in human colorectal cancer. *Cancer Lett.* 403, 86–97. doi: 10.1016/j.canlet.2017.05.013
- Suvanish Kumar, V. S., Pretorius, E., and Rajanikant, G. K. (2018). The synergistic combination of everolimus and paroxetine exerts post-ischemic neuroprotection in vitro. *Cell Mol. Neurobiol.* 38 (7), 1383–1397. doi: 10.1007/s10571-018-0605-6
- Taheem, D. K., Foyt, D. A., Loaiza, S., Ferreira, S. A., Ilic, D., Auner, H. W., et al. (2018). Differential regulation of human bone marrow mesenchymal stromal cell chondrogenesis by hypoxia inducible factor-1alpha hydroxylase inhibitors. *Stem. Cells* 36 (9), 1380–1392. doi: 10.1002/stem.2844
- Tal, R., Shaish, A., Barshack, I., Polak-Charcon, S., Afek, A., Volkov, A., et al. (2010). Effects of hypoxia-inducible factor-1alpha overexpression in pregnant mice: possible implications for preeclampsia and intrauterine growth restriction. *Am. J. Pathol.* 177 (6), 2950–2962. doi: 10.2353/ajpath.2010.090800
- Tian, G., Guo, L., and Gao, W. (2010). Use of compound Chinese medicine in the treatment of lung cancer. *Curr. Drug Discov. Technol.* 7 (1), 32–36. doi: 10.2174/157016310791162776
- Toth, R. K., and Warfel, N. A. (2017). Strange bedfellows: nuclear factor, erythroid 2-like 2 (Nrf2) and hypoxia-inducible factor 1 (HIF-1) in tumor hypoxia. *Antioxidants (Basel)* 6 (2), E27. doi: 10.3390/antiox6020027
- Toullec, A., Buard, V., Rannou, E., Tarlet, G., Guipaud, O., Robine, S., (2018). HIF-1alpha deletion in the endothelium, but not in the epithelium, protects from radiation-induced enteritis. *Cell Mol. Gastroenterol. Hepatol.* 5 (1), 15–30. doi: 10.1016/j.jcmgh.2017.08.001
- Trollmann, R., Muhlberger, T., Richter, M., Boie, G., Feigenspan, A., Brackmann, F., et al. (2018). Differential regulation of angiogenesis in the developing mouse brain in response to exogenous activation of the hypoxia-inducible transcription factor system. *Brain Res.* 1688, 91–102. doi: 10.1016/j.brainres.2018.03.012
- Tsai, I. T., Kuo, C. C., Liou, J. P., and Chang, J. Y. (2018). Novel microtubule inhibitor MPT0B098 inhibits hypoxia-induced epithelial-to-mesenchymal transition in head and neck squamous cell carcinoma. *J. Biomed. Sci.* 25 (1), 28. doi: 10.1186/s12929-018-0432-6
- Tsang, C. M., Cheung, K. C., Cheung, Y. C., Man, K., Lui, V. W., Tsao, S. W., et al. (2015). Berberine suppresses Id-1 expression and inhibits the growth and development of lung metastases in hepatocellular carcinoma. *Biochim. Biophys. Acta.* 1852 (3), 541–551. doi: 10.1016/j.bbdis.2014.12.004
- Tyska-Czochara, M., Lasota, M., and Majka, M. (2018). Caffeic acid and metformin inhibit invasive phenotype induced by TGF-beta1 in C-4I and HTB-35/SiHa human cervical squamous carcinoma cells by acting on different molecular targets. *Int. J. Mol. Sci.* 19 (1), E266. doi: 10.3390/ijms19010266
- Wang, F. R., and Jiang, Y. S. (2015). Effect of treatment with baicalein on the intracerebral tumor growth and survival of orthotopic glioma models. *J. Neurooncol.* 124 (1), 5–11. doi: 10.1007/s11060-015-1804-3
- Wang, B. S., Zhang, L. S., Song, D. M., Zhang, J. H., and Liu, Y. M. (2009). [Effect of genesenside Rg3 on apoptosis of Hep-2 and expression of HIF-1alpha in human laryngeal cancer cell line under anoxic conditions]. *Zhong. Yao. Cai.* 32 (1), 102–106.
- Wang, C., Wang, Z., Zhang, X., Zhang, X., Dong, L., Xing, Y., et al. (2012). Protection by silibinin against experimental ischemic stroke: up-regulated pAkt, pmTOR, HIF-1alpha and Bcl-2, down-regulated Bax, NF-kappaB expression. *Neurosci. Lett.* 529 (1), 45–50. doi: 10.1016/j.neulet.2012.08.078
- Wang, Z., Wang, N., Han, S., Wang, D., Mo, S., Yu, L., (2013). Dietary compound isoliquiritigenin inhibits breast cancer neoangiogenesis via VEGF/VEGFR-2 signaling pathway. *PLoS One* 8 (7), e68566. doi: 10.1371/journal.pone.0068566
- Wang, D., Xin, Y., Tian, Y., Li, W., Sun, D., and Yang, Y. (2017). Pseudolaric acid B inhibits gastric cancer cell metastasis in vitro and in haematogenous dissemination

- model through PI3K/AKT, ERK1/2 and mitochondria-mediated apoptosis pathways. *Exp. Cell. Res.* 352 (1), 34–44. doi: 10.1016/j.yexcr.2017.01.012
- Wang, X. P., Wang, Q. X., Lin, H. P., and Chang, N. (2017). Anti-tumor bioactivities of curcumin on mice loaded with gastric carcinoma. *Food Funct.* 8 (9), 3319–3326. doi: 10.1039/C7FO00555E
- Wang, W., Xu, B., Xuan, H., Ge, Y., Wang, Y., Wang, L., et al. (2018). Hypoxia-inducible factor 1 in clinical and experimental aortic aneurysm disease. *J. Vasc. Surg.* 68 (5), 1538–1550 e2. doi: 10.1016/j.jvs.2017.09.030
- Wei, Y., Hong, H., Zhang, X., Lai, W., Wang, Y., Chu, K., et al. (2017). Salidroside inhibits inflammation through PI3K/Akt/HIF signaling after focal cerebral ischemia in rats. *Inflammation* 40 (4), 1297–1309. doi: 10.1007/s10753-017-0573-x
- Weih, M., Bergk, A., Isaev, N. K., Ruscher, K., Megow, D., Riepe, M., et al. (1999). Induction of ischemic tolerance in rat cortical neurons by 3-nitropropionic acid: chemical preconditioning. *Neurosci. Lett.* 272 (3), 207–210. doi: 10.1016/S0304-3940(99)00594-7
- Woodley, D. T., Fan, J., Cheng, C. F., Li, Y., Chen, M., Bu, G., et al. (2009). Participation of the lipoprotein receptor LRP1 in hypoxia-HSP90 α autocrine signaling to promote keratinocyte migration. *J. Cell. Sci.* 122 (Pt 10), 1495–1498. doi: 10.1242/jcs.047894
- Wu, C., Chen, J., Chen, C., Wang, W., Wen, L., Gao, K., et al. (2015). Wnt/ β -catenin coupled with HIF-1 α /VEGF signaling pathways involved in galangin neurovascular unit protection from focal cerebral ischemia. *Sci. Rep.* 5, 16151. doi: 10.1038/srep16151
- Xing, Y., Mi, C., Wang, Z., Zhang, Z. H., Li, M. Y., Zuo, H. X., et al. (2018). Fraxinellone has anticancer activity *in vivo* by inhibiting programmed cell death-ligand 1 expression by reducing hypoxia-inducible factor-1 α and STAT3. *Pharmacol. Res.* 135, 166–180. doi: 10.1016/j.phrs.2018.08.004
- Xu, W., Yang, G., Xu, Y., Zhang, Q., Fu, Q., Yu, J., et al. (2014). The possibility of traditional Chinese medicine as maintenance therapy for advanced nonsmall cell lung cancer. *Evid. Based Complement. Alternat. Med.* 2014, 278917. doi: 10.1155/2014/278917
- Yamakawa, M., Liu, L. X., Belanger, A. J., Date, T., Kuriyama, T., Goldberg, M. A., et al. (2004). Expression of angiopoietins in renal epithelial and clear cell carcinoma cells: regulation by hypoxia and participation in angiogenesis. *Am. J. Physiol. Renal. Physiol.* 287 (4), F649–F657. doi: 10.1152/ajprenal.00028.2004
- Yang, X., Yang, B., Cai, J., Zhang, C., Zhang, Q., Xu, L., et al. (2013). Berberine enhances radiosensitivity of esophageal squamous cancer by targeting HIF-1 α *in vitro* and *in vivo*. *Cancer. Biol. Ther.* 14 (11), 1068–1073. doi: 10.4161/cbt.26426
- Yeh, S. H., Hung, J. J., Gean, P. W., and Chang, W. C. (2008). Hypoxia-inducible factor-1 α protects cultured cortical neurons from lipopolysaccharide-induced cell death *via* regulation of NRI expression. *J. Neurosci.* 28 (52), 14259–14270. doi: 10.1523/JNEUROSCI.4258-08.2008
- Yen, T. L., Hsu, C. K., Lu, W. J., Hsieh, C. Y., Hsiao, G., Chou, D. S., et al. (2012). Neuroprotective effects of xanthohumol, a prenylated flavonoid from hops (*Humulus lupulus*), in ischemic stroke of rats. *J. Agric. Food Chem.* 60 (8), 1937–1944. doi: 10.1021/jf204909p
- Yen, T. L., Ong, E. T., Lin, K. H., Chang, C. C., Jayakumar, T., Lin, S. C., et al. (2014). Potential advantages of Chinese medicine Taohong Siwu Decoction () combined with tissue-plasminogen activator for alleviating middle cerebral artery occlusion-induced embolic stroke in rats. *Chin. J. Integr. Med.* doi: 10.1007/s11655-014-1847-x
- Yeom, C. J., Zeng, L., Zhu, Y., Hiraoka, M., and Harada, H. (2011). Strategies to assess hypoxic/hif-1-active cancer cells for the development of innovative radiation therapy. *Cancers (Basel)* 3 (3), 3610–3631. doi: 10.3390/cancers3033610
- Yu, X., Tong, Y., Kwok, H. F., Sze, S. C., Zhong, L., Lau, C. B., et al. (2012). Anti-angiogenic activity of Erxian Decoction, a traditional Chinese herbal formula, in zebrafish. *Biol. Pharm. Bull.* 35 (12), 2119–2127. doi: 10.1248/bpb.12-00130
- Yuan, C., Wang, H., and Yuan, Z. (2019). Ginsenoside Rg1 inhibits myocardial ischemia and reperfusion injury *via* HIF-1 α -ERK signalling pathways in a diabetic rat model. *Pharmazie* 74 (3), 157–162.
- Zagzag, D., Zhong, H., Scalzitti, J. M., Laughner, E., Simons, J. W., and Semenza, G. L. (2000). Expression of hypoxia-inducible factor 1 α in brain tumors: association with angiogenesis, invasion, and progression. *Cancer* 88 (11), 2606–2618. doi: 10.1002/1097-0142(20000601)88:11<2606::AID-CNCR25>3.0.CO;2-W
- Zaman, K., Ryu, H., Hall, D., O'Donovan, K., Lin, K. I., Miller, M. P., (1999). Protection from oxidative stress-induced apoptosis in cortical neuronal cultures by iron chelators is associated with enhanced DNA binding of hypoxia-inducible factor-1 and ATF-1/CREB and increased expression of glycolytic enzymes, p21(waf1/cip1), and erythropoietin. *J. Neurosci.* 19 (22), 9821–9830. doi: 10.1523/JNEUROSCI.19-22-09821.1999
- Zdravlevic, M., Vucetic, M., Daher, B., Marchiq, I., Parks, S. K., and Pouyssegur, J. (2018). Disrupting the 'Warburg effect' re-routes cancer cells to OXPHOS offering a vulnerability point *via* 'ferroptosis'-induced cell death. *Adv. Biol. Regul.* 68, 55–63. doi: 10.1016/j.jbior.2017.12.002
- Zeinali, T., Mansoori, B., Mohammadi, A., and Baradaran, B. (2018). Regulatory mechanisms of miR-145 expression and the importance of its function in cancer metastasis. *Biomed. Pharmacother.* 109, 195–207. doi: 10.1016/j.biopha.2018.10.037
- Zhang, Z. G., and Chopp, M. (2009). Neurorestorative therapies for stroke: underlying mechanisms and translation to the clinic. *Lancet Neurol.* 8 (5), 491–500. doi: 10.1016/S1474-4422(09)70061-4
- Zhang, S., Zhang, Z., Sandhu, G., Ma, X., Yang, X., Geiger, J. D., et al. (2007). Evidence of oxidative stress-induced BNP3 expression in amyloid beta neurotoxicity. *Brain Res.* 1138, 221–230. doi: 10.1016/j.brainres.2006.12.086
- Zhang, Z., Yan, J., Chang, Y., ShiDu Yan, S., and Shi, H. (2011). Hypoxia inducible factor-1 as a target for neurodegenerative diseases. *Curr. Med. Chem.* 18 (28), 4335–4343. doi: 10.2174/092986711797200426
- Zhang, Q., Qian, Z., Pan, L., Li, H., and Zhu, H. (2012). Hypoxia-inducible factor 1 mediates the anti-apoptosis of berberine in neurons during hypoxia/ischemia. *Acta. Physiol. Hung.* 99 (3), 311–323. doi: 10.1556/APhysiol.99.2012.3.8
- Zhang, C., Yang, X., Zhang, Q., Yang, B., Xu, L., Qin, Q., et al. (2014). Berberine radiosensitizes human nasopharyngeal carcinoma by suppressing hypoxia-inducible factor-1 α expression. *Acta. Otolaryngol.* 134 (2), 185–192. doi: 10.3109/00016489.2013.850176
- Zhang, Q., Zhang, C., Yang, X., Yang, B., Wang, J., Kang, Y., et al. (2014a). Berberine inhibits the expression of hypoxia induction factor-1 α and increases the radiosensitivity of prostate cancer. *Diagn. Pathol.* 9, 98. doi: 10.1186/1746-1596-9-98
- Zhang, Q., Bian, H., Li, Y., Guo, L., Tang, Y., and Zhu, H. (2014b). Preconditioning with the traditional Chinese medicine Huang-Lian-Jie-Du-Tang initiates HIF-1 α -dependent neuroprotection against cerebral ischemia in rats. *J. Ethnopharmacol.* 154 (2), 443–452. doi: 10.1016/j.jep.2014.04.022
- Zhang, K., Han, E. S., Dellinger, T. H., Lu, J., Nam, S., Anderson, R. A., et al. (2017). Cinnamon extract reduces VEGF expression *via* suppressing HIF-1 α gene expression and inhibits tumor growth in mice. *Mol. Carcinog.* 56 (2), 436–446. doi: 10.1002/mc.22506
- Zhang, L., Chen, C., Duanmu, J., Wu, Y., Tao, J., Yang, A., et al. (2018). Cryptotanshinone inhibits the growth and invasion of colon cancer by suppressing inflammation and tumor angiogenesis through modulating MMP/TIMP system, PI3K/Akt/mTOR signaling and HIF-1 α nuclear translocation. *Int. Immunopharmacol.* 65, 429–437. doi: 10.1016/j.intimp.2018.10.035
- Zhou, Z. L., Luo, Z. G., Yu, B., Jiang, Y., Chen, Y., Feng, J. M., et al. (2010). Increased accumulation of hypoxia-inducible factor-1 α with reduced transcriptional activity mediates the antitumor effect of triptolide. *Mol. Cancer* 9, 268. doi: 10.1186/1476-4598-9-268
- Zhu, H., and Zhang, S. (2018). Hypoxia inducible factor-1 α /vascular endothelial growth factor signaling activation correlates with response to radiotherapy and its inhibition reduces hypoxia-induced angiogenesis in lung cancer. *J. Cell. Biochem.* 119 (9), 7707–7718. doi: 10.1002/jcb.27120
- Zhu, P., Wu, Y., Yang, A., Fu, X., Mao, M., and Liu, Z. (2017). Catalpol suppressed proliferation, growth and invasion of CT26 colon cancer by inhibiting inflammation and tumor angiogenesis. *Biomed. Pharmacother.* 95, 68–76. doi: 10.1016/j.biopha.2017.08.049
- Zou, X., Wu, Z., Huang, J., Liu, P., Qin, X., Chen, L., et al. (2018). The role of matrix metalloproteinase-3 in the doxycycline attenuation of intracranial venous hypertension-induced angiogenesis. *Neurosurgery* 83 (6), 1317–1327. doi: 10.1093/neuros/nyx633

Conflict of Interest Statement: The authors declare that the research was conducted in the absence of any commercial or financial relationships that could be construed as a potential conflict of interest.

Copyright © 2019 Hong, Shi, Wang, Tan, Wang and Feng. This is an open-access article distributed under the terms of the Creative Commons Attribution License (CC BY). The use, distribution or reproduction in other forums is permitted, provided the original author(s) and the copyright owner(s) are credited and that the original publication in this journal is cited, in accordance with accepted academic practice. No use, distribution or reproduction is permitted which does not comply with these terms.



C-Phycocyanin Ameliorates Mitochondrial Fission and Fusion Dynamics in Ischemic Cardiomyocyte Damage

Jinchao Gao^{1†}, Lidong Zhao^{2†}, Jinfeng Wang³, Lihang Zhang¹, Dandan Zhou², Jinlong Qu⁴, Hao Wang¹, Ming Yin¹, Jiang Hong^{2*} and Wenjuan Zhao^{1*}

¹ Engineering Research Center of Cell & Therapeutic Antibody, Ministry of Education, School of Pharmacy, Shanghai Jiao Tong University, Shanghai, China, ² Department of Internal and Emergency Medicine, Shanghai General Hospital, Shanghai Jiao Tong University School of Medicine (Originally Named "Shanghai First People's Hospital"), Shanghai, China, ³ College of Chemistry and Environmental Engineering, Shandong University of Science and Technology, Qingdao, China, ⁴ Department of Emergency and Critical Care, Shanghai Changzheng Hospital, Second Military Medical University, Shanghai, China

OPEN ACCESS

Edited by:

Yuliang Wang,
Shanghai Jiao Tong University, China

Reviewed by:

Mario Chiong,
Universidad de Chile, Chile
Fu-Ming Shen,
Second Military Medical University,
China
Haiyan Lou,
Shandong University, China

*Correspondence:

Wenjuan Zhao
zhaowj@sjtu.edu.cn
Jiang Hong
jhong.pku@163.com

[†]These authors have contributed
equally to this work.

Specialty section:

This article was submitted to
Ethnopharmacology,
a section of the journal
Frontiers in Pharmacology

Received: 24 January 2019

Accepted: 07 June 2019

Published: 28 June 2019

Citation:

Gao J, Zhao L, Wang J, Zhang L,
Zhou D, Qu J, Wang H, Yin M,
Hong J and Zhao W (2019)
C-Phycocyanin Ameliorates
Mitochondrial Fission and Fusion
Dynamics in Ischemic
Cardiomyocyte Damage.
Front. Pharmacol. 10:733.
doi: 10.3389/fphar.2019.00733

Mitochondrial dysfunction is a predominant risk factor in ischemic heart disease, in which the imbalance of mitochondrial fusion and fission deteriorates mitochondrial function and might lead to cardiomyocyte death. C-phycocyanin (C-pc), an active component from blue-green algae, such as *Spirulina platensis*, has been reported to have anti-apoptosis and anti-oxidation functions. In this study, the effects of C-pc on mitochondrial dynamics of cardiomyocytes was examined using an oxygen-glucose deprivation/reoxygenation (OGD/R) model in H9c2 cells, an *in vitro* model to study the ischemia in the heart. Cell viability assay showed that C-pc dose-dependently reduced OGD/R-induced cell death. Intracellular reactive oxygen species production induced by OGD/R was decreased in C-pc-treated groups in a dose-dependent manner as well. H9c2 cells subjected to OGD/R showed excessive mitochondrial fission and diminished mitochondrial fusion. C-pc treatment significantly ameliorated unbalanced mitochondrial dynamics induced by OGD/R and regulated mitochondrial remodeling through inhibiting mitochondrial fission while promoting fusion. The enhanced expressions of dynamin 1-like protein and mitochondrial fission 1 protein induced by OGD/R were suppressed by C-pc, while the subdued expressions of mitochondrial fusion proteins mitofusins 1 and 2 and optic atrophy 1 induced by OGD/R increased in C-pc-treated groups. Triple immunofluorescence staining revealed that C-pc treatment reduced the recruitment of dynamin 1-like protein from cytoplasm to mitochondrial membranes. Furthermore, C-pc protected H9c2 cells against OGD/R-induced cytochrome c/apoptotic protease activating factor-1 intrinsic apoptosis and suppressed the phosphorylations of extracellular signal-regulated kinase and c-Jun N-terminal kinase. These results suggest that C-pc protects cardiomyocytes from ischemic damage by affecting mitochondrial fission and fusion dynamics and reducing apoptosis and, thus, may be of potential as a prophylactic or therapeutic agent for ischemic heart disease.

Keywords: C-phycocyanin, mitochondrial dynamics, fission, fusion, apoptosis, cardiomyocytes, ischemia

INTRODUCTION

Ischemic heart disease (IHD) is a common disease that accounts for the major proportion of cardiovascular diseases, causing numerous deaths globally (Goff et al., 2014). It is generally known that cardiac circulation insufficiency is a primary risk factor, causing oxygen free radical production and myocardial energy metabolism disturbance (Chouchani et al., 2014; Kornfeld et al., 2015). Furthermore, the blood reperfusion inevitably leads to detrimental effects such as apoptosis-induced cardiomyocyte death (Hausenloy and Yellon, 2013). These consequences bring about mitochondrial dysfunction of myocardial cell, especially an abnormal mitochondrial dynamics, which are regulated due to two opposing processes, mitochondrial fission and fusion (Han et al., 2018). The dynamic balance of fusion and fission of mitochondria is essential in determining their morphology, number, subcellular distribution, and function. The core protein factors for mitochondrial fission and fusion are dynamin proteins that possess membrane-remodeling properties. A growing literature supports the role of abnormal fission and fusion in heart failure (Knowlton et al., 2014; Dorn, 2016). Although the current treatments for IHD could improve blood supply for the heart, it is still an intractable obstruction to completely restore the balance of mitochondrial dynamics in time. Thus, reversion of abnormal mitochondrial dynamics is a hard but significant step toward improving treatment for the patients.

In the past decade, mitochondrial fusion and fission imbalance has been one of the high-profile topics in cardiovascular diseases (Del Campo et al., 2018), neurodegenerative diseases (Ammal Kaidery and Thomas, 2018; Godoy et al., 2018), obesity (Knott and Bossy-Wetzel, 2010), etc. Mitochondria are highly dynamic organelles constantly going through fusion and fission (Kasahara et al., 2013). Mitochondrial fission is a divisive phenomenon in which a single mitochondrion separates into two or more mitochondria followed by fragmentation of mitochondria and rapidly high energy demand, and on the other hand, mitochondrial fusion is an inverse process, two or more mitochondria form into a single mitochondrion (Franco et al., 2016; Haroon and Vermulst, 2016). By consuming lots of energy (Piquereau et al., 2013), cardiomyocytes keep the balance of mitochondrion fusion and fission when facing to the suitable energy requirement and having favorable metabolic condition (Diaz and Moraes, 2008; Li and Liu, 2018). Growing individuals have emphasized the role of mitochondrial fusion and fission in the process of IHD and heart failure. Increased mitochondrial fission and decreased mitochondrial fusion in myocardial ischemia/reperfusion (I/R) injury will disturb vascular homeostasis leading to cardiomyocyte apoptosis (Karbowski et al., 2004; Ashrafian et al., 2010; Yang et al., 2017). Timothy Wai and his colleagues showed that imbalanced fusion protein optic atrophy 1 (Opa1) processing and mitochondrial fragmentation would cause heart failure in mice (Wai et al., 2015). Moreover, previous research revealed that upregulation of mammalian fission protein fission mitochondrial 1 (FIS-1) powerfully promoted apoptosis, while Opa1 might perform as an anti-apoptotic protein to keep spontaneous apoptosis in check (Lee et al., 2004). Therefore, maintaining favorable balance of mitochondrial fusion and

fission or ameliorating excessive mitochondrial fission in IHD is essential for homeostasis of cardiomyocytes.

Lots of attention has been spent on the implications of antioxidants in cardiovascular disease (Zhang et al., 2008; Hatch et al., 2014). Unfortunately, clinical trials proved that the traditional antioxidants targeting reactive oxygen species (ROS) directly are in general ineffective and sometimes harmful in the context of cardiovascular pathology. The major reason for the failure of traditional antioxidants in the clinical studies is that ROS at lower levels exerts physiological effects by involving in signaling pathways while pathological ROS at excessive levels induces cell damage. Therefore, modulate molecular events upstream and downstream of ROS production, i.e., improve mitochondrial functions, may overcome the limitations of traditional antioxidants. Mitochondria-based therapeutics that alleviate mitochondrial dysfunction and maintain the balance of mitochondrial dynamics seem to be a promising therapeutic approach for myocardial ischemia and heart damage (Kornfeld et al., 2015).

Algae are capable of photosynthesis and have been used in traditional Chinese medicine for a variety of biological activities. The extracts of cyanobacteria, blue-green algae, have been found to show widespread pharmacological activities in treating wound healing (Gunes et al., 2017), neuroprotection (Lee et al., 2018), obesity (Seo et al., 2018), and inflammatory diseases (Gonzalez et al., 1999; Bermejo et al., 2008; Zahran and Emam, 2018). C-phycocyanin (C-pc) is one of the active components extracted and purified from blue-green algae, *Spirulina platensis* (Liu et al., 2016). Previous experiments found that C-phycocyanin (C-pc) served as a natural antioxidant (Remirez et al., 2002) and had anticancer (Jiang et al., 2018), anti-inflammatory, and anti-apoptotic activities (Romay et al., 2003). Studies have also showed that C-pc attenuated the formation of ROS and inhibited apoptosis in cardiomyocytes (Khan et al., 2006). However, whether C-pc affects mitochondrial dynamics or helps to balance abnormal mitochondrial fission and fusion in cardiomyocytes after I/R is unknown. Therefore, we used an oxygen-glucose deprivation/reoxygenation (OGD/R) model in H9c2 cells, an *in vitro* model to study the ischemia in the heart, to investigate the role of C-pc in mitochondrial fission and fusion dynamics. In the present study, we found that C-pc not only changed mitochondrial morphology from diminutive and globular to filamentous form but also decreased mitochondrial fission protein levels and elevated fusion protein levels, reversing excessive mitochondrial fission induced by OGD/R injury. Since excessive mitochondrial fission protein dynamin-like protein 1 (DLP-1) is triggered to cytochrome c release (Strack et al., 2013), while fusion protein Opa1 could prevent cytochrome c leakage from mitochondria (Frezza et al., 2006), our study showed that C-pc significantly decreased cytochrome c and apoptotic protease activating factor-1 (Apaf1) and inhibited the activation of procaspase-9 in H9c2 cells induced by OGD/R. Furthermore, C-pc possibly exerted its effects by directly or indirectly modulating extracellular signal-regulated kinase 1/2 (ERK1/2) and c-Jun N-terminal protein kinase (JNK) pathway. Collectively, for the first time, we found that C-pc powerfully ameliorated excessive mitochondrial fission and promoted mitochondrial

fusion, maintaining the balance of mitochondrial dynamics and protecting cardiomyocytes from intrinsic apoptosis. It might be a potential candidate agent against I/R injury of heart for further development.

MATERIALS AND METHODS

Cell Culture

The myoblast cell line H9c2, derived from embryonic rat heart ventricle, was obtained from the Cell Bank of Chinese Academy of Sciences (Shanghai, China). Cells were cultured in a HERAccl 150i CO₂-Incubator (Thermo Fisher Scientific Inc., USA) in Dulbecco's modified Eagle's medium (DMEM, Grand Island, NY, USA) supplemented with 10% fetal bovine serum and 1% penicillin/streptomycin (GIBCO-Invitrogen, Grand Island, NY) in a humidified incubator with 5% CO₂/95% air atmosphere at 37°C.

Induction of OGD/R and Treatment

For induction of I/R *in vitro*, H9c2 cells were exposed to hypoxic conditions (oxygen deprivation, 0.5% O₂) for 24 h in a low-glucose DMEM medium (pH 7.4) containing 5.3 mM KCl, 44.0 mM NaHCO₃, 110.3 mM NaCl, 0.9 mM NaH₂PO₄, and

1.8 mM CaCl₂ at 37°C (oxygen–glucose deprivation). After hypoxia, the cells were reoxygenated and transferred to a normal culture condition (normoxic/normoglycemic) for 24 h at 37°C (reoxygenation).

To study the protective effect of C-pc, H9c2 cells were treated with C-pc (Sigma-Aldrich St. Louis, MO, USA) at different dosage (0, 10, 20, 40, and 80 µg/ml) 2 h before the hypoxia–oxygenation onset and lasted until the end of reoxygenation in C-pc-treated groups. The time schedule of the induction of OGD/R and C-pc treatment is shown in **Figure 1A**. The group C0 was exposed to OGD/R and treated with sterile phosphate-buffered saline (PBS). Groups C10, C20, and C40 were treated with C-pc at the concentration of 10, 20, and 40 µg/ml, respectively, in addition to the exposure to OGD/R. Cells in the control groups were cultivated under the normal conditions without exposing to OGD/R.

Assessment of Cell Viability

Cell viability was assessed by cell counting kit-8 (cck-8) assays (Dojindo, Kumamoto, Japan). The H9c2 cells were seeded and cultured in a 96-well cell plate at 2×10^4 cells/well for 24 h. Mediums with different dosages of C-pc (0, 10, 20, and 40-µg/ml) were used to treat cells for 24 h to detect the effect of C-pc. Afterward, cck-8 was added into the medium according to

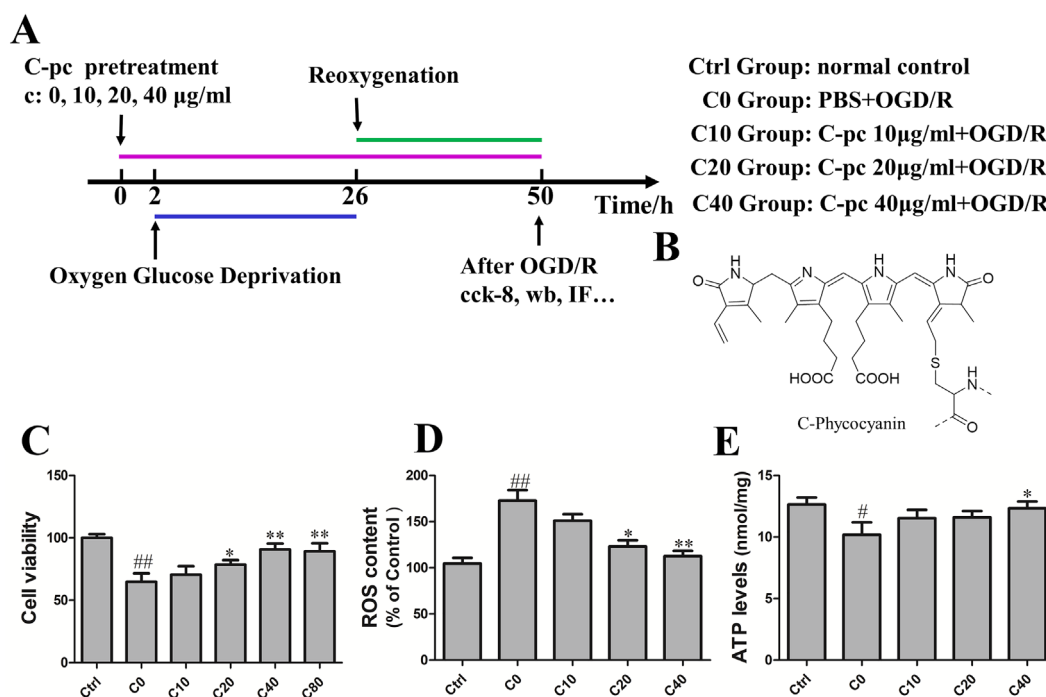


FIGURE 1 | C-phycocyanin dose-dependently reduced oxygen–glucose deprivation/reoxygenation (OGD/R)-induced cell death and reactive oxygen species (ROS) in H9c2 cells. **(A)** Experiment design. The group C0 was exposed to OGD/R and treated with sterile phosphate-buffered saline (PBS). Groups C10, C20, and C40 were treated with C-phycocyanin (C-pc) at the concentration of 10, 20, and 40 µg/ml, respectively, in addition to the exposure to OGD/R. Cells in the control groups were cultivated under the normal conditions without exposing to OGD/R. **(B)** Chemical structure of the C-pc (Bharathiraja et al., 2016). **(C)** Effects of C-pc on OGD/R-induced cell death. Cell viability was detected by cell counting kit-8 (cck-8) assay. **(D)** Effects of C-pc on OGD/R-induced intracellular ROS. **(E)** Effects of C-pc on mitochondrial function assessed by an ATP detection kit. The ATP level was normalized by protein levels (per milligram per milliliter). Data were expressed as mean ± SEM (n = 5). [#]*P* < 0.05, ^{##}*P* < 0.01 versus control (normal) group; ^{*}*P* < 0.05, ^{**}*P* < 0.01 versus C0 (OGD/R model) group. *P* < 0.05 was considered as statistically significant.

manufacturer's instructions and incubated for 2 h. Finally, the absorbance value was measured at 490 nm with a microplate reader to manifest cell viability determination.

Determination of Intracellular Reactive Oxygen Species Levels

Intracellular ROS levels were determined using dichloro-dihydro-fluorescein diacetate (Beyotime, China), which can cross the intracellular matrix where it is oxidized by ROS and produce fluorescent dichlorofluorescein. The H9c2 cells were seeded and cultured in 96-well cell plate at 2×10^4 cells/well for 24 h. H9c2 cells were incubated with 10% dichloro-dihydro-fluorescein diacetate for 30 min at 37°C in a humidified incubator, and then, the plates were washed using DMEM without serum three times.

Determination of Adenosine Triphosphate Levels

Adenosine triphosphate (ATP) levels were determined using an ATP detection kit (Beyotime, China). The H9c2 cells were seeded and cultured in a six-well cell plate at 2×10^4 cells/well. The supernatant medium was substituted by PBS, and the cells were harvested using lysis buffer at 4°C. Then, lysis buffer was centrifuged at 12,000×g for 5 min, and obtained supernatant medium was intermingled with reagent. The data were analyzed by a multimode reader (Tecan M200, Switzerland). Finally, the ATP level was normalized by protein level (per milligram per milliliter).

Western Blotting

H9c2 cells were harvested and washed with PBS for 3 min. Protein was extracted using radioimmunoprecipitation assay buffer with phenylmethylsulfonyl fluoride (1%, v/v) and protease/phosphatase inhibitor cocktails (Beyotime, Haimen, China). The concentrations of protein in samples were detected with bicinchoninic acid protein assay kit (Beyotime Biotechnology, Shanghai, China). Protein samples were separated by 8–15% sodium dodecyl sulfate polyacrylamide gel electrophoresis depending on the molecular weight of target protein and then transferred onto polyvinylidene difluoride membranes, blocked with 5% nonfat dry milk for 2 h at room temperature, incubated with specific primary antibodies at 4°C overnight (antibodies source was provided in **Supplementary material Table 1**). The following day, the polyvinylidene difluoride membrane was washed for three times with tris-buffered saline with Tween 20 (TBS-T) and incubated with the appropriate horseradish peroxidase secondary antibody for 2 h. After washing with tris-buffered saline with Tween 20 for three times, the blots were detected using an enhanced chemiluminescence (Millipore Billerica, USA) in multifunction imaging system (Tanon 5200 Multi, Shanghai, China).

Immunocytochemistry

H9c2 cells were fixed with 4% paraformaldehyde in PBS for 15 min, permeabilized with 0.5% Triton X-100 for 15 min, then blocked with 10% goat serum for 1 h. Afterward, the cells were incubated with primary antibodies at 4°C overnight. The

next day, the cells were washed with PBS and incubated with proper fluorescence-conjugated secondary antibodies (1:200 dilution) for 60 min, then washed with PBS, and the nuclei were counterstained with 4',6-diamidino-2-phenylindole for 7 min. Images were taken using a fluorescent microscope (OLYMPUS DP72, Japan) and a confocal microscope (Leica TCS SP8, Germany).

Staining of Mitochondria

H9c2 cells grew on coverslips inside a petri dish filled with DMEM. When cells reached the desired confluence, the media was removed from the dish and added with pre-warmed (37°C) staining solution containing mitochondrion-selective probe Mito-Tracker Red (MT-red) (Invitrogen, Carlsbad, CA, USA). The cells were co-stained with MT-red for 25 min under growth conditions. According to the procedures recommended by the manufacturer, the optimal concentration of MT-red was determined to 1 mM in preliminary experiments. After staining, cells were washed with fresh, pre-warmed DMEM and then fixed with freshly prepared, pre-warmed DMEM containing 2–4% formaldehyde. After fixation, H9c2 cells were incubated in PBS containing 0.2% Triton X-100 for 10 min and washed with PBS.

Statistical Analysis

Results were represented as mean \pm SEM. Comparisons involving more than two groups used one-way ANOVA followed by Fisher's *post hoc* test. Comparisons of two groups used the two-tailed Student's *t* test. $P < 0.05$ was considered as statistically significant.

RESULTS

C-Phycocyanin Dose-Dependently Mitigated Cell Death, Reduced Reactive Oxygen Species, and Ameliorated Mitochondrial Function Induced by Oxygen–Glucose Deprivation/Reoxygenation in H9c2 Cells

During I/R, cardiomyocyte death attributed to the deterioration of heart damage. Cell viability was tested by cck-8 assay to determine the promising effect of C-pc on H9c2 cells subjected by OGD/R. As shown in **Figure 1C**, cell viability of H9c2 cells was significantly decreased in C0 group subjected by OGD/R compared with normal control group. In contrast, C-pc dose-dependently mitigated the cell death induced by OGD/R, as cell viabilities in C10, C20, and C40 groups increased with the concentration of C-pc. However, C-pc treatment at the dosage of 80 μ g/ml was not more effective than that of 40 μ g/ml. Trypan blue staining was also performed to determine the cell viability in case that cck-8 assay might be affected by mitochondrial function. The results of trypan blue staining and cck-8 were consistent. When treated with C-pc (40 μ g/ml), there was obviously greater cell viability and fewer cell deaths in H9c2 cells subjected to OGD/R (data not shown). So, C-pc was used at the concentration from 0 to 40 μ g/ml in later experiments.

Increased generation of ROS was suggested as a major contributor to the pathogenetic damage of I/R injury. We thus measured the levels of intracellular ROS. Compared with the normal control group, the ROS levels dramatically elevated in OGD/R treatment group. Similarly, the OGD/R-induced production of intracellular ROS was inhibited in C-pc-treated groups in a dose-dependent manner as well (**Figure 1D**). Moreover, the function of the mitochondria was also assessed by the levels of ATP. C-pc at the dose of 40 $\mu\text{g/ml}$ significantly enhanced the reduced ATP levels induced by OGD/R, improving OGD/R-induced inhibition of mitochondrial function (**Figure 1E**). Additionally, treatment with 40 $\mu\text{g/ml}$ C-pc for 50 h did not significantly affect the cell viability, mitochondrial morphology, and ATP level of normal H9c2 cells (supplementary data).

C-Phycocyanin Alleviated Mitochondrial Morphology Changes Induced by Oxygen–Glucose Deprivation/Reoxygenation

Mitochondria are dynamic organelles undergoing alteration of mitochondrial morphology of fusion and fission. The disruption of the balance between fission and fusion was one important source that led to the production of ROS and cell damage. To examine the effect of C-pc on the mitochondrial morphology of H9c2 cells subjected to OGD/R, the mitochondrion-selective probe MT-red was used to visualize mitochondria by fluorescence microscopy. In normal control cells, most mitochondria exhibited a filamentous structure as shown in **Figure 2**. Mitochondrial morphology in OGD/R-treated (C0) group differed from that in control cells and manifested as diminutive and globular shapes, suggesting excessive mitochondrial fission that occurred in H9c2 cells under the oxygen deficit and energy debt during OGD/R. The abnormal mitochondrial morphology was gradually improved with the administration of C-pc by increasing concentration, as

the mitochondrial morphology had a general tendency toward filamentous mitochondria, which was the characterization of mitochondrial fusion and existed in normal H9c2 cells (**Figure 2**). Collectively, these results demonstrated that C-pc ameliorates mitochondrial morphology change that might be associated with mitochondrial fusion and fission balance in H9c2 cells after OGD/R.

C-Phycocyanin Reduced the Expression of Mitochondrial Fission Proteins Dynamin-Like Protein 1 and Fission Mitochondrial 1, Suppressed Dynamin-Like Protein 1 Phosphorylation, and Transportation in H9c2 Cells Induced by Oxygen–Glucose Deprivation/Reoxygenation

A number of proteins, including DLP-1 and FIS-1, are involved in mitochondrial fission. Then, we detected the protein levels of DLP-1, DLP-1 phosphorylation, and FIS-1 by Western blot and DLP-1 transportation by immunocytochemistry. The levels of mitochondrial fission proteins, DLP-1 and FIS-1, remarkably increased in H9c2 cells that suffered from OGD/R compared with those in the normal control group ($P < 0.01$, **Figure 3A, B, and D**). The elevated levels of mitochondrial fission proteins induced by OGD/R were significantly reduced by the administration of C-pc in a dose-dependent manner (**Figure 3A, B, and D**). The expression of DLP-1 was even back to a near-normal level (**Figure 3D**). Phosphorylation of DLP-1 regulated the association of DLP-1 with mitochondria. To determine the effects of C-pc on DLP1-mediated fission, we examined the effect of C-pc on DLP-1 phosphorylation at serine 616 that has been shown to increase mitochondrial fission and found that C-pc treatment made a significant reduction in OGD/R-induced DLP-1 phosphorylation.

Mitochondrial morphology assay

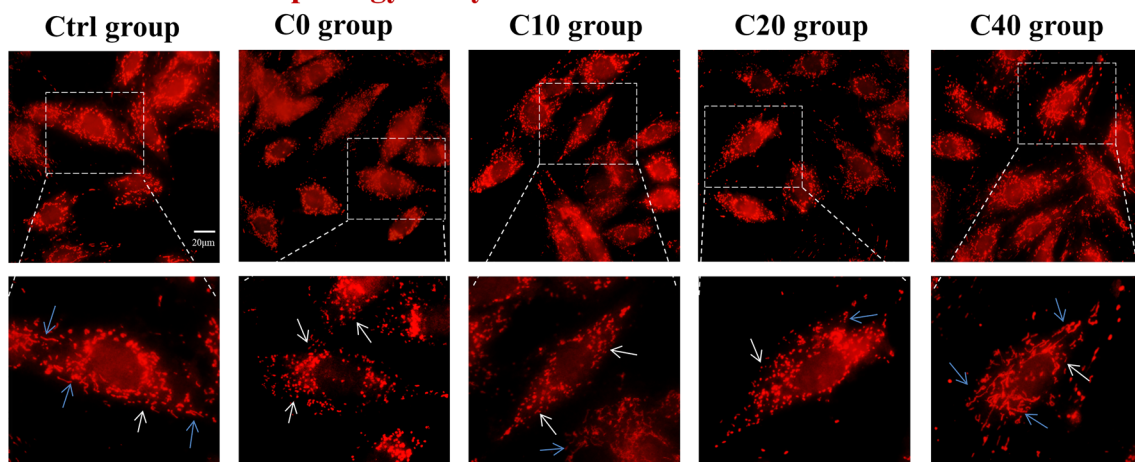


FIGURE 2 | C-phycocyanin alleviated mitochondrial morphology changes induced by OGD/R. The mitochondrial morphology of H9c2 cells was visualized by mitochondrion-selective probe Mito-Tracker. Cells were treated with C-pc (0, 10, 20, and 40 $\mu\text{g/ml}$) or phosphate-buffered saline (PBS) and subjected to OGD/R except the control group. Representative images showed the morphology of mitochondria (scale bar 20 μm). The images in the dotted box are shown at a higher resolution on the below. The white arrow showed the diminutive and globular mitochondria, and the blue arrow showed filamentous mitochondria.

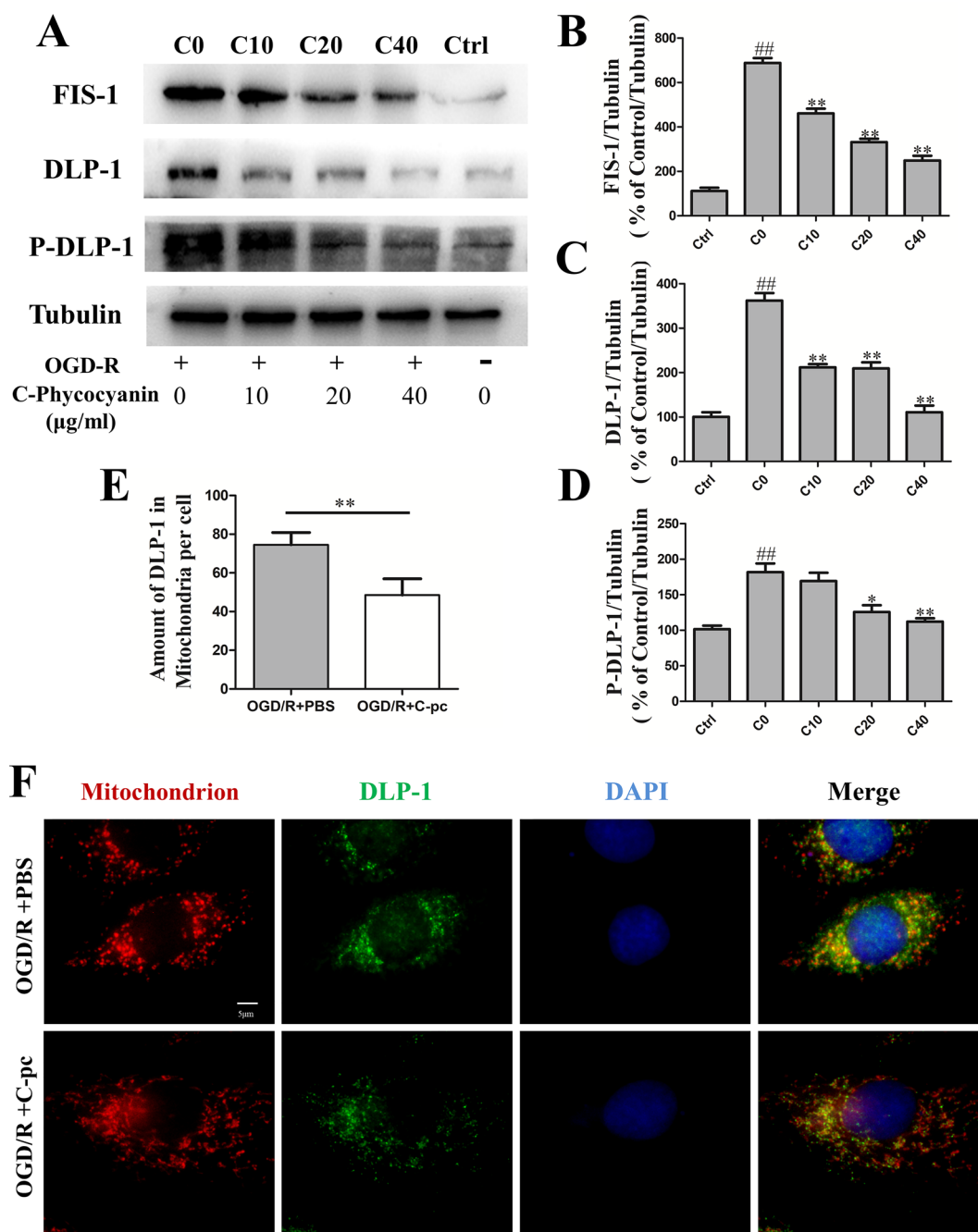


FIGURE 3 | C-phycocyanin reduced the expression of mitochondrial fission proteins DLP-1 and Fis1, suppressed DLP-1 phosphorylation, and transportation in H9c2 cells induced by OGD/R. **(A)** Representative Western blot images show the expression of mitochondrial fission proteins (FIS-1 and DLP-1) and DLP-1 phosphorylation. **(B–D)** Densitometric quantitation is shown as percentage protein expression of FIS-1 **(B)**, DLP-1 **(C)**, and P-DLP-1 **(D)**. **(E)** Quantification analysis of the amount of DLP-1 in mitochondria (co-localization of DLP-1 and mitochondria). **(F)** Representative images from immunofluorescence staining of H9c2 cells treated with PBS or C-pc (40 μg/ml) to OGD/R exposure. The cells were immunostained with 4',6-diamidino-2-phenylindole (blue), Mito-Tracker (red), and anti-DLP-1 antibody (green). Data were expressed as mean ± SEM ($n = 5$). $^*P < 0.05$, $^{##}P < 0.01$ versus control (normal) group; $^*P < 0.05$, $^{**}P < 0.01$ versus C0 (OGD/R model) group. $P < 0.05$ was considered as statistically significant.

In order to directly monitor the DLP-1 on mitochondrial surface, the localization and quantification of DLP-1 were further detected by immunocytochemistry. Consistent with the inhibitory effect in the expression of fission proteins induced by OGD/R, not only the total DLP-1, as indicated by weaker fluorescent intensity than that in OGD/R models (Figure 3F), but also the amount of DLP-1 on mitochondria, as the coexisted immunostaining of DLP-1 and mitochondria (Figure 3F), were remarkably decreased by the treatment of C-pc (40 µg/ml), as shown in Figure 3E, suggesting C-pc could mitigate OGD/R-impaired recruitment of DLP-1 from cytoplasm to mitochondrial surface, where DLP-1 could work effectively.

C-Phycocyanin Promoted Mitochondrial Fusion Proteins Mitofusins 1 and 2 and Optic Atrophy 1 Expression

Mitochondrial fusion was confirmed to be regulated by fusion proteins including mitofusins (Mfn1 and Mfn2) and Opa1. We performed Western blot to investigate whether C-pc attenuated the inhibition of fusion proteins expression induced by OGD/R to keep the balance of mitochondrial dynamics. The results showed that outer mitochondrial membrane proteins Mfn1 and Mfn2 in the control group were observably higher than those in C0 group that suffered from OGD/R (Figure 4B–C, $P < 0.05$). Similarly, the level of inner mitochondrial membrane protein Opa1 had similar change (Figure 4D, $P < 0.01$). Additionally, the abnormal outer mitochondrial membranes of both Mfn1 and Mfn2 in C0 group were significantly improved when the cells were treated with a low-dose C-pc (10 µg/ml) and even came back to the level of the control group (Figure 4B–C). However, only when treated with much higher concentration of C-pc (40 µg/ml), the inner mitochondrial membrane protein Opa1 got back to the normal level as that in the control group. These results correlated with that OGD/R-induced damage on the inner membrane of the mitochondria that was more serious than that on the outer membrane in H9c2 cells (Figure 4B–C).

Meanwhile, we carried out immunofluorescence to determine the quantification of Opa1 in C0 and C40 groups. The same results were obtained with Western blot. Thus, these results indicate that C-pc potentially prevents the decrease of fusion proteins Mfn1, Mfn2, and Opa1 expression induced by OGD/R.

C-Phycocyanin Attenuated Intrinsic Apoptosis Induced by OGD/R Injury in H9c2 Cells

Apoptosis played a crucial role of cardiomyocyte death in IHD. Focusing on the mitochondria of H9c2 cells, we investigated whether C-pc could attenuate mitochondrial apoptosis induced by acute OGD/R injury in H9c2 cells. The Western blot results showed that under the OGD/R, there was a higher level of cytochrome c in the C0 group than the control group. Cytochrome c is the main factor of intrinsic apoptosis, which releases from mitochondria and associates with the complex of apoptotic protease activating factor-1 (Apaf1) and procaspase-9. As expected, the protein level of Apaf1 and activated procaspase-9

in the C0 group was significantly increased than that in the control group (Figure 5B–D). These results demonstrate the increase of H9c2 cells' intrinsic apoptosis that occurred with OGD/R injury. In the treatment of C-pc (40 µg/ml), the protein level of cytochrome c and Apaf1 was significantly decreased, and the activation of procaspase-9 was also inhibited compared with that of the C0 group ($P < 0.01$). In addition, H9c2 cells treated with C-pc exceedingly inhibited the Bax expression (Figure 5E).

C-Phycocyanin Modulated Phosphorylation of Extracellular Signal-Regulated Kinase 1/2, c-Jun N-Terminal Protein Kinase Induced by Oxygen-Glucose Deprivation/Reoxygenation Injury in H9c2 Cells

Mitogen-activated protein kinases (MAPKs) were involved in various fundamental cellular processes, including proliferation, differentiation, apoptosis, and OGD/R injury. The Western blot was used to detect the levels of ERK1/2, JNK, p38 MAPK, and phosphorylation after H9c2 cells suffered from OGD/R. The results showed that the phosphorylation of ERK1/2 was obviously elevated in the C0 group (twofold over control Figure 6A), which could be attenuated by treatment with C-pc. Furthermore, a significant increase in the activation of JNK was observed in the C0 group compared with that in the control group (7.39-fold over control Figure 6C). C-pc modulated phosphorylation of JNK with the same trend of ERK1/2. However, OGD/R treatment seemed to have no effect on p38 MAPK, and C-pc also could not influence p38 MAPK signaling pathway (Figure 6D).

DISCUSSION

Based on the cardioprotective effects of C-pc, we paid attention to the effects on mitochondrial dynamics and used it to treat H9c2 cells in OGD/R model. Fortunately, we found that C-pc effectively inhibited ROS production and kept the balance of mitochondrial dynamics. Additionally, the decrease of excessive mitochondrial fission inhibited mitochondrial apoptosis via cytochrome c/Apaf1 pathway. These protective effects of C-pc play an essential role in preventing cardiomyocytes from the death triggered by OGD/R *in vitro*.

Cardiomyocytes consume lots of energy, in which 90% of ATP is produced by mitochondria (Li and Liu, 2018). The complicated and subtle balance of mitochondrial fusion and fission should be in no doubt that it is crucial for cardiomyocyte homeostasis. Previous research has suggested that Opa1 mutant and Mfn2 knockout mice displayed significantly greater mitochondrial dysfunction than those in the control group inducing cardiomyocyte death (Chen et al., 2012; Zhao et al., 2012). Further, decreased DLP-1 expression in cardiomyocytes could enhance myocardial contractility, while inhibition of Mfn2 could decrease contractility (Givvimani et al., 2015). These results indicate that gene defect or mutant of fusion protein accelerates cardiomyocyte death, and mitochondrial fission is not beneficial for ischemic myocardial protection. Excessive fission proteins contribute to mitochondrial fragmentation, which can

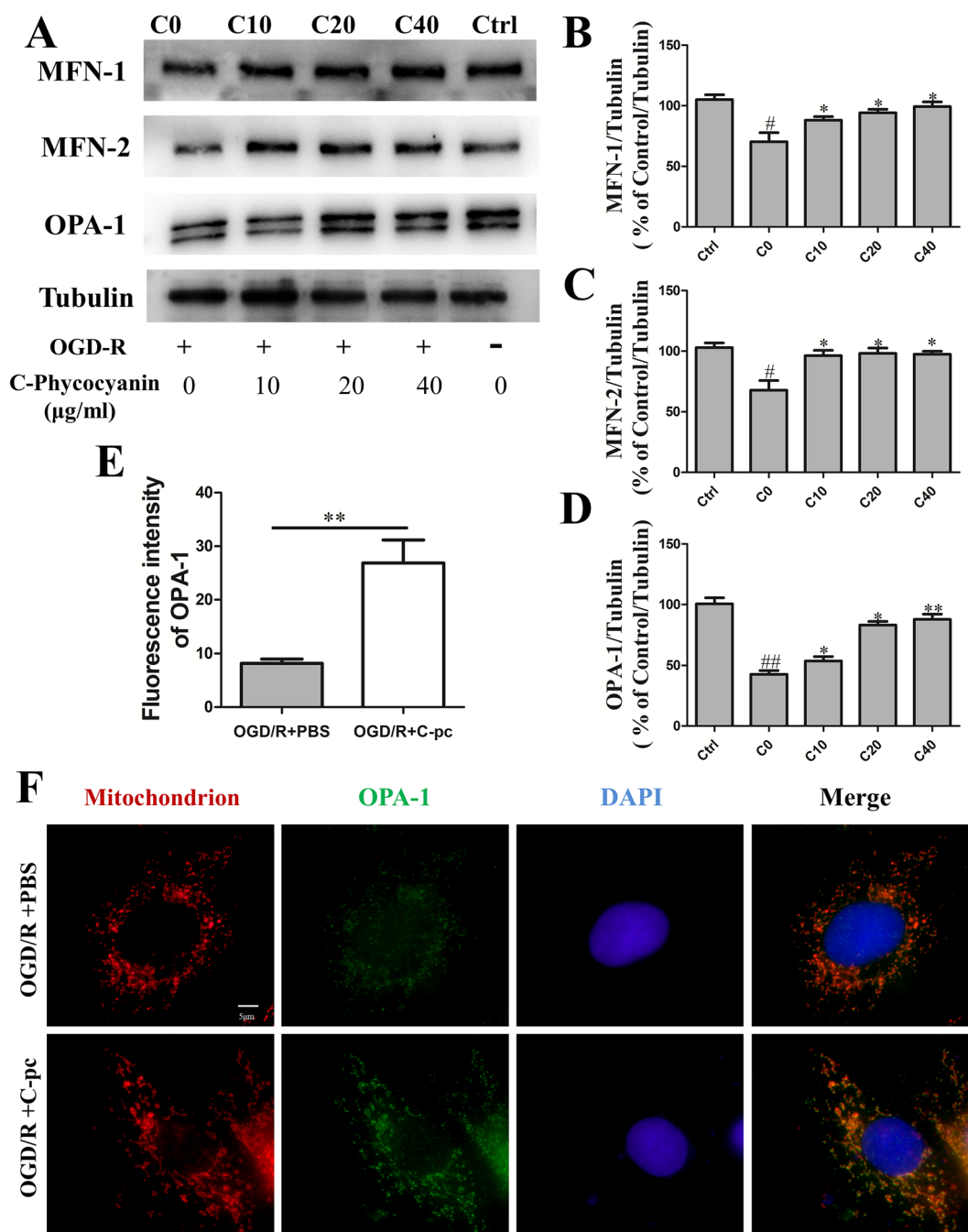


FIGURE 4 | C-phycocyanin promoted mitochondrial fusion proteins Mfn1, Mfn2, and Opa1 expression. **(A)** Representative Western blot images show the expression of mitochondrial fusion proteins MFN-1, MFN-2, and OPA-1. **(B–D)** Densitometric quantitation is shown as percentage protein expression of mitochondrial outer membrane: MFN-1 expression **(B)**, MFN-2 expression **(C)**, and mitochondrial inner membrane OPA-1 expression **(D)**. Vertical coordinates used (protein/ β -actin)/(control/ β -actin). **(E)** Quantification analysis of the fluorescence intensity of OPA-1 on H9c2 cell treated with PBS or C-pc (40 μ g/ml) after OGD/R exposure. **(F)** Representative images from immunofluorescence staining of H9c2 cells treated with PBS or C-pc (40 μ g/ml) to OGD/R exposure. The cells were immunostained with 4',6-diamidino-2-phenylindole (blue), Mito-Tracker (red), and anti-OPA-1 antibody (green). Data were expressed as mean \pm SEM ($n = 5$). [#] $P < 0.05$, ^{##} $P < 0.01$ versus control (normal) group; ^{*} $P < 0.05$, ^{**} $P < 0.01$ versus C0 (OGD/R model) group. $P < 0.05$ was considered as statistically significant.

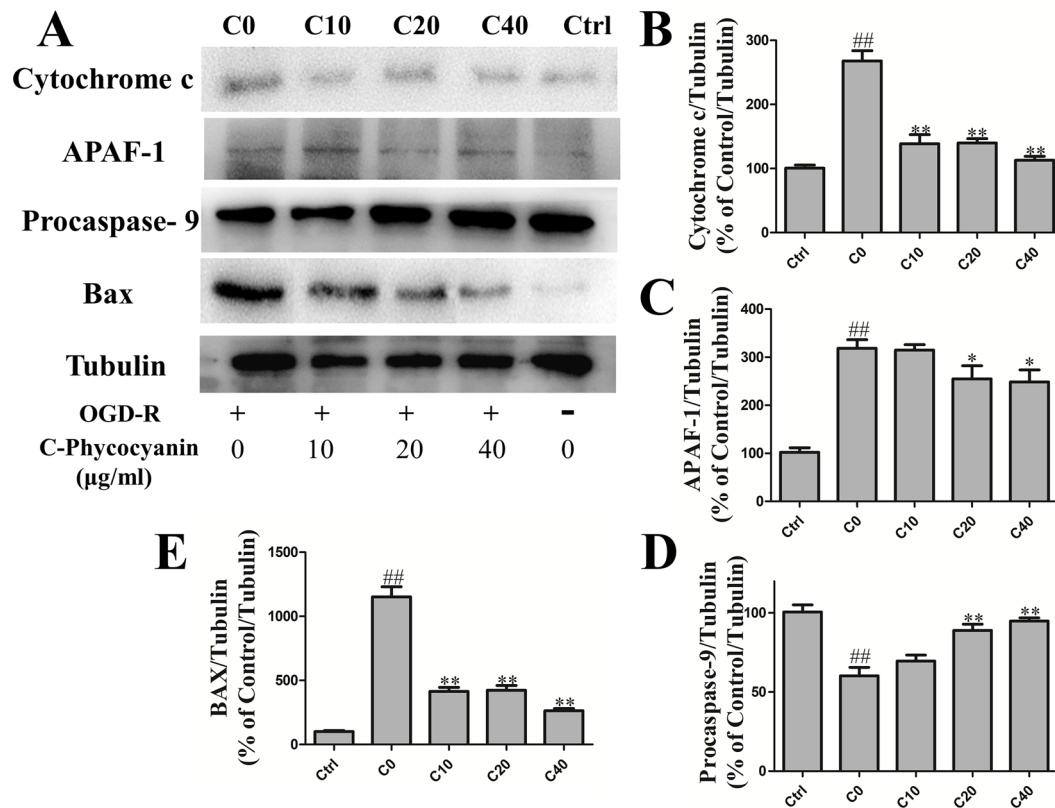


FIGURE 5 | C-phycocyanin attenuated intrinsic apoptosis induced by OGD/R injury in H9c2 cells. **(A)** The Western blot of endogenous apoptosis pathway proteins and Bax. **(B–E)** The Western blotting of cytochrome c expression **(B)**, Apaf-1 **(C)** and procaspase-9 **(D)**, and Bax **(E)** in H9c2 cells. For detecting protein expression, cells were treated with C-pc (0, 10, 20, and 40 $\mu\text{g/ml}$) or PBS and subjected to OGD/R expect control group. Data were expressed as mean \pm SEM ($n = 5$). [#] $P < 0.05$, ^{##} $P < 0.01$ versus control (normal) group; ^{*} $P < 0.05$, ^{**} $P < 0.01$ versus C0 (OGD/R model) group.

induce a metabolic switch from fatty acid to glucose utilization and generate massive mitochondria, consuming plentiful energy in the heart (Wai et al., 2015). However, it almost stores no spare energy in sustained ischemic condition. In other words, mitochondrial fusion represents a recognized strategy to allow survival during nutrient deprivation and cellular stress (Gomes et al., 2011). The observed fragmentation might be the result of DLP-1-mediated fission and of impaired mitochondrial fusion (Karbowski et al., 2004). Here, our work highlights the importance of the balance of mitochondrial dynamics, and C-pc can inhibit excessive mitochondrial fission induced by OGD/R in cardiomyocyte.

Apoptosis has been recognized as one of the major factors of cardiomyocyte death induced by I/R. It has been studied that C-pc could exert anticancer effects *via* upregulation of Fas and cleaved caspase-3 protein levels, while downregulation of the Bcl-2 protein level in MDA-MB-231 cells to induce apoptosis (Jiang et al., 2018). Conversely, C-pc played a protective effect in cardiomyocytes by upregulating anti-apoptotic protein (Khan et al., 2006). Also, inhibition of oxidative stress by C-pc prevented cisplatin-induced nephrotoxicity (Fernandez-Rojas et al., 2014). Considering that C-pc treatment decreases ROS production, affects mitochondrial dynamics greatly, and improves cardiomyocyte survival, it is possible that C-pc can mediate its protective action in cardiomyocytes by suppressing intrinsic apoptosis that is less

known before. Earlier studies have demonstrated that ischemic and hypoxic stage caused cardiomyocyte apoptosis that were associated with mitochondrial fission and fusion (Ong et al., 2010; Ikeda et al., 2015). On the one hand, Opa1 can regulate cristae shape, and Mfns can inhibit mitochondrial outer membrane permeabilization preventing cytochrome c, a proapoptotic factor, leakage (Frezza et al., 2006; Chen et al., 2009). On the other hand, inhibition of mitochondrial fission can increase inner membrane proton leak that contributes to decrease ROS production and susceptibility to apoptotic stimuli (Lee and Yoon, 2014; Wang et al., 2015). To further investigate this possibility, H9c2 cells were synchronized and subjected by OGD/R for 48 h. Finally, we observed that C-pc significantly reduced cytochrome c release from mitochondria and inhibited the activation of endogenous apoptotic pathways (Figure 5A). H9c2 cells are commonly used to generate oxygen–glucose deprivation–nutrition resumption (OGD/R) models to simulate myocardial I/R injury *in vitro*, as they are derived from heart tissue. However, we should also be careful about using H9c2 cells in the present study, as Apaf-1, a molecule in the pathway of apoptosis, was expressed in H9c2 cells but not cardiomyocytes, which might make H9c2 cells more sensitive to apoptosis than cardiomyocytes (Sanchis et al., 2003). Thus, more research on the cardioprotective effects of C-pc in cardiomyocytes *in vivo* is needed for ensuring its potential use in treatment of IHD.

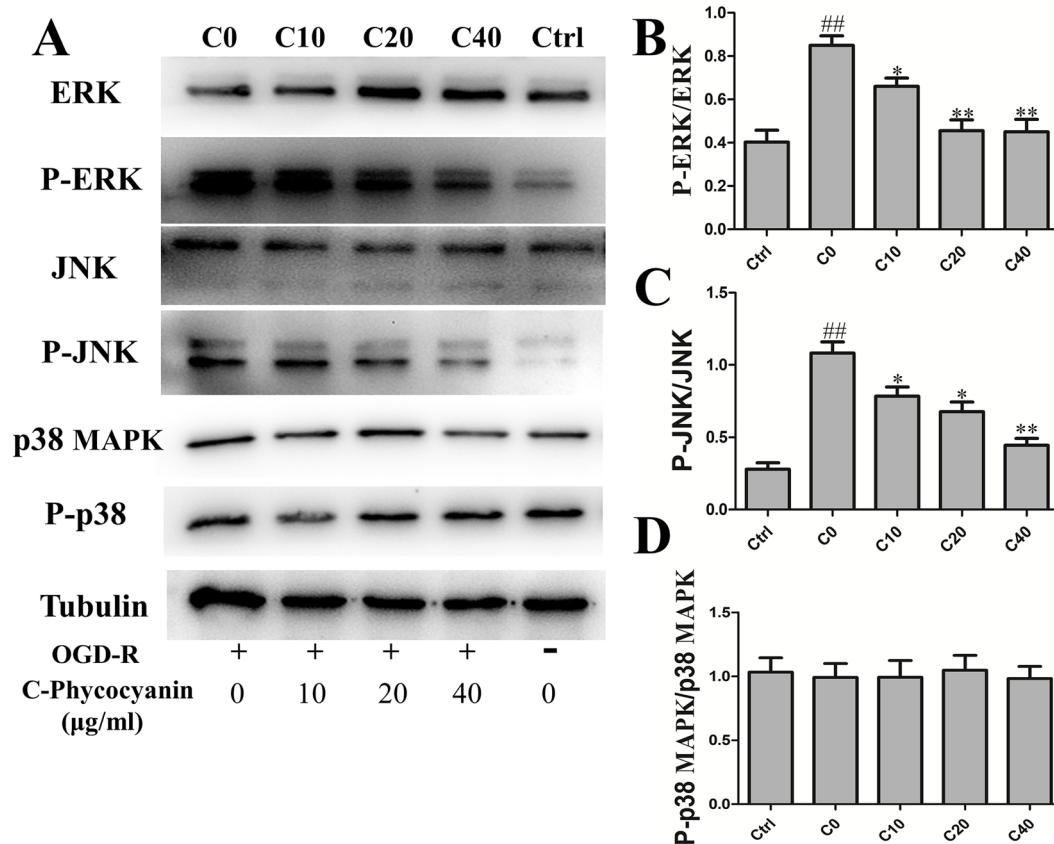


FIGURE 6 | C-phycocyanin modulated phosphorylation of ERK 1/2, c-Jun N-terminal protein kinase (JNK) induced by OGD/R injury in H9c2 cells. **(A)** The Western blotting of MAPK pathway. **(B–D)** The ratio of Western blotting results P-ERK/ERK **(B)**, P-JNK/JNK **(C)**, and P-p38 MAPK/p38 **(D)** expression in H9c2 cells. Vertical coordinates used phosphorylation/non-phosphorylation. Data were expressed as mean \pm SEM ($n = 5$). [#] $P < 0.05$, ^{##} $P < 0.01$ versus control (normal) group; ^{*} $P < 0.05$, ^{**} $P < 0.01$ versus C0 (OGD/R model) group. $P < 0.05$ was considered as statistically significant.

The molecular weight of monomeric C-pc is about 40 kD, which is an obstruction for entering into cytoplasm directly to exert protective action. Mitogen-activated protein kinases (MAPKs) are involved in various fundamental cellular processes, including cell apoptosis and survival. We speculate that whether these enzymes are activated through a sequential phosphorylation cascade that affects fission and fusion protein expression and apoptosis by C-pc directly or indirectly. Previous studies have shown that extracellular signal-regulated kinase (ERK) is well-documented for apoptosis induced by DNA-damaging agents (Fehrenbacher et al., 2008) and various antitumor compounds (Kim et al., 2008). Further, on the presence of ROS, sustained ERK can be activated (Cagnol and Chambard, 2010). Our results show that ERK is activated in H9c2 induced by OGD/R and C-pc can significantly suppress ERK activity. The ERK activity is associated with intrinsic apoptotic pathway and ROS production leading to cells death, while the inhibition of ERK activity by C-pc modulates its participation in mitochondrial dynamics. Pyakurel et al. showed that the activation of ERK phosphorylated Mfn1 causing the inhibition of mitochondrial fusion and stimulation of apoptotic mitochondrial permeabilization (Pyakurel et al., 2015).

Furthermore, activation of ERK can accelerate phosphorylation of DLP-1, which leads to mitochondrial fragmentation and facilitates apoptosis (Strack et al., 2013). The c-Jun N-terminal protein kinase (JNK) also plays an important role in the regulation of cell apoptosis (Weng et al., 2016). Here, we demonstrated that the JNK activity significantly increased in response to OGD/R in H9c2. Indeed, C-pc can inhibit the phosphorylation of ERK1/2 and JNK and improve cardiomyocyte survival.

In conclusion, our results suggest that C-pc can keep the balance of mitochondrial dynamics and suppress mitochondrial apoptosis *via* cytochrome c/Apaf1 pathway induced by OGD/R (Figure 7). C-pc might be a new therapeutic alternative or potential cardioprotectant to ameliorate excessive mitochondrial fission in IHD.

AUTHOR CONTRIBUTIONS

WZ and JH contributed to the design of the study, served as the study coordinators, and edited the manuscript. JG designed the study, performed experiments, collected and analyzed the data, and wrote the manuscript. LZ performed experiments and

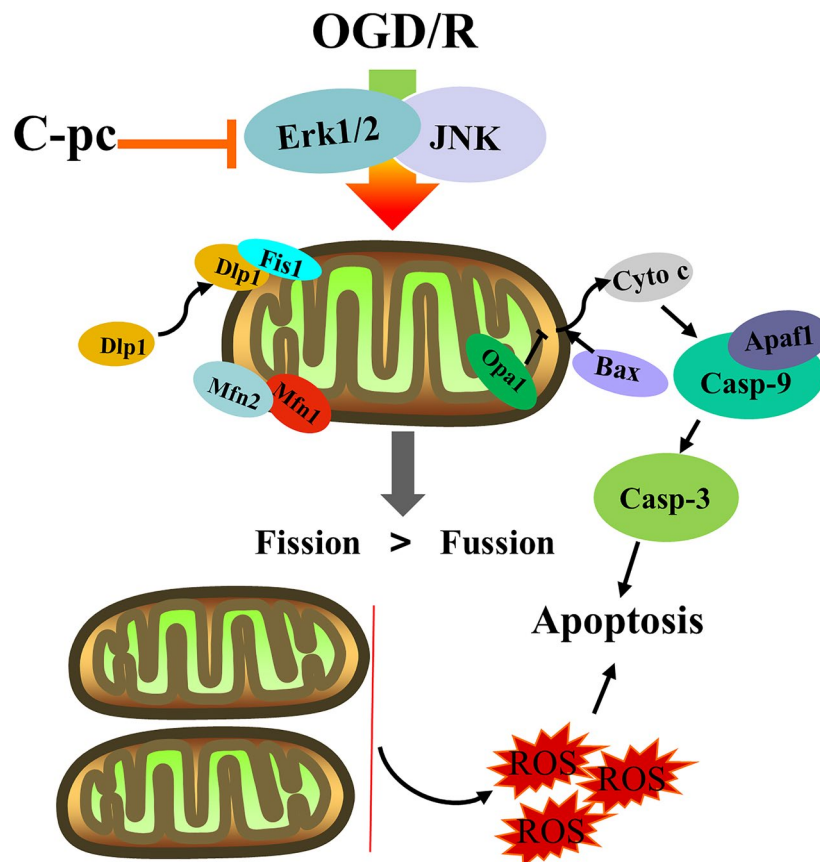


FIGURE 7 | The effects of C-phycocyanin in H9c2 cells that suffered from OGD/R injury. C-pc decreases the unnormal mitochondrial dynamics by suppressing the expression of fission proteins and promoting the expression of fusion proteins by extracellular inhibition of ERK1/2 and JNK. C-pc also inhibits Dlp-1 phosphorylation and the recruitment of Dlp1 from cytoplasm to mitochondrial surface. Further, the effect of C-pc on inhibition of excessive mitochondrial fission ameliorates mitochondrial apoptosis via cytochrome c/Apaf1 pathway.

collected and analyzed the data. JW, LZ, DZ, JQ, HW, and MY helped perform experiments and analyzed data. All authors have read and approved the final manuscript.

FUNDING

This study was supported by grants from the National Natural Science Foundation of China (grant no. 81471232, 81570293)

REFERENCES

- Ammal Kaidery, N., and Thomas, B. (2018). Current perspective of mitochondrial biology in Parkinson's disease. *Neurochem Int.* 117, 91–113. doi: 10.1016/j.neuint.2018.03.001
- Ashrafian, H., Docherty, L., Leo, V., Towilson, C., Neilan, M., Steeples, V., et al. (2010). A mutation in the mitochondrial fission gene Dnm1l leads to cardiomyopathy. *PLoS Genet.* 6 (6), e1001000. doi: 10.1371/journal.pgen.1001000
- Bermejo, P., Pinero, E., and Villar, A. M. (2008). Iron-chelating ability and antioxidant properties of phycocyanin isolated from a protean extract of *Spirulina platensis*. *Food Chem.* 110 (2), 436–445. doi: 10.1016/j.foodchem.2008.02.021

and the Science and Technology Commission of Shanghai Municipality (14431901400).

SUPPLEMENTARY MATERIAL

The Supplementary Material for this article can be found online at: <https://www.frontiersin.org/articles/10.3389/fphar.2019.00733/full#supplementary-material>

- Bharathiraja, S., Seo, H., Manivasagan, P., Santha Moorthy, M., Park, S., and Oh, J. (2016). *In vitro* photodynamic effect of phycocyanin against breast cancer cells. *Mol.* 21 (11). doi: 10.3390/molecules21111470
- Cagnol, S., and Chambard, J. C. (2010). ERK and cell death: mechanisms of ERK-induced cell death—apoptosis, autophagy and senescence. *FEBS J.* 277 (1), 2–21. doi: 10.1111/j.1742-4658.2009.07366.x
- Chen, L., Gong, Q., Stice, J. P., and Knowlton, A. A. (2009). Mitochondrial OPA1, apoptosis, and heart failure. *Cardiovasc. Res.* 84 (1), 91–99. doi: 10.1093/cvr/cvp181
- Chen, L., Liu, T., Tran, A., Lu, X., Tomilov, A. A., Davies, V., et al. (2012). OPA1 mutation and late-onset cardiomyopathy: mitochondrial dysfunction

- and mtDNA instability. *J. Am. Heart. Assoc.* 1 (5), e003012. doi: 10.1161/JAHA.112.003012
- Chouchani, E. T., Pell, V. R., Gaude, E., Aksentijevic, D., Sundier, S. Y., Robb, E. L., et al. (2014). Ischaemic accumulation of succinate controls reperfusion injury through mitochondrial ROS. *Nature* 515 (7527), 431–+. doi: 10.1038/nature13909
- Del Campo, A., Bustos, C., Mascayano, C., Acuna-Castillo, C., Troncoso, R., and Rojo, L. E. (2018). Metabolic Syndrome and Antipsychotics: The Role of Mitochondrial Fission/Fusion Imbalance. *Front. Endocrinol. (Lausanne)* 9, 144. doi: 10.3389/fendo.2018.00144
- Diaz, F., and Moraes, C. T. (2008). Mitochondrial biogenesis and turnover. *Cell Calcium* 44 (1), 24–35. doi: 10.1016/j.ceca.2007.12.004
- Dorn, G. (2016). Mitochondrial fission/fusion and cardiomyopathy. *Curr. Opin. Genet. Dev.* 38, 38–44. doi: 10.1016/j.gde.2016.03.001
- Fehrenbacher, N., Bastholm, L., Kirkegaard-Sorensen, T., Rafn, B., Bottzauw, T., Nielsen, C., et al. (2008). Sensitization to the lysosomal cell death pathway by oncogene-induced down-regulation of lysosome-associated membrane proteins 1 and 2. *Cancer Res.* 68 (16), 6623–6633. doi: 10.1158/0008-5472.CAN-08-0463
- Fernandez-Rojas, B., Medina-Campos, O. N., Hernandez-Pando, R., Negrette-Guzman, M., Huerta-Yepez, S., and Pedraza-Chaverri, J. (2014). C-Phycocyanin prevents cisplatin-induced nephrotoxicity through inhibition of oxidative stress. *Food Funct.* 5 (3), 480–490. doi: 10.1039/C3FO60501A
- Franco, A., Kitsis, R. N., Fleischer, J. A., Gavathiotis, E., Kornfeld, O. S., Gong, G., et al. (2016). Correcting mitochondrial fusion by manipulating mitofusin conformations. *Nature* 540 (7631), 74–79. doi: 10.1038/nature20156
- Frezza, C., Cipolat, S., Martins de Brito, O., Micaroni, M., Beznoussenko, G. V., Rudka, T., et al. (2006). OPA1 controls apoptotic cristae remodeling independently from mitochondrial fusion. *Cell* 126 (1), 177–189. doi: 10.1016/j.cell.2006.06.025
- Givvimani, S., Pushpakumar, S. B., Metreveli, N., Veeranki, S., Kundu, S., and Tyagi, S. C. (2015). Role of mitochondrial fission and fusion in cardiomyocyte contractility. *Int. J. Cardiol.* 187, 325–333. doi: 10.1016/j.ijcard.2015.03.352
- Godoy, J. A., Valdivieso, A. G., and Inestrosa, N. C. (2018). Nicotine Modulates Mitochondrial Dynamics in Hippocampal Neurons. *Mol. Neurobiol.* 55 (12), 8965–8977. doi: 10.1007/s12035-018-1034-8
- Goff, D. C., Jr., Lloyd-Jones, D. M., Bennett, G., Coady, S., D'Agostino, R. B., Sr., Gibbons, R., et al. (2014). 2013 ACC/AHA guideline on the assessment of cardiovascular risk: a report of the American College of Cardiology/American Heart Association Task Force on Practice Guidelines. *J. Am. Coll. Cardiol.* 63 (25 Pt B), 2935–2959. doi: 10.1016/j.jacc.2013.11.005
- Gomes, L. C., Di Benedetto, G., and Scorrano, L. (2011). During autophagy mitochondria elongate, are spared from degradation and sustain cell viability. *Nat. Cell. Biol.* 13 (5), 589–598. doi: 10.1038/ncb2220
- Gonzalez, R., Rodriguez, S., Romay, C., Ancheta, O., Gonzalez, A., Armesto, J., et al. (1999). Anti-inflammatory activity of phycocyanin extract in acetic acid-induced colitis in rats. *Pharmacol. Res.* 39 (1), 55–59. doi: 10.1006/phrs.1998.0409
- Gunes, S., Tamburaci, S., Dalay, M. C., and Deliloglu Gurhan, I. (2017). In vitro evaluation of Spirulina platensis extract incorporated skin cream with its wound healing and antioxidant activities. *Pharm. Biol.* 55 (1), 1824–1832. doi: 10.1080/13880209.2017.1331249
- Han, Q., Li, G., Ip, M. S., Zhang, Y., Zhen, Z., Mak, J. C., et al. (2018). Haemin attenuates intermittent hypoxia-induced cardiac injury via inhibiting mitochondrial fission. *J. Cell. Mol. Med.* 22 (5), 2717–2726. doi: 10.1111/jcmm.13560
- Haroon, S., and Vermulst, M. (2016). Linking mitochondrial dynamics to mitochondrial protein quality control. *Curr. Opin. Genet. Dev.* 38, 68–74. doi: 10.1016/j.gde.2016.04.004
- Hatch, A. L., Gurel, P. S., and Higgs, H. N. (2014). Novel roles for actin in mitochondrial fission. *J. Cell. Sci.* 127 (Pt 21), 4549–4560. doi: 10.1242/jcs.153791
- Hausenloy, D. J., and Yellon, D. M. (2013). Myocardial ischemia-reperfusion injury: a neglected therapeutic target. *J. Clin. Invest.* 123 (1), 92–100. doi: 10.1172/JCI62874
- Ikeda, Y., Shirakabe, A., Maejima, Y., Zhai, P., Sciarretta, S., Toli, J., et al. (2015). Endogenous Drp1 mediates mitochondrial autophagy and protects the heart against energy stress. *Circ. Res.* 116 (2), 264–278. doi: 10.1161/CIRCRESAHA.116.303356
- Jiang, L., Wang, Y., Liu, G., Liu, H., Zhu, F., Ji, H., et al. (2018). C-Phycocyanin exerts anti-cancer effects via the MAPK signaling pathway in MDA-MB-231 cells. *Cancer Cell Int.* 18, 12. doi: 10.1186/s12935-018-0511-5
- Karbowski, M., Arnoult, D., Chen, H. C., Chan, D. C., Smith, C. L., and Youle, R. J. (2004). Quantitation of mitochondrial dynamics by photolabeling of individual organelles shows that mitochondrial fusion is blocked during the Bax activation phase of apoptosis. *J. Cell Biol.* 164 (4), 493–499. doi: 10.1083/jcb.200309082
- Kasahara, A., Cipolat, S., Chen, Y., Dorn, G. W., 2nd, and Scorrano, L. (2013). Mitochondrial fusion directs cardiomyocyte differentiation via calcineurin and Notch signaling. *Science* 342 (6159), 734–737. doi: 10.1126/science.1241359
- Khan, M., Varadharaj, S., Ganesan, L. P., Shobha, J. C., Naidu, M. U., Parinandi, N. L., et al. (2006). C-phycocyanin protects against ischemia-reperfusion injury of heart through involvement of p38 MAPK and ERK signaling. *Am. J. Physiol. Heart Circ. Physiol.* 290 (5), H2136–H2145. doi: 10.1152/ajpheart.01072.2005
- Kim, Y. H., Lee, D. H., Jeong, J. H., Guo, Z. S., and Lee, Y. J. (2008). Quercetin augments TRAIL-induced apoptotic death: involvement of the ERK signal transduction pathway. *Biochem. Pharmacol.* 75 (10), 1946–1958. doi: 10.1016/j.bcp.2008.02.016
- Knott, A. B., and Bossy-Wetzell, E. (2010). Impact of nitric oxide on metabolism in health and age-related disease. *Diabetes Obes. Metab.* 12 Suppl 2, 126–133. doi: 10.1111/j.1463-1326.2010.01267.x
- Knowlton, A. A., Chen, L., and Malik, Z. A. (2014). Heart failure and mitochondrial dysfunction: the role of mitochondrial fission/fusion abnormalities and new therapeutic strategies. *J. Cardiovasc. Pharmacol.* 63 (3), 196–206. doi: 10.1097/01.fjc.0000432861.55968.a6
- Kornfeld, O. S., Hwang, S., Disatnik, M. H., Chen, C. H., Qvit, N., and Mochly-Rosen, D. (2015). Mitochondrial reactive oxygen species at the heart of the matter new therapeutic approaches for cardiovascular diseases. *Circ. Res.* 116 (11), 1783–1799. doi: 10.1161/CIRCRESAHA.116.305432
- Lee, H., and Yoon, Y. (2014). Transient contraction of mitochondria induces depolarization through the inner membrane dynamin OPA1 protein. *J. Biol. Chem.* 289 (17), 11862–11872. doi: 10.1074/jbc.M113.533299
- Lee, H. Y., Ryu, G. H., Choi, W. Y., Yang, W. Y., Lee, H. W., and Ma, C. J. (2018). Protective effect of water extracted spirulina maxima on glutamate-induced neuronal cell death in mouse hippocampal HT22 cell. *Pharmacogn. Mag.* 14 (54), 242–247. doi: 10.4103/pm.pm_191_17
- Lee, Y. J., Jeong, S. Y., Karbowski, M., Smith, C. L., and Youle, R. J. (2004). Roles of the mammalian mitochondrial fission and fusion mediators FIS-1, Drp1, and Opa1 in apoptosis. *Mol. Biol. Cell.* 15 (11), 5001–5011. doi: 10.1091/mbc.e04-04-0294
- Li, Y. Z., and Liu, X. H. (2018). Novel insights into the role of mitochondrial fusion and fission in cardiomyocyte apoptosis induced by ischemia/reperfusion. *J. Cell. Physiol.* 233 (8), 5589–5597. doi: 10.1002/jcp.26522
- Liu, Q., Huang, Y., Zhang, R., Cai, T., and Cai, Y. (2016). Medical application of spirulina platensis derived C-phycocyanin. *Evid. Based Complement Alternat. Med.* 2016, 7803846. doi: 10.1155/2016/7803846
- Ong, S. B., Subrayan, S., Lim, S. Y., Yellon, D. M., Davidson, S. M., and Hausenloy, D. J. (2010). Inhibiting mitochondrial fission protects the heart against ischemia/reperfusion injury. *Circulation* 121 (18), 2012–2022. doi: 10.1161/CIRCULATIONAHA.109.906610
- Piquereau, J., Caffin, F., Novotova, M., Lemaire, C., Veksler, V., Garnier, A., et al. (2013). Mitochondrial dynamics in the adult cardiomyocytes: which roles for a highly specialized cell? *Front. Physiol.* 4, 102. doi: 10.3389/fphys.2013.00102
- Pyakurel, A., Savoia, C., Hess, D., and Scorrano, L. (2015). Extracellular regulated kinase phosphorylates mitofusin 1 to control mitochondrial morphology and apoptosis. *Mol. Cell.* 58 (2), 244–254. doi: 10.1016/j.molcel.2015.02.021
- Remirez, D., Fernandez, V., Tapia, G., Gonzalez, R., and Videla, L. A. (2002). Influence of C-phycocyanin on hepatocellular parameters related to liver oxidative stress and Kupffer cell functioning. *Inflamm. Res.* 51 (7), 351–356. doi: 10.1007/PL00000314
- Romay, C., Gonzalez, R., Ledon, N., Ramirez, D., and Rimbau, V. (2003). C-phycocyanin: a biliprotein with antioxidant, anti-inflammatory and neuroprotective effects. *Curr. Protein Pept. Sci.* 4 (3), 207–216. doi: 10.2174/1389203033487216
- Sanchis, D., Mayorga, M., Ballester, M., and Comella, J. X. (2003). Lack of Apaf-1 expression confers resistance to cytochrome c-driven apoptosis in cardiomyocytes. *Cell. Death Differ.* 10 (9), 977–986. doi: 10.1038/sj.cdd.4401267
- Seo, Y. J., Kim, K. J., Choi, J., Koh, E. J., and Lee, B. Y. (2018). Spirulina maxima extract reduces obesity through suppression of adipogenesis and activation of

- browning in 3T3-L1 cells and high-fat diet-induced obese mice. *Nutrients* 10 (6), 712. doi: 10.3390/nu10060712
- Strack, S., Wilson, T. J., and Cribbs, J. T. (2013). Cyclin-dependent kinases regulate splice-specific targeting of dynamin-related protein 1 to microtubules. *J. Cell. Biol.* 201 (7), 1037–1051. doi: 10.1083/jcb.201210045
- Wai, T., Garcia-Prieto, J., Baker, M. J., Merkwirth, C., Benit, P., Rustin, P., et al. (2015). Imbalanced OPA1 processing and mitochondrial fragmentation cause heart failure in mice. *Science* 350 (6265), aad0116. doi: 10.1126/science.aad0116
- Wang, L., Yu, T. Z., Lee, H., O'Brien, D. K., Sesaki, H., and Yoon, Y. (2015). Decreasing mitochondrial fission diminishes vascular smooth muscle cell migration and ameliorates intimal hyperplasia. *Cardiovasc. Res.* 106 (2), 272–283. doi: 10.1093/cvr/cvv005
- Weng, Q., Liu, Z., Li, B., Liu, K., Wu, W., and Liu, H. (2016). Oxidative stress induces mouse follicular granulosa cells apoptosis via JNK/FoxO1 Pathway. *PLoS One* 11 (12), e0167869. doi: 10.1371/journal.pone.0167869
- Yang, Y., Zhao, L., and Ma, J. (2017). Penicillamine hydrochloride preconditioning provides cardiac protection in a rat model of myocardial ischemia/reperfusion injury via the mechanism of mitochondrial dynamics mechanism. *Eur. J. Pharmacol.* 813, 130–139. doi: 10.1016/j.ejphar.2017.07.031
- Zahrn, W. E., and Emam, M. A. (2018). Renoprotective effect of *Spirulina platensis* extract against nicotine-induced oxidative stress-mediated inflammation in rats. *Phytomedicine* 49, 106–110. doi: 10.1016/j.phymed.2018.06.042
- Zhang, W. J., Bird, K. E., McMillen, T. S., LeBoeuf, R. C., Hagen, T. M., and Frei, B. (2008). Dietary alpha-lipoic acid supplementation inhibits atherosclerotic lesion development in apolipoprotein E-deficient and apolipoprotein E/low-density lipoprotein receptor-deficient mice. *Circulation* 117 (3), 421–428. doi: 10.1161/CIRCULATIONAHA.107.725275
- Zhao, T., Huang, X., Han, L., Wang, X., Cheng, H., Zhao, Y., et al. (2012). Central role of mitofusin 2 in autophagosome-lysosome fusion in cardiomyocytes. *J. Biol. Chem.* 287 (28), 23615–23625. doi: 10.1074/jbc.M112.379164

Conflict of Interest Statement: The authors declare that the research was conducted in the absence of any commercial or financial relationships that could be construed as a potential conflict of interest.

The handling editor declared a shared affiliation, though no other collaboration, with several of the authors JG, LZ, WZ, MY, and HW at time of review.

Copyright © 2019 Gao, Zhao, Wang, Zhang, Zhou, Qu, Wang, Yin, Hong and Zhao. This is an open-access article distributed under the terms of the Creative Commons Attribution License (CC BY). The use, distribution or reproduction in other forums is permitted, provided the original author(s) and the copyright owner(s) are credited and that the original publication in this journal is cited, in accordance with accepted academic practice. No use, distribution or reproduction is permitted which does not comply with these terms.



Traditional Chinese Medicine for Coronary Heart Disease: Clinical Evidence and Possible Mechanisms

Ke-Jian Zhang^{1†}, Qun Zheng^{1†}, Peng-Chong Zhu^{1†}, Qiang Tong¹, Zhuang Zhuang¹, Jia-Zhen Zhu¹, Xiao-Yi Bao¹, Yue-Yue Huang¹, Guo-Qing Zheng^{2*} and Yan Wang^{1*}

¹ Department of Cardiology, the Second Affiliated Hospital and Yuying Children's Hospital of Wenzhou Medical University, Wenzhou, China, ² Department of Neurology, the Second Affiliated Hospital and Yuying Children's Hospital of Wenzhou Medical University, Wenzhou, China

OPEN ACCESS

Edited by:

Tie-Jun Li,
Second Military Medical University,
China

Reviewed by:

Amy Botta,
York University,
Canada
Linda Zhong,
Hong Kong Baptist University,
Hong Kong

*Correspondence:

Guo-Qing Zheng
gq_zheng@sohu.com
Yan Wang
wywzchina@sina.com

[†]These authors contributed equally
to this work

Specialty section:

This article was submitted to
Ethnopharmacology,
a section of the journal
Frontiers in Pharmacology

Received: 06 January 2019

Accepted: 01 July 2019

Published: 02 August 2019

Citation:

Zhang K-J, Zheng Q, Zhu P-C,
Tong Q, Zhuang Z, Zhu J-Z, Bao X-Y,
Huang Y-Y, Zheng G-Q and Wang Y
(2019) Traditional Chinese Medicine
for Coronary Heart Disease: Clinical
Evidence and Possible Mechanisms.
Front. Pharmacol. 10:844.
doi: 10.3389/fphar.2019.00844

Coronary heart disease (CHD) remains a major cause of mortality with a huge economic burden on healthcare worldwide. Here, we conducted a systematic review to investigate the efficacy and safety of Chinese herbal medicine (CHM) for CHD based on high-quality randomized controlled trials (RCTs) and summarized its possible mechanisms according to animal-based researches. 27 eligible studies were identified in eight database searches from inception to June 2018. The methodological quality was assessed using seven-item checklist recommended by Cochrane Collaboration. All the data were analyzed using Rev-Man 5.3 software. As a result, the score of study quality ranged from 4 to 7 points. Meta-analyses showed CHM can significantly reduce the incidence of myocardial infarction and percutaneous coronary intervention, and cardiovascular mortality ($P < 0.05$), and increase systolic function of heart, the ST-segment depression, and clinical efficacy ($P < 0.05$). Adverse events were reported in 11 studies, and CHMs were well tolerated in patients with CHD. In addition, CHM exerted cardioprotection for CHD, possibly altering multiple signal pathways through anti-inflammatory, anti-oxidation, anti-apoptosis, improving the circulation, and regulating energy metabolism. In conclusion, the evidence available from present study revealed that CHMs are beneficial for CHD and are generally safe.

Keywords: Traditional Chinese medicine, coronary heart disease, high-quality randomized controlled trials, clinical evidence, possible mechanisms, systematic review

INTRODUCTION

Coronary heart disease (CHD) incurs a huge economic burden on healthcare and society (Dunbar et al., 2018). According to the epidemiological data from 1990 to 2013, 92.94 million people were suffering from this disease, which eventually led to 8.1 million deaths (Murray et al., 2015; Roth et al., 2015). Current treatments for CHD include coronary revascularization, drug intervention, risk factor control, cardiac rehabilitation, and lifestyle improvement (Arslan et al., 2018). Among them, percutaneous coronary intervention (PCI) and coronary artery bypass grafting are the most effective (Roffi et al., 2016). However, PCI is mainly for the treatment of locally severe stenotic vessels and has limited therapeutic effect on extensive coronary stenosis and microcirculation lesions (Heusch and Gersh, 2017). Meanwhile, the prognosis of patients treated with PCI is sometimes not ideal because myocardial ischemia/reperfusion injury, no reflow, coronary dissection, stent thrombosis, and acute coronary occlusion still exist (Hausenloy and Yellon, 2013; Arslan et al., 2018). Although

the technology of coronary intervention is still improving and conventional medicine is constantly updating, novel treatments that can stabilize arterial plaque, improve microcirculation, and angina symptoms; prevent acute myocardial infarction; delay the development of ischemic cardiomyopathy; ultimately reduce PCI; and improve prognosis are urgently needed.

Traditional Chinese medicine (TCM) includes herbal medicine (CHM), acupuncture, and other non-pharmacological therapies, which is a holistic approach to health and healing (Xu et al., 2013). CHM has been used to treat CHD for thousands of years, and in modern time, many claimed randomized controlled trials (RCT) have reported some TCM Fufang exerted the cardioprotective function (Han et al., 2008; Gao et al., 2010; Chung et al., 2013; Liu et al., 2013). However, most of these studies are poor methodological quality, leading that there is still insufficient evidence to support routine use of CHMs for CHD. Thus, the Cochrane group guidelines for clinical reviews may exclude the “not-so-good” studies (Chan et al., 2012). In addition, in a TCM reviewing process, researchers may need to include such high-quality studies about a medical certain issue to identify current problems and areas worthy of improvement for its future development (Chan et al., 2012). Thus, we performed a systematic review to assess the efficacy and safety of CHM for CHD according to high-quality studies with at least four domains of “yes” in Cochrane risk of bias (RoB) tool (Li et al., 2015).

METHODS

Search Strategy and Study Selection

Studies estimating the efficacy of CHMs in patients with CHD were systematically searched from EMBASE, PubMed, Cochrane Library, Wangfang database, China National Knowledge Infrastructure (CNKI), VIP database (VIP), and China Biology Medicine disc (CBM) from inception to the end of June 2018. The key words were used as follows: “coronary disease OR acute coronary syndrome OR myocardial infarction OR myocardial ischemia” AND “herb OR traditional Chinese medicine OR Chinese Materia Medica.” Moreover, reference lists of potential articles were searched for relevant studies.

Inclusion and Exclusion Criteria

The inclusion criteria were prespecified as follows: (1) RCTs that investigated the efficacy and safety of CHM for CHD were included. Quasi-randomized trials, such as those in which patients were allocated according to date of birth and order of admission number, were excluded. If a three-arm design was used in a study, we extracted data only for the group(s) involving CHM and the control group(s). (2) All participants were patients with a diagnosis of CHD based on one of the following criteria: (1) The guideline of unstable or stable angina from Chinese cardiovascular association in different years, (2) the guideline of unstable or stable angina from American College of Cardiology (ACC) or American Heart Association (AHA) or European Society of Cardiology (ESC) or World Health Organization (WHO) in different years, (3) be diagnosed by

coronary angiography, (4) patients after PCI, and (5) diagnostic criteria made by other authors with comparable definitions were also used. (3) The treatment interventions included CHMs used as monotherapies or adjunct with conventional medicine (i.e., antiplatelet, stable plaque, control ventricular rate) or supportive treatment (i.e., nutrition support, exercise therapy, psychotherapy). Interventions for control group were restricted to no intervention, placebo, conventional medicine, and supportive treatment. Studies comparing a CHM agent with another CHM agent were excluded. (4) The primary outcome measures were the incidence of myocardial infarction and/or the incidence of PCI and/or cardiovascular mortality and/or the level of ST-segment depression and/or indicators which represent systolic and diastolic function of the heart in cardiac ultrasound. The secondary outcome measures were clinical effective rating, and the safety of co-administration of CHM. The exclusion criteria were prespecified as follows: (1) no predetermined outcome index; (2) compared or combined with other Chinese herb medicine; (3) not randomized, double-blind, placebo-controlled designed; (4) no control group; and (5) double publication.

Data Extraction

Two authors independently reviewed each included study and extracted following aspects of details: (1) name of first author, year of publication; (2) diagnostic criteria; (3) detail information of participants for each study, including sample size, gender composition, and mean age; (4) detail information of treatment and control group, including therapeutic drug dosage, method of administration, and duration of treatment; and (5) outcome measures and intergroup differences. The data of predetermined primary and secondary outcomes were extracted for further qualitative and quantitative syntheses. We made efforts to contact authors for further information when some records' published data were only in graphical format or not in the publication. And the numerical values were measured from the graphs by digital ruler software when response was not received from authors.

Risk of Bias in Individual Studies

The methodological quality of each included study was evaluated by two authors with the seven-item checklist recommended by Cochrane Collaboration (Higgins and Green, 2012). Only RCTs with a cumulative score of at least four points were included in our systematic review. Any disagreements from two authors were dealt with through discussion with the corresponding author (GQZ).

Statistical Analysis

The statistical analysis was conducted *via* RevMan version 5.3. A fixed-effects model (FEM) or random-effects model (REM) was conducted to analyze pooled effects. When the outcome measurements in all included studies in meta-analysis were based on the same scale, weighted mean difference (WMD) with 95% confidence intervals was calculated as a summary statistic, otherwise standard mean difference (SMD) was calculated.

Heterogeneity between study results was investigated based on a standard chi-square test and I^2 statistic. A fixed-effects model ($I^2 < 50\%$) or a random-effects model ($I^2 > 50\%$) was used depending on the value of I^2 . Funnel plots were used to visually estimate publication bias. A probability value 0.05 was considered statistically significant.

CHM Composition and Possible Mechanisms of Active Ingredients

Specific herbs in the CHM formulae were recorded. The frequency of use for particular herb was calculated and those used at a high frequency that are described in detail. Animal-based mechanism studies of active ingredients from frequently used herbs were searched. The following information was recorded for such studies: identity of active ingredients and their herbal sources, suggested mechanisms and implicated signaling pathways, first author's name and publication year of the citation, and structure of active ingredients.

RESULTS

Study Selection

A total of 2,158 studies were retrieved after systematical searches from the database, of which 287 were reduplicated and irrelevant studies. After screening title and abstract, 180 were excluded because they were: (1) animal trial, (2) case report, (3) review article, and (4) meeting abstract. After reviewing the full text of the remaining 87 articles, 60 studies were excluded if: (1) no predetermined outcome index; (2) compared or combined with other CHM; (3) not randomized, double-blind, and placebo-controlled designed; (4) no control group; (5) double publication; and (6) data of result was not available. Ultimately, 27 studies with Cochrane RoB score ≥ 4 (Lu et al., 2006; Qiao et al., 2006; Lu et al., 2008; Cheng et al., 2009; Chu et al., 2010; Qiu et al., 2009; Wang et al., 2009; Zhang et al., 2010; Shang et al., 2011; Mo et al., 2012; Wang S. H. et al., 2012; Wang Y. G. et al., 2012; Chen et al., 2013; Shang et al., 2013; Hu et al., 2014; Liu et al., 2014; Lu et al., 2014; Sun, 2014; Xu et al., 2014; Xu et al., 2015; Zhang et al., 2015; Duan et al., 2016; Mao et al., 2016; Wang et al., 2016; Zhu et al., 2016; Wang et al., 2017; Yang et al., 2017) were selected (Figure 1).

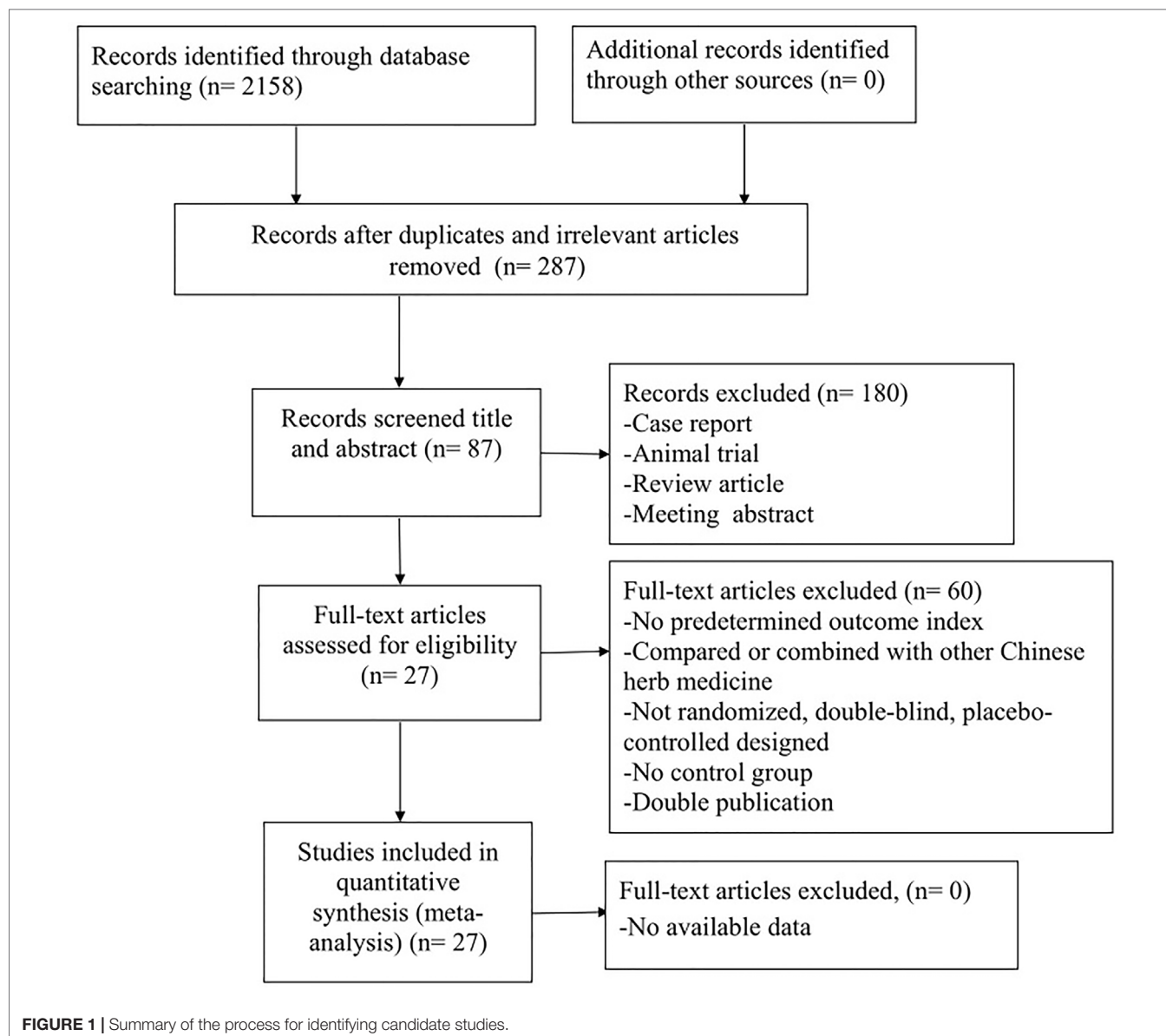
Characteristics of Included Studies

17 studies (Lu et al., 2006; Qiao et al., 2006; Cheng et al., 2009; Chu et al., 2010; Qiu et al., 2009; Mo et al., 2012; Wang S. H. et al., 2012; Wang Y. G. et al., 2012; Chen et al., 2013; Hu et al., 2014; Liu et al., 2014; Lu et al., 2014; Sun, 2014; Xu et al., 2014; Xu et al., 2015; Duan et al., 2016; Zhu et al., 2016; Wang et al., 2017; Yang et al., 2017) were published in Chinese and 10 studies (Lu et al., 2008; Wang et al., 2009; Zhang et al., 2010; Chu et al., 2010; Shang et al., 2011; Shang et al., 2013; Xu et al., 2015; Zhang et al., 2015; Mao et al., 2016; Wang et al., 2016) in English between 2006 and 2017. All studies were conducted in China. The sample size of the included studies ranged from 57 to 4,870 with a total of 11,732 participants, including 5,916 patients in treatment groups and 5,816 patients serving as controls. Of 27

included studies, 18 studies (Cheng et al., 2009; Qiu et al., 2009; Wang et al., 2009; Shang et al., 2011; Mo et al., 2012; Wang S. H. et al., 2012; Shang et al., 2013; Hu et al., 2014; Liu et al., 2014; Sun, 2014; Xu et al., 2014; Zhang et al., 2015; Duan et al., 2016; Wang et al., 2016; Zhu et al., 2016; Wang et al., 2017; Yang et al., 2017) were based on patients with angina pectoris of CHD and nine studies (Lu et al., 2006; Qiao et al., 2006; Lu et al., 2008; Chu et al., 2010; Zhang et al., 2010; Chen et al., 2013; Lu et al., 2014; Xu et al., 2015; Mao et al., 2016) were based on patients with acute coronary syndrome. Comparisons of CHM plus a conventional treatment (i.e., antiplatelet, stable plaque, control ventricular rate) *versus* a conventional treatment were conducted in 26 trials, and comparisons of CHM *versus* a placebo were performed in one trial (Hu et al., 2014). The CHMs were administered orally (i.e., tablets, capsules, granules, or decoction). The duration of follow-up was varied from 4 weeks to 4.5 years. All studies accounted for baseline comparability. The incidence of myocardial infarction (MI) was utilized as outcome measure in 10 studies (Lu et al., 2006; Lu et al., 2008; Wang et al., 2009; Shang et al., 2011; Shang et al., 2013; Lu et al., 2014; Sun, 2014; Xu et al., 2015; Mao et al., 2016; Wang et al., 2016), the incidence of PCI in five studies (Lu et al., 2006; Lu et al., 2008; Wang et al., 2009; Shang et al., 2013; Wang et al., 2016), cardiovascular mortality in seven studies (Lu et al., 2008; Wang et al., 2009; Shang et al., 2013; Sun, 2014; Xu et al., 2015; Mao et al., 2016; Wang et al., 2016), left ventricular ejection fraction (LVEF) in five studies (Qiao et al., 2006; Qiu et al., 2009; Chen et al., 2013; Sun, 2014; Mao et al., 2016), the ventricular wall motion score in two studies (Qiao et al., 2006; Chen et al., 2013), and the level of ST-segment elevation in three studies (Chu et al., 2010; Hu et al., 2014; Sun, 2014). The efficiency of angina improved was reported in 12 studies (Lu et al., 2006; Chu et al., 2010; Shang et al., 2011; Mo et al., 2012; Wang S. H. et al., 2012; Hu et al., 2014; Lu et al., 2014; Sun, 2014; Zhang et al., 2015; Duan et al., 2016; Zhu et al., 2016; Yang et al., 2017), the usage of nitroglycerin in two studies (Sun, 2014; Xu et al., 2014), low-density lipoprotein (LDL) in four studies (Lu et al., 2008; Wang Y. G. et al., 2012; Zhu et al., 2016; Wang et al., 2017), hypersensitive C-reactive protein (hsCRP) in two studies (Mo et al., 2012; Wang S. H. et al., 2012), the degree of coronary artery stenosis in two studies (Lu et al., 2006; Yang et al., 2017), and the rate of coronary restenosis in two studies (Shang et al., 2011; Lu et al., 2014). The overall characteristics of included studies are shown in Table 1.

Study Quality

The quality score of study ranged from 4 to 7 in a total of 7 points. Of which, six studies (Lu et al., 2006; Chu et al., 2010; Wang et al., 2009; Liu et al., 2014; Xu et al., 2015; Wang et al., 2016) got 7 points, three studies (Zhang et al., 2015; Duan et al., 2016; Mao et al., 2016) got 6 points, 15 studies (Qiao et al., 2006; Lu et al., 2008; Cheng et al., 2009; Qiu et al., 2009; Zhang et al., 2010; Shang et al., 2011; Mo et al., 2012; Wang S. H. et al., 2012; Chen et al., 2013; Shang et al., 2013; Hu et al., 2014; Xu et al., 2014; Zhu et al., 2016; Wang et al., 2017) got 5 points, and three studies (Lu et al., 2014; Sun, 2014; Yang et al., 2017) got 4 points. All 27 included studies had random allocation, including 10 (Qiao et al., 2006; Cheng et al., 2009; Qiu et al., 2009; Mo et al., 2012; Wang S. H.



et al., 2012; Chen et al., 2013; Lu et al., 2014; Sun, 2014; Zhu et al., 2016) in which a random number table was used, eight (Lu et al., 2006; Chu et al., 2010; Wang et al., 2009; Shang et al., 2011; Wang Y. G. et al., 2012; Liu et al., 2014; Duan et al., 2016; Wang et al., 2017) that employed a computer generated random sample set, three (Xu et al., 2015; Zhang et al., 2015; Wang et al., 2016) that applied block randomization, and six (Lu et al., 2008; Zhang et al., 2010; Shang et al., 2013; Hu et al., 2014; Xu et al., 2014; Mao et al., 2016) that stated that randomization was used without providing methodological details. Of the 27 included studies, all studies reported blinding of participants and personnel and withdraw bias. Additionally, nine studies (Lu et al., 2006; Chu et al., 2010; Wang et al., 2009; Liu et al., 2014; Xu et al., 2015; Zhang et al., 2015; Duan et al., 2016; Mao et al., 2016; Wang et al., 2016) reported using allocation concealment; eight studies (Lu et al., 2006; Chu et al., 2010; Wang et al., 2009; Liu et al., 2014; Xu et al., 2015;

Zhang et al., 2015; Duan et al., 2016; Wang et al., 2016) applied blinding specifically during outcome measure assessment, and 22 studies (Lu et al., 2006; Qiao et al., 2006; Lu et al., 2008; Cheng et al., 2009; Chu et al., 2010; Qiu et al., 2009; Wang et al., 2009; Zhang et al., 2010; Shang et al., 2011; Mo et al., 2012; Wang S. H. et al., 2012; Chen et al., 2013; Shang et al., 2013; Hu et al., 2014; Liu et al., 2014; Xu et al., 2014; Xu et al., 2015; Mao et al., 2016; Wang et al., 2016; Zhu et al., 2016; Wang et al., 2017) reported selective reporting. No study provided sample size estimation information. The methodological quality is concluded in **Table 2**.

Effectiveness

The Incidence of MI and PCI

Meta-analysis of 10 studies (Lu et al., 2006; Lu et al., 2008; Wang et al., 2009; Shang et al., 2011; Shang et al., 2013; Lu et al., 2014;

TABLE 1 | Characteristics of the 27 included studies.

Study (years)	Diagnostic criteria	Number of participants (male/female), mean age (years)		Interventions		Conventional medicine or basic treatment	Duration of treatment	Outcome index	Intergroup differences
		Trial	Control	Trial	Control				
Lu et al., 2006	After PCI	60 58.94 ± 10.79	58 57.1 ± 9.81	Xiongshao capsule (0.5g, tid, p.o).	Placebo	Clopidogrel, aspirin; atorvastatin, low molecular weight heparin	6 months	1. Cardiovascular mortality 2. The rate of coronary restenosis 3. The degree of coronary artery stenosis 4. The efficiency of angina pectoris 5. Myocardial infarction rate 6. The incidence of PCI	1. P < 0.05 2. P < 0.05 3. P < 0.05 4. P < 0.05 5. P < 0.05 6. P < 0.05
Qiao et al., 2006	After PCI	30 (17/13) 64.0 ± 11.2	29 (18/11) 65.7 ± 12.2	Tongguan capsule (three doses, tid, p.o).	Placebo	Anticoagulant, antiplatelet, anti-infection	1 month	1. LVEF 2. The ventricular wall motion score 3. Survey of angina pectoris in Seattle	1. P < 0.05 2. P < 0.05 3. P < 0.05
Lu et al., 2008	Documented previous myocardial infarction	2,429 58.35 ± 9.02	2,441 58.35 ± 9.02	Xuezhikang capsule (0.6g, bid, p.o).	Placebo	Other drugs that do not affect blood lipids	4.5 years	1. Myocardial infarction rate 2. Cardiovascular mortality 3. The incidence of PCI 4. TC 5. TG 6. HDL-C 7. LDL-C	1. P < 0.05 2. P < 0.05 3. P < 0.05 4. P < 0.01 5. P < 0.01 6. P < 0.01 7. P < 0.01
Cheng et al., 2009	The guideline of chronic stable angina from China, 2007	41 (37/4) 49.97 ± 6.19	41 (39/2) 51.12 ± 7.33	Qingre Quyu granule (6g, bid, p.o).	Placebo	Aspirin, bisoprolol fumarate, isosorbide dinitrate sustained release tablets	25 weeks	1. Number of atherosclerotic plaques 2. Arterial plaque score 3. Intima thickness of carotid artery 4. hsCRP	1. P < 0.05 2. P < 0.05 3. P < 0.05 4. P < 0.05
Qiu et al., 2009	The guideline of acute myocardial infarction from China, 2001	51 (45/6) 57.82 ± 10.23	52 (44/8) 55.79 ± 11.06	Compound <i>Salvia</i> tablet and Xinyue capsule	Placebo	Antiplatelet agents, anticoagulant, β blocker, angiotensin converting enzyme inhibitor, nitrates, and lipid-regulating drugs	3 months	1. LVEF	1. P < 0.05
Wang et al., 2009	The guideline of unstable angina pectoris from ACC/AHA USA, 2002	32 (12/20) 61.65 ± 8.15	31 (13/18) 64.47 ± 9.21	Shenshao tablet (0.3g, qd, p.o).	Placebo	Aspirin, isosorbide, mononitrate, simvastatin, Benner Pury, amlodipine, metoprolol	4 weeks	1. Frequency of angina pectoris 2. Seattle score 3. The incidence of PCI 4. Acute myocardial infarction rate	1. P < 0.05 2. P < 0.05 3. P > 0.05 4. P > 0.05
Chu et al., 2010	After PCI	28 (18/10); 61.7 ± 9.6	29 (20/9); 58.8 ± 8.9	Xuefu Zhuyu capsule	Placebo	Clopidogrel, aspirin, low molecular weight heparin, metoprolol tartrate, atorvastatin	4 weeks	1. The efficiency of angina pectoris 2. Electrocardiogram curative effect 3. Survey of angina pectoris in Seattle	1. P < 0.05 2. P < 0.05 3. P < 0.05

(Continued)

TABLE 1 | Continued

Study (years)	Diagnostic criteria	Number of participants (male/female), mean age (years)		Interventions		Conventional medicine or basic treatment	Duration of treatment	Outcome index	Intergroup differences
		Trial	Control	Trial	Control				
Zhang et al., 2010	The guideline of segment elevation myocardial infarction from WHO	108 (92/16) 58.5 ± 10.6	111 (96/15) 57.6 ± 11.2	Tongxinluo (2.08g, qd, p.o).	Placebo	Aspirin, clopidogrel	180 days	1. The incidence of no reflow of myocardium	1. P = 0.0031
Shang et al., 2011	The guideline of stable angina pectoris from WHO	73 (50/23) 67.79 ± 4.77	79 (52/27) 66.7 ± 4.16	Chuangxiongol (250mg, tid, p.o).	Placebo	Aspirin, tilopidine, diltiazem, nitroglycerin, heparin	6 months	1. Restenosis rate 2. The efficiency of angina pectoris 3. Cardiovascular mortality 4. Acute myocardial infarction rate 5. The incidence of PCI	1. P > 0.05 2. P < 0.01 3. P > 0.05 4. P > 0.05 5. P > 0.05
Mo et al., 2012	The guideline of criteria for the naming and diagnosis of ischemic heart disease	60 (43/17) 67.15 ± 4.87	60 (42/18) 66.22 ± 5.12	Yixin Mai granule (one dose, tid, p.o).	Placebo	Isosorbide, metoprolol, fosinopril, aspirin	4 weeks	1. hsCRP 2. IL-6 3. IL-18 4. The efficiency of angina pectoris	1. P < 0.01 2. P < 0.01 3. P < 0.01 4. P = 0.037
Wang S. H. et al., 2012	The guideline of unstable angina pectoris from ACC/AHA USA, 2002	33 (26/7) 60.2 ± 9	33 (25/8) 62.7 ± 7.1	Tablets of betel (1.5g, bid, p.o).	Placebo	Aspirin, simvastatin, isosorbide, dinitrate	28 days	1. The efficiency of angina pectoris 2. Electrocardiogram efficiency 3. Nitroglycerin consumption 4. hsCRP 5. sCD40L	1. P < 0.05 2. P > 0.05 3. P < 0.05 4. P < 0.05 5. P < 0.05
Wang Y. G. et al., 2012	The guideline of chronic stable angina from China, 2007	76	72	Double ginseng capsule and Tongguan capsule (four doses, tid, p.o).	Placebo	Original treatment	6 months	1. TG 2. TC 3. HDL-C 4. LDL-C	1. P < 0.05 2. P > 0.05 3. P < 0.05 4. P < 0.05
Chen et al., 2013	After PCI	30 (17/13) 65.5 ± 7.5	30 (16/14) 63.8 ± 6.3	Tongguan capsule (three doses, tid, p.o).	Placebo	Clopidogrel, aspirin, low molecular weight heparin	3 months	1. LVEF 2. The ventricular wall motion score 3. The number of endothelial progenitor cell in peripheral blood	1. P < 0.05 2. P < 0.05 3. P < 0.05
Shang et al., 2013	The guideline of chronic stable angina from China, 2004	1,746 (1,191/555) 58.35 ± 9.02	1,759 (1,260/499) 58.28 ± 8.99	QSYQ (0.5g, tid, p.o).	Placebo	Antihypertensive drugs, hypoglycemic agent, lipid-lowering medicine	12 months	1. Cardiovascular mortality 2. Myocardial infarction rate 3. The incidence of PCI	1. P > 0.05 2. P > 0.05 3. P > 0.05
Hu et al., 2014	The guideline of chronic stable angina from China, 2007	192 57.82 ± 10.23	99 57.82 ± 10.23	Reachable film (three doses, tid, p.o).	Placebo	NM	4 weeks	1. The efficiency of angina pectoris 2. The total curative effect of TCM Syndrome 3. Electrocardiogram efficiency	1. P < 0.05 2. P < 0.05 3. P < 0.05

(Continued)

TABLE 1 | Continued

Study (years)	Diagnostic criteria	Number of participants (male/female), mean age (years)		Interventions		Conventional medicine or basic treatment	Duration of treatment	Outcome index	Intergroup differences
		Trial	Control	Trial	Control				
Liu et al., 2014	The guideline of chronic stable angina from China, 2007	120 59.21 ± 7.92	120 60.64 ± 7.69	Chek Shincen Tongxin granule	Placebo	Aspirin, atorvastatin	4 weeks	1. Body limitation 2. Stable state of angina pectoris 3. Episodes of angina pectoris 4. Satisfaction with treatment 5. The degree of understanding of disease 6. Electrocardiogram efficiency	1. P < 0.05 2. P < 0.05 3. P < 0.05 4. P < 0.05 5. P < 0.05 6. P < 0.05
Lu et al., 2014	After PCI	90 (48/42) 60.2 ± 6.9	90 (46/44) 61.8 ± 7.2	Tongxinluo capsule (three doses, tid, p.o).	Placebo	Original treatment	12 months	1. The incidence of coronary restenosis 2. The degree of coronary restenosis 3. The efficiency of angina pectoris 4. Myocardial infarction rate 5. Cardiovascular mortality	1. P < 0.05 2. P < 0.01 3. P = 0.04 4. P = 0.19 5. P > 0.05
Sun, 2014	The guideline of chronic unstable angina from China, 2007	64 (42/22) 70.81 ± 10.76	64 (44/20) 69.8 ± 10.98	Musk Baixin pill (two doses, tid, p.o).	Placebo	Isosorbide dinitrate tablets, atorvastatin, thiazepine, enteric aspirin	6 months	1. The efficiency of angina pectoris 2. Myocardial infarction rate 3. Cardiovascular mortality 4. Nitroglycerin consumption 5. Electrocardiogram efficiency 6. LVEF	1. P < 0.05 2. P < 0.05 3. P > 0.05 4. P < 0.01 5. P < 0.05 6. P < 0.05
Xu et al., 2014	The guideline of unstable angina pectoris from ACC/AHA USA, 2002	55 (29/26) 69.47 ± 8	59 (33/26) 70.41 ± 8.6	Shenzhu Guanxin recipe (12g, qd, p.o).	Placebo	Conventional western medicine (unspecified)	12 weeks	1. The efficiency of angina pectoris 2. The duration of angina pectoris 3. Total use of nitroglycerin 4. The degree of physical activity induced by angina pectoris 5. The degree of angina pectoris	1. P < 0.05 2. P < 0.05 3. P < 0.05 4. P < 0.05 5. P < 0.01
Xu et al., 2015	After PCI	113 (86/27) 70.35 ± 9.61	74 (51/23) 68.08 ± 10.38	Shenzhu Guanxin recipe	Placebo	Aspirin, ticlopidine, diltiazem, glyceryl, trinitrate, heparin	3 months	1. Angina pectoris score 2. Cardiovascular mortality 3. Myocardial ischemia rate	1. P = 0.66 2. P = 0.33 3. P = 0.63
Zhang et al., 2015	The guideline of unstable angina pectoris from ACC/AHA USA, 2002	119 (56/63) 59.46 ± 6.524	120 (52/68) 58.82 ± 7.061	Wufuxinnaoqing capsules	Placebo	Antiplatelet, aggregation, ACEI or ARB, statin two hydrogen arsenide	12 weeks	1. The efficiency of angina pectoris 2. Nitroglycerin consumption	1. P < 0.01 2. P < 0.01

(Continued)

TABLE 1 | Continued

Study (years)	Diagnostic criteria	Number of participants (male/female), mean age (years)		Interventions		Conventional medicine or basic treatment	Duration of treatment	Outcome index	Intergroup differences
		Trial	Control	Trial	Control				
Duan et al., 2016	The guideline of chronic stable angina from China, 2007	64 (38/26) 59.7 ± 6.34	67 (47/20) 60.7 ± 6.44	Live heart pill (two doses, tid, p.o).	Placebo	Conventional western medicine (unspecified)	8 weeks	1. Symptom score of angina pectoris 2. Nitroglycerin consumption 3. Electrocardiogram plate movement 4. Seattle scale 5. Syndromes of traditional Chinese Medicine 6. hsCRP 7. Blood lipid	1. P < 0.01 2. P < 0.01 3. P < 0.01 4. P < 0.01 5. P < 0.01 6. P > 0.05 7. P > 0.05
Mao et al., 2016	After PCI	42 67.54 ± 8.39	41 68.38 ± 10.41	Danlou tablet	Placebo	Conventional western medicine (unspecified)	90 days	1. Left ventricular end diastolic volume index 2. End systolic volume index of left ventricle 3. LVEF 4. Cardiovascular mortality 5. Myocardial infarction rate	1. P < 0.001 2. P < 0.001 3. P < 0.001 4. P < 0.05 5. P < 0.05
Wang et al., 2016	The guideline of unstable angina pectoris from ACCF/AHA USA, 2007	109 (72/37) 62.89 ± 9.23	110 (74/36) 63.89 ± 10.03	Danlou tablet (4.5g, qd, p.o).	Placebo	Antiplatelet, aggregation, anticoagulant, lipid-lowering, improvement of myocardial, remodeling, step-down	90 days	1. Cardiovascular mortality 2. Myocardial infarction rate 3. Reconstructive rate of blood vessels 4. Troponin 5. hsCRP	1. P > 0.05 2. P = 0.04 3. P > 0.05 4. P > 0.05 5. P > 0.05
Zhu et al., 2016	The guideline of chronic stable angina from China, 2007	76 (48/28) 51.8 ± 1.6	74 (46/28) 51.5 ± 1.4	Traditional Chinese medicine prescription (10 mg, tid, p.o).	Placebo	Isosorbide, aspirin, atorvastatin	4 weeks	1. The efficiency of angina pectoris 2. Electrocardiogram efficiency 3. TG 4. TC 5. HDL-C 6. LDL-C 7. TCM syndrome score	1. P < 0.05 2. P < 0.05 3. P < 0.05 4. P < 0.05 5. P < 0.05 6. P < 0.05 7. P < 0.05
Wang et al., 2017	The guideline of unstable angina pectoris from ACC/AHA USA, 2011	40 (17/23) 70.68 ± 6.87	40 (21/19) 71.65 ± 4.32	Xuesaitong soft capsule (0.66g, bid, p.o).	Placebo	Conventional western medicine (unspecified)	4 weeks	1. TC 2. TG 3. HDL 4. LDL 5. Survey of angina pectoris in Seattle	1. P < 0.05 2. P < 0.05 3. P < 0.05 4. P < 0.05 5. P < 0.05
Yang et al., 2017	The guideline of chronic stable angina from China, 2014	33 (20/13) 61.18 ± 6.61	33 (21/12) 61.03 ± 7.51	Coronary Ningtong prescription	Placebo	Aspirin enteric-coated tablets, simvastatin tablets, isosorbide mononitrate, metoprolol	24 weeks	1. Coronary stenosis 2. The efficiency of angina pectoris	1. P < 0.05 2. P < 0.05

PCI, percutaneous coronary intervention; LVEF, left ventricular ejection fraction; hsCRP, high sensitive C reactive protein; TC, total cholesterol; TG, total glycerol three fat; HDL, high density lipoprotein; LDL, low density lipoprotein; STEMI, segment elevation myocardial infarction; WHO, world health organization; NM, not mention; QSYQ, Qi-Shen-Yi-Qi dripping pills.

TABLE 2 | Quality assessment of included studies.

Study	A	B	C	D	E	F	G	Total
Lu et al., 2006	1	1	1	1	1	1	1	7
Qiao et al., 2006	1	0	1	0	1	1	1	5
Lu et al., 2008	1	0	1	0	1	1	1	5
Chu et al., 2010	1	1	1	1	1	1	1	7
Cheng et al., 2009	1	0	1	0	1	1	1	5
Qiu et al., 2009	1	0	1	0	1	1	1	5
Wang et al., 2009	1	1	1	1	1	1	1	7
Zhang et al., 2010	1	0	1	0	1	1	1	5
Shang et al., 2011	1	0	1	0	1	1	1	5
Mo et al., 2012	1	0	1	0	1	1	1	5
Wang S. H. et al., 2012	1	0	1	0	1	1	1	5
Wang Y. G. et al., 2012	1	0	1	0	1	1	1	5
Chen et al., 2013	1	0	1	0	1	1	1	5
Shang et al., 2013	1	0	1	0	1	1	1	5
Lu et al., 2014	1	0	1	0	1	0	1	4
Hu et al., 2014	1	0	1	0	1	1	1	5
Liu et al., 2014	1	1	1	1	1	1	1	7
Sun, 2014	1	0	1	0	1	0	1	4
Xu et al., 2014	1	0	1	0	1	1	1	5
Xu et al., 2015	1	1	1	1	1	1	1	7
Zhang et al., 2015	1	1	1	1	1	0	1	6
Duan et al., 2016	1	1	1	1	1	0	1	6
Mao et al., 2016	1	1	1	0	1	1	1	6
Wang et al., 2016	1	1	1	1	1	1	1	7
Zhu et al., 2016	1	0	1	0	1	1	1	5
Wang et al., 2017	1	0	1	0	1	1	1	5
Yang et al., 2017	1	0	1	0	1	0	1	4

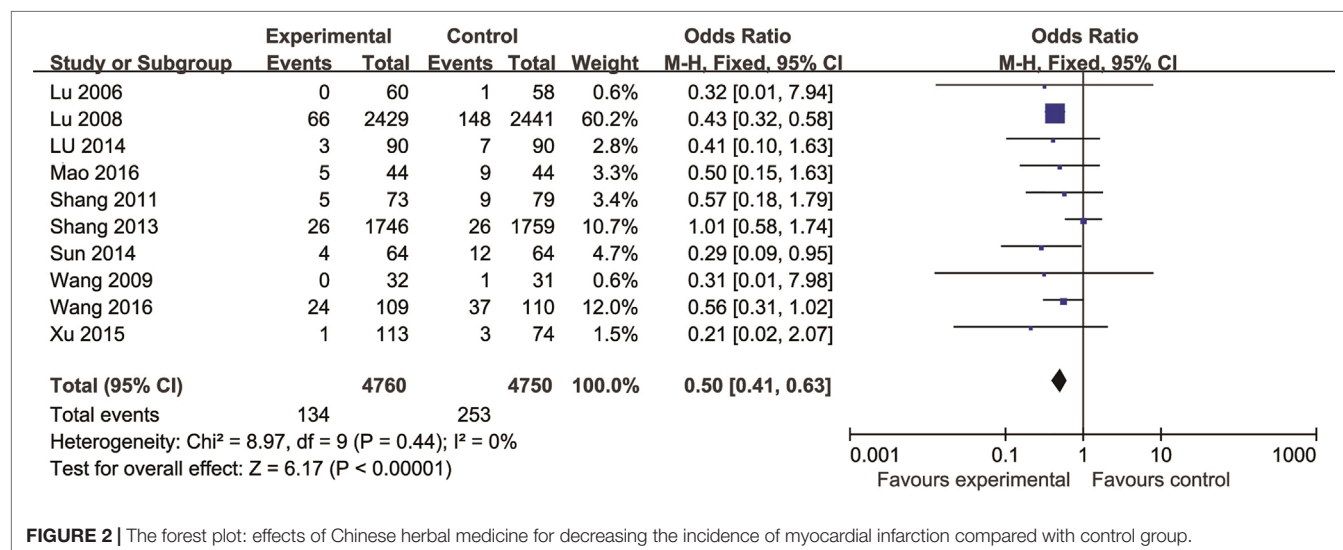
A, adequate sequence generation; B, concealment of allocation; C, blinding of participants and personnel; D, blinding of outcome assessment; E, incomplete out-come data; F, selective reporting; G, other bias; 1, low risk of bias, the information of the domain was adequate in the text; 0, high risk of bias, the information of the domain was inadequate in the text.

Sun, 2014; Xu et al., 2015; Mao et al., 2016; Wang et al., 2016) found a significant difference in favor of CHM for decreasing the incidence of MI compared with control group (n = 9510, OR = 0.50, 95% CI (0.41, 0.63), $P < 0.00001$, $I^2 = 0\%$) (Figure 2). Meta-analysis of five studies (Lu et al., 2006; Lu et al., 2008; Wang et al., 2009; Shang et al., 2013; Wang et al., 2016) showed CHM existed significant effect for decreasing the incidence of PCI compared

with control group (n = 8775, OR = 0.66, 95% CI (0.51, 0.86), $P = 0.002$, $I^2 = 0\%$) (Figure 3).

Cardiovascular Mortality

Seven studies (Wang et al., 2009; Shang et al., 2013; Sun, 2014; Xu et al., 2015; Mao et al., 2016; Wang et al., 2016) reported

**FIGURE 2 |** The forest plot: effects of Chinese herbal medicine for decreasing the incidence of myocardial infarction compared with control group.

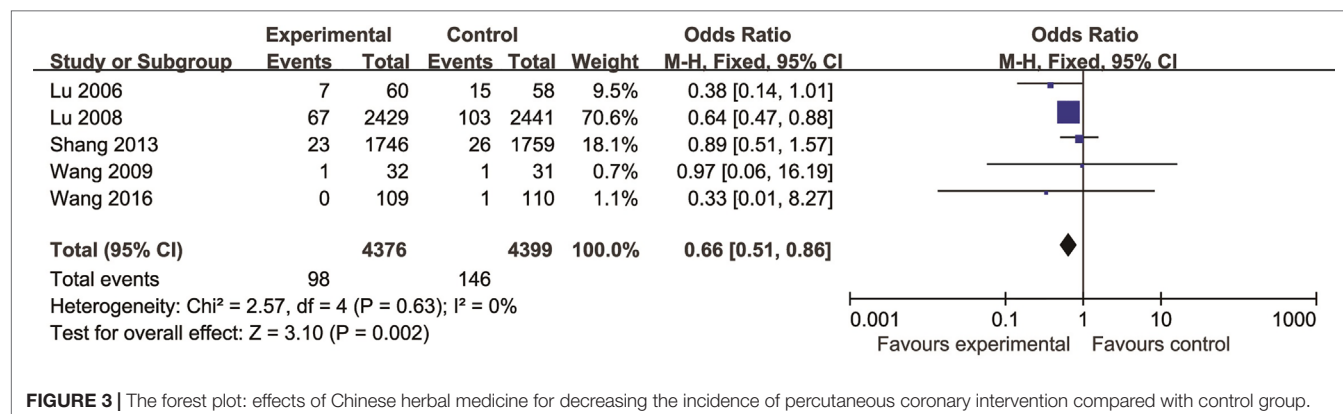


FIGURE 3 | The forest plot: effects of Chinese herbal medicine for decreasing the incidence of percutaneous coronary intervention compared with control group.

cardiovascular mortality as the outcome measure. Of which, there were no deaths were found in three studies (Lu et al., 2008; Wang et al., 2009; Wang et al., 2016). Meta-analysis of remaining four studies (Shang et al., 2013; Sun, 2014; Xu et al., 2015; Mao et al., 2016) showed CHM existed significant effect for decreasing cardiovascular mortality compared with control group ($n = 9,060$, $OR = 0.73$, 95% CI: 0.58, 0.93, $P = 0.009$, $I^2 = 15\%$) (Figure 4).

Systolic and Diastolic Functions of the Heart in Cardiac Ultrasound and the Level of ST-Segment Depression in Electrocardiogram

For systolic function, five studies (Qiao et al., 2006; Qiu et al., 2009; Chen et al., 2013; Sun, 2014; Mao et al., 2016) showed CHM existed significant effect for increasing LVEF compared with control group ($P < 0.05$). For diastolic function, there was no study involving related indicators as outcome measure. Two studies (Qiao et al., 2006; Chen et al., 2013) showed that CHM could decrease the ventricular wall motion score compared with control ($P < 0.05$). In addition, meta-analysis of three studies (Chu et al., 2010; Hu et al., 2014; Sun, 2014) reported that CHM can increase degree of decline in the ST-segment compared with control ($n = 473$, $OR = 2.51$, 95% CI: 1.64~3.83, $P < 0.0001$, $I^2 = 0\%$) (Figure 5).

Clinical Efficacy

Compared with controls, meta-analysis of 12 studies (Lu et al., 2006; Chu et al., 2010; Shang et al., 2011; Mo et al., 2012; Wang S. H. et al., 2012; Hu et al., 2014; Lu et al., 2014; Sun, 2014; Zhang et al., 2015; Duan et al., 2016; Zhu et al., 2016; Yang et al., 2017) showed that the efficiency of angina improved more obviously in the TCM group than that in the control group ($n = 1711$, $OR = 0.21$, 95% CI: 0.17~0.26, $P = 0.09$, $I^2 = 41\%$) (Figure 6); two studies (Sun, 2014; Xu et al., 2014) for reducing the usage of nitroglycerin ($n = 242$, $MD = -0.71$, 95% CI: -0.91~-0.51, $P < 0.00001$, $I^2 = 0\%$) (Figure 7), four studies (Lu et al., 2008; Wang Y. G. et al., 2012; Zhu et al., 2016; Wang et al., 2017) for reducing LDL ($n = 5,248$, $SMD = -0.67$, 95% CI: -0.73~-0.61, $P < 0.00001$, $I^2 = 0\%$) (Figure 8), two studies (Mo et al., 2012; Wang S. H. et al., 2012) for reducing hsCRP ($n = 182$, $OR = -0.95$, 95% CI: -1.26~-0.64, $P < 0.00001$, $I^2 = 0\%$) (Figure 9), two studies (Lu et al., 2006; Yang et al., 2017) for reducing the degree of coronary artery stenosis ($P < 0.05$), and two studies (Shang et al., 2011; Lu et al., 2014) for reducing the rate of coronary restenosis ($P < 0.05$).

The Safety of Co-Administration of CHM

Adverse events were reported in 11 studies (Lu et al., 2006; Chu et al., 2010; Wang et al., 2009; Zhang et al., 2010; Shang et al.,

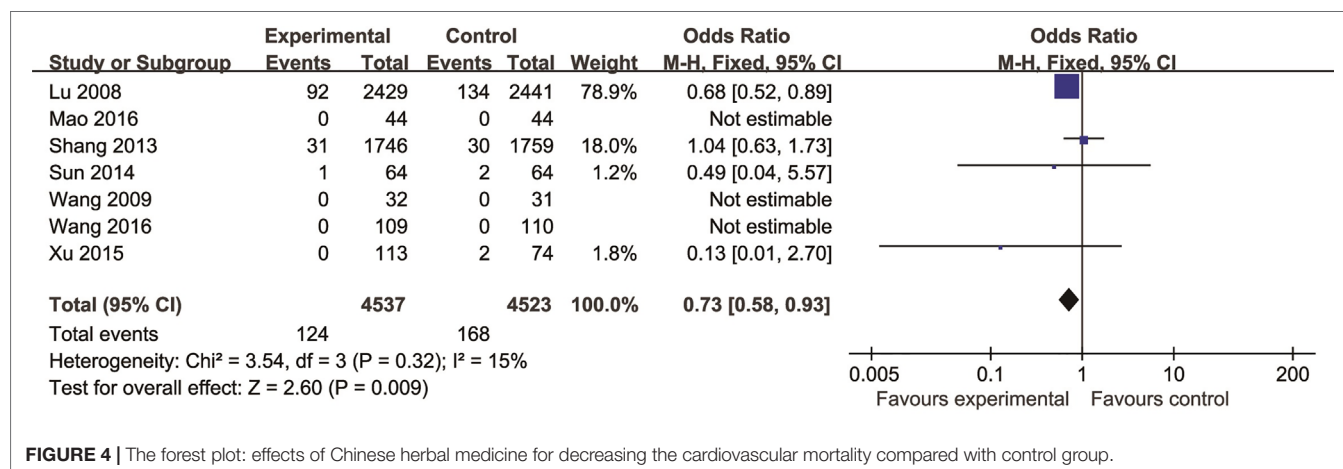
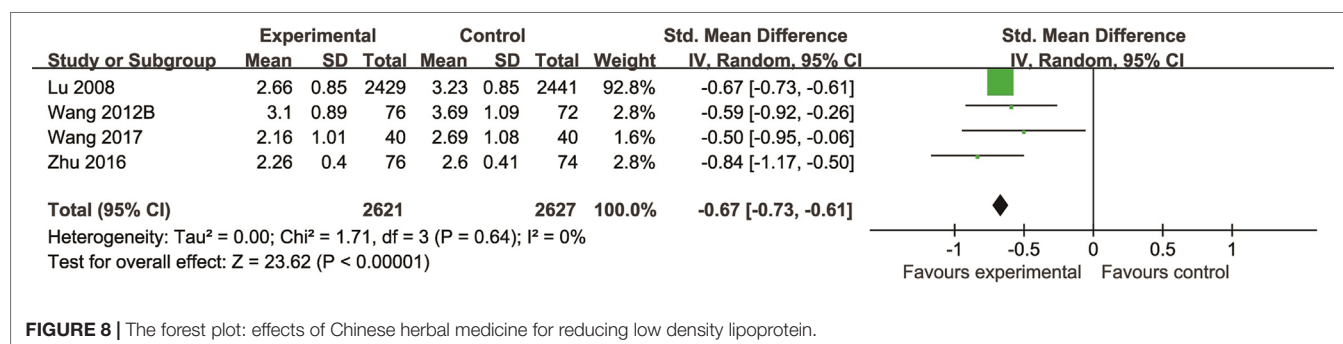
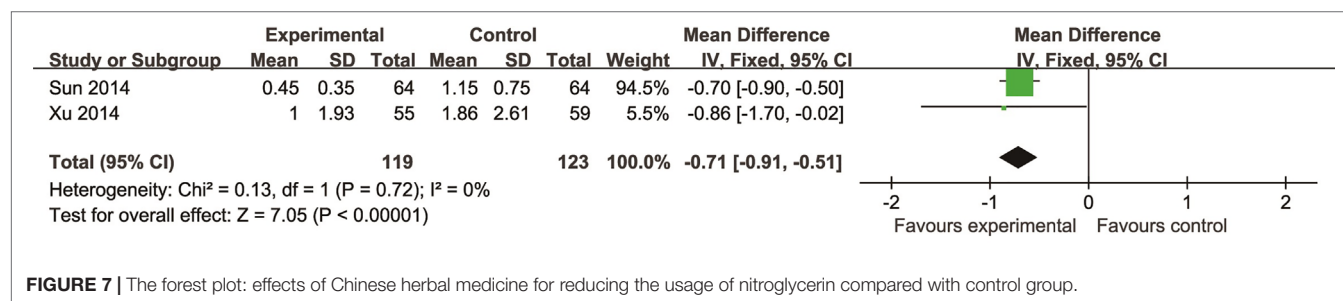
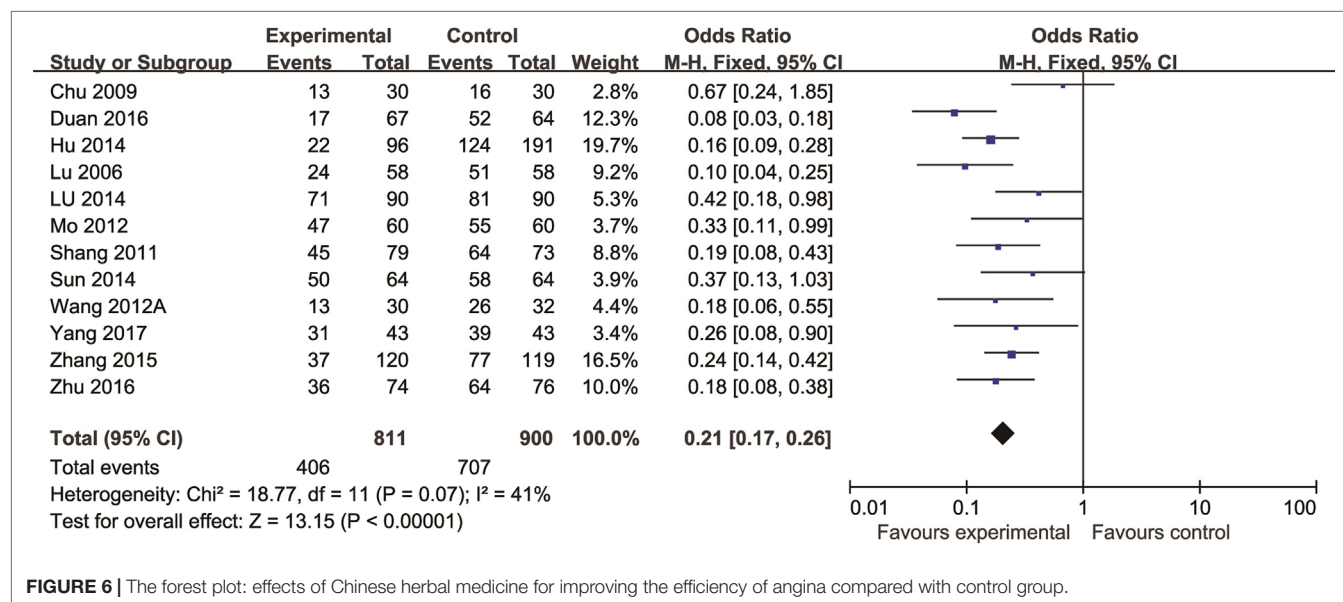
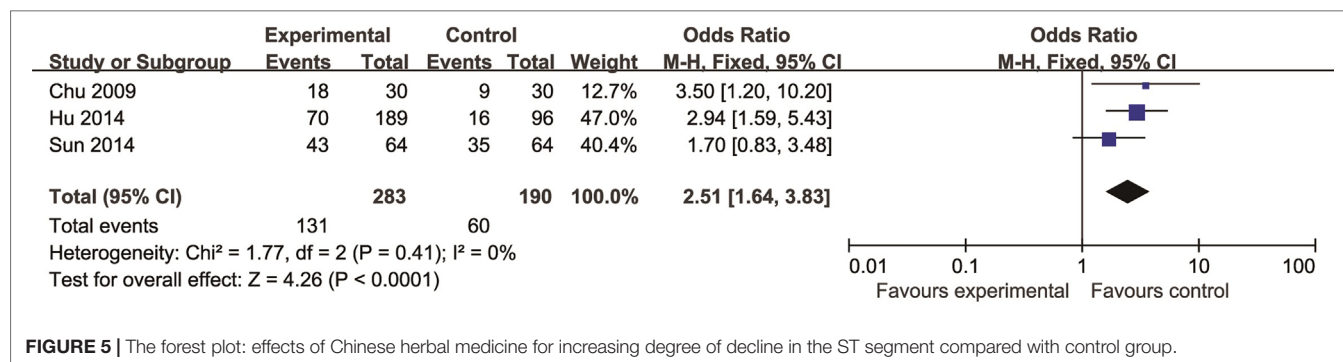
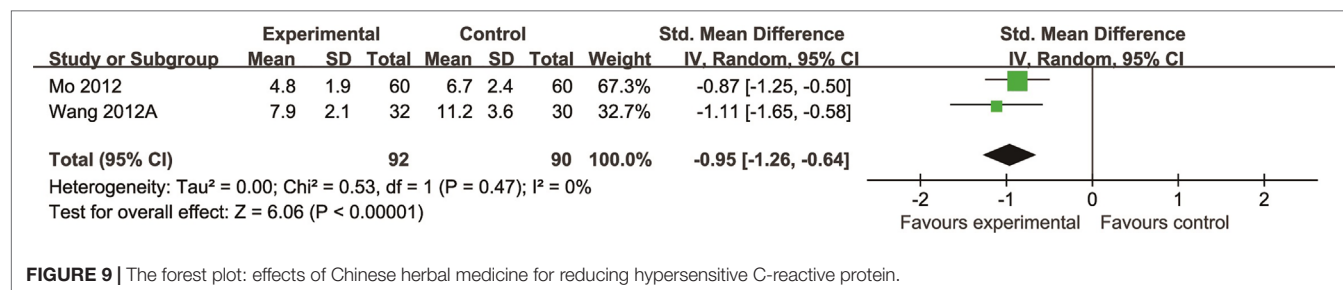


FIGURE 4 | The forest plot: effects of Chinese herbal medicine for decreasing the cardiovascular mortality compared with control group.





2011; Shang et al., 2013; Sun, 2014; Zhang et al., 2015; Wang et al., 2016; Zhu et al., 2016; Yang et al., 2017), analyzed but not observed in four studies (Lu et al., 2008; Cheng et al., 2009; Chen et al., 2013; Liu et al., 2014), and not analyzed in 12 studies (Qiao et al., 2006; Qiu et al., 2009; Mo et al., 2012; Wang S. H. et al., 2012; Wang Y. G. et al., 2012; Lu et al., 2014; Hu et al., 2014; Xu et al., 2014; Xu et al., 2015; Duan et al., 2016; Mao et al., 2016; Wang et al., 2017). In the 11 studies with adequate information about adverse events, a total of 106/5,134 (2.06%) patients suffered adverse events in the treatment groups and 118/5,167 (2.28%) patients in control groups. Gastrointestinal discomfort symptoms, including nausea, stomachache, vomiting, diarrhea, anorexia, and constipation, were the most frequently occurring adverse events, affecting 74/106 (69.8%) patients in the treatment groups and 80/118 (67.8%) in control group patients. Allergy, hemorrhage, hepatic insufficiency, headache, and urinary tract infection were reported frequently also, affecting 20/106 (18.8%) patients in the treatment groups and 26/118 (22.0%) of patients in the control groups. The majority of above adverse events were mild and resolved by stopping related drugs and symptomatic treatment. Although some serious adverse events such as heart failure (1/106), cerebral hemorrhage (1/106), pericardial tamponade (1/106), coronary bypass surgery (1/106), and death (1/106) were reported in the two groups, there was no significant difference between the two groups.

Ingredients of CHM Formulae and Frequently Used Herbs

The ingredients of CHM in each RCT are listed in Table 3. The most frequently used herbs across all formulae were *Miltiorrhiza* (nine formulae), pseudo-ginseng (seven formulae), ginseng (seven formulae), *Radix Paeoniae rubra* (six formulae), *Astragalus membranaceus* (five formulae), rhizome of *Chuanxiong* (five formulae), leech (five formulae), borneol (five formulae), and safflower (four formulae). Chinese *Angelica*, *Achyranthes bidentata*, *Rehmannia glutinosa*, peach kernel, liquorice, hawthorn, *Trichosanthes*, *Cinnamomum*, *Poria*, aloes, *Rhizoma Corydalis*, and ginkgo biloba were also frequently used.

Possible Mechanism of Herbal Benefits for CHD

A total of 45 experimental studies (Jormalainen et al., 2004; Liu et al., 2008; Chen et al., 2008; He et al., 2008; Nizamutdinova et al., 2008; Wang et al., 2008; Liu et al., 2010; Liu et al., 2010; Tang

et al., 2010; Zhang et al., 2010; Liu and Niu, 2011; Liu et al., 2011; Pan et al., 2011; Wu et al., 2011; Zhai et al., 2011; Liu et al., 2012; Lv et al., 2012; Zhu et al., 2013; Lim et al., 2013; Tu et al., 2013; Wang et al., 2013; Yin et al., 2013; Zhang et al., 2013; He et al., 2014; Li et al., 2014; Liu et al., 2014; Park et al., 2014; Qian et al., 2014; Tang et al., 2014; Tao et al., 2014; Wei et al., 2014; Xue et al., 2014; Zhang et al., 2014; Deng et al., 2015; Lu et al., 2015; Wang et al., 2015; Xia et al., 2015; Yu et al., 2015; Chen et al., 2016; Fan et al., 2016; Hu et al., 2016; Leng et al., 2015; Ma et al., 2016; Meng et al., 2016; Yu et al., 2016) were identified in our electronic searches to investigate the effects and mechanisms of the main active components of single flavored Chinese medicine which were frequently used on I/R injury models (Table 4). The possible mechanisms of them are summarized as follows: (1) oxidative stress is important reaction after myocardial ischemia. The function of free radical scavenging system is decreased in myocardial ischemia. Large amounts of free radicals was produced by the unbalanced endogenous antioxidant systems, which further leads to the peroxidation of lipids, proteins and nucleic acids, the biochemical alteration (reducing SOD, and GSH-Px, and increasing MDA), and further led to cardiomyocyte death (Yellon and Hausenloy, 2007). Based on these observations, antioxidant therapy is the key step considered to prevent I/R injury. In our study, *Salvia miltiorrhiza*, salvianolic acid B, tanshinone IIA, notoginsenoside R1, ginsenoside Rb1, ginsenoside Rb3, astragaloside IV, and ligustrazine could enhance SOD (Chan et al., 2012; Lv et al., 2012; Liu et al., 2014; Tang et al., 2014; Xue et al., 2014; Wang et al., 2015; Xia et al., 2015) and attenuate chondriokinesis to reduce the release of MDA (Liu et al., 2011; Chan et al., 2012; Liu et al., 2014; Tang et al., 2014; Xue et al., 2014; Xia et al., 2015); borneol, ginsenoside Rd, and hydroxysafflor yellow A could reduce ROS (He et al., 2008; Liu and Niu, 2011; Wang et al., 2013). *S. miltiorrhiza* and hydroxysafflor yellow A (Hu et al., 2016) exhibit antioxidant effects via PI3K/Akt signaling pathway; tanshinone IIA (Wei et al., 2014) increases NADPH oxidase via AMPK/Akt/PKC pathway; and astragaloside IV (Zhang et al., 2014) could reduce ROS via the PI3K/Akt/mTOR pathway. Our study showed TCM could improve the antioxidant function to reduce the damage of myocardial ischemia. (2) Apoptosis was an energy-requiring programmed cell death (Zhang and Xu, 2000). Apoptosis can be activated extrinsically by sarcolemmal receptors such as FAS: FAS(CD 95) and tumor necrosis factor alpha (TNF- α) (Kleinbongard et al., 2011), or intrinsically by cytochrome c which initiates the caspase cascade activation result in intracellular proteolysis. In addition, the opening of mitochondrial permeability transition pore (MPTP) conduces the mitochondrial matrix swelling, then leading to rupture of the outer membrane and release of cytochrome c,

TABLE 3 | Ingredients of Chinese herbal medicine formulae.

Study (years)	Prescription	Ingredients of herb prescription	Usage of prescription	Preparations	Quality control
Chu et al., 2010	Xuefu Zhuyu capsule	Peach kernel, <i>Angelica sinensis</i> , rhizome of <i>Chuanxiong</i> , safflower, <i>Radix Paeoniae rubra</i> , <i>Radix Rehmanniae</i> , <i>Fructus aurantii</i> , <i>Radix Bupleuri</i> , <i>Platycodon grandiflorum</i> , <i>Radix Achyranthis bidentatae</i> , and liquorice	3#tid po	Capsule	Traditional Chinese patented medicine WY: Z12020223
Qiao et al., 2006 Chen et al., 2013	Tongguan capsule	<i>Astragalus membranaceus</i> , <i>Miltiorrhiza</i> , leech, etc.	3#tid po	Capsule	Produced by The Second Affiliated Hospital Of Guangzhou University Of Traditional Chinese Medicine
Cheng et al., 2009	Qingre Quyu granule	<i>Fructus trichosanthis</i> 15g, <i>Miltiorrhiza</i> 30g, hawthorn 30g, <i>Fritillaria thunbergii</i> 10g, pseudo-ginseng 3g, <i>Lignum Millettiae</i> 30g, and the seed of cowherb 15g	1#bid po	Decoction	Produced by China Pharmaceutical Materials Group Company
Lu et al., 2006 Shang et al., 2011 Wang et al., 2017	Xiongshao capsule Xuesaitong soft capsule	Rhizome of <i>Chuanxiong</i> and <i>Radix Paeoniae rubra</i> Pseudo-ginseng	2#tid po 2#bid po	Capsule Capsule	Unreported Traditional Chinese patented medicine WY: Z19990022
Mo et al., 2012	Yixin Mai granule	Ginseng, cassia twig, <i>Fructus trichosanthis</i> , leech, and <i>Poria cocos</i>	1#tid po	Decoction	Produced by Ruikang Hospital Affiliated to Guangxi College of Traditional Chinese Medicine
Liu et al., 2014	Red ginseng Tongxin granule	<i>Radix Paeoniae rubra</i> 10g, Agilawood 1g, <i>Angelica sinensis</i> 10g, orange peel 10g, <i>Rhizoma Corydalis</i> 6g, rhizome of <i>Chuanxiong</i> 6g, <i>Miltiorrhiza</i> 10g, astragalus 6g, peach kernel 10g, and safflower 10g	Unreported	Decoction	Produced by Jiangyin Tianjiang Pharmaceutical Co., Ltd.
Zhu et al., 2016	Traditional Chinese medicine prescription	Hawthorn, <i>Miltiorrhiza</i> , ginkgo leaf, lentil, <i>Psoralea</i> , sapanwood, <i>Ganoderma</i> , <i>Polygonum multiflorum</i> , <i>Cornus officinalis</i> , <i>Alisma orientalis</i> , <i>Radix Paeoniae alba</i> , cinnamon, <i>Pericarpium Citri reticulatae</i> , liquorice, <i>Fructus cnidii</i> , cicada slough, and <i>Ramuli Umcariae Cumuncis</i>	1#tid po	Capsule	Unreported
Wang et al., 2009	Shenshao tablet	<i>Radix Paeoniae alba</i> and ginseng	4#tid po	Tablet	Traditional Chinese patented medicine WY: Z19990059
Xu et al., 2015 Xu et al., 2014	Shenzhu Guanxin recipe	Ginseng 5g, <i>Rhizoma Atractylodis</i> 10g, <i>Radix Notoginseng</i> 10g, <i>Rhizoma Pinelliae</i> 10g, leech 3g, <i>Radix Panacis quinquefolium</i> 5g, and <i>Folium nelumbinis</i> 15g	50ml qd po	Decoction	Produced by Jiangxi Jiangyin Pharmaceutical Factory
Wang et al., 2012 Wang et al., 2016 Mao et al., 2016	Danlou tablet	<i>Fructus trichosanthis</i> , <i>Allium macrostemon</i> , the root of kudzu vine, rhizome of <i>Chuanxiong</i> , <i>Miltiorrhiza</i> , <i>Radix Paeoniae rubra</i> , <i>Alisma orientalis</i> , <i>Astragalus membranaceus</i> , <i>Curcuma aromatica</i> , and <i>Drynaria</i> rhizome	4.5g qd po	Tablet	Traditional Chinese patented medicine WY: YBZ17382006
Zhang et al., 2010 Lu et al., 2014	Tongxinluo capsule	Ginseng, leech, scorpion, red peony root, cicada slough, soil turtle worm, centipede, sandalwood, <i>Lignum acronychiae</i> , frankincense, jujube nut, and borneol	Before PCI: 8# qd po After PCI: 4#tid po	Capsule	Traditional Chinese patented medicine WY: Z19980015
Qiu et al., 2009	Compound <i>Salvia</i> tablet and Xinyue capsule	<i>Miltiorrhiza</i> 450mg, pseudo-ginseng 141mg, borneol 8mg, ginseng 50mg	Unreported	Capsule	Traditional Chinese patented medicine WY: Z44023372 and Z20030073
Hu et al., 2014	Kodaling tablet	<i>Rhizoma Corydalis</i>	3#tid po	Tablet	Produced by Zhejiang KangEnbei Pharmaceutical Co., Ltd.
Duan et al., 2016	Live heart pill	Ginseng, <i>Radix Aconiti carmichaeli</i> , <i>Ganoderma lucidum</i> , safflower, musk, bezoar, bear bile, pearl, toad venom, and borneol	2#tid po	Tablet	Traditional Chinese patented medicine WY: Z44021835

(Continued)

TABLE 3 | Continued

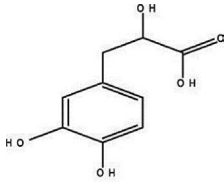
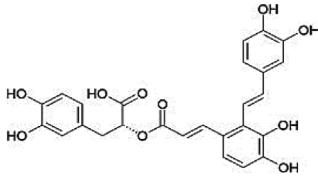
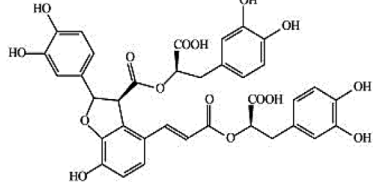
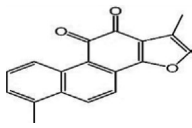
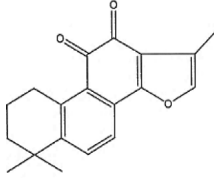
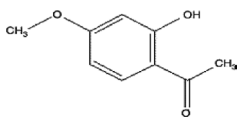
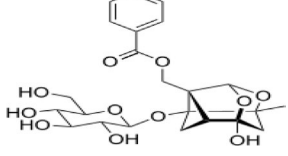
Study (years)	Prescription	Ingredients of herb prescription	Usage of prescription	Preparations	Quality control
Zhang et al., 2015	Wufuxinnaoqing	Safflower oil, borneol, vitamin E, and vitamin B6	2#tid po	Capsule	Produced by Shineway Pharmaceutical Group Co., Ltd.
Lu et al., 2008	Xuezhikang capsule	Red yeast Chinese rice	600mg bid po	Capsule	Produced by the Beijing WBL Peking University Biotech Co. Ltd. Unreported in detail
Shang et al., 2013	Qi-Shen-Yi-Qi dripping pills	<i>Miltiorrhizae</i> , pseudo-ginseng, <i>Lignum Dalbergiae odoriferae</i> , and <i>Astragalus membranaceus</i>	0.5g tid po	Pill	Unreported
Yang et al., 2017	Coronary Ningtong prescription	<i>Astragalus membranaceus</i> 30g, <i>Miltiorrhiza</i> 30g, mulberry parasitism 30g, <i>Gynostemma pentecox</i> 30g, hawthorn 30g, the root of kudzu vine 30g, <i>Herba Rhodiolae</i> 30g, <i>Fructus trichosanthis</i> 15g, <i>Allium macrostemon</i> 15g, <i>Rhizoma Pinellinae praeparata</i> 15g, immature bitter orange 10g, safflower 10g, <i>Rhizoma Sparganii</i> 10g, <i>Zedoaria</i> 10g, <i>Rhizoma coptidis</i> 6g, pseudo-ginseng 3g, and leech 3g	100ml bid po	Decoction	Unreported
Sun, 2014	Musk Baoxin pill	artificial musk, ginseng, cinnamon, toad venom, storax, artificial bezoar, and borneol	2#tid po	Pill	Produced by Shanghai and Huangyao Pharmaceutical Industry
Wang et al., 2012	Double ginseng capsule And Tongguan capsule	<i>Miltiorrhiza</i> , ginseng, <i>Herba Rhodiolae</i> , pseudo-ginseng and <i>Lignum Dalbergiae odoriferae</i>	4#tid po	Capsule	Produced by Shaanxi Pharmaceutical Group Shaanxi New Drug Technology Development Center

d, day; #: tablet; PCI, Percutaneous Coronary Intervention; Co., Ltd, Company Limited.

activating the caspase cascade, ultimately resulting in the apoptotic cell death (Heusch et al., 2010). Proapoptotic and antiapoptotic proteins of the Bcl family interact with the MPTP (Baines, 2009). In present study, *S. miltiorrhiza*, salvianolic acid A, salvianolic acid B, paeonol, paeoniflorin, ginsenoside Rb1, ginsenoside Rb3, ginsenoside Rd, ginsenoside Rg3, and ligustrazine could increase Bcl-2 expression (Nizamutdinova et al., 2008; Wang et al., 2008; Tang et al., 2010; Zhai et al., 2011; Wang et al., 2013; Liu et al., 2014; Wang et al., 2015; Fan et al., 2016) and the Bcl-2/Bax ratio (Nizamutdinova et al., 2008; Tang et al., 2010; Wu et al., 2011; Zhai et al., 2011; Wang et al., 2013; Liu et al., 2014; Wang et al., 2015; Chen et al., 2016; Fan et al., 2016). Three studies (Wang et al., 2008; Zhang et al., 2013; Chen et al., 2016) reported that salvianolic acid A, tanshinone IIA, and ginsenoside Rb1 exhibit anti-apoptotic effects via PI3K/Akt signaling pathway, and one study (Wang et al., 2013) reported that ginsenoside Rd could decrease caspase-3 and caspase-9 activities. (3) The inflammation during myocardial I/R injury was reviewed by previous studies (Marchant et al., 2012). The excessive inflammation can lead to cardiomyocyte damage. When the myocardium got reperused, the NF- κ B pathway was activated by pattern recognition receptors, culminating in promoted cytokine expression. *S. miltiorrhiza*, tanshinone I, tanshinone IIA, paeonol, notoginsenoside r1, ginsenoside Re, ginsenoside Rg1, ligustrazine, astragaloside IV, and astragalus polysaccharides were shown to exert anti-inflammatory effects by decreasing TNF- α (Zhang et al., 2010; Lim et al., 2013; Tu et al., 2013; Deng et al., 2015; Lu et al., 2015; Xia et al., 2015),

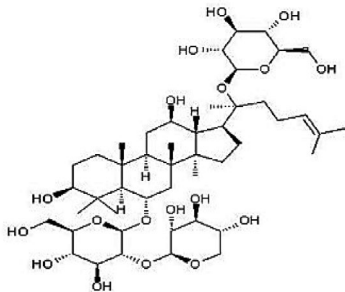
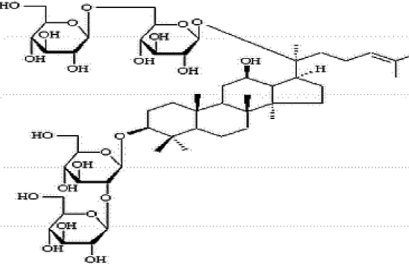
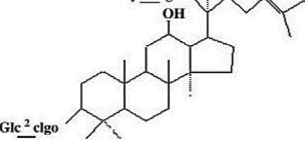
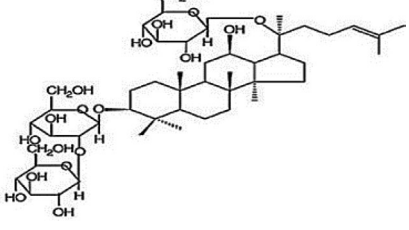
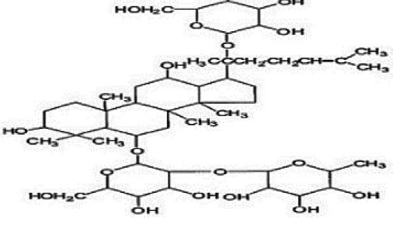
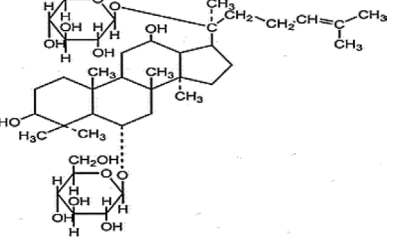
IL-6 (Chen et al., 2008; Zhang et al., 2010), IL-8 (Li et al., 2014), and NF- κ B (Tu et al., 2013; Qian et al., 2014; Deng et al., 2015; Lu et al., 2015). Two studies (Qian et al., 2014; Zhu et al., 2013) reported that ligustrazine and astragalus polysaccharides exhibit anti-inflammatory effects via inhibiting P38MAPK pathway, and one study (Zhang et al., 2010) reported that tanshinone IIA could decrease TNF- α and IL-6 via PI3K/Akt pathway. (4) Nitric oxide is an essential modulator of cardiovascular system. The NO can decrease intracellular calcium concentration in vascular smooth muscle cells, which further induces vasodilation (Schulz et al., 2004). Salvianolic acid B, tanshinone IIA, ginsenoside Rb1, ginsenoside Rg3, ligustrazine, astragaloside IV, and hydroxysafflor yellow A were shown to improve circulation by increasing NO expression (Liu et al., 2008; Liu et al., 2010; Pan et al., 2011; Lv et al., 2012; Leng et al., 2015; Wang et al., 2015) via up-regulating eNOS phosphorylation (Liu et al., 2008; Liu et al., 2010; Pan et al., 2011; Lv et al., 2012; Leng et al., 2015; Wang et al., 2015). (5) *S. miltiorrhiza* and notoginsenoside r1 were shown to regulate energy metabolism via p-JNK-NF-kappaB-TRPC6 pathway (Meng et al., 2016) and ROCK-dependent ATP5D modulation separately (He et al., 2014; Li et al., 2014). (6) Hirudin was shown to attenuate coagulation and enhance microvascular flow during reperfusion (Jormalainen et al., 2004). Thus, antioxidant, anti-apoptotic, circulation improvement, anti-inflammatory, and energy metabolism regulation actions have been promoted as important mechanisms of herbal compounds used to treat I/R injury.

TABLE 4 | Mechanisms of the main active components of single flavored Chinese Medicine on organic injury induced by ischemia/reperfusion.

Active ingredients	Herb source	Possible mechanisms (signaling pathway)	Citation	Structure
Salvia miltiorrhiza	Miltiorrhiza	<ol style="list-style-type: none"> 1. Regulation of energy metabolism (p-JNK-NF-kappaB-TRPC6 pathway) 2. Attenuation of oxidative stress (Akt/Nrf2/HO-1 pathway) 3. Anti-inflammation 4. Anti-apoptosis (increase expression of Bcl-2 and increase Bcl-2/Bax ratio, affect Akt, and ERK1/2 phosphorylation) 	<ol style="list-style-type: none"> 1. Meng et al., 2016 2. Hu et al., 2016 3. Yin et al., 2013 4. Yu et al., 2015; Fan et al., 2016 	
Salvianolic acid A	Miltiorrhiza	<ol style="list-style-type: none"> 1. Anti-apoptosis (increase Bcl-2/Bax ratio via JNK/PI3K/Akt signaling pathway) 	<ol style="list-style-type: none"> 1. Chen et al., 2016 	
Salvianolic acid B	Miltiorrhiza	<ol style="list-style-type: none"> 1. Improve circulation (increase expression of NO via up-regulating eNOS phosphorylation) 2. Attenuation of oxidative stress (increase SOD and decrease MDA) 3. Anti-apoptosis 	<ol style="list-style-type: none"> 1. Pan et al., 2011 2. Xue et al., 2014 3. Xue et al., 2014 	
Tanshinone I	Miltiorrhiza	<ol style="list-style-type: none"> 1. Anti-inflammation 	<ol style="list-style-type: none"> 1. Park et al., 2014 	
Tanshinone IIA	Miltiorrhiza	<ol style="list-style-type: none"> 1. Improve circulation (increase expression of NO via up-regulating eNOS phosphorylation) 2. Attenuation of oxidative stress (increase SOD and HO-1, decrease MDA, increase NADPH oxidase via AMPK/Akt/PKC pathway) 3. Anti-inflammation (decrease TNF-alpha and IL-6 via PI3K/Akt-dependent pathway) 4. Anti-apoptosis (decrease caspase-3 activity via Akt/FOXO3A/Bim-mediated signal pathway) 	<ol style="list-style-type: none"> 1. Pan et al., 2011 2. Tang et al., 2014; Wei et al., 2014 3. Zhang et al., 2010 4. Zhang et al., 2013 	
Paeonol	Radix Paeoniae rubra	<ol style="list-style-type: none"> 1. Anti-inflammation 2. Anti-apoptosis (increase expression of Bcl-2 and increase Bcl-2/Bax ratio) 	<ol style="list-style-type: none"> 1. Ma et al., 2016 2. Nizamutdinova et al., 2008 	
Paeoniflorin	Radix Paeoniae rubra	<ol style="list-style-type: none"> 1. Anti-apoptosis (increase expression of Bcl-2 and increased Bcl-2/Bax ratio) 	<ol style="list-style-type: none"> 1. Tang et al., 2010 	

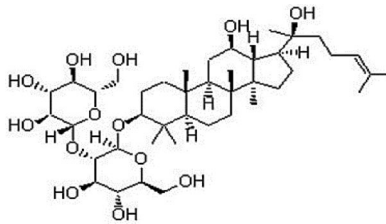
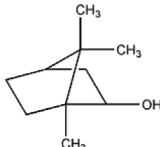
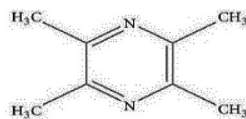
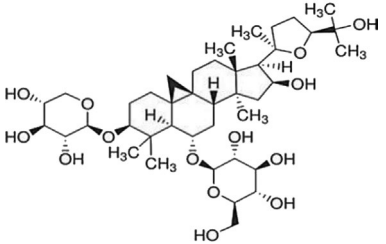
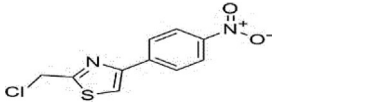
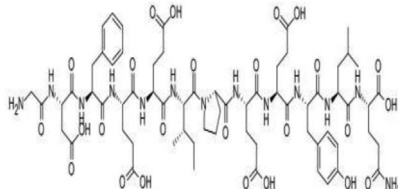
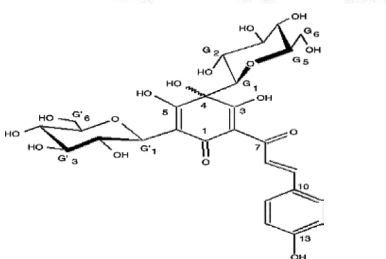
(Continued)

TABLE 4 | Continued

Active ingredients	Herb source	Possible mechanisms (signaling pathway)	Citation	Structure
Notoginsenoside r1	Pseudo-Ginseng	<ol style="list-style-type: none"> 1. Anti-inflammation (decrease IL-6, IL-8, and TNF-α) 2. Regulation of energy metabolism (ROCK-dependent ATP5D modulation) 3. Anti-apoptosis (increase Bcl-2 expression) 4. Attenuation of oxidative stress (increase SOD, and decrease MDA) 5. Attenuation of endoplasmic reticulum stress 	<ol style="list-style-type: none"> 1. Chen et al., 2008; Li et al., 2014; Xia et al., 2015 2. He et al., 2014; Li et al., 2014 3. Liu et al., 2010 4. Xia et al., 2015 5. Yu et al., 2016 	
Ginsenoside Rb1	Ginseng	<ol style="list-style-type: none"> 1. Anti-apoptosis (increase Bcl-2 expression and increased Bcl-2/Bax ratio via PI3K/Akt pathway) 2. Attenuation of oxidative stress (increase SOD, and decrease MDA) 3. Improve circulation (increase NO expression via up-regulating eNOS phosphorylation) 	<ol style="list-style-type: none"> 1. Wang et al., 2008; Wu et al., 2011 2. Chan et al., 2012 3. Leng et al., 2015 	
Ginsenoside Rb3	Ginseng	<ol style="list-style-type: none"> 1. Attenuation of oxidative stress (increase SOD, and decrease MDA) 2. Anti-apoptosis (increase Bcl-2 expression and increase Bcl-2/Bax ratio) 	<ol style="list-style-type: none"> 1. Liu et al., 2014 2. Liu et al., 2014 	
Ginsenoside Rd	Ginseng	<ol style="list-style-type: none"> 1. Attenuation of oxidative stress (decrease ROS) 2. Anti-apoptosis (increase Bcl-2 expression and increase Bcl-2/Bax ratio, decrease caspase-3 and caspase-9 activity via mitochondrial-dependent apoptotic pathway) 	<ol style="list-style-type: none"> 1. Wang et al., 2013 2. Wang et al., 2013 	
Ginsenoside Re	Ginseng	<ol style="list-style-type: none"> 1. Anti-inflammation (decrease TNF-α) 	<ol style="list-style-type: none"> 1. Lim et al., 2013 	
Ginsenoside Rg1	Ginseng	<ol style="list-style-type: none"> 1. Anti-inflammation (decrease TNF-α and IL-1β, in part via the NF-κB signaling pathway) 	<ol style="list-style-type: none"> 1. Tao et al., 2014; Deng et al., 2015 	

(Continued)

TABLE 4 | Continued

Active ingredients	Herb source	Possible mechanisms (signaling pathway)	Citation	Structure
Ginsenoside Rg3	Ginseng	<ol style="list-style-type: none"> 1. Attenuation of oxidative stress (increase SOD) 2. Anti-apoptosis (increase Bcl-2 expression and increase Bcl-2/Bax ratio) 3. Improve circulation (increase NO expression via up-regulating eNOS phosphorylation) 	<ol style="list-style-type: none"> 1. Wang et al., 2015 2. Wang et al., 2015 3. Wang et al., 2015 	
Borneol	Borneol	<ol style="list-style-type: none"> 1. Attenuation of oxidative stress (decrease ROS) 	<ol style="list-style-type: none"> 1. Liu and Niu, 2011 	
Ligustrazine	Rhizome of <i>Chuanxiong</i>	<ol style="list-style-type: none"> 1. Attenuation of oxidative stress (increase SOD and decrease MDA) 2. Improve circulation (increase NO expression via up-regulating eNOS phosphorylation) 3. Anti-inflammation (decrease the expression of NF-κB via inhibiting P38MAPK pathway) 4. Anti-apoptosis (increase Bcl-2 expression and increase Bcl-2/Bax ratio) 	<ol style="list-style-type: none"> 1. Liu et al., 2011; Lv et al., 2012 2. Lv et al., 2012 3. Qian et al., 2014 4. Zhai et al., 2011 	
Astragaloside IV	Astragalus membranaceus	<ol style="list-style-type: none"> 1. Promoting angiogenesis (increase the expression of VEGF) 2. Anti-apoptosis (increase Bcl-2 expression and increase Bcl-2/Bax ratio, decrease caspase-3) 3. Anti-inflammation (decrease the expression of TNF-alpha and NF-κB) 4. Improve circulation (increase NO expression via up-regulating eNOS phosphorylation) 5. Attenuation of oxidative stress (reduce ROS to via the PI3K/Akt/mTOR pathway) 	<ol style="list-style-type: none"> 1. Yu et al., 2015 2. Tu et al., 2013; Lu et al., 2015 3. Tu et al., 2013; Lu et al., 2015 4. Liu et al., 2010 5. Zhang et al., 2014 	
Astragalus polysaccharides	Astragalus membranaceus	<ol style="list-style-type: none"> 1. Anti-inflammatory (via the p38 MAPK signaling pathway) 	<ol style="list-style-type: none"> 1. Zhu et al., 2013 	
Hirudin	Leech	<ol style="list-style-type: none"> 1. Attenuate coagulation and enhance microvascular flow during reperfusion 	<ol style="list-style-type: none"> 1. Jormalainen et al., 2004 	
Hydroxysafflower yellow A	Safflower	<ol style="list-style-type: none"> 1. Attenuation of oxidative stress (Akt/Nrf2/HO-1 pathway, decrease ROS) 2. Improve circulation (increase NO expression via up-regulating eNOS phosphorylation) 	<ol style="list-style-type: none"> 1. He et al., 2008; Hu et al., 2016 2. Liu et al., 2008 	

HO-1, heme oxygenase-1; SOD, super oxide dismutase; PI3K, phosphatidylinositol 3-kinase; ROS, reactive oxygen species; eNOS, endothelial nitric oxide synthase; MDA, malonaldehyde; NADPH, nicotinamide adenine dinucleotide phosphate; VEGF, vascular endothelial growth factor; NF- κ B, nuclear factor κ B.

TABLE 5 | Different syndromes of coronary heart disease and the classification of herbs according to syndrome differentiation therapy for different syndromes.

Syndrome	Syndrome differentiation therapy for different syndromes	Representative herbs in the theory of traditional Chinese medicine mentioned in present study
Syndrome of coagulation cold in heart vessel	1. Dispelling cold 2. Dredging channel blockade and yang	1. Cinnamon, <i>Psoralea</i> , <i>Ramuli Umcariae Cumuncis</i> 2. <i>Angelica sinensis</i> , radix <i>Paeoniae rubra</i> , pseudo-ginseng, rhizome Of <i>Chuanxiong</i> , frankincense, <i>Miltiorrhiza</i> , safflower, peach kernel, rhizoma <i>Corydalis</i> , leech, soil turtle worm, <i>Lignum Millettiae</i> , ginkgo leaf, sapanwood, red yeast Chinese, <i>Allium macrostemon</i>
Syndrome of qi stagnation in heart and chest	1. Dispersing stagnated liver qi for regulating qi-flowing	1. Hawthorn, <i>Fructus aurantii</i> , <i>Lignum acronychiae</i> , Agilawood, radix <i>Bupleuri</i> , rhizoma <i>Corydalis</i>
Syndrome of blockade of heart blood	1. Promoting blood circulation for removing blood stasis	1. <i>Angelica sinensis</i> , radix <i>Paeoniae rubra</i> , pseudo-ginseng, rhizome Of <i>Chuanxiong</i> , frankincense, <i>Miltiorrhiza</i> , safflower, peach kernel, rhizoma <i>Corydalis</i> , leech, soil turtle worm, <i>Lignum Millettiae</i> , ginkgo leaf, sapanwood, red yeast Chinese rice
Syndrome of turbid phlegm blocking heart	1. Dredging yang for resolving turbidity 2. Eliminating phlegm for resolving masses	1. <i>Allium macrostemon</i> 2. <i>Rhizoma Pinelliae</i> , liquorice, <i>Platycodon grandiflorum</i> , <i>Fritillaria thunbergii</i> , orange peel
Syndrome of deficiency of both qi and yin	1. Benefiting qi and nourishing yin 2. Promoting blood circulation for dredging vessels	1. <i>Angelica sinensis</i> , ginseng, <i>Astragalus Membranaceus</i> , radix <i>Panacis quinquefolium</i> , <i>Rhizoma Atractylodis</i> , liquorice 2. <i>Radix Paeoniae Rubra</i> , pseudo-ginseng, rhizome Of <i>Chuanxiong</i> , frankincense, <i>Miltiorrhiza</i> , safflower, peach kernel, rhizoma <i>Corydalis</i> , leech, soil turtle worm, <i>Lignum Millettiae</i> , ginkgo leaf, sapanwood, red yeast Chinese rice, musk
Syndrome of yin deficiency of heart and kidney	1. Nourishing yin and clearing heat 2. Activating blood circulation for nourishing heart	1. <i>Angelica sinensis</i> , borneol, <i>Cassia</i> twig, cicada slough, <i>Fructus trichosanthis</i> , <i>Fritillaria thunbergii</i> , orange peel, <i>Folium nelumbinis</i> , bezoar, bear bile, pearl, toad venom, <i>Gynostemma pentecox</i> , <i>Rhizoma Coptidis</i> , liquorice 2. <i>Radix Paeoniae rubra</i> , pseudo-ginseng, rhizome of <i>Chuanxiong</i> , frankincense, <i>Miltiorrhiza</i> , safflower, peach kernel, rhizoma <i>Corydalis</i> , leech, soil turtle worm, <i>Lignum Millettiae</i> , ginkgo leaf, sapanwood, red yeast Chinese rice
Syndrome of yang deficiency of heart and kidney	1. Warmly tonifying yang qi and inspiring heart yang	1. Ginseng, <i>Astragalus Membranaceus</i> , radix <i>Panacis quinquefolium</i> , <i>Rhizoma Atractylodis</i> , liquorice, <i>Ganoderma</i> , <i>Herba Rhodiola</i>

DISCUSSION

Summary of Evidence

This is the first clinical systematic review of 27 high-quality RCTs involving 11,732 participants to estimate the efficacy and safety of CHMs for CHD. The evidence available from present study revealed that CHMs are beneficial for CHD and are generally safe. In addition, CHM exerted cardioprotection for CHD, possibly altering multiple signal pathways through anti-inflammation, anti-oxidation, anti-apoptosis, circulation improvement, and energy metabolism regulation.

Limitations

First, there were still some methodological weaknesses in the primary studies although we included high-quality studies. Only nine of the 27 included studies (Lu et al., 2006; Chu et al., 2010; Wang et al., 2009; Liu et al., 2014; Xu et al., 2015; Zhang et al., 2015; Duan et al., 2016; Mao et al., 2016; Wang et al., 2016) reported allocation concealment, and eight included studies (Lu et al., 2006; Chu et al., 2010; Wang et al., 2009; Liu et al., 2014; Xu et al., 2015; Zhang et al., 2015; Duan et al., 2016; Wang et al., 2016) reported blinding during outcome assessment. It is worth noting that an average 18% more “beneficial” effect in trials with inadequate or unclear concealment of allocation compared with adequate concealment (Higgins and Green, 2012). And blinding during outcome assessment is an essential method to avoid systemic errors which existed in the outcome assessment of non-blinded studies (Higgins and Green, 2012).

Second, English and Chinese literatures were included only in present study and the absence of studies written in other languages may generate selective bias in a certain degree. Third, no included trials were reported to have been registered, and negative findings were less likely to be published, which may lead to the efficacy being overestimated.

Implications

The findings from present study indicate that CHM paratherapy is beneficial for CHD and is well tolerated. Thus, we recommended, at least to an extent, to use CHMs for CHD, especially selected case. Further study should identify specific CHM and/or indications of CHM. In addition, the findings of the most frequently used herbs such as *Miltiorrhiza*, pseudo-ginseng, ginseng, *Radix Paeoniae rubra*, *Astragalus membranaceus*, rhizome of *Chuanxiong*, leech, borneol, and safflower and their main active components should be considered as further development of herbal prescriptions and component injection for CHD.

Some methodological weaknesses still existed in the primary studies. Recommendations for further research are as follows: (1) the CONSORT 2010 statement (Schulz et al., 2010), CONSORT for TCM (Bian et al., 2011), RCTs investigating CHM (Flower et al., 2012), and CONSORT Extension for Chinese Herbal Medicine Formulas 2017 (Cheng et al., 2017) should be abided by for the design. (2) Clinic trials should be registered in a generally accessible database (www.clinicaltrials.com) prior to first case inclusion. It allows verification of predefined study hypothesis and end-points of the study, which would help to the

report of negative findings and reduce publication bias (Rongen and Wever, 2015). (3) In view of trials with insufficient statistical power that runs the risk of over estimating therapeutic efficacy (Kjaergard et al., 2001), the further studies are recommended to provide statistical information of sample size estimation. (4) In order to ensure the efficacy of TCM, the identity and quantity of the herbal preparations should be described clearly in further research. (5) The safety of TCM has been increasingly concerned by both medical workers and the public.

The frequency of use for particular herb was calculated and those used at a high frequency that are described in detail in the part 3.6 and **Table 3**. The high-frequency herbs that we selected can ignite the treatment based on syndrome differentiation according to the herbal functions **Table 5**. Ginseng and *Astragalus membranaceus* benefit qi; *Miltiorrhiza*, pseudo-ginseng, *Radix Paeoniae rubra*, rhizome of *Chuanxiong*, leech, and safflower promote blood circulation for removing blood stasis; and borneol has function of resuscitation with aromatics for relieving pain. Thus, we can also deduce that the main patterns of CHD are qi deficiency and blood stasis. The selected high-frequency herbs are composed of a herbal prescription for CHD, which can be used for clinic and as a candidate for RCT.

Cardioprotection by anti-inflammation, antioxidant, anti-apoptosis, and circulation improvement for myocardial I/R injury (Xu et al., 2014) was an innovative strategy for antagonizing the injurious biochemical and molecular events that eventually resulted in irreversible ischemic injury (Wu and He, 2010). The included preclinical trials presented the main active components of the most frequently used herbs that performed anti-inflammatory, anti-oxidation, anti-apoptosis, energy metabolism regulation, and circulation improvement mechanisms in

multiple models of I/R injury through multiple signal pathways, including the PI3K/Akt signaling pathway, AMPK/Akt/PKC pathway, PI3K/Akt/mTOR pathway, mitochondrial-dependent apoptotic pathway, P38MAPK pathway, eNOS phosphorylation, and p-JNK-NF-kappaB-TRPC6 pathway. Further studies of CHM for CHD should explore the multi-drug, multi-target signal pathway using novel techniques such as network pharmacological approach.

Conclusion

The findings from present study indicate that CHMs are beneficial for CHD and are generally safe. In addition, CHM exerted cardioprotection for CHD, possibly altering multiple signal pathways through anti-inflammatory, anti-oxidation, anti-apoptosis, circulation improvement, and energy metabolism regulation mechanisms.

AUTHOR CONTRIBUTIONS

Study conception and design: GQZ, YW, KJZ, and QZ. Acquisition, analysis and/or interpretation of data: QZ, KJZ, JZZ, XYB, QT, PCZ, ZZ, YYH, GQZ, YW. Final approval and overall responsibility for this published work: GQZ and YW.

FUNDING

This project was supported by the grant of National Natural Science Foundation of China (81573750/81473491/81173395/H2902).

REFERENCES

- Arslan, F., Bongartz, L., Ten Berg, J. M., Jukema, J. W., Appelman, Y., Liem, A. H., et al. (2018). ESC guidelines for the management of acute myocardial infarction in patients presenting with ST-segment elevation: comments from the Dutch ACS working group. *Neth. Heart J.* 26 (9), 417–421. doi: 10.1007/s12471-018-1134-0
- Baines, C. P. (2009). The mitochondrial permeability transition pore and ischemia-reperfusion injury. *Basic Res. Cardiol.* 104 (2), 181–188. doi: 10.1007/s00395-009-0004-8
- Bian, Z., Liu, B., Moher, D., Wu, T., Li, Y., Shang, H., et al. (2011). Consolidated standards of reporting trials (CONSORT) for traditional Chinese medicine: current situation and future development. *Front. Med.* 5 (2), 171–177. doi: 10.1007/s11684-011-0132-z
- Chan, K., Shaw, D., Simmonds, M. S., Leon, C. J., Xu, Q., Lu, A., et al. (2012). Good practice in reviewing and publishing studies on herbal medicine, with special emphasis on traditional Chinese medicine and Chinese materia medica. *J. Ethnopharmacol.* 140 (3), 469–475. doi: 10.1016/j.jep.2012.01.038
- Chen, P., Zhu, C. L., and Zhang, M. Z. (2013). Effect of Tongguan capsule on the number of endothelial progenitor cells in the peripheral blood of patients with coronary artery disease after PCI. *Zhongguo Zhong Xi Yi Jie He Za Zhi* 33 (7), 873–876. doi: 10.7661/CJIM.2013.07.0873
- Chen, Q., Xu, T., Li, D., Pan, D., Wu, P., Luo, Y., et al. (2016). JNK/PI3K/Akt signaling pathway is involved in myocardial ischemia/reperfusion injury in diabetic rats: effects of salvianolic acid A intervention. *Am. J. Transl. Res.* 8, 2534–2548.
- Chen, W. X., Wang, F., Liu, Y. Y., Zeng, Q. J., Sun, K., Xue, X., et al. (2008). Effect of notoginsenoside R1 on hepatic microcirculation disturbance induced by gut ischemia and reperfusion. *World J. Gastroenterol.* 14, 29–37. doi: 10.3748/wjg.14.29
- Cheng, C. W., Wu, T. X., Shang, H. C., Li, Y. P., Altman, D. G., Moher, D., et al. (2017). CONSORT extension for Chinese herbal medicine formulas 2017: recommendations, explanation, and elaboration. *Ann. Intern. Med.* 167 (2), W21–W34. doi: 10.7326/M16-2977
- Cheng, W. L., Wang, Y., Cai, Z., Ke, Y. N., Liu, X. F., and Fan, S. Y. (2009). Effect of Qingre Quyu G ranule on the vulnerable atherosclerotic plaque of carotid artery in patients with stable coronary artery disease. *Zhongguo Zhong Xi Yi Jie He Za Zhi* 29 (12), 1085–1088. doi: 10.3321/j.issn:1003-5370.2009.12.007
- Chu, F. Y., Wang, J., Yao, K. W., and Li, Z. Z. (2010). Effect of Xuefu Zhuyu Capsule on the symptoms and signs and health-related quality of life in the unstable angina patients with blood-stasis syndrome after percutaneous coronary intervention: a randomized controlled trial. *Chin. J. Integr. Med.* 16 (5), 399–405. doi: 10.1007/s11655-010-9999-9
- Chung, V. C., Chen, M., Ying, Q., Tam, W. W., Wu, X. Y., Ma, P. H., et al. (2013). Add-on effect of chinese herbal medicine on mortality in myocardial infarction: systematic review and meta-analysis of randomized controlled trials. *Evid. Based Complementary Altern. Med.* 2013, 675906. doi: 10.1155/2013/675906
- Deng, Y., Yang, M., Xu, F., Zhang, Q., Zhao, Q., Yu, H., et al. (2015). Combined salvianolic Acid B and Ginsenoside Rg1 exerts cardioprotection against ischemia/reperfusion injury in rats. *PLoS One* 10, e0135435. doi: 10.1371/journal.pone.0135435
- Duan, W. H., Xu, H., Wang, C. P., Gao, H. C., Li, Y. L., and Chen, Y. S. (2016). A multicenter, randomized, double-blind, placebo-controlled clinical study of HuoXin Wan (concentrated pill) for the treatment of stable angina pectoris

- with the syndrome of qi deficiency and blood stasis. *Chin. J. Evid. Based Med.* 8 (9), 1110–1115. doi: 10.3969/j.issn.1674-4055.2016.09.29
- Dunbar, S. B., Khavjou, O. A., Bakas, T., Hunt, G., Kirch, R. A., Leib, A. R., et al. (2018). American Heart Association. Projected costs of informal caregiving for cardiovascular disease: 2015 to 2035: a policy statement from the American Heart Association. *Circulation* 137 (19), e558–e577. doi: 10.1161/CIR.0000000000000570
- Fan, G., Yu, J., Asare, P. F., Wang, L., Zhang, H., Zhang, B., et al. (2016). Danshensu alleviates cardiac ischemia/reperfusion injury by inhibiting autophagy and apoptosis via activation of mTOR signalling. *J. Cell Mol. Med.* 20 (10), 1908–1919. doi: 10.1111/jcmm.12883
- Flower, A., Witt, C., Liu, J. P., Ulrich-Merzenich, G., Yu, H., and Lewith, G. (2012). Guidelines for randomised controlled trials investigating Chinese herbal medicine. *J. Ethnopharmacol.* 140, 550–554. doi: 10.1016/j.jep.2011.12.017
- Gao, Z. Y., Zhang, J. C., Xu, H., Shi, D. Z., Fu, C. G., Qu, D., et al. (2010). Analysis of relationships among syndrome, therapeutic treatment, and Chinese herbal medicine in patients with coronary artery disease based on complex networks. *Zhong Xi Yi Jie He Xue Bao* 8 (3), 238–243. doi: 10.3736/jcim20100307
- Han, J. Y., Fan, J. Y., Horie, Y., Miura, S., Cui, D. H., Ishii, H., et al. (2008). Ameliorating effects of compounds derived from *Salvia miltiorrhiza* root extract on microcirculatory disturbance and target organ injury by ischemia and reperfusion. *Pharmacol. Ther.* 117 (2), 280–295. doi: 10.1016/j.pharmthera.2007.09.008
- Hausenloy, D. J., and Yellon, D. M. (2013). Myocardial ischemia-reperfusion injury: a neglected therapeutic target. *J. Clin. Invest.* 123 (1), 92–100. doi: 10.1172/JCI62874
- He, H., Liu, Q., Shi, M., Zeng, X., Yang, J., Wu, L., et al. (2008). Cardioprotective effects of hydroxysafflor yellow A on diabetic cardiac insufficiency attributed to up-regulation of the expression of intracellular calcium handling proteins of sarcoplasmic reticulum in rats. *Phytother. Res.* 22 (8), 1107–1114. doi: 10.1002/ptr.2468
- He, K., Yan, L., Pan, C. S., Liu, Y. Y., Cui, Y. C., Hu, B. H., et al. (2014). ROCK-dependent ATP5D modulation contributes to the protection of notoginsenoside NR1 against ischemia-reperfusion-induced myocardial injury. *Am. J. Physiol. Heart Circ. Physiol.* 307, H1764–H1776. doi: 10.1152/ajpheart.00259.2014
- Heusch, G., and Gersh, B. J. (2017). The pathophysiology of acute myocardial infarction and strategies of protection beyond reperfusion: a continual challenge. *Eur. Heart J.* 38 (11), 774–784. doi: 10.1093/eurheartj/ehw224
- Heusch, G., Boengler, K., and Schulz, R. (2010). Inhibition of mitochondrial permeability transition pore opening: the Holy Grail of cardioprotection. *Basic Res. Cardiol.* 105 (2), 151–154. doi: 10.1007/s00395-009-0080-9
- Higgins, J. P. T., and Green, S. (2012). *Cochrane Handbook for Systematic Reviews of Interventions*. Version 5.0.1, Updated March 2011. Oxford, UK: the Cochrane Collaboration. <http://www.cochrane-handbook.org/>.
- Hu, J. N., Qu, W., Zhang, Q. M., Jiang, M. X., Ye, W., and Wang, R. W. (2014). To observe the clinical efficacy and safety on treating and angina pectoris coronary heart disease with Kodaling Tablets. *Clin. J. Chin. Med.* 6 (5), 31–34. doi: 10.3969/j.issn.1674-7860.2014.05.014
- Hu, T., Wei, G., Xi, M., Yan, J., Wu, X., Wang, Y., et al. (2016). Synergistic cardioprotective effects of Danshensu and hydroxysafflor yellow A against myocardial ischemia-reperfusion injury are mediated through the Akt/Nrf2/HO-1 pathway. *Int. J. Mol. Med.* 38, 83–94. doi: 10.3892/ijmm.2016.2584
- Jormalainen, M., Vento, A. E., Wartiovaara-Kautto, U., Suojaranta-Ylinen, R., Rämö, O. J., Petäjä, J., et al. (2004). Recombinant hirudin enhances cardiac output and decreases systemic vascular resistance during reperfusion after cardiopulmonary bypass in a porcine model. *J. Thorac. Cardiovasc. Surg.* 128 (2), 189–196. doi: 10.1016/j.jtcvs.2003.11.058
- Kjaergard, L. L., Villumsen, J., and Gluud, C. (2001). Reported methodologic quality and discrepancies between large and small randomized trials in meta-analyses. *Ann. Intern. Med.* 135, 982–989. doi: 10.7326/0003-4819-135-11-200112040-00010
- Kleimborgard, P., Schulz, R., and Heusch, G. (2011). TNF- α in myocardial ischemia/reperfusion, remodeling and heart failure. *Heart Fail. Rev.* 16 (1), 49–69. doi: 10.1007/s10741-010-9180-8
- Leng, X., Zhang, L. D., Jia, L. Q., Zang, A. Y., Cao, J., Li, Q. F., et al. (2015). Effect of ginsenoside Rb1 on isoproterenol-induced acute myocardial ischemia in rats and its mechanism of action. *Chin. J. Exp. Trad. Med. Formulae* 21 (24), 104–108. doi: 10.13422/j.cnki.syfjx.2015240104
- Li, C., Li, Q., Liu, Y. Y., et al. (2014). Protective effects of Notoginsenoside R1 on intestinal ischemia-reperfusion injury in rats. *Am. J. Physiol. Gastrointest. Liver Physiol.* 306, G111–G122. doi: 10.1152/ajpgi.00123.2013
- Li, H. Q., Wei, J. J., Xia, W., Li, J. H., Liu, A. J., Yin, S. B., et al. (2015). Promoting blood circulation for removing blood stasis therapy for acute intracerebral hemorrhage: a systematic review and meta-analysis. *Acta Pharmacol. Sin.* 36 (6), 659–675. doi: 10.1038/aps.2014.139
- Lim, K. H., Lim, D. J., and Kim, J. H. (2013). Ginsenoside-Re ameliorates ischemia and reperfusion injury in the heart: a hemodynamics approach. *J. Ginseng Res.* 37 (3), 283–292. doi: 10.5142/jgr.2013.37.283
- Liu, J., and Niu, P. W. (2011). Protective effects of chuan xiong qin against ischemia/reperfusion injury in rats. *China Prac. Med.* 6, 29–30. doi: 10.14163/j.cnki.11-5547/r.2011.02.021
- Liu, C. E., Wu, S. X., and Ye, G. (2012). Mechanism of ginsenoside Rb1 against myocardial apoptosis during ischemia-reperfusion injury in diabetic rats. *J. Emerg. Trad. Chin. Med.* 21 (7), 1080–1081. doi: 10.3969/j.issn.1009-0959.2010.03.054
- Liu, G. Y., Zhang, Z., Li, Z., and Yang, G. L. (2014). Integrative interventions stable angina syndrome of blood stasis due to qi deficiency clinical efficacy. *Chin. Arch. Trad. Chin. Med.* 32 (11), 2616–2618. doi: 10.13193/j.issn.1673-7717.2014.11.016
- Liu, J., Ding, Y. J., Lin, N., and Shu, B. (2010). Protective effect of astragaloside on cardiac function injury induced by myocardial ischemia in Beagles. *China Prac. Med.* 5 (33), 12–15. doi: 10.3969/j.issn.1673-7555.2010.33.006
- Liu, Q., Li, J., Wang, J., Li, J., Janicki, J. S., and Fan, D. (2013). Effects and mechanisms of Chinese herbal medicine in ameliorating myocardial ischemia-reperfusion injury. *Evid. Based Complementary Altern. Med.* 2013, 925625. doi: 10.1155/2013/925625
- Liu, R., Zhang, L., Lan, X., Li, L., Zhang, T. T., Sun, J. H., et al. (2011). Protection by borneol on cortical neurons against oxygen-glucose deprivation/reperfusion: involvement of anti-oxidation and anti-inflammation through nuclear transcription factor KappaB signaling pathway. *Neuroscience* 176, 408–419. doi: 10.1016/j.neuroscience.2010.11.029
- Liu, W. J., Tang, H. T., Jia, Y. T., Ma, B., Fu, J. F., Wang, Y., et al. (2010). Notoginsenoside R1 attenuates renal ischemia-reperfusion injury in rats. *Shock* 34, 314–320. doi: 10.1097/SHK.0b013e3181ceede4
- Liu, X., Jiang, Y., Yu, X., Fu, W., Zhang, H., and Sui, D. (2014). Ginsenoside-Rb3 protects the myocardium from ischemia-reperfusion injury via the inhibition of apoptosis in rats. *Exp. Ther. Med.* 8, 1751–1756. doi: 10.3892/etm.2014.2007
- Liu, Y. N., Zhou, Z. M., and Chen, P. (2008). Evidence that hydroxysafflor yellow A protects the heart against ischaemia-reperfusion injury by inhibiting mitochondrial permeability transition pore opening. *Clin. Exp. Pharmacol. Physiol.* 35 (2), 211–216. doi: 10.1111/j.1440-1681.2007.04814.x
- Lu, H. W., Zhang, J., Chen, X., and Zheng, C. (2014). Clinical observation on tongxinluo capsule combined with outline western medicine in the prevention of restenosis after percutaneous coronary intervention in 90 cases. *J. Trad. Chin. Med.* 55 (24), 2117–2120. doi: 10.13288/j.11-2166/r.2014.24.013
- Lu, M., Tang, F., Zhang, J., Luan, A., Mei, M., Xu, C., et al. (2015). Astragaloside IV attenuates injury caused by myocardial ischemia/reperfusion in rats via regulation of toll-like receptor 4/Nuclear Factor- κ B signaling pathway. *Phytother. Res.* 4, 599–606. doi: 10.1002/ptr.5297
- Lu, X. Y., Shi, D. Z., Xu, H., Chen, K. Y., and Lv, S. Z. (2006). Clinical study on effect of Xiongshao Capsule on restenosis after percutaneous coronary intervention. *Zhongguo Zhong Xi Yi Jie He Za Zhi* 26 (1), 13–17. doi: 10.3321/j.issn:1003-5370.2006.01.006
- Lu, Z., Kou, W., Du, B., Wu, Y., Zhao, S., Brusco, O. A., et al. (2008). Chinese Coronary Secondary Prevention Study Group, Li S. Effect of Xuezhikang, an extract from red yeast Chinese rice, on coronary events in a Chinese population with previous myocardial infarction. *Am. J. Cardiol.* 101 (12), 1689–1693. doi: 10.1016/j.amjcard.2008.02.056
- Lv, L., Jiang, S. S., Xu, J., Gong, J. B., and Cheng, Y. (2012). Protective effect of ligustrazine against myocardial ischemia reperfusion in rats: the role of endothelial nitric oxide synthase. *Clin. Exp. Pharmacol. Physiol.* 39, 20–27. doi: 10.1111/j.1440-1681.2011.05628.x
- Ma, L., Chuang, C. C., Weng, W., Zhao, L., Zheng, Y., Zhang, J., et al. (2016). Paeonol protects rat heart by improving regional blood perfusion during no-reflow. *Front. Physiol.* 7, 298. doi: 10.3389/fphys.2016.00298

- Mao, S., Wang, L., Ouyang, W. W., Zhou, Y. S., Qi, J. Y., and Guo, L. H. (2016). Traditional Chinese medicine, Danlou tablets alleviate adverse left ventricular remodeling after myocardial infarction: results of a double-blind, randomized, placebo-controlled, pilot study. *BMC Complement. Altern. Med.* 16, 1–8. doi: 10.1186/s12906-016-1406-4
- Marchant, D. J., Boyd, J. H., Lin, D. C., Granville, D. J., Garmaroudi, F. S., McManus, B. M., et al. (2012). Inflammation in myocardial diseases. *Circ. Res.* 110 (1), 126–144. doi: 10.1161/CIRCRESAHA.111.243170
- Meng, Y., Li, W. Z., Shi, Y. W., Zhou, B. F., Ma, R., and Li, W. P. (2016). Danshensu protects against ischemia/reperfusion injury and inhibits the apoptosis of H9c2 cells by reducing the calcium overload through the p-JNK-NF-kappaB-TRPC6 pathway. *Int. J. Mol. Med.* 37, 258–266. doi: 10.3892/ijmm.2015.2419
- Mo, Q. Y., Fang, X. M., Zhang, C., Wu, S. J., He, J. S., Wang, Q., et al. (2012). Effect of YIXINMAI granule on high-sensitivity c-reactive protein, interlenkin-6 and interlenkin-18 in patients with coronary artery disease. *Guangxi Med. J.* 34 (5), 537–539. doi: 10.3969/j.issn.0253-4304.2012.05.007
- Murray, C. J., Barber, R. M., Foreman, K. J., Abbasoglu Ozgoren, A., Abd-Allah, F., Abera, S. F., et al. (2015). Global, regional, and national disability-adjusted life years (DALYs) for 306 diseases and injuries and healthy life expectancy (HALE) for 188 countries, 1990–2013: quantifying the epidemiological transition. *Lancet* 386 (10009), 2145–2191. doi: 10.1016/S0140-6736(15)61340-X
- Nizamutdinova, I. T., Jin, Y. C., Kim, J. S., Yean, M. H., Kang, S. S., Kim, Y. S., et al. (2008). Paeonol and paeoniflorin, the main active principles of *Paeonia albiflora*, protect the heart from myocardial ischemia/reperfusion injury in rats. *Planta Med.* 74, 14–18. doi: 10.1055/s-2007-993775
- Pan, H., Li, D., Fang, F., Chen, D., Qi, L., Zhang, R., et al. (2011). Salvianolic acid A demonstrates cardioprotective effects in rat hearts and cardiomyocytes after ischemia/reperfusion injury. *J. Cardiovasc. Pharmacol.* 58, 535–542. doi: 10.1097/FJC.0b013e31822de355
- Park, J. H., Park, O. K., Cho, J. H., Chen, B. H., Kim, I. H., Ahn, J. H., et al. (2014). Anti-inflammatory effect of tanshinone I in neuroprotection against cerebral ischemia-reperfusion injury in the gerbil hippocampus. *Neurochem. Res.* 39, 1300–1312. doi: 10.1007/s11064-014-1312-4
- Qian, W., Xiong, X., Fang, Z., Lu, H., and Wang, Z. (2014). Protective effect of tetramethylpyrazine on myocardial ischemia-reperfusion injury. *Evid. Based Complement. Altern. Med.* 2014, 107501. doi: 10.1155/2014/107501
- Qiao, Z. Q., Zhang, M. Z., Liu, H., Cheng, K. L., and Li, S. (2006). A randomized double-blind placebo-controlled clinical trial of Tongguan Capsule in improving cardiac function after percutaneous coronary intervention in patients with coronary heart disease. *Chin. Arch. Trad. Chin. Med.* 24 (9), 1667–1668. doi: 10.7666/d.y738108
- Qiu, S. L., Jin, M., Zhu, T. G., Quan, X., Liang, Y., and Shi, D. Z. (2009). Effect of replenishing Qian nourishing yin to promote the blood circulation on 103 patients with acute myocardial infarction after reperfusion. *J. Cap. Med. Univ.* 30 (4), 426–429. doi: 10.3969/j.issn.1006-7795.2009.04.005
- Roffi, M., Patrono, C., Collet, J. P., Mueller, C., Valgimigli, M., Andreotti, F., et al. (2016). 2015 ESC Guidelines for the management of acute coronary syndromes in patients presenting without persistent ST-segment elevation. Task Force for the Management of Acute Coronary Syndromes in Patients Presenting without Persistent ST-Segment Elevation of the European Society of Cardiology (ESC). *G. Ital. Cardiol. (Rome)* 17 (10), 831–872. doi: 10.1714/2464.25804
- Rongen, G. A., and Wever, K. E. (2015). Cardiovascular pharmacotherapy: innovation stuck in translation. *Eur. J. Pharmacol.* 759, 200–204. doi: 10.1016/j.ejphar.2015.03.035
- Roth, G. A., Huffman, M. D., Moran, A. E., Feigin, V., Mensah, G. A., Naghavi, M., et al. (2015). Global and regional patterns in cardiovascular mortality from 1990 to 2013. *Circulation* 132 (17), 1667–1678. doi: 10.1161/CIRCULATIONAHA.114.008720
- Schulz, K. F., Altman, D. G., Moher, D., CONSORT Group. (2010). CONSORT 2010 statement: updated guidelines for reporting parallel group randomized trials. *BMJ* 340, c332. doi: 10.1136/bmj.c332
- Schulz, R., Kelm, M., and Heusch, G. (2004). Nitric oxide in myocardial ischemia/reperfusion injury. *Cardiovasc. Res.* 61 (3), 402–413. doi: 10.1016/j.cardiores.2003.09.019
- Shang, H. C., Zhang, J. H., Yao, C., Liu, B. Y., Gao, X. M., and Ren, M. (2013). Qi-Shen-Yi-Qi dripping pills for the secondary prevention of myocardial infarction: a randomised clinical trial. *Evid. Based Complement. Altern. Med.* 2013, 738391. doi: 10.1155/2013/738391
- Shang, Q. H., Xu, H., Lu, X. Y., Wen, C., Shi, D. Z., and Chen, K. J. (2011). A multi-center randomized double-blind placebo-controlled trial of Xiongshao Capsule in preventing restenosis after percutaneous coronary intervention: a subgroup analysis of senile patients. *Chin. J. Integr. Med.* 17 (9), 669–674. doi: 10.1007/s11655-011-0843-7
- Sun, S. Z. (2014). Observation on efficacy and safety of Shexiang Baoxin Pills in the treatment of unstable angina pectoris of coronary heart disease in elderly patients. *Mod. J. Integr. Trad. Chin. West. Med.* 23 (4), 391–393. doi: 10.3969/j.issn.1008-8849.2014.04.020
- Tang, H., Pan, C. S., Mao, X. W., Liu, Y. Y., Yan, L., Zhou, C. M., et al. (2014). Role of NADPH oxidase in total salvianolic acid injection attenuating ischemia-reperfusion impaired cerebral microcirculation and neurons: implication of AMPK/Akt/PKC. *Microcirculation* 21, 615–627. doi: 10.1111/micc.12140
- Tang, N. Y., Liu, C. H., Hsieh, C. T., and Hsieh, C. L. (2010). The anti-inflammatory effect of paeoniflorin on cerebral infarction induced by ischemia-reperfusion injury in Sprague-Dawley rats. *Am. J. Chin. Med.* 38, 51–64. doi: 10.1142/S0192415X10007786
- Tao, T., Chen, F., Bo, L., Xie, Q., Yi, W., Zou, Y., et al. (2014). Ginsenoside Rg1 protects mouse liver against ischemia-reperfusion injury through anti-inflammatory and anti-apoptosis properties. *J. Surg. Res.* 191, 231–238. doi: 10.1016/j.jss.2014.03.067
- Tu, L., Pan, C. S., Wei, X. H., Yan, L., Liu, Y. Y., Fan, J. Y., et al. (2013). Astragaloside IV protects heart from ischemia and reperfusion injury via energy regulation mechanisms. *Microcirculation* 20 (8), 736–747. doi: 10.1111/micc.12074
- Wang, J., He, Q. Y., and Zhang, Y. L. (2009). Effect of shenshao tablet on the quality of life for coronary heart disease patients with stable angina pectoris. *Chin. J. Integr. Med.* 15 (5), 328–332. doi: 10.1007/s11655-009-0328-0
- Wang, J., Qiao, L., Li, Y., and Yang, G. (2008). Ginsenoside Rb1 attenuates intestinal ischemia-reperfusion-induced liver injury by inhibiting NF-kappaB activation. *Exp. Mol. Med.* 40, 686–698. doi: 10.3858/emmm.2008.40.6.686
- Wang, J., Teng, F., Liu, Y. M., and Chen, G. (2017). Invention effect of xuesaitong for coronary heart disease unstable angina with blood stasis and relevant microRNA. *Chin. J. Exp. Trad. Med. Formulae* 23 (9), 11–16. doi: 10.13422/j.cnki.syfjx.2017190011
- Wang, L., Zhao, X. J., Mao, S., Liu, S. N., Guo, X. F., and Guo, L. H. (2016). Efficacy of danlou tablet in patients with non-ST elevation acute coronary syndrome undergoing percutaneous coronary intervention: results from a multicentre, placebo-controlled, randomized trial. *Evid. Based Complement. Altern. Med.* 2016, 7960503. doi: 10.1155/2016/7960503
- Wang, S. H., Wang, J., Li, J., Xiong, X. J., Ye, Y., and Zhu, M. J. (2012). Efficacy assessment of treating patients with coronary heart disease angina of phlegm and stasis mutual obstruction syndrome by Danlou Tablet. *Zhongguo Zhong Xi Yi Jie He Za Zhi* 32 (8), 1051–1055. doi: 10.7661/CJIM.2012.8.1051
- Wang, Y. G., You, J. Z., Qi, J., Shang, P. J., Wang, Q. A., and Zhong, W. (2012). The influence on blood lipids, blood rheology and TCM syndromes by Shuangshen Tongguan capsule on patients with stable angina. *Mod. Trad. Chin. Med.* 32 (5), 4–7.
- Wang, Y., Hu, Z., Sun, B., Xu, J., Jiang, J., and Luo, M. (2015). Ginsenoside Rg3 attenuates myocardial ischemia/reperfusion injury via Akt/endothelial nitric oxide synthase signaling and the Bcl2 lymphoma/Bcl2 lymphoma-associated X protein pathway. *Mol. Med. Rep.* 11, 4518–4524. doi: 10.3892/mmr.2015.3336
- Wang, Y., Li, X., Wang, X., Lau, W., Wang, Y., Xing, Y., et al. (2013). Ginsenoside Rd attenuates myocardial ischemia/reperfusion injury via Akt/GSK-3beta signaling and inhibition of the mitochondria-dependent apoptotic pathway. *PLoS One* 8, e70956. doi: 10.1371/journal.pone.0070956
- Wei, B., Li, W. W., Ji, J., Hu, Q. H., and Ji, H. (2014). The cardioprotective effect of sodium tanshinone IIA sulfonate and the optimizing of therapeutic time window in myocardial ischemia/reperfusion injury in rats. *Atherosclerosis* 235, 318–327. doi: 10.1016/j.atherosclerosis.2014.05.924
- Wu, Y., and He, L. (2010). Advances in research on mechanisms of myocardial ischemia-reperfusion injury and related therapeutic drugs. *Prog. Pharm. Sci.* 34 (7), 305–312. doi: 10.3969/j.issn.1001-5094.2010.07.003
- Wu, Y., Xia, Z. Y., Dou, J., Zhang, L., Xu, J. J., Zhao, B., et al. (2011). Protective effect of ginsenoside Rb1 against myocardial ischemia/reperfusion injury in streptozotocin-induced diabetic rats. *Mol. Biol. Rep.* 38, 4327–4335. doi: 10.1007/s11033-010-0558-4
- Xia, K. P., Ca, H. M., and Shao, C. Z. (2015). Protective effect of notoginsenoside R1 in a rat model of myocardial ischemia reperfusion injury by regulation of

- vitamin D3 upregulated protein 1/NF-kappaB pathway. *Pharmazie* 70, 740–744. doi: 10.1691/ph.2015.5694
- Xu, M. (2014). Research on main mechanisms of myocardial ischemia reperfusion injury and related drug therapy. *Pract. Pharm. Clin. Remed.* 17 (8), 1052–1055. doi: 10.14053/j.cnki.ppcr.2014.08.068
- Xu, D. P., Wang, X., Sheng, X. G., Lin, Y., Li, S., and Zheng, Z. Y. (2014). Double-blind, randomized, controlled clinical trial of Shenzhu Guanxin prescription for treatment of stable angina due to coronary heart disease. *J. Guangzhou Univ. Trad. Chin. Med.* 31 (2), 173–177. doi: 10.13359/j.cnki.gzxbtcm.2014.02.001
- Xu, D. P., Wu, H. L., Lan, T. H., Wang, X., Sheng, X. G., and Lin, Y. (2015). Effect of Shenzhu Guanxin recipe on patients with angina pectoris after percutaneous coronary intervention: a prospective, randomized controlled trial. *Chin. J. Integr. Med.* 21 (6), 408–416. doi: 10.1007/s11655-015-2040-6
- Xu, Q., Bauer, R., Hendry, B. M., Fan, T. P., Zhao, Z., Duez, P., et al. (2013). The quest for modernisation of traditional Chinese medicine. *BMC Complement. Altern. Med.* 13, 132. doi: 10.1186/1472-6882-13-132
- Xue, L., Wu, Z., Ji, X. P., Gao, X. Q., and Guo, Y. H., (2014). Effect and mechanism of salvianolic acid B on the myocardial ischemia-reperfusion injury in rats. *Asian Pac. J. Trop. Med.* 7 (4), 280–284. doi: 10.1016/S1995-7645(14)60038-9
- Yang, H., Yang, B., and Xiong, Q. X. (2017). Effect of coronary Ningtong prescription combined with metoprolol on coronary heart disease and angina pectoris. *Shaanxi J. Trad. Chin. Med.* 38 (8), 1006–1007. doi: 10.3969/j.issn.1000-7369.2017.08.010
- Yellon, D. M., and Hausenloy, D. J. (2007). Myocardial reperfusion injury. *N. Engl. J. Med.* 357 (11), 1121–1135. doi: 10.1056/NEJMr071667
- Yin, Y., Guan, Y., Duan, J., Wei, G., Zhu, Y., Quan, W., et al. (2013). Cardioprotective effect of Danshensu against myocardial ischemia/reperfusion injury and inhibits apoptosis of H9c2 cardiomyocytes via Akt and ERK1/2 phosphorylation. *Eur. J. Pharmacol.* 699, 219–226. doi: 10.1016/j.ejphar.2012.11.005
- Yu, J. M., Zhang, X. B., Jiang, W., Wang, H. D., and Zhang, Y. N., (2015). Astragalosides promote angiogenesis via vascular endothelial growth factor and basic fibroblast growth factor in a rat model of myocardial infarction. *Mol. Med. Rep.* 12 (5), 6718–6726. doi: 10.3892/mmr.2015.4307
- Yu, Y., Sun, G., Luo, Y., Wang, M., Chen, R., Zhang, J., et al. (2016). Cardioprotective effects of Notoginsenoside R1 against ischemia/reperfusion injuries by regulating oxidative stress-and endoplasmic reticulum stress- related signaling pathways. *Sci. Rep.* 6 (5), 21730. doi: 10.1038/srep21730
- Zhai, Z. Y., Yang, J. H., Hang, S.M., Wu, B. H., Xin, D., Zhou, L. H., et al. (2011). Role of Janus kinase 2/signal transducer and activator of transcription 3 signaling pathway in attenuation of myocardial ischemia-reperfusion injury by teramethylpyrazine in rats. *Chin. J. Anesthesiol.* 31, 1005–1008. doi: 10.3760/cma.j.issn.0254-1416.2011.08.029
- Zhang, J. H., and Xu, M. (2000). DNA fragmentation in apoptosis. *Cell Res.* 10 (3), 205–211. doi: 10.1038/sj.cr.7290049
- Zhang, H. T., Jia, Z. H., Zhang, J., Ye, Z. K., Yang, W. X., Tian, Y. Q. (2010). No-reflow protection and long-term efficacy for acute myocardial infarction with Tongxinluo: a randomized double-blind placebo-controlled multicenter clinical trial (ENLEAT Trial). *Chin. Med. J. (Engl.)* 123 (20), 2858–2864.
- Zhang, J., Ma, C. L., and Wang, G. Z. (2014). Improvement effects of astragaloside IV on myocardial focal ischemia-reperfusion injury and its influence in PI3K/Akt/mTOR signaling pathway. *J. Jilin Univ. (Med. Ed.)* 40 (5), 991–996. doi: 10.13481/j.1671-587x.20140517
- Zhang, M. Q., Zheng, Y. L., Chen, H., Tu, et al. (2013). Sodium tanshinone IIA sulfonate protects rat myocardium against ischemia-reperfusion injury via activation of PI3K/Akt/FOXO3A/Bim pathway. *Acta Pharmacol. Sin.* 34 (11), 1386–1396. doi: 10.1038/aps.2013.91
- Zhang, Y., Wei, L., Sun, D., et al. (2010). Tanshinone IIA pretreatment protects myocardium against ischaemia/reperfusion injury through the phosphatidylinositol 3-kinase/Akt-dependent pathway in diabetic rats. *Diabetes Obes. Metab.* 12 (4), 316–322. doi: 10.1111/j.1463-1326.2009.01166.x
- Zhang, Z.F., Xu, F. Q., Liu, H. X., Wang, F. R., Zhao, M. J., Sun, L. J., et al. (2015). A multicenter, randomized, double-blind clinical study on wufuxinnaoping soft capsule in treatment of chronic stable angina patients with blood stasis syndrome. *Chin. J. Integr. Med.* 21 (8), 571–578. doi: 10.1007/s11655-014-1953-9
- Zhu, H. Y., Gao, Y. H., Wang, Z. Y., Xu, B., Wu, A. M., Wei, Y. X., et al. (2013). Astragalus polysaccharide suppresses the expression of adhesion molecules through the regulation of the p38 mapk signaling pathway in human cardiac microvascular endothelial cells after ischemia-reperfusion injury. *Evid. Based Complement Altern. Med.* 2013:280493. doi: 10.1155/2013/280493
- Zhu, Q. H., Wang, M. R., Qeng, J. F., Chen, S. J., and Xiao, Y. S., et al. (2016). Clinical effect of self-made traditional prescription on premature coronary heart disease diagnosed as tcm syndrome of phlegm turbidity and blood stasis. *Zhongguo Zhong Xi Yi Jie He Za Zhi* 8 (9), 92–95. doi: 10.3969/j.issn.1008-5971.2016.08.025

Conflict of Interest Statement: The authors declare that the research was conducted in the absence of any commercial or financial relationships that could be construed as a potential conflict of interest.

Copyright © 2019 Zhang, Zheng, Zhu, Tong, Zhuang, Zhu, Bao, Huang, Zheng and Wang. This is an open-access article distributed under the terms of the Creative Commons Attribution License (CC BY). The use, distribution or reproduction in other forums is permitted, provided the original author(s) and the copyright owner(s) are credited and that the original publication in this journal is cited, in accordance with accepted academic practice. No use, distribution or reproduction is permitted which does not comply with these terms.



Anisodamine Ameliorates Hyperkalemia during Crush Syndrome through Estradiol-Induced Enhancement of Insulin Sensitivity

Jian-Guang Yu^{1*}, Bo-Shi Fan^{2,3}, Jin-Min Guo⁴, Yun-Jie Shen¹, Ye-Yan Hu¹ and Xia Liu^{2*}

¹ Department of Pharmacy, Shanghai Chest Hospital, Shanghai Jiao Tong University, Shanghai, China, ² Department of Pharmacology, Second Military Medical University, Shanghai, China, ³ Department of Thoracic Surgery, Sixth Medical Center of PLA General Hospital, Beijing, China, ⁴ Department of Pharmacy, 960 Hospital of the Joint Logistics Support Force of the Chinese People's Liberation Army, Jinan, China

OPEN ACCESS

Edited by:

Zhang Yuefan,
Shanghai University,
China

Reviewed by:

Ying Peng,
Institute of Materia Medica,
China
He-Hui Xie,
Shanghai Jiao Tong University,
China
Yi Zhun Zhu,
Macau University of Science and
Technology, Macau

*Correspondence:

Jian-Guang Yu
yueqingqiu@163.com
Xia Liu
lxflying@aliyun.com

Specialty section:

This article was submitted to
Ethnopharmacology,
a section of the journal
Frontiers in Pharmacology

Received: 12 September 2019

Accepted: 12 November 2019

Published: 29 November 2019

Citation:

Yu J-G, Fan B-S, Guo J-M, Shen Y-J,
Hu Y-Y and Liu X (2019) Anisodamine
Ameliorates Hyperkalemia
during Crush Syndrome through
Estradiol-Induced Enhancement
of Insulin Sensitivity.
Front. Pharmacol. 10:1444.
doi: 10.3389/fphar.2019.01444

Hyperkalemia is a major cause of on-site death in crush syndrome (CS), which is more severe and common in male victims. Anisodamine is a belladonna alkaloid and widely used in China for treatment of shock through activation of $\alpha 7$ nicotinic acetylcholine receptor ($\alpha 7$ nAChR). The present work was designed to study the protective effect of anisodamine in CS and the possible role of estradiol involved. Male and ovariectomized female CS mice exhibited lower serum estradiol and insulin sensitivity, and higher potassium compared to the relative female controls at 6 h after decompression. There was no gender difference in on-site mortality in CS mice within 24 h after decompression. Serum estradiol increased with similar values in CS mice of both gender compared to that in normal mice. Anisodamine decreased serum potassium and increased serum estradiol and insulin sensitivity in CS mice, and methyllycaconitine, selective antagonist of $\alpha 7$ nAChR, counteracted such effects of anisodamine. Treatment with anisodamine or estradiol increased serum estradiol and insulin sensitivity, decreased serum potassium and on-site mortality, and eliminated the difference in these parameters between CS mice received ovariectomy or its sham operation. Anisodamine could also increase blood pressure in CS rats within 3.5 h after decompression, which could also be attenuated by methyllycaconitine, without influences on heart rate. These results suggest that activation of $\alpha 7$ nAChR with anisodamine could decrease serum potassium and on-site mortality in CS through estradiol-induced enhancement of insulin sensitivity.

Keywords: anisodamine, estradiol, $\alpha 7$ nicotinic acetylcholine receptor, crush syndrome, hyperkalemia, insulin sensitivity

INTRODUCTION

Crush syndrome (CS), due to compression of the extremities or other parts of the body, is characterized by rhabdomyolysis-induced metabolic disorders (e.g. hyperkalemia), hypovolemic shock, and acute kidney injury, etc. (Better, 1997; Oda et al., 1997; Bywaters and Beall, 1998; Slater and Mullins, 1998; Sever et al., 2015). CS in great earthquakes, is the most common cause of death,

apart from trauma (Ukai, 1997). Up to 20% victims suffering from CS died of cardiac arrest caused by hyperkalemia or hypovolemic shock shortly after decompression (Ashkenazi et al., 2005), and hyperkalemia is the most important and fatal medical complication in CS patients. Male CS victims were characterized by higher serum potassium at admission and more frequently faced with fatal hyperkalemia after mass disasters (Sever et al., 2002; Sever et al., 2003; Sever et al., 2004). However, causes of gender difference in serum potassium during CS remain unclear, and drugs to safely reduce on-site mortality in CS, except for intravenous fluid resuscitation, are still clinically vacant (Sever and Vanholder, 2013).

Anisodamine (Ani) is a belladonna alkaloid isolated from the Chinese medicinal herb *Scopolia tangutica* Maxim of the Solanaceae family, and it has been used clinically for decades primarily to ameliorate circulatory disorders such as disseminated intravascular coagulation and septic shock. Our previous studies found that Ani could indirectly activate $\alpha 7$ nicotinic acetylcholine receptor ($\alpha 7$ nAChR) to decrease serum potassium through enhancement of insulin sensitivity, resulting in decline of on-site mortality in CS, and Ani might be a promising on-site remedy for CS (Fan et al., 2016). Activation of $\alpha 7$ nAChR was reported to increase serum estradiol (E_2) level in ovariectomized rats (Ma et al., 2015). In addition, plenty of researches have demonstrated that E_2 administration could ameliorate insulin resistance and enhance insulin sensitivity (Park et al., 2017; Qiu et al., 2018; Torres et al., 2018; Yan et al., 2019). Therefore, we speculated that gender difference in serum potassium during CS depends on level of serum E_2 ; E_2 could decrease serum potassium through elevation of insulin sensitivity, and even to decrease on-site mortality in CS.

The present work was designed to study the protective effect of Ani on serum potassium and on-site mortality in CS and the possible role of E_2 involved. The influence of Ani on blood pressure after decompression in CS was also examined. Here, we show for the first time that activation of $\alpha 7$ nAChR with Ani could increase serum E_2 which further enhances insulin sensitivity to decrease serum potassium, contributing to the decline of on-site mortality in CS.

MATERIALS AND METHODS

Animals and Reagents

C57BL/6 mice (22–25 g, male; 20–22 g, female) and Sprague-Dawley rats (230–270 g, male) were purchased from Sino-British SIPPR/BK Laboratory Animals (Shanghai, China). Animals were housed at 22°C under a 12-h light/dark cycle, with free access to water and standard rodent chow (Peng et al., 2007). The use and care of animals were in compliance with institutional guidelines for health and care of experimental animals. Ani hydrochloride (purity 95%) was purchased from Fu-Ma Chemical & Engineering Company (Hangzhou, China). Methyllycaconitine (MLA) citrate was purchased from Sigma-Aldrich (St. Louis, MO, USA). 17β - E_2 was purchased from Mei-Lun Biology Company (Dalian, China).

Ovariectomy Surgery

Female mice were bilaterally ovariectomized as previously described (Sun et al., 2018). Briefly, mice were anesthetized with 10% chloral hydrate (0.03 mL/kg, i.p.). The dorsal skin was shaved and sterilized. The ovaries were exteriorized with the associated fat pad and fallopian tubes via a midline dorsal skin and muscle layer incision at the right or left side of the vertebral column, and then the wounds were closed. During sham operation for ovariectomy (OVX) surgery, mice received the same operation except for isolation and removal of the ovaries.

Preparation of CS Models

CS Models were prepared as previously described (Fan et al., 2016). In general, mice were anesthetized with a combination of ketamine (15 mg/kg, i.p.) and diazepam (0.15 mg/kg, i.p.) after 6-h fast, while rats were anesthetized with a combination of ketamine (10 mg/kg, i.p.) and diazepam (0.1 mg/kg, i.p.) after an overnight fast. The animals were fixed in prone position, with hind limbs (2 and 4.5 cm from the ankles up for mice and rats respectively) compressed by 20 kg weights for 5 h.

Serum Biochemical Assays

Serum K^+ and glucose levels in mice were measured with a Hitachi 7600-120 automated chemistry analyzer (Hitachi, Tokyo, Japan). Mice serum insulin and E_2 levels were determined by ELISA according to the manufacturer's instructions (Shanghai Enzyme-linked Biotechnology, Shanghai, China). Homeostasis model assessment of insulin resistance (HOMA-IR) index = fasting serum insulin (mIU/L) \times fasting serum glucose (mmol/L)/22.5. Quantitative insulin sensitivity check index (QUICKI) = $1/[\log(\text{fasting serum glucose}) + \log(\text{fasting serum insulin})]$.

Blood Pressure Measurement

Systolic blood pressure (SBP), diastolic blood pressure (DBP), mean blood pressure (MBP), and heart rate (HR) were continuously recorded as previously described with minor modifications (Liu et al., 2012; Yu et al., 2013). Briefly, rats were anesthetized with a combination of ketamine (50 mg/kg, i.p.) and diazepam (5 mg/kg, i.p.). A polyethylene catheter was inserted into the ascending aorta through left common carotid artery for blood pressure measurement and another polyethylene catheter was inserted into left external jugular vein for drug injection. After a two-day recovery period, blood pressure and HR were determined under a conscious condition.

Experimental Protocols

Experiment 1: Gender Difference of Serum K^+ , E_2 , Insulin Sensitivity, and Mortality in Mice With CS

Female mice were randomly divided into normal group ($n = 6$) and CS model group ($n = 6$, mice received compression). Twelve male mice were divided and treated similarly. Blood samples were collected from vena cava at 6 h after decompression, and serum K^+ , E_2 , insulin, and glucose levels were measured, as well

as in “normal” groups. CS models were established in another group of mice ($n = 20$ per gender). Survival time was monitored for 24 h after decompression.

Experiment 2: Influences of Ani on Serum K^+ , E_2 , and Insulin Sensitivity in Mice With CS

Male mice were randomly divided into five groups ($n = 6$ per group): 1) normal: mice received normal saline (i.p.); 2) CS model: mice received normal saline (i.p.); 3) MLA (10 mg/kg); 4) Ani (28 mg/kg); 5) Ani (28 mg/kg) + MLA (10 mg/kg). CS models were established in groups 2 to 5. Ani was given i.p. at 30 min before decompression, and MLA was given i.p. 30 min earlier. Blood samples were collected from vena cava at 6 h after decompression, and serum K^+ , E_2 , insulin, and glucose levels were measured, as well as in “normal” group.

Experiment 3: Influences of OVX and Ani/ E_2 Treatment on Serum K^+ , E_2 , and Insulin Sensitivity in Mice With CS

Female mice were randomly divided into four groups ($n = 6$ per group) 2 weeks after OVX surgery: 1) normal: mice received normal saline (i.p.); 2) CS model: mice received normal saline (i.p.); 3) Ani (28 mg/kg); 4) E_2 (100 mg/kg). CS models were established in the later three groups. Four groups ($n = 6$ per group) of female mice were treated similarly 2 weeks after sham operation for OVX surgery. Ani and E_2 were given i.p. at 30 min before decompression. Blood samples were collected from vena cava at 6 h after decompression, and serum K^+ , E_2 , insulin, and glucose levels were measured, as well as in “normal” group.

Experiment 4: Effects of Ani and E_2 on Mortality in Mice With CS

Female mice were randomly divided into three groups ($n = 20$ per group) 2 weeks after OVX surgery: 1) CS model: mice received normal saline (i.p.); 2) Ani (28 mg/kg); 3) E_2 (100 mg/kg). CS models were established in all the groups. Three groups ($n = 20$ per group) of female mice were treated similarly 2 weeks after sham operation for OVX surgery. Ani and E_2 were given i.p. at 30 min before decompression. Survival time was monitored for 24 h after decompression.

Experiment 5: Influences of Ani on Blood Pressure in Rats With CS

Male rats were randomly divided into five groups ($n = 6$ per group): 1) normal: rats received normal saline (i.p.); 2) CS model: rats received normal saline (i.p.); 3) MLA (7 mg/kg); 4) Ani (20 mg/kg); 5) Ani (20 mg/kg) + MLA (7 mg/kg). After catheterization and recovery for 2 d, CS models were established in groups 2 to 5. Ani was injected i.p. at 30 min before decompression, and MLA was injected i.p. 30 min earlier. Blood pressure was monitored for 3.5 h since 30 min before decompression, as well as in “normal” group.

Statistical Analysis

Data are shown as mean \pm SD. T test or t' test was used for data of experiments involving only two groups. ANOVA was used for

data of experiments involving more than two groups, followed by Bonferroni test or Games-Howell test. Kaplan-Meier analysis was used for survival time analysis, followed by a log-rank test. Survival rate between two groups were analyzed with Fisher's exact test. $P < 0.05$ was considered statistically significant. Analyses were performed using SPSS 21.0 (SPSS, Inc., Chicago, IL, USA).

RESULTS

Gender Difference of Serum K^+ , E_2 , and Mortality in Mice With CS

Serum K^+ level at 6 h after decompression was significantly higher in male mice (+7.6%, $P < 0.01$, **Figure 1A**) compared with that in female mice, and there was no difference in serum K^+ between normal female and male mice. Male mice had significantly lower serum E_2 level than female mice whether compressed or not. Furthermore, serum E_2 was much higher in both female and male CS models (+18.7%, +47.1% respectively, **Figure 1B**) than that in normal mice. The mortality within 24 h was 60% and 70% for female and male CS models respectively (**Figure 1C**).

Ani Decreases Serum K^+ and Increases Serum E_2 in Mice With CS

Serum K^+ was significantly lower in Ani (−16.5%, $P < 0.01$, **Figure 2A**) treated mice compared with that in model controls, and significantly higher in Ani + MLA group compared with that in Ani group (+12.4%, $P < 0.05$). Serum E_2 was significantly higher in Ani (+113.7%, $P < 0.01$, **Figure 2B**) treated mice compared with that in model controls, and significantly lower in Ani + MLA group compared with that in Ani group (−43.4%, $P < 0.05$).

Influences of OVX and Ani/ E_2 Treatment on Serum K^+ and E_2 in Mice With CS

Serum K^+ was significantly higher in CS models received OVX surgery (+9.5%, $P < 0.05$, **Figure 3A**) compared with that in those received sham operation for OVX surgery. Serum K^+ decreased in CS models received OVX surgery or its sham operation through Ani (−14.9%, −11.8% respectively) or E_2 (−15.1%, −9.5% respectively) treatment. OVX surgery did not affect serum K^+ in normal mice. OVX surgery-induced difference in serum K^+ was eliminated by both Ani and E_2 treatment. Serum E_2 was significantly lower in mice received OVX surgery compared with that in those received sham operation for OVX surgery, except for those received E_2 treatment (**Figure 3B**). Serum E_2 increased in CS models received OVX surgery or its sham operation through Ani (+31.5%, +12.6% respectively) or E_2 (+95.4%, +13.8% respectively) treatment.

Ani and E_2 Decreases Mortality in Mice With CS

The mortality within 24 h was much lower in Ani and E_2 groups compared with that in CS model controls received OVX surgery (30% and 25% vs. 70%, **Figure 4B**) or its sham operation (20%

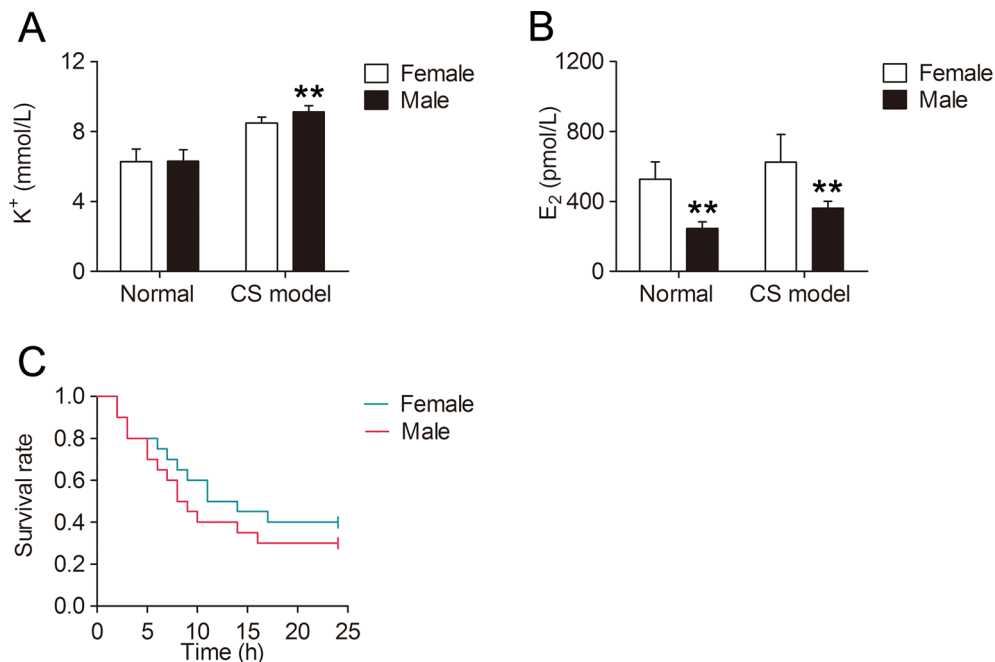


FIGURE 1 | Gender difference of serum K^+ , E_2 , and mortality in mice with crush syndrome (CS). Blood samples of mice with CS were collected at 6 h after decompression ($n = 6$ per group). Serum K^+ level was significantly lower in female CS models than that in male (**A**). Serum E_2 level was much higher in both female and male CS models than that in normal mice (**B**). There was no significant difference in survival time between female and male CS models (**C**, $n = 20$ per group). ** $P < 0.01$ vs. female.

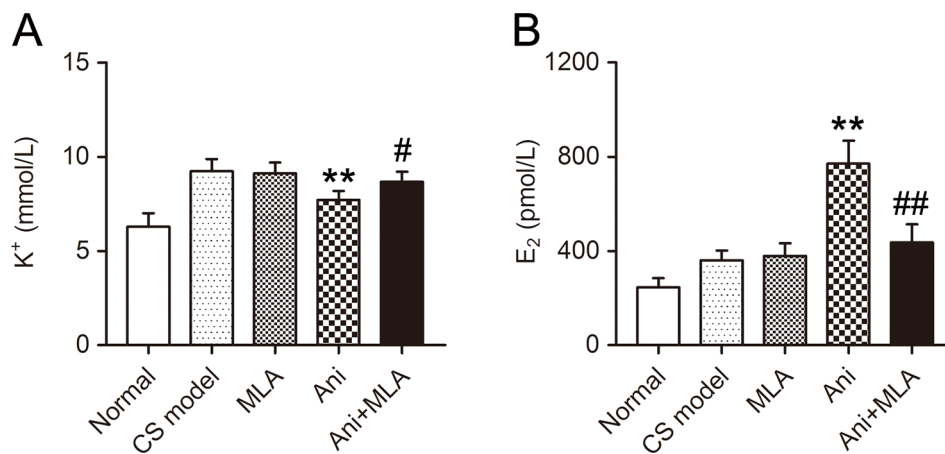


FIGURE 2 | Anisodamine (Ani) decreases serum K^+ and increases serum E_2 in male mice with crush syndrome (CS). Ani (28 mg/kg, i.p.) was administrated at 30 min before decompression in mice with CS, and methyllycaconitine (MLA) (10 mg/kg, i.p.) was given 30 min earlier. Blood samples were collected at 6 h after decompression. Ani decreased serum K^+ level after decompression, and MLA significantly counteracted such effect of Ani (**A**). Ani increased serum E_2 level after decompression, and MLA significantly counteracted such effect of Ani (**B**). $N = 6$ per group. ** $P < 0.01$ vs. CS model. # $P < 0.05$, ## $P < 0.01$ vs. Ani.

and 20% vs. 60%, **Figure 4A**). Survival time was significantly longer in Ani and E_2 groups compared with that in CS model controls received OVX surgery (log-rank testing $\chi^2 = 6.84$, $P = 0.009$, $\chi^2 = 8.00$, $P = 0.005$ respectively) or its sham operation (log-rank testing $\chi^2 = 5.65$, $P = 0.017$, $\chi^2 = 5.98$, $P = 0.014$ respectively).

Ani Increases Insulin Sensitivity in Mice With CS

Treatment with Ani significantly reduced serum insulin ($P < 0.01$, **Figure 5A**) and HOMA-IR ($P < 0.01$, **Figure 5C**), elevated QUICKI index ($P < 0.01$, **Figure 5D**), and slightly reduced serum glucose level (**Figure 5B**) in mice with CS, indicating a higher

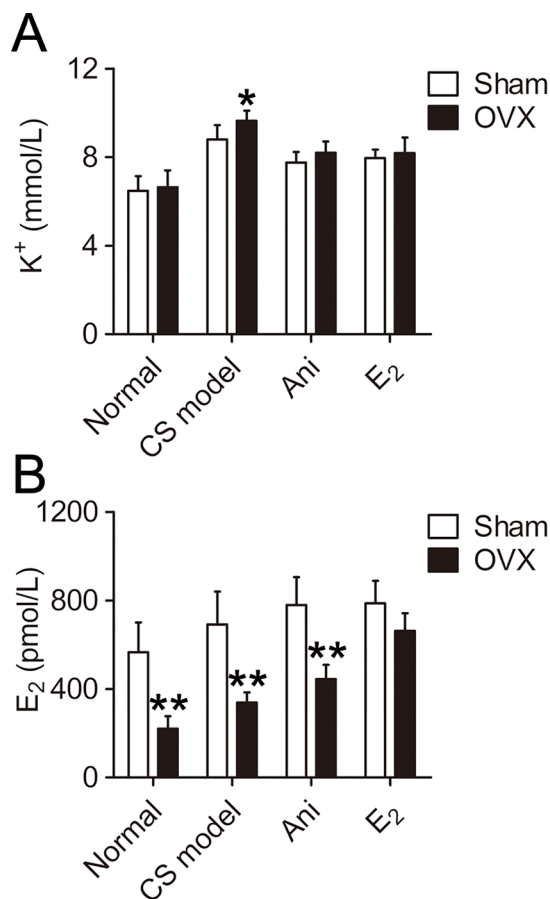


FIGURE 3 | Influences of ovariectomy (OVX) and anisodamine (Ani)/ E_2 treatment on serum K^+ and E_2 in mice with crush syndrome (CS). Ani (28 mg/kg, i.p.) or E_2 (100 mg/kg, i.p.) was administrated at 30 min before decompression in mice with CS 2 weeks after OVX surgery or its sham operation. Blood samples were collected at 6 h after decompression. OVX increases serum K^+ level after decompression. Both Ani and E_2 eliminated OVX-induced difference in serum K^+ and decreased serum K^+ in CS models (**A**). OVX decreased serum E_2 level, and E_2 treatment narrowed such difference. Both Ani and E_2 increased serum E_2 in CS models received OVX surgery (**B**). N = 6 per group. * $P < 0.05$, ** $P < 0.01$ vs. sham. Sham, sham operation for OVX surgery.

insulin sensitivity in Ani treated mice. However, MLA attenuated the effect of Ani on insulin sensitivity, reflected by elevated serum insulin ($P < 0.01$), glucose, and HOMA-IR ($P < 0.01$), and reduced QUICKI index ($P < 0.01$).

Gender Difference of Insulin Sensitivity in Mice With CS

Insulin sensitivity was significantly lower in male CS models compared with that in female CS models, reflected by higher serum insulin level ($P < 0.01$, **Figure 6A**) and HOMA-IR ($P < 0.05$, **Figure 6C**), and lower QUICKI index ($P < 0.05$, **Figure 6D**). Serum glucose level was not significantly affected by gender in CS models (**Figure 6B**). There was no difference in insulin sensitivity between normal female and male mice.

Influences of OVX and Ani/ E_2 Treatment on Insulin Sensitivity in Mice With CS

Insulin sensitivity was significantly lower in CS models received OVX surgery compared with that in those received sham operation for OVX surgery, reflected by elevated serum insulin ($P < 0.05$, **Figure 7A**) and HOMA-IR ($P < 0.05$, **Figure 7C**), and reduced QUICKI index ($P < 0.05$, **Figure 7D**). Serum glucose level was not significantly affected by OVX surgery (**Figure 7B**). Insulin sensitivity increased in CS models received OVX surgery or its sham operation through Ani or E_2 treatment, reflected by reduced serum insulin, glucose and HOMA-IR, and elevated QUICKI index. OVX surgery did not affect insulin sensitivity in normal mice. OVX surgery-induced difference in insulin sensitivity was eliminated by both Ani and E_2 treatment.

Ani Increases Blood Pressure in Rats With CS

SBP, DBP, and MBP decreased gradually after decompression in rats with CS. Treatment with Ani significantly increased SBP (105 ± 9.4 vs. 84 ± 13 mmHg, $P < 0.05$, **Figure 8A**) and MBP (88 ± 9.3 vs. 73 ± 14 mmHg, $P < 0.05$, **Figure 8C**) at 2.5 h after decompression and increased SBP (102 ± 7.9 vs. 77 ± 9.9

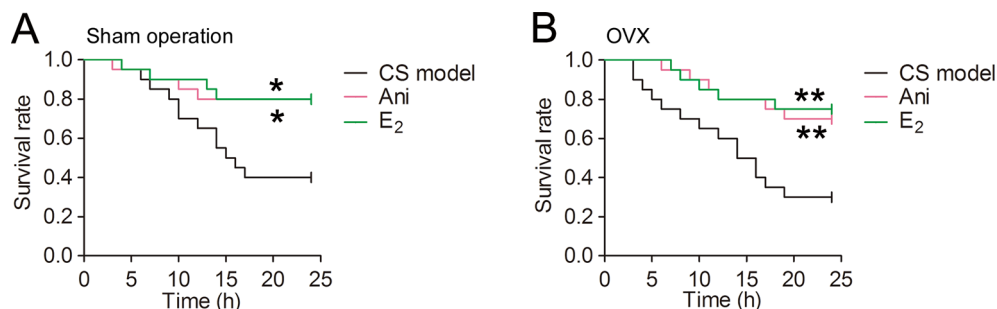


FIGURE 4 | Anisodamine (Ani) and E_2 decreases mortality in mice with crush syndrome (CS). Ani (28 mg/kg, i.p.) or E_2 (100 mg/kg, i.p.) was administrated at 30 min before decompression in mice with CS 2 weeks after ovariectomy (OVX) surgery or its sham operation. Both Ani and E_2 prolonged survival time in mice with CS received OVX surgery (**B**) or its sham operation (**A**). N = 20 per group. * $P < 0.05$, ** $P < 0.01$ vs. CS model.

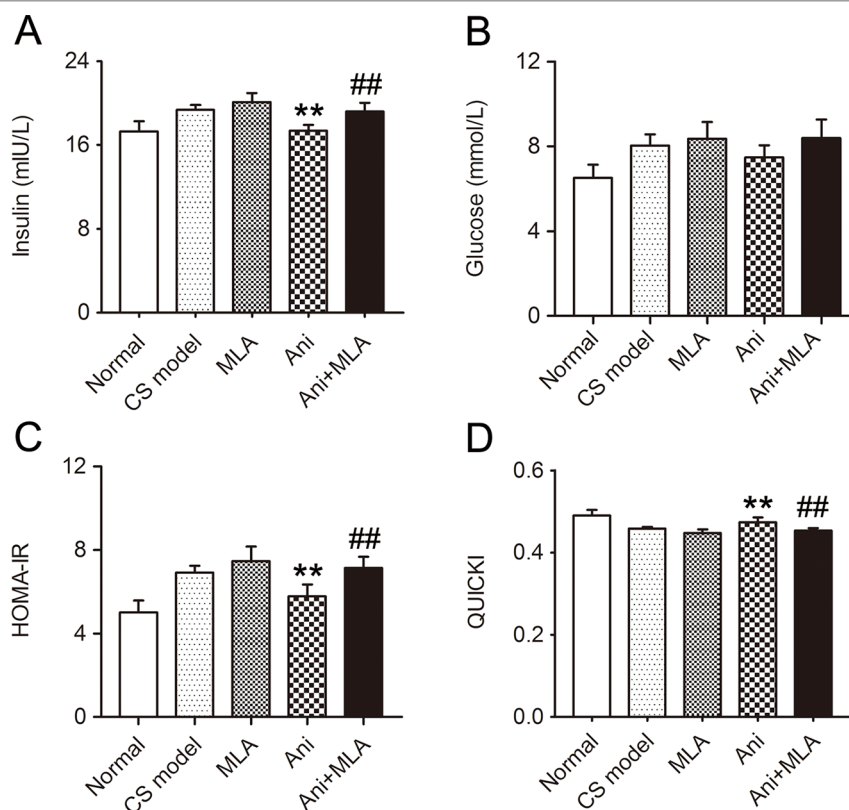


FIGURE 5 | Anisodamine (Ani) increases insulin sensitivity in male mice with crush syndrome (CS). Ani (28 mg/kg, i.p.) was administrated at 30 min before decompression in mice with CS, and methyllycaconitine (MLA) (10 mg/kg, i.p.) was given 30 min earlier. Blood samples were collected at 6 h after decompression. Ani reduced serum insulin level (A) and homeostasis model assessment of insulin resistance index (C), elevated quantitative insulin sensitivity check index (D) after decompression, but had no significant effect on serum glucose level (B). MLA significantly counteracted such effects of Ani. N = 6 per group. ** $P < 0.01$ vs. CS model. ## $P < 0.01$ vs. Ani.

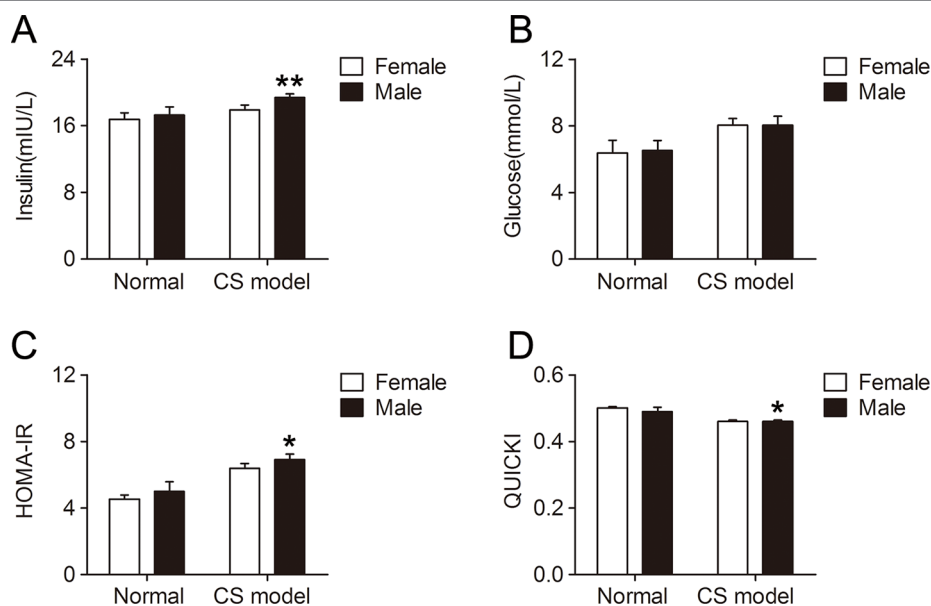


FIGURE 6 | Gender difference of insulin sensitivity in mice with crush syndrome (CS). Blood samples of mice with CS were collected at 6 h after decompression. Female CS models exhibited lower serum insulin level (A) and homeostasis model assessment of insulin resistance index (C), and higher quantitative insulin sensitivity check index (D) than that in male. Serum glucose level was not affected by gender in CS models (B). N = 6 per group. * $P < 0.05$, ** $P < 0.01$ vs. female.

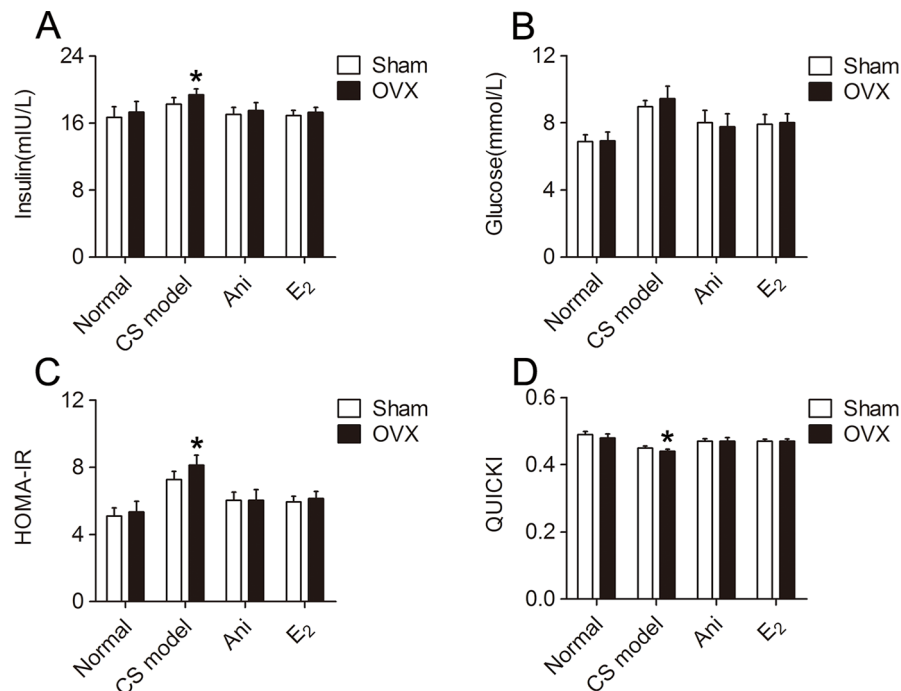


FIGURE 7 | Influences of ovariectomy (OVX) and Anisodamine (Ani)/E₂ treatment on insulin sensitivity in mice with crush syndrome (CS). Ani (28 mg/kg, i.p.) or E₂ (100 mg/kg, i.p.) was administrated at 30 min before decompression in mice with CS 2 weeks after OVX surgery or its sham operation. Blood samples were collected at 6 h after decompression. OVX elevated serum insulin level (A) and homeostasis model assessment of insulin resistance index (C), reduced quantitative insulin sensitivity check index (D) after decompression, but had no significant effect on serum glucose level (B). Both Ani and E₂ eliminated OVX-induced difference in insulin sensitivity and increased insulin sensitivity in CS models. N = 6 per group. **P* < 0.05 vs. Sham, sham operation for OVX surgery.

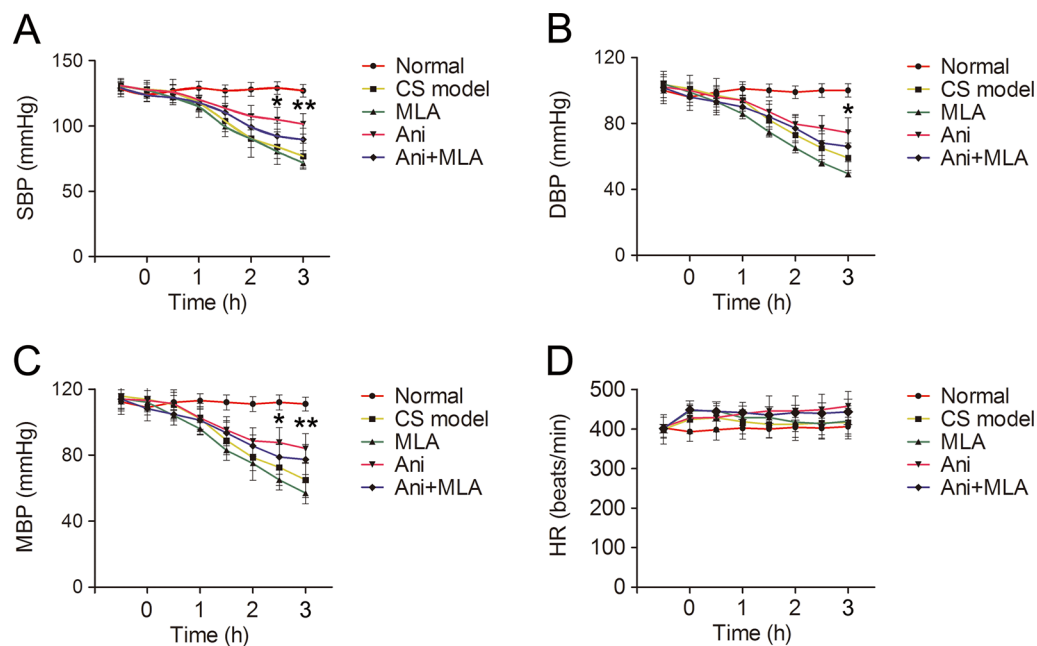


FIGURE 8 | Anisodamine (Ani) increases blood pressure in rats with crush syndrome (CS). Ani (20 mg/kg, i.p.) was administrated at 30 min before decompression in rats with CS, and methyllycaconitine (MLA) (7 mg/kg, i.p.) was given 30 min earlier. Blood pressure was monitored for 3.5 h since 30 min before decompression. Systolic blood pressure (SBP), diastolic blood pressure (DBP), mean blood pressure (MBP) decreased gradually after decompression in rats with CS. Ani significantly increased SBP and MBP at 2.5 h after decompression and increased SBP (A), DBP (B), and MBP (C) at 3 h after decompression. MLA attenuated the effect of Ani on blood pressure. Heart rate (HR) was not affected by compression, decompression, or drug administration (D). N = 6 per group. **P* < 0.05, ***P* < 0.01 vs. CS model.

mmHg, $P < 0.01$), DBP (74 ± 9.0 vs. 60 ± 9.0 mmHg, $P < 0.05$, **Figure 8B**) and MBP (84 ± 9.6 vs. 65 ± 11 mmHg, $P < 0.01$) at 3 h after decompression compared with that in model controls. MLA attenuated the effect of Ani on blood pressure. HR was not affected by compression, decompression, or drug administration (**Figure 8D**).

DISCUSSION

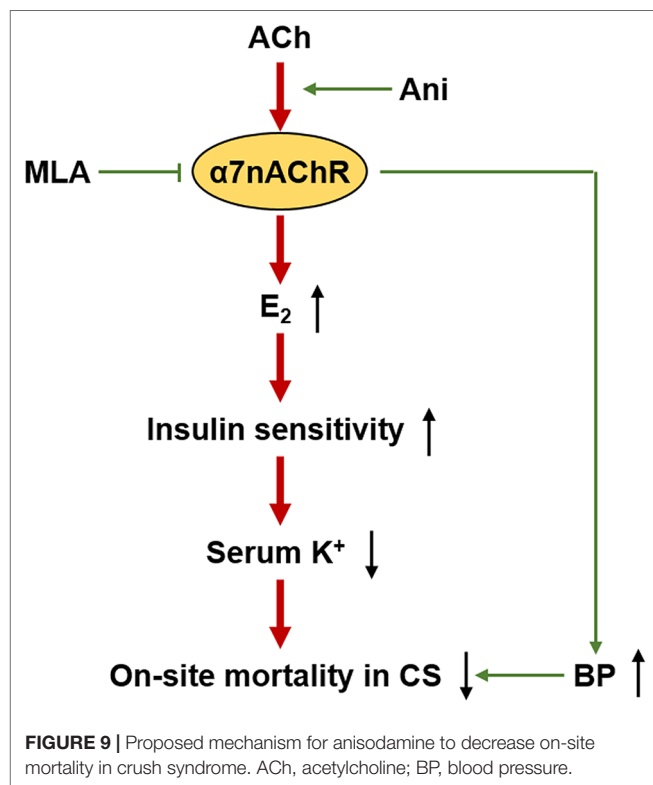
Hyperkalemia, occurring shortly after decompression, is a major cause of on-site death in CS (Ashkenazi et al., 2005). Sever and his research team reported that serum potassium is the most significant predictor of dialysis needs in the CS victims recued during the first 3 days (Sever et al., 2003). Though there is no gender difference in serum potassium in the healthy, it's puzzling that both severity and frequency of hyperkalemia is higher in male CS victims, represented as higher serum potassium at admission (5.0% higher than female) and more dialysis needs; however, there is no difference in mortality between female and male (16.1% vs. 14.3%) victims (Sever et al., 2002; Sever et al., 2003; Sever et al., 2004). Consistent with these studies, we observed no gender differences in serum potassium in normal mice, and slightly higher serum potassium in male CS mice (7.6% higher than female), which was not high enough to cause a gender difference in on-site mortality. Furthermore, OVX was performed to remove the main source of endogenous E_2 , the major female sex hormone, in female mice. As expected, serum E_2 was dramatically decreased after OVX, and serum potassium was higher in OVX mice after decompression compared to that in sham-operated mice. All the above-findings indicated the important role of E_2 in gender difference of serum potassium during CS.

As known, stress can down-regulate the hypothalamic-pituitary-gonadal axis and subsequent production of endogenous sex hormones (Toufexis et al., 2014; Rasmusson et al., 2017). Interestingly, our results demonstrated that serum E_2 was increased in both female and male CS mice with similar values, 98.42 pmol/L for female and 115.48 pmol/L for male. Coincidentally, serum E_2 was increased in all CS mice received OVX or its sham operation with similar values, 125.35 pmol/L for sham operation and 117.72 pmol/L for OVX. Treatment with E_2 was reported to decrease plasma potassium in OVX rats (Zheng et al., 2006). Normally, quantities of serum E_2 , estrogen receptor ($ER\alpha$ and $ER\beta$), and G protein-coupled ER (GPER) in tissue are in a homeostasis, therefore, gonads-sourced E_2 could only alleviate the increase of serum potassium within limits. Although serum potassium was lower in CS female mice, with far higher serum E_2 than that in male or OVX mice, it was still dramatically higher than normal level. From the above, the increased part of serum E_2 might originate from sources outside of gonads, such as adipose tissue, and act as a defense against sudden increase of serum potassium in CS.

Ani is widely used clinically for varieties of shock treatment in China, especially septic shock with fewer and less severe adverse effects compared with atropine (Li et al., 1999). Our previous

studies showed that Ani could decrease on-site mortality in CS through modest reduction ($\sim 10\% \sim 20\%$) of serum potassium, and such effect was mediated by indirect activation of $\alpha 7nAChR$ (Fan et al., 2016), which was verified with MLA, selective antagonist of $\alpha 7nAChR$, in the present study. PNU-282987, selective $\alpha 7nAChR$ agonist, has been reported to increase serum E_2 level and $ER\alpha$ and $ER\beta$ expression in OVX rats (Ma et al., 2015). We found that Ani might increase serum E_2 in CS mice and MLA might counteract such effect of Ani. Treatment with Ani increased serum E_2 , and decreased serum potassium and on-site mortality in all CS mice received OVX or its sham operation. Serum E_2 was reported to have a negative correlation with major arrhythmic cardiovascular events in patients with arrhythmogenic right ventricular cardiomyopathy/dysplasia that may lead to sudden cardiac death (Akdis et al., 2017). E_2 could also prevent hyperkalemia-induced Ca^{2+} loading and hypercontracture in cardiomyocytes, which might exert cardioprotective effects during hyperkalemic cardioplegia (Jovanovic et al., 1998). We found that exogenous supplement of E_2 exerted similar influence to Ani on serum potassium and on-site mortality. Disagreed with the result of Ma et al. that serum E_2 was even higher in PNU-282987-treated OVX rats than that in sham-operated rats (Ma et al., 2015), a great gap still existed in serum E_2 between sham-operated and OVX mice after Ani treatment; however, difference in serum potassium had been eliminated by Ani. Herein, decline of serum potassium in CS mainly depends on E_2 originating from sources outside of gonads. E_2 was reported to increase expression of $\alpha 7nAChR$ in the brain and kidney of animals (Miller et al., 1982; Miller et al., 1984; Centeno et al., 2006; el-Mas et al., 2011). In addition, E_2 and other ER agonists could increase $ER\alpha$, $ER\beta$, and GPER expression respectively (Pisolato et al., 2016; Wang et al., 2019). Taken together, there might be a crosstalk between $\alpha 7nAChR$ and E_2 , as well as ERs, to regulate the expression of each other, which is the basis for Ani to ameliorate hyperkalemia and decrease on-site mortality in CS.

Enhancement of insulin sensitivity may decrease serum potassium, accompanying reduction of serum glucose. We previously proved that activation of $\alpha 7nAChR$ decreases serum potassium in CS through elevation of insulin sensitivity, during which insulin downstream signaling molecules, such as phosphoinositide 3-kinase, mammalian target of rapamycin, and signal transducer and activator of transcription 3, were involved. Inhibition of the above-mentioned signaling molecules could decrease extracellular potassium (Fan et al., 2016). E_2 has been reported to enhance insulin sensitivity and ameliorate insulin resistance in lots of experiments (Park et al., 2017; Qiu et al., 2018; Torres et al., 2018; Yan et al., 2019). In the present study, insulin sensitivity after decompression was lower in male and OVX female mice compared to the relative controls. Both Ani and exogenous supplement of E_2 could increase insulin sensitivity after decompression and eliminate the difference between sham-operated and OVX mice. In addition, E_2 could also stimulate activity and expression of Na/K-ATPase (Obradovic et al., 2014; Obradovic et al., 2015), which pumps sodium out of cells while pumping



potassium into cells and plays an important role in insulin-induced decline of serum potassium (Chibalin et al., 2001; Al-Khalili et al., 2004). Therefore, Ani could decrease serum potassium during CS through E_2 -based activation of insulin signaling pathway.

We also examined the influence of Ani on hypovolemic shock in CS rats shortly after decompression in this study. Treatment with Ani could alleviate hypotension in CS rats induced by long-sustained compression, which could be attenuated by MLA, without influences on HR. Our previous study showed that Ani could increase blood pressure and decrease mortality in rats with hemorrhagic shock, which indirectly proved the causality between elevation of blood pressure and decline of mortality associated with hypovolemic shock during CS. Besides hyperkalemia-induced cardiac arrest, E_2 could also exert neuroprotective effects after hypovolemic cardiac arrest (Semenas et al., 2011). Therefore, activation of $\alpha 7nAChR$ with Ani could benefit both hyperkalemia and hypovolemic shock in CS through participation of E_2 .

REFERENCES

Akdis, D., Saguner, A. M., Shah, K., Wei, C., Medeiros-Domingo, A., von Eckardstein, A., et al. (2017). Sex hormones affect outcome in arrhythmogenic right ventricular cardiomyopathy/dysplasia: from a stem cell derived cardiomyocyte-based model to clinical biomarkers of disease outcome. *Eur. Heart J.* 38, 1498–1508. doi: 10.1093/eurheartj/ehx011

CONCLUSION

This study demonstrates that activation of $\alpha 7nAChR$ with Ani could ameliorate hyperkalemia during CS through E_2 -induced enhancement of insulin sensitivity, and thus to decrease on-site mortality (Figure 9). Ani could also alleviate hypovolemic shock in CS, during which the study about effect of E_2 is still required. Moreover, Ani and E_2 are encouraging drugs for on-site remedy of CS, which needs further investigations.

LIMITATIONS

In the present study, effect of Ani on serum E_2 in CS was well proved, as well as the effect of E_2 on serum potassium and even on-site mortality. However, participation of ERs ($ER\alpha$, $ER\beta$, and GPER) in this process was not verified. Therefore, examination of ER expression and application of ER knockout mice is still required in further investigations.

DATA AVAILABILITY STATEMENT

The raw data supporting the conclusions of this manuscript will be made available by the authors, without undue reservation, to any qualified researcher.

ETHICS STATEMENT

The animal study was reviewed and approved by Ethics Committee of Second Military Medical University.

AUTHOR CONTRIBUTIONS

J-GY and XL designed the study and experiments. J-GY, B-SF, and J-MG performed the experiments. Y-JS and Y-YH analyzed the data. J-GY and B-SF wrote the paper.

FUNDING

This work was supported by Grants from the National Natural Science Foundation of China (81773726), National Science and Technology Major Project (2018ZX09J18110-003-001), and Innovation Cultivating Foundation of 6th Medical Center, PLA General Hospital (CXPY201829).

Al-Khalili, L., Kotova, O., Tsuchida, H., Ehren, I., Feraille, E., Krook, A., et al. (2004). ERK1/2 mediates insulin stimulation of $Na(+)$, $K(+)$ -ATPase by phosphorylation of the alpha-subunit in human skeletal muscle cells. *J. Biol. Chem.* 279, 25211–25218. doi: 10.1074/jbc.M402152200

Ashkenazi, I., Isakovitch, B., Kluger, Y., Alfici, R., Kessel, B., and Better, O. S. (2005). Prehospital management of earthquake casualties buried under rubble. *Prehosp. Disaster Med.* 20, 122–133. doi: 10.1017/s1049023x00002302

- Better, O. S. (1997). History of the crush syndrome: from the earthquakes of Messina, Sicily 1909 to Spitak, Armenia 1988. *Am. J. Nephrol.* 17, 392–394. doi: 10.1159/000169127
- Bywaters, E. G., and Beall, D. (1998). Crush injuries with impairment of renal function. 1941. *J. Am. Soc. Nephrol.* 9, 322–332.
- Centeno, M. L., Henderson, J. A., Pau, K. Y., and Bethea, C. L. (2006). Estradiol increases alpha7 nicotinic receptor in serotonergic dorsal raphe and noradrenergic locus coeruleus neurons of macaques. *J. Comp. Neurol.* 497, 489–501. doi: 10.1002/cne.21026
- Chibalin, A. V., Kovalenko, M. V., Ryder, J. W., Feraille, E., Wallberg-Henriksson, H., and Zierath, J. R. (2001). Insulin- and glucose-induced phosphorylation of the Na(+),K(+)-adenosine triphosphatase alpha-subunits in rat skeletal muscle. *Endocrinology* 142, 3474–3482. doi: 10.1210/endo.142.8.8294
- el-Mas, M. M., el-Gowilly, S. M., Gohar, E. Y., Ghazal, A. R., and Abdel-Rahman, A. A. (2011). Estrogen dependence of the renal vasodilatory effect of nicotine in rats: role of alpha7 nicotinic cholinergic receptor/eNOS signaling. *Life Sci.* 88, 187–193. doi: 10.1016/j.lfs.2010.11.009
- Fan, B. S., Zhang, E. H., Wu, M., Guo, J. M., Su, D. F., Liu, X., et al. (2016). Activation of alpha7 nicotinic acetylcholine receptor decreases on-site mortality in crush syndrome through insulin signaling-Na/K-ATPase pathway. *Front. Pharmacol.* 7, 79. doi: 10.3389/fphar.2016.00079
- Jovanovic, S., Jovanovic, A., Shen, W. K., and Terzic, A. (1998). Protective action of 17beta-estradiol in cardiac cells: implications for hyperkalemic cardioplegia. *Ann. Thorac. Surg.* 66, 1658–1661. doi: 10.1016/s0003-4975(98)00893-5
- Li, Q. B., Pan, R., Wang, G. F., and Tang, S. X. (1999). Anisodamine as an effective drug to treat snakebites. *J. Nat. Toxins* 8, 327–330.
- Liu, A. J., Zang, P., Guo, J. M., Wang, W., Dong, W. Z., Guo, W., et al. (2012). Involvement of acetylcholine-alpha7nAChR in the protective effects of arterial baroreflex against ischemic stroke. *CNS Neurosci. Ther.* 18, 918–926. doi: 10.1111/cns.12011
- Ma, F., Gong, F., Lv, J., Gao, J., and Ma, J. (2015). Effects of a7nAChR agonist on the tissue estrogen receptor expression of castrated rats. *Int. J. Clin. Exp. Pathol.* 8, 13421–13425.
- Miller, M. M., Silver, J., and Billiar, R. B. (1982). Effects of ovariectomy on the binding of [125I]-alpha bungarotoxin (2.2 and 3.3) to the suprachiasmatic nucleus of the hypothalamus: an *in vivo* autoradiographic analysis. *Brain Res.* 247, 355–364. doi: 10.1016/0006-8993(82)91261-6
- Miller, M. M., Silver, J., and Billiar, R. B. (1984). Effects of gonadal steroids on the *in vivo* binding of [125I]alpha-bungarotoxin to the suprachiasmatic nucleus. *Brain Res.* 290, 67–75. doi: 10.1016/0006-8993(84)90736-4
- Obradovic, M., Stewart, A. J., Pitt, S. J., Labudovic-Borovic, M., Sudar, E., Petrovic, V., et al. (2014). In vivo effects of 17beta-estradiol on cardiac Na(+)/K(+)-ATPase expression and activity in rat heart. *Mol. Cell. Endocrinol.* 388, 58–68. doi: 10.1016/j.mce.2014.03.005
- Obradovic, M., Zafirovic, S., Jovanovic, A., Milovanovic, E. S., Mousa, S. A., Labudovic-Borovic, M., et al. (2015). Effects of 17beta-estradiol on cardiac Na(+)/K(+)-ATPase in high fat diet fed rats. *Mol. Cell. Endocrinol.* 416, 46–56. doi: 10.1016/j.mce.2015.08.020
- Oda, J., Tanaka, H., Yoshioka, T., Iwai, A., Yamamura, H., Ishikawa, K., et al. (1997). Analysis of 372 patients with Crush syndrome caused by the Hanshin-Awaji earthquake. *J. Trauma* 42, 470–475; discussion 475–476. doi: 10.1097/00005373-199703000-00015
- Park, Y. M., Pereira, R. I., Erickson, C. B., Swibas, T. A., Cox-York, K. A., and Van Pelt, R. E. (2017). Estradiol-mediated improvements in adipose tissue insulin sensitivity are related to the balance of adipose tissue estrogen receptor alpha and beta in postmenopausal women. *PloS One* 12, e0176446. doi: 10.1371/journal.pone.0176446
- Peng, Y., Xu, S., Chen, G., Wang, L., Feng, Y., and Wang, X. (2007). 1-3-n-Butylphthalide improves cognitive impairment induced by chronic cerebral hypoperfusion in rats. *J. Pharmacol. Exp. Ther.* 321, 902–910. doi: 10.1124/jpet.106.118760
- Pisolato, R., Lombardi, A. P., Vicente, C. M., Lucas, T. F., Lazari, M. F., and Porto, C. S. (2016). Expression and regulation of the estrogen receptors in PC-3 human prostate cancer cells. *Steroids* 107, 74–86. doi: 10.1016/j.steroids.2015.12.021
- Qiu, J., Bosch, M. A., Meza, C., Navarro, U. V., Nestor, C. C., Wagner, E. J., et al. (2018). Estradiol protects proopiomelanocortin neurons against insulin resistance. *Endocrinology* 159, 647–664. doi: 10.1210/en.2017-00793
- Rasmussen, A. M., Marx, C. E., Pineles, S. L., Locci, A., Scioli-Salter, E. R., Nillni, Y. I., et al. (2017). Neuroactive steroids and PTSD treatment. *Neurosci. Lett.* 649, 156–163. doi: 10.1016/j.neulet.2017.01.054
- Semenas, E., Sharma, H. S., Nozari, A., Basu, S., and Wiklund, L. (2011). Neuroprotective effects of 17beta-estradiol after hypovolemic cardiac arrest in immature piglets: the role of nitric oxide and peroxidation. *Shock* 36, 30–37. doi: 10.1097/SHK.0b013e3182150f43
- Sever, M. S., and Vanholder, R. (2013). Management of crush victims in mass disasters: highlights from recently published recommendations. *Clin. J. Am. Soc. Nephrol.* 8, 328–335. doi: 10.2215/CJN.07340712
- Sever, M. S., Ereke, E., Vanholder, R., Yurugen, B., Kantarci, G., Yavuz, M., et al. (2002). Renal replacement therapies in the aftermath of the catastrophic Marmara earthquake. *Kidney Int.* 62, 2264–2271. doi: 10.1046/j.1523-1755.2002.00669.x
- Sever, M. S., Ereke, E., Vanholder, R., Kantarci, G., Yavuz, M., Turkmen, A., et al. (2003). Serum potassium in the crush syndrome victims of the Marmara disaster. *Clin. Nephrol.* 59, 326–333. doi: 10.5414/cnp59326
- Sever, M. S., Ereke, E., Vanholder, R., and Lameire, N. (2004). Effect of gender on various parameters of crush syndrome victims of the Marmara earthquake. *J. Nephrol.* 17, 399–404.
- Sever, M. S., Lameire, N., Van Biesen, W., and Vanholder, R. (2015). Disaster nephrology: a new concept for an old problem. *Clin. Kidney J.* 8, 300–309. doi: 10.1093/ckj/sfv024
- Slater, M. S., and Mullins, R. J. (1998). Rhabdomyolysis and myoglobinuric renal failure in trauma and surgical patients: a review. *J. Am. Coll. Surg.* 186, 693–716. doi: 10.1016/s1072-7515(98)00089-1
- Sun, Y., Qin, Z., Wan, J. J., Wang, P. Y., Yang, Y. L., Yu, J. G., et al. (2018). Estrogen weakens muscle endurance via estrogen receptor-p38 MAPK-mediated orosomucoid (ORM) suppression. *Exp. Mol. Med.* 50, e463. doi: 10.1038/emmm.2017.307
- Torres, M. J., Kew, K. A., Ryan, T. E., Pennington, E. R., Lin, C. T., Buddo, K. A., et al. (2018). 17beta-Estradiol Directly Lowers Mitochondrial membrane microviscosity and improves bioenergetic function in skeletal muscle. *Cell Metab.* 27, 167–179 e167. doi: 10.1016/j.cmet.2017.10.003
- Toufexis, D., Rivarola, M. A., Lara, H., and Viau, V. (2014). Stress and the reproductive axis. *J. Neuroendocrinol.* 26, 573–586. doi: 10.1111/jne.12179
- Ukai, T. (1997). The Great Hanshin-Awaji Earthquake and the problems with emergency medical care. *Ren. Fail.* 19, 633–645. doi: 10.3109/08860229709109029
- Wang, J., Yu, R., Han, Q. Q., Huang, H. J., Wang, Y. L., Li, H. Y., et al. (2019). G-1 exhibit antidepressant effect, increase of hippocampal ERs expression and improve hippocampal redox status in aged female rats. *Behav. Brain Res.* 359, 845–852. doi: 10.1016/j.bbr.2018.07.017
- Yan, H., Yang, W., Zhou, F., Li, X., Pan, Q., Shen, Z., et al. (2019). Estrogen improves insulin sensitivity and suppresses gluconeogenesis via the transcription factor foxo1. *Diabetes* 68, 291–304. doi: 10.2337/db18-0638
- Yu, J. G., Song, S. W., Shu, H., Fan, S. J., Liu, A. J., Liu, C., et al. (2013). Baroreflex deficiency hampers angiogenesis after myocardial infarction via acetylcholine-alpha7-nicotinic ACh receptor in rats. *Eur. Heart J.* 34, 2412–2420. doi: 10.1093/eurheartj/ehr299
- Zheng, W., Shi, M., You, S. E., Ji, H., and Roesch, D. M. (2006). Estrogens contribute to a sex difference in plasma potassium concentration: a mechanism for regulation of adrenal angiotensin receptors. *Gen. Med.* 3, 43–53. doi: 10.1016/s1550-8579(06)80193-2

Conflict of Interest: The authors declare that the research was conducted in the absence of any commercial or financial relationships that could be construed as a potential conflict of interest.

Copyright © 2019 Yu, Fan, Guo, Shen, Hu and Liu. This is an open-access article distributed under the terms of the Creative Commons Attribution License (CC BY). The use, distribution or reproduction in other forums is permitted, provided the original author(s) and the copyright owner(s) are credited and that the original publication in this journal is cited, in accordance with accepted academic practice. No use, distribution or reproduction is permitted which does not comply with these terms.



Edible Bird's Nest Protects Against Hyperglycemia-Induced Oxidative Stress and Endothelial Dysfunction

Dharmani Devi Murugan^{1*}, Zuhaida Md Zain¹, Ker Woon Choy²,
Nor Hisam Zamakshshari³, Mel June Choong⁴, Yang Mooi Lim⁵
and Mohd Rais Mustafa^{1*}

¹ Department of Pharmacology, Faculty of Medicine, University of Malaya, Kuala Lumpur, Malaysia, ² Department of Anatomy, Faculty of Medicine, Universiti Teknologi MARA, Sungai Buloh, Malaysia, ³ Centre for Natural Product Research and Drug Discovery (CENAR), Wellness Research Cluster, University of Malaya, Kuala Lumpur, Malaysia, ⁴ Centre for Cancer Research, Faculty of Medicine and Health Sciences, University Tunku Abdul Rahman, Selangor, Malaysia, ⁵ Department of Pre-clinical Sciences, Centre for Cancer Research, Faculty of Medicine and Health Sciences, University Tunku Abdul Rahman, Selangor, Malaysia

OPEN ACCESS

Edited by:

Issy Laher,
University of British
Columbia, Canada

Reviewed by:

Xiao Yu Tian,
The Chinese University of
Hong Kong, China
Esraa Shosha,
Augusta University, United States

*Correspondence:

Dharmani Devi Murugan
dharmani79@um.edu.my
Mohd Rais Mustafa
rais@um.edu.my

Specialty section:

This article was submitted to
Ethnopharmacology,
a section of the journal
Frontiers in Pharmacology

Received: 29 May 2019

Accepted: 13 December 2019

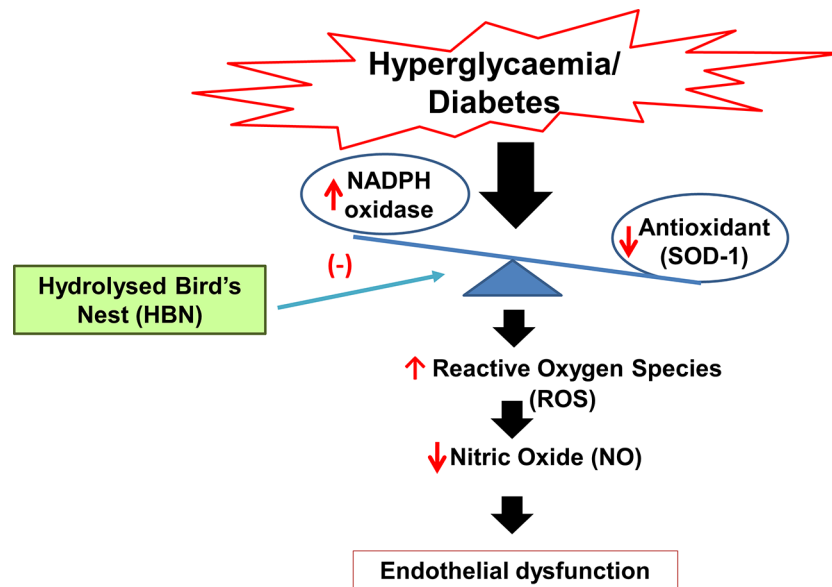
Published: 04 February 2020

Citation:

Murugan DD, Md Zain Z, Choy KW,
Zamakshshari NH, Choong MJ,
Lim YM and Mustafa MR (2020) Edible
Bird's Nest Protects Against
Hyperglycemia-Induced Oxidative
Stress and Endothelial Dysfunction.
Front. Pharmacol. 10:1624.
doi: 10.3389/fphar.2019.01624

Increased oxidative stress by hyperglycemia is a major cause of vascular complications in diabetes. Bird's nest, which is made from the saliva of swiftlets has both medicinal and nutritional values dated back to ancient China. However, its role in improving endothelial dysfunction due to diabetes is yet to be elucidated. The present study examined the protective effect and mechanism of action of the aqueous extract of hydrolyzed edible bird nest (HBN) on endothelium in models of diabetes, *in vitro* and *in vivo*. Male *db/m+* and *db/db* mice were orally administered with or without HBN and glibenclamide for 28 days, followed by vascular reactivity studies in mouse aortas. Human umbilical vein endothelial cells (HUVECs) and isolated mouse aorta from C57BL/6J were treated with high glucose (HG), HBN, sialic acid (SA), glibenclamide, and apocynin, respectively. The effects of HBN on reactive oxygen species (ROS) production and nitric oxide (NO) bioavailability were assessed by Western blot, 2',7'-dichlorofluorescein-diacetate (DCF-DA), and 4-amino-5-methylamino-2',7' difluorofluorescein (DAF-FM DA) in HUVECs, isolated mouse aorta, and *db/db* diabetic mice. HBN significantly reversed the endothelial dysfunction in diabetic mice and isolated mouse aorta. HBN normalized ROS over-production of NOX2 and nitrotyrosine, reversed the reduction of anti-oxidant marker, SOD-1 as well as restored NO bioavailability in both HUVECs challenged with HG and in *db/db* diabetic mice. Similarly, HG-induced elevation of oxidative stress in HUVECs were reversed by SA, glibenclamide, and apocynin. This attests that HBN restores endothelial function and protects endothelial cells against oxidative damage induced by HG in HUVECs, isolated mouse aorta, and *db/db* diabetic mice *via* modulating ROS mechanism, which subsequently increases NO bioavailability. This result demonstrates the potential role of HBN in preserving endothelial function and management of micro- or macrovascular complications in diabetes.

Keywords: hydrolyzed bird's nest, hyperglycemia, oxidative stress, endothelial dysfunction, reactive oxygen species, nitric oxide



GRAPHICAL ABSTRACT | Mechanism of action of hydrolyzed bird's nest on hyperglycemia-induced endothelial dysfunction.

INTRODUCTION

The endothelium plays a pivotal role in physiology and pathophysiology of the vasculature, including modulating the vascular tone, cellular adhesion, smooth muscle, cell proliferation, thromboresistance, and inflammation of vessel wall (Sena et al., 2013). Under normal physiological condition, the healthy endothelium maintains a fine balance between vasoconstriction and vasodilatation factors (Sena et al., 2013). Nitric oxide (NO) is among the endothelium-derived factor which controls the vasodilatory effect whereas factors such as reactive oxygen species (ROS), thromboxane, and endothelin 1 exerts vasoconstrictor effects (Just et al., 2008; Loscalzo, 2013). Endothelial dysfunction is commonly associated with increased cellular oxidative stress and with decreased nitric oxide (NO) bioavailability, resulting in dysregulation of vascular tone and ultimately compromised cardiovascular function (Pitocco et al., 2010). Endothelial dysfunction is correlated with various cardiovascular and metabolic diseases such as hypertension, atherosclerosis, and diabetes mellitus (Sena et al., 2013).

Over the years, hyperglycemia-induced oxidative stress has been known as a key process in the onset of diabetic complications (Matough et al., 2012). Hyperglycemia causes excessive production of ROS, especially superoxide anions (O_2^-) which are generated through partial reduction of molecular oxygen to O_2^- by NADPH oxidase, uncoupled endothelial nitric oxide synthase (eNOS), mitochondrial electron transport chain as well as xanthine oxidase (Jay et al., 2006). O_2^- will react with NO to form the toxic peroxynitrite ($ONOO^-$), which uncouples eNOS to produce more superoxide anions. This vicious continuous cascade of events reduces NO bioavailability and leads to endothelial dysfunction (Schulz et al., 2008).

The edible bird's nest is made from the saliva of swiftlets inhabiting the limestone caves. Edible bird's nest has been used in Chinese cuisine mainly in the form of bird's nest soup since 1,200 years ago as it is believed to enhance energy levels, prevent aging, and improve overall well-being (Ma and Liu, 2012). Edible bird's nest has lethal dose (LD_{50}) cut off more than 5,000 mg/kg and is classified as category 5 or unclassified category of globally harmonized classification system (GHS), therefore it is safe to be taken by humans (Haghani et al., 2016). Furthermore, there are scientific reports of its anti-oxidative, anti-inflammatory, influenza virus inhibitory effect, hemagglutination-inhibitory activities, and bone-strengthening effects (Kong et al., 1987; Guo et al., 2006; Matsukawa et al., 2011; Ma and Liu, 2012; Vimala et al., 2012; Yida et al., 2014). In 2015, Yida et al. showed that edible bird's nest prevents high-fat diet- (HFD) induced insulin resistance in rats. However, thus far, the protective effect of edible bird's nest in glucotoxicity condition has not been studied. Therefore, the present study investigated the effect of hydrolyzed bird's nest (HBN) in abating oxidative stress and improving endothelial dysfunction in the hyperglycemia-induced oxidative stress in models of diabetes, *in vitro*, *ex vivo*, and *in vivo*.

MATERIALS AND METHODS

Quantification of Sialic Acid in Hydrolyzed Bird's Nest

The HBN was prepared and kindly provided by Professor YL from University Tunku Abdul Rahman, Malaysia. A voucher specimen was deposited in the Nature Inspired UM Natural

Products Library, University Malaya (voucher number UMCNA1801). Briefly, the raw edible birds nest sample eluted in distilled water was boiled at 80°C for an hour. The extracts were filtered with membrane filter paper and the resulting filtrates were lyophilized and stored at -80°C for further use. Liquid chromatography-mass spectrometry quadrupole-time of flight (LCMS Q-TOF) was used to determine the amount of sialic acid, one of the active compounds in HBN. The LCMS Q-TOF protocol was adapted from Marni et al., 2014 with slight modification (Marni et al., 2014). Briefly, a series of a standard solution of sialic acid with different concentration (50, 25, 12.5, 6.3, 3.1, and 1.5 µg/mL) and 10 mg/mL of HBN were prepared in distilled water. The samples were sonicated for 10 min and were subjected for LCMS Q-TOF analysis. The C-18 reversed phased column with diameter 4.6 × 250 mm was used with a mobile phase of water: methanol (1:1), the flow rate of 2 mL.min⁻¹, sample quantity of 10 µL, and column temperature 25° C. HBN and standard sialic acid were run in triplicates. A linear graph was plotted using standard sialic acid and the sialic acid content in HBN was determined from the standard curve. A standard solution graph of concentration versus area was plotted. Finally, the sialic acid concentration of each extract was determined based on the graph.

Animals

Male *db/m+* and *db/db* mice (10 weeks old) were obtained from The Jackson Laboratories (Bar Harbor, ME, USA) for the *in vivo* experiment while male C57BL/6J (12 weeks old) mice were obtained from the Monash University (Sunway Campus, Malaysia) for the *ex vivo* experiments. All the experimental procedures were approved by the University of Malaya Animal Care and Ethics Committee (Ethics Reference No: 2015-180709) and accredited by Association for Assessment and Accreditation of Laboratory Animal Care International (AAALAC). Animal study was carried out in strict accordance with the established institutional guidelines and the NIH guidelines on the use of experimental animals. The animals were housed in a well-ventilated room maintained at a temperature of 23°C with 12 h light/dark cycles, 30–40% humidity and had free access to standard rat chow (Specialty Feeds Pty Ltd., Glen Forrest, Australia) and filtered tap water.

Ex Vivo Culture of Mouse Aortic Rings

The male C57BL/6J mice were euthanized using carbon dioxide (CO₂), and the aorta was carefully isolated and immersed in sterile phosphate buffer saline (PBS). The aortas were cleaned from fat and connective tissues under the microscope and cut into several segments of approximately 2 mm in length. The aortic rings were incubated in normal glucose (NG, 2.5 mM) or high glucose (HG, 30 mM) with or without co-incubation of HBN (15 and 30 µg/mL), sialic acid (20 µg/mL), glibenclamide (10 µM), apocynin (20 µM), and compound C for 48 h at 37°C in Dulbecco's Modified Eagle's Media (DMEM; Gibco, Gaithersburg, MD, USA) with 10% fetal bovine serum (FBS; Gibco), 100 µg/mL streptomycin, and 100 U/mL penicillin (Lau et al., 2013). The concentrations of HBN used in this study were determined using MTT assay (data not shown).

HBN Treatment in *db/db* Mice

The male *db/db* mice male randomly assigned into four groups (n = 6 per group) of mice receiving: (a) vehicle (distilled water); (b) hydrolyzed bird's nest (75 mg/kg); (c) hydrolyzed bird's nest (150 mg/kg); (d) glibenclamide (1mg/kg) by oral gavage for four weeks. The *db/m+* mice (n = 6) was used as the non-diabetic control. The animals were humanely sacrificed by CO₂ inhalation at the end of treatment. Blood samples were collected from inferior vena cava after an overnight fast, and the serum were stored at -80°C for total nitrate/nitrite assay. The aorta was excised and cleaned of adjacent connective tissues and fat and cut into rings for functional studies and some arteries were snap-frozen in liquid nitrogen and stored at -80°C for further experiments.

Functional Study

The aortic rings from the treated groups and organ-cultured rings were mounted on myograph chamber containing 5 mL of oxygenated Krebs solution which consists mM of NaCl 119, NaHCO₃ 25, KCl 4.7, KH₂PO₄ 1.2, MgSO₄·7H₂O 1.2, glucose 11.7, and CaCl₂·2H₂O 2.5. The aortic rings were maintained at 37°C and stretched to optimal baseline tension of 3 millinewtons (mN) in a Multi-Wire Myograph System (Danish Myo Technology, Aarhus, Denmark) and continuously oxygenated with 95% O₂ and 5% CO₂. The changes of isometric tension of aortic rings in response to different drugs were recorded using the PowerLab LabChart 6.0 recording system (AD Instruments, Australia). The rings were equilibrated for approximately 45 min and pre-contracted with high 60 mM KCl solution followed by three times of washing with Krebs solution. Once the tension stabilized and returns to baseline, phenylephrine (3 µM) was added to induce contraction followed by generation of endothelium-dependent relaxation (EDR) by cumulative addition of acetylcholine (ACh) from 3 to 10 nM. The endothelium-independent relaxation (EIR) was generated by the addition of sodium nitroprusside (SNP) from 1 nM to 10 µM. Each experiment was conducted on separate rings from six mice. Concentration-response curves for relaxations were conveyed as the percentage of reduction in contraction induced by phenylephrine before the application of ACh or SNP. The maximum effect (R_{max}) and concentration inducing 50% of R_{max} (pEC₅₀) were determined from the cumulative concentration-response curves.

Detection of Vascular Superoxide Formation

Lucigenin-enhanced chemiluminescence assay was used in this study to quantify the production of vascular superoxide anion. The organ-cultured rings from each group were incubated for 45 min at 37°C in Krebs-HEPES buffer (in mM: NaCl 99.0, NaHCO₃ 25, KCl 4.7, KH₂PO₄ 1.0, MgSO₄ 1.2, glucose 11.0, CaCl 22.5, and Na-HEPES 20.0) in the presence of diethylthiocarbamic acid (DETCA, 1 mM) and β-nicotinamide adenine dinucleotide phosphate (β-NADPH, 0.1 mM). DETCA acts as an inactivator for superoxide dismutase (SOD) while β-NADPH acts as a substrate for NADPH oxidase. The NADPH

oxidase inhibitor, diphenylene iodonium (DPI; 5 mM) was then added as a positive control. Before measurement, a solution containing lucigenin (5 mM) and β -NADPH (0.1 mM) in Krebs-HEPES buffer was added into each well of 96-well Optiplate. Background photo emissions were measured every 30 s for 20 min using Hidex plate CHAMELEONTM V (Finland). After addition of the rings into the wells, the measurement was taken again. The rings were then dried for 48 h at 65°C and weighed. The data were expressed as average counts per weight of dried vessel (mg) and was compared over the normal glucose (Choy et al., 2017).

Cell Culture

Human umbilical vein endothelial cells (HUVECs, Lonza, Basel, Switzerland, No. CC-2517) were cultured in normal glucose endothelial cell medium (ECM) supplemented with 10% fetal bovine serum (FBS), 100 U/mL penicillin, 100 μ g/mL streptomycin, and 50 μ g/L endothelial cell growth supplement (all ScienCell, Carlsbad, CA). The cells were incubated in a humidified atmosphere containing 5% CO₂ at 37°C. Cells from passages 5 to 9 were used for the current study. Experiments were performed once the cells reached 80% confluency. The cells were then starved for 4 h in FBS-free ECM before treatment with either normal glucose (5.5 mM, NG) and high glucose (HG, 30mM) co-treated with hydrolyzed bird's nest HBN (30 μ g/mL), sialic acid (20 μ g/mL), glibenclamide (10 μ M), and apocynin (20 μ M) for 48 h. Another set was incubated with osmotic control, mannitol (25 mM) (Lau et al., 2013).

Measurement of Intracellular ROS Generation

The amount of intracellular ROS generation in HUVECs was measured using DCF-DA fluorescein (Invitrogen, CA, USA) dye. ROS was detected after formation of fluorescent DCF product inside the cell due to oxidation of DCF-DA. In brief, 1×10^4 HUVECs were seeded into 96 well plates. After overnight incubation in 5% CO₂ at 37°C, the cells were starved and treated as described. Another set of cells were treated with H₂O₂ (200 μ M), the ROS inducer 4 h before the end of 48 h incubation as a positive control. The treated cells were incubated for 48 h and the media was then removed. The wells were rinsed with phosphate buffered saline PBS followed by addition of 10 μ M of DCF-DA into each well. The absorbance was then measured kinetically for 1 h using a fluorescent multimode reader (Infinite M1000 Pro; Tecan US, Morrisville, NC) at fluorescence excitation and emission of 492/517 nm. The data was presented as the fluorescent intensity (a.u.) at 50th minute after addition of DCF-DA dye.

Measurement of NO Production in HUVECs

The amount NO production in HUVECs was measured using DAF-FM diacetate (Invitrogen, CA, USA) dye (Namin et al., 2013). Basically, NO within the cells will react with DAF-FM diacetate to form fluorescent benzotriazole. The confluent HUVECs were seeded into 96 well plates and treated accordingly as described in the previous section. HUVECs treated with calcium ionophore (A23187, 5 μ M) were used as

positive control. After 48 h incubation, the media was removed and rinsed with PBS three times. Five micrograms of DAF dye was added into each well, and the absorbance was measured kinetically for 1 h using a fluorescent multimode reader (Infinite M1000 Pro; Tecan US, Morrisville, NC) at fluorescence excitation and emission of 495/515nm. The results were presented as a value of fluorescent intensity (a.u) at 50th minute after addition of the dye.

Measurement of Total Nitrite/Nitrate Levels

Total nitrite and nitrate level from the mice serum was detected using Nitrate/Nitrite Colorimetric Assay Kit (Cayman Chemical Company, Ann Arbor, MI, USA) according to the manufacturer's protocol. Absorbance was measured using a plate reader (Tecan, Mannedorf, Switzerland) with an absorbance of 540nm. The results are expressed in μ M.

Western Blot

Protein samples from the treated mouse aorta and HUVECs were lysed in ice-cold 1X RIPA buffer consists of EGTA 1 mM, EDTA 1 mM, NaF 1 mM, leupeptin 1 μ g/mL, aprotinin 5 μ g/mL, PMSF 100 μ g/mL, sodium orthovanadate 1 mM, and β -glycerolphosphate 2 mg/mL. The lysates were collected and centrifuged at 20,000 g for 20 min. Protein concentrations were determined using standard Lowry assay protocol by (Bio-Rad Laboratories, Hercules, CA, USA). Fifteen micrograms of protein samples were electrophoresed at 100 V through 7.5% or 10% SDS-polyacrylamide gels based on the size of target proteins and transferred to an Immobilon-P polyvinylidene difluoride membrane (Millipore, Billerica, MA, USA). The membranes were blocked from any non-specific binding by 3% bovine serum albumin (BSA) in 0.05% Tween 20 PBS with gentle shaking. The membranes were then incubated with primary antibodies against NADPH oxidase 2 (NOX-2; 1:1,000, Abcam), nitrotyrosine (1:1,000, Abcam) superoxide dismutase-1 (SOD-1; 1:1,000, Santa Cruz), phosphorylated endothelial nitric oxide synthase (p-eNOS) at Ser1177 (1:1,000, Abcam), endothelial nitric oxide synthase (eNOS) (1:1,000, BD Transduction laboratory, San Diego, CA, USA), and β -actin (1:10,000, Abcam) at 4°C overnight. Following incubation, the membranes were washed three times with TBS-T and incubated with horseradish peroxidase-conjugated secondary antibodies (DakoCytomation, Carpinteria, CA, USA) for 2 h at room temperature. Finally, the enhanced chemiluminescence detection system (ECL reagents, Millipore Corporation, Billerica, MA) was added onto the membrane and exposed on X-ray films. The films were then automatically processed and developed by SRX-101 (Konica, Wayne, NJ). The densitometry analysis was performed using Quantity One software (Bio-Rad). The respective protein expression levels for nitrotyrosine, NOX-2, and SOD-1 were normalized to β -actin, p-eNOS to eNOS, and then compared with control.

Data Analysis

Results are presented as mean \pm SEM from n experiments. Concentration-response curves were fixed to a sigmoidal curve using non-linear regression using the statistical software GraphPad Prism version 4 (GraphPad Software Inc.,

San Diego, CA, USA). Statistical significance was determined using two-tailed Student's *t*-test for comparison of two groups and a one-way ANOVA followed by Bonferroni multiple comparison tests for comparisons of more than two groups. $P < 0.05$ was considered statistically significant.

RESULTS

Sialic Acid Content in Hydrolyzed Bird's Nest

Six difference standards of sialic acid (N-acetylneuraminic acid) were run on the LCMS Q-TOF and result was plotted. The standard graph for sialic acid was obtained from the calibration equation $y = (3 \times 10^6)x + 532,337$ ($R^2 = 0.9931$) where y is the peak area and x is the weight of sialic acid content in the extract. The LCMS spectrum for standard together with HBN is shown in **Figure 1**. Sialic acid appeared at the retention time of 4.9 min of the LCMS spectrum. The amount of sialic acid in the sample was determined based on the molecular weight of 309.107 g/mol and their retention time. From this analysis, it shows that HBN contained 1.26 μg sialic acid/mg.

HBN Ameliorated Endothelial Dysfunction in Mouse Aorta

To determine the role of HBN treatment in high glucose-induced endothelial dysfunction in mice, we examined EDR and EIR in

response to ACh and SNP respectively in a concentration-dependent manner. Aorta from mice treated with HG for 48 h displayed 48% relaxation to ACh-induced relaxation compared to control group which showed 85% relaxation. Co-treatment with HBN (15 and 30 $\mu\text{g}/\text{mL}$) restored the impaired relaxation to ACh in a concentration-dependent manner, with HBN at 30 $\mu\text{g}/\text{mL}$ being an effective concentration in the HG-treated aorta. HBN alone did not affect the ACh relaxation in the NG-treated aorta (**Figure 2A** and **Table 1**). Additionally, co-incubation with sialic acid (20 $\mu\text{g}/\text{mL}$), glibenclamide (10 μM), and apocynin (20 μM) reversed the HG-induced impairment of relaxation to ACh (**Figure 2B** and **Table 1**). SNP-induced relaxations were similar in all groups, reflecting the lacked changes in the sensitivity of vascular smooth muscle to NO (**Figures 2C–D** and **Table 1**).

The maximal relaxation and sensitivity to ACh in the aorta from *db/db* mice treated with vehicle was significantly lesser compared to the non-diabetic group (R_{max} : $57.04 \pm 3.29\%$ vs. $95.03 \pm 1.31\%$, respectively). Four-weeks treatment with HBN (150 mg/kg) and glibenclamide (1 mg/kg) reversed the impaired ACh-induced relaxation in *db/db* aorta (**Figure 3A** and **Table 2**) while no significant changes was observed in SNP-induced relaxation (**Figure 3B** and **Table 2**).

HBN Reduced High Glucose-Induced Vascular Superoxide Production and Intercellular ROS Formation

HG produced high levels of vascular superoxide anions (**Figure 4A**) in isolated mouse aorta and intercellular ROS in HUVECs

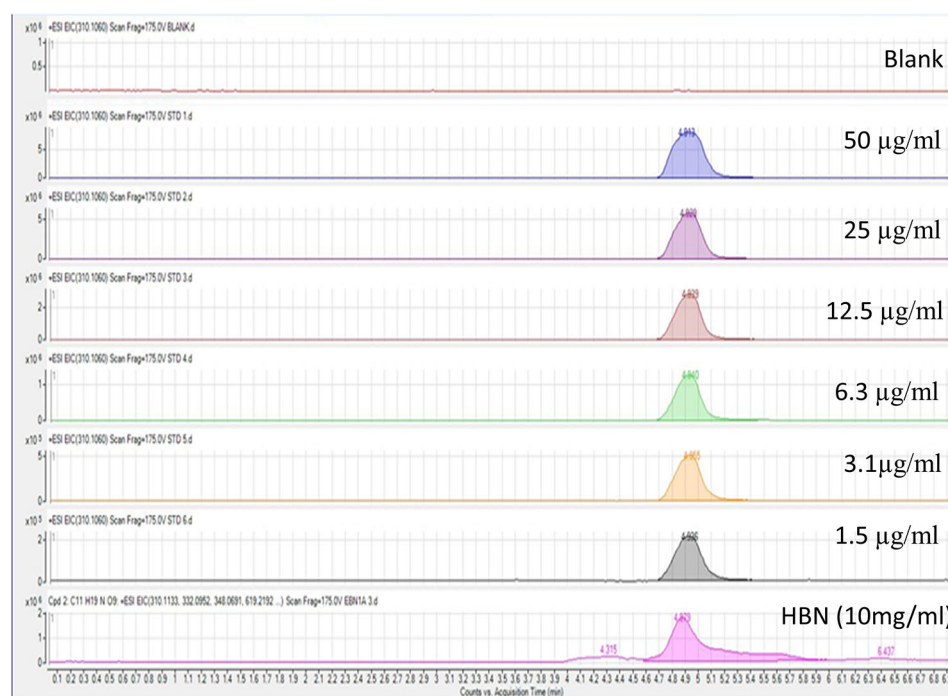


FIGURE 1 | Liquid chromatography-mass spectrometry spectrum of standard sialic acid at different concentrations and 10 mg/mL hydrolyzed bird nest (HBN). HBN contained 1.26 μg sialic acid/mg HBN based on their molecular weight and retention time.

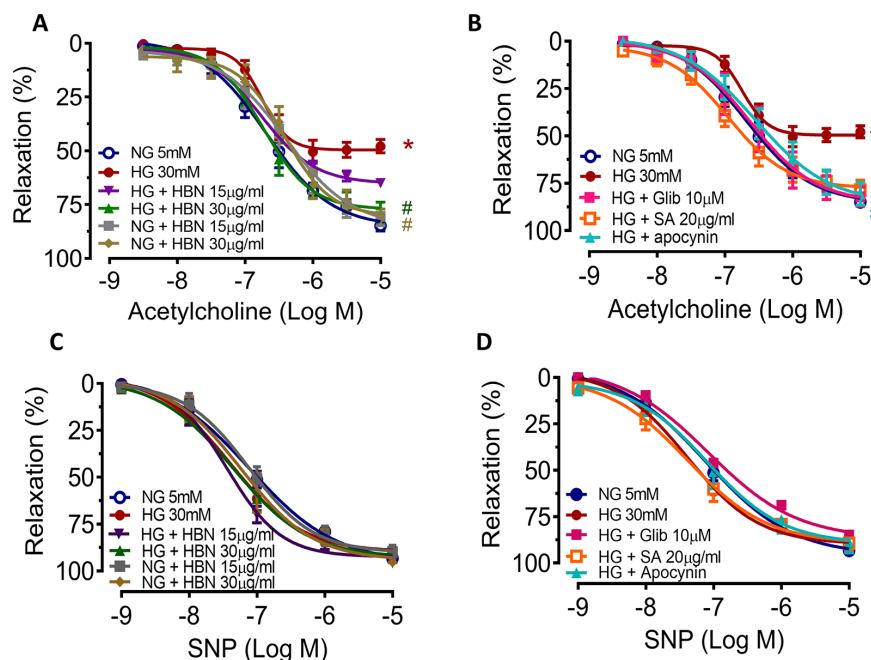


FIGURE 2 | The effect of isolated aorta from C57BL/6J treated with normal glucose (NG, 5 mM), high glucose (HG, 30 mM), hydrolyzed bird nest (HBN, 15 and 30 μ g/mL), sialic acid (SA, 20 μ g/mL), glibenclamide (Glib, 10 μ M), and apocynin (20 μ M) for 48 h in acetylcholine-induced endothelium-dependent relaxation (EDR) (**A**, **B**) and sodium nitroprusside-induced endothelium-independent relaxation (EIR) (**C**, **D**). Results are means \pm SEM of six experiments. * $P < 0.05$ compared with NG, # $P < 0.05$ when compared with HG.

TABLE 1 | Agonist sensitivity (pEC_{50}) and % maximum relaxation (R_{max}) of acetylcholine (ACh)-induced endothelium-dependent relaxation and sodium nitroprusside (SNP)-induced EIR in isolated aorta from C57BL/6J mice treated with normal glucose (NG, 5 mM), high glucose (HG, 30 mM), hydrolyzed bird nest (HBN, 15 and 30 μ g/mL), sialic acid (SA, 20 μ g/mL), glibenclamide (Glib, 10 μ M), and apocynin (20 μ M) for 48 h.

Groups	ACh		SNP	
	pEC_{50} (log M)	R_{max} (%)	pEC_{50} (log M)	R_{max} (%)
NG	-6.69 ± 0.10	84.88 ± 2.48	-7.11 ± 0.12	93.30 ± 1.52
NG + HBN (15 μ g/mL)	-6.40 ± 0.19	80.26 ± 4.58	-7.12 ± 0.14	89.86 ± 3.46
NG + HBN (30 μ g/mL)	-6.42 ± 0.11	79.73 ± 2.64	-7.23 ± 0.18	95.24 ± 2.55
HG	-6.75 ± 0.07	$47.92 \pm 3.12^*$	-7.39 ± 0.13	91.53 ± 2.07
HG + HBN (15 μ g/mL)	-6.76 ± 0.06	64.97 ± 1.70	-7.44 ± 0.09	95.57 ± 1.25
HG + HBN (30 μ g/mL)	-6.73 ± 0.09	$79.10 \pm 5.14^{\#}$	-7.35 ± 0.17	93.38 ± 2.34
HG + Glib	-6.63 ± 0.18	$82.13 \pm 5.03^{\#}$	-7.08 ± 0.21	84.87 ± 1.70
HG + SA	-6.95 ± 0.14	$78.67 \pm 5.18^{\#}$	-7.38 ± 0.20	89.33 ± 3.89
HG + Apocynin	-6.54 ± 0.17	$80.68 \pm 5.93^{\#}$	-7.09 ± 0.23	88.77 ± 5.85

Results are means \pm SEM ($n = 6$). * $P < 0.05$ compared with NG, # $P < 0.05$ when compared with HG.

(Figure 4B) compared to NG, as measured by LEC and DCF-DA respectively. Co-treatment with HBN (30 μ g/mL) significantly reduced the production of vascular superoxide anion and intercellular ROS in HUVECs compared to HG. Similarly, co-treatment with sialic acid (20 μ g/mL), glibenclamide (10 μ M), and apocynin (20 μ M) reduced the vascular superoxide anion and intercellular ROS in HUVECs. The level of vascular superoxide anion and intercellular ROS in HUVECs in HBN alone in HG was similar to the NG-treated group.

HBN Restored High Glucose-Induced Production of NO in HUVECs and NO Level in *db/db* Mice

The reduced level of NO in HUVECs in response to HG was reversed by co-treatment with HBN (30 μ g/mL), sialic acid (20 μ g/mL), glibenclamide (10 μ M), and apocynin (20 μ M). Meanwhile, the positive control, calcium ionophore (A23187) significantly increased the NO level. HBN and mannitol co-treatment did not affect NO level in the NG-treated aorta (Figure 5A).

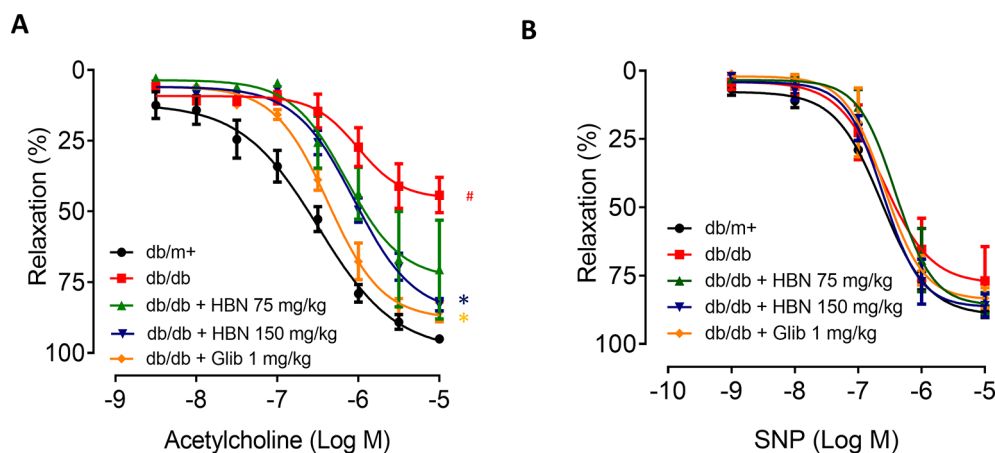


FIGURE 3 | The effect of four week's treatment of hydrolyzed bird nest (HBN, 75 and 150 mg/kg) and glibenclamide (1 mg/kg) on **(A)** acetylcholine-induced endothelium-dependent relaxation (EDR) and **(B)** sodium nitroprusside-induced endothelium-independent relaxation (EIR) in db/db mice. Results are means \pm SEM of six experiments. # $P < 0.05$ compared with db/m+, * $P < 0.05$ when compared with db/db.

TABLE 2 | Agonist sensitivity (pEC_{50}) and % maximum relaxation (R_{max}) of acetylcholine-induced endothelium-dependent relaxation and sodium nitroprusside (SNP)-induced EIR in isolated aorta from db/db mice treated with glibenclamide (1 mg/kg), HBN (75 mg/kg) and HBN (150 mg/kg).

Groups	Ach		SNP	
	pEC_{50} (log M)	R_{max} (%)	pEC_{50} (log M)	R_{max} (%)
db/m+	-6.49 ± 0.11	95.03 ± 1.31	-6.62 ± 0.08	88.27 ± 2.12
db/db	-5.93 ± 0.15 ###	57.04 ± 3.29	-6.59 ± 0.28	76.91 ± 12.49
db/db + HBN 75mg/kg	-6.19 ± 0.22	70.56 ± 17.45	-6.41 ± 0.16	85.16 ± 3.92
db/db + HBN 150 mg/kg	-6.05 ± 0.07 ***	83.01 ± 2.17	-6.61 ± 0.13	85.98 ± 4.20
db/db + glibenclamide 1 mg/kg	-6.37 ± 0.06 ***	85.55 ± 3.48	-6.59 ± 0.17	83.21 ± 3.71

Results are means \pm SEM ($n = 6$). ### $P < 0.001$ compared with db/m+, *** $P < 0.001$ when compared with db/db.

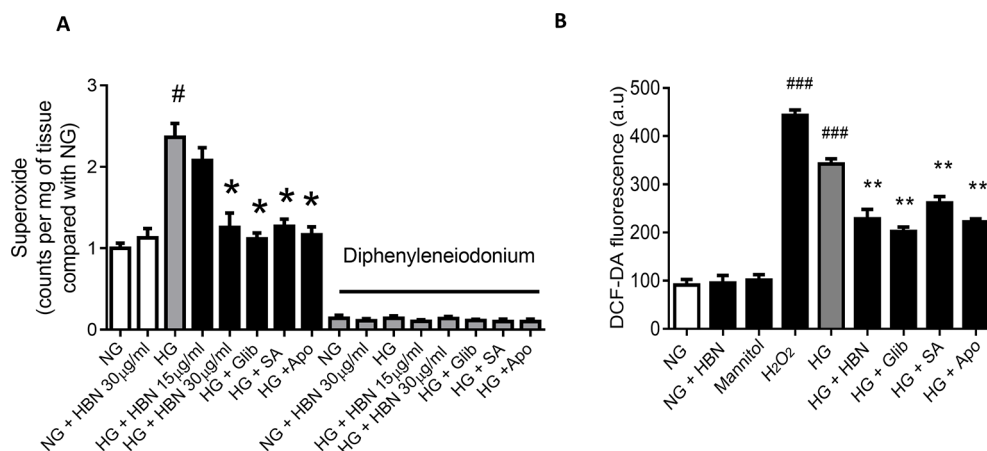


FIGURE 4 | (A) Superoxide production measured by lucigenin-enhanced chemiluminescence assay in the aorta of C57BL/6J mice in the absence and presence of diphenyleneiodonium, NOX inhibitor and **(B)** level of intercellular ROS measured by DCF-DA assay after treatment with normal glucose (NG, 5 mM), high glucose (HG, 30 mM), mannitol (25 mM), H₂O₂ (200 μ M), calcium ionophore (A23187, 5 μ M), Hydrolysed bird nest (HBN, 30 μ g/ml), sialic acid (SA, 20 μ g/ml), glibenclamide (Glib, 10 μ M) and apocynin (Apo, 20 μ M) in HUVECs for 48 hours. Results are means \pm SEM of 6 independent experiments. # $P < 0.05$ and ### $P < 0.001$ compared with NG, * $P < 0.05$ and ** $P < 0.01$ compared to HG.

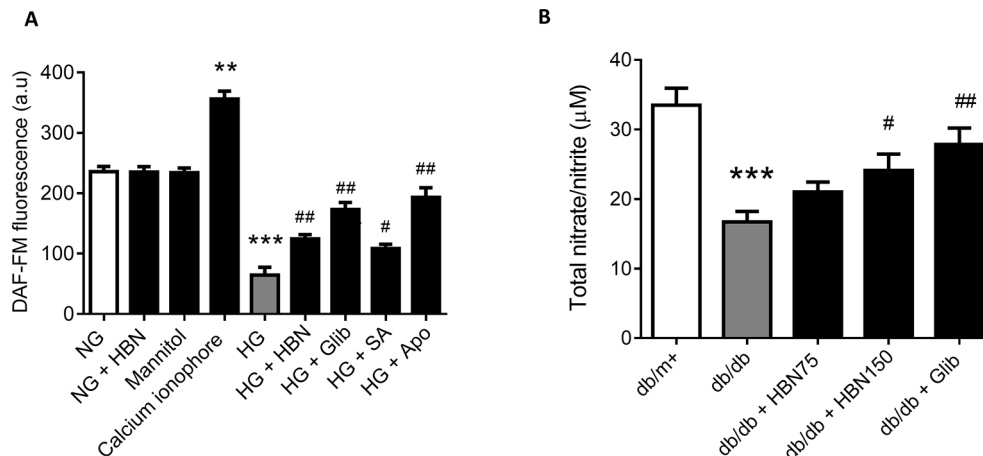


FIGURE 5 | (A) Nitric oxide (NO) level as measured by DAF-FM after treatment with normal glucose (NG, 5 mM), high glucose (HG, 30 mM), mannitol (25mM), H₂O₂ (200 μM), calcium ionophore (A23187, 5 μM), hydrolyzed bird nest (HBN, 30 μg/mL), sialic acid (SA, 20 μg/mL), glibenclamide (Glib, 10 μM), and apocynin (Apo, 20 μM) in HUVECs for 48 h. **(B)** in serum of db/db mice treated with hydrolyzed bird nest (HBN, 75 and 150 mg/kg) and glibenclamide (1 mg/kg) for four weeks. Results are mean ± SEM of three experiments. **P < 0.01 and ***P < 0.001 compared to control; #P < 0.05 and ##P < 0.01 compared to HG.

The level of NO in *db/db* mice was depleted about 50% compared to the *db/m+* which demonstrated a reduction from 33.5 μM to 16.7 μM (**Figure 5B**). Treatment with HBN (150 mg/kg) increased the level of NO up to 24 μM compared to vehicle control. Meanwhile, the positive control, glibenclamide (1 mg/kg) significantly increased the NO level to 27.9 μM (**Figure 5B**). This results from *in vivo* study is in agreement with the *in vitro* study.

HBN Inhibited High Glucose-Induced Oxidative Stress Associated Proteins in HUVECs and *db/db* Mouse Aorta

The effects of HBN were next explored on high glucose-induced oxidative stress associated proteins. NADPH oxidase 2 (NOX-2) and nitrotyrosine proteins were up-regulated in HG-induced HUVECs (**Figures 6A–C**) and in diabetic mouse aorta

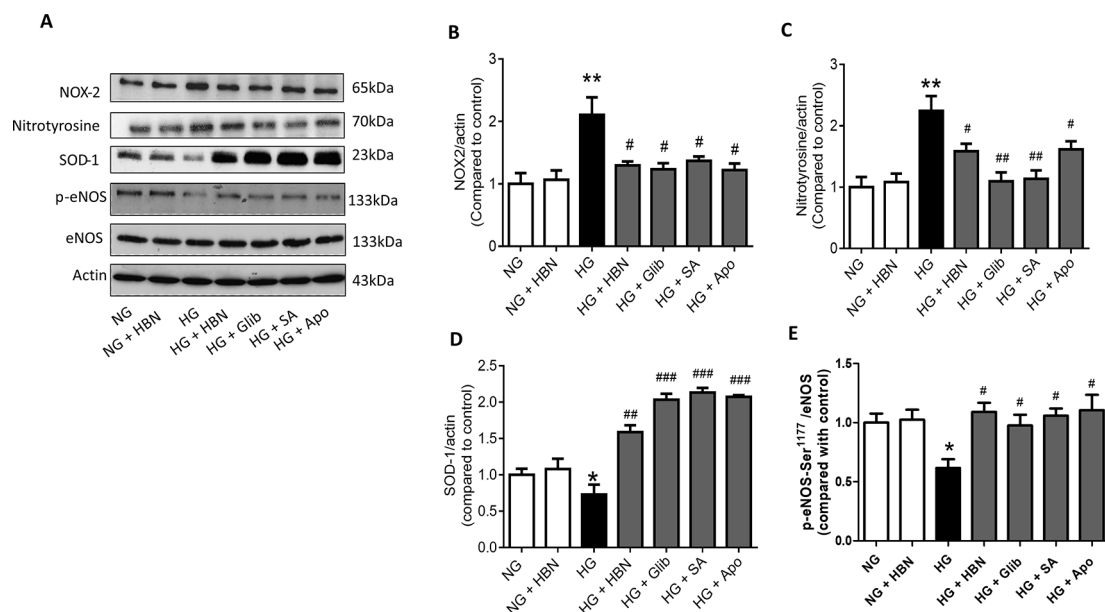


FIGURE 6 | Western blot and quantitative data showing proteins in HUVECs treated with normal glucose (NG, 5 mM), high glucose (HG, 30 mM), hydrolyzed bird nest (HBN, 30 μg/mL), sialic acid (SA, 20 μg/mL), glibenclamide (Glib, 10 μM), and apocynin (Apo, 20 μM) for 48 h. Results are means + SEM of four separate experiments. *P < 0.05 and **P < 0.01 compared to control; #P < 0.05, ##P < 0.01 and ###P < 0.001 compared to HG.

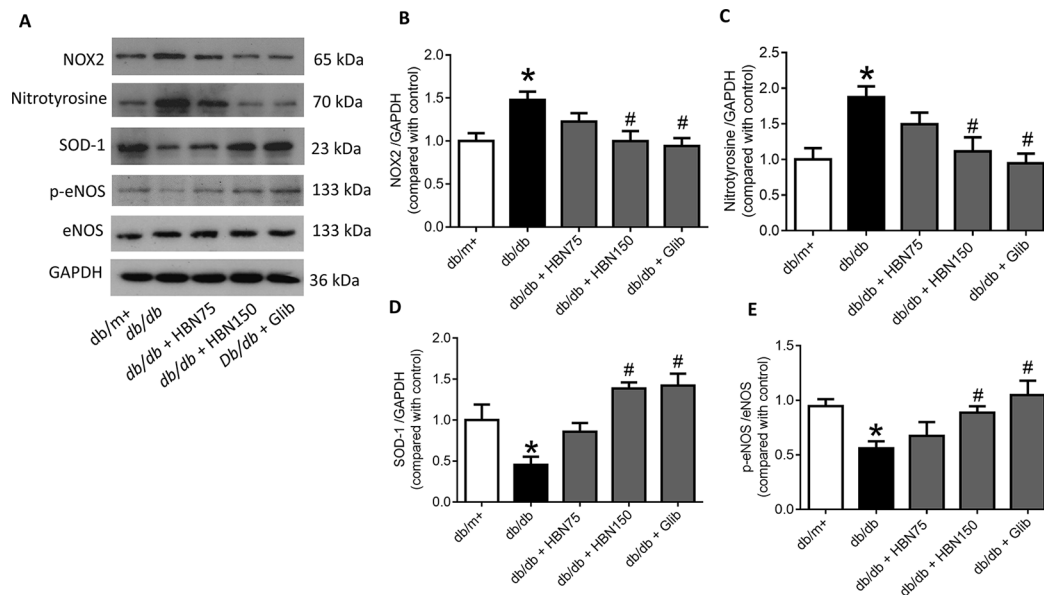


FIGURE 7 | Western blot and quantitative data showing proteins in aorta of *db/db* mice treated with hydrolyzed bird nest (HBN, 75 and 150 mg/kg), and glibenclamide (1 mg/kg) for four weeks. Results are means + SEM of six separate experiments. * $P < 0.05$ compared to *db/m+*; # $P < 0.05$ compared to *db/db*.

(Figures 7A–C). In contrast, the antioxidant protein (SOD-1) and eNOS activity were decreased in HG-induced HUVECs (Figures 6A, D, and E) and in diabetic mouse aorta (Figures 7A, D, and E). Co-treatment of HG with HBN (30 µg/mL), sialic acid (20 µg/mL), glibenclamide (10 µM), and apocynin (20 µM) significantly reversed the elevated levels of NOX-2 (Figure 6B) and nitrotyrosine (Figure 6C) as well as increased the downregulated SOD-1 (Figure 6D) and p-eNOS (Figure 6E) protein levels induced by HG. No significant changes were observed between the NG and the NG + HBN group. Four-weeks treatment with 150 mg/kg HBN and 1 mg/kg glibenclamide to *db/db* mice significantly reversed the elevated vascular NOX-2 (Figure 7B) and nitrotyrosine (Figure 7C), while increased the reduced SOD-1 (Figure 7D) and p-eNOS (Figure 7E) protein levels compared to the *db/db* mice.

DISCUSSION

The present study provides experimental evidence that treatment with HBN effectively restored the impaired endothelium-dependent relaxations in mice aortas exposed to high glucose condition. In addition, the current work showed HBN reduced the expression of ROS markers (NOX-2 and nitrotyrosine), increased expression of SOD-1 and phosphorylated eNOS in HUVECs and aorta of *db/db* mice. These results indicate HBN treatment attenuates the hyperglycemia-induced endothelial dysfunction through the reduction in oxidative stress and increasing the NO bioavailability.

Increased oxidative stress and reduced nitric oxide (NO) bioavailability play a causal role in endothelial cell dysfunction occurring in the vasculature of diabetic patients (Rajendran et al., 2013). Prolonged exposure to high glucose *in vitro* or *in vivo* has

been shown to inhibit ACh-induced endothelium-dependent relaxation, while not affecting SNP-induced endothelium-independent relaxation (Lau et al., 2013; Mangipudi and Hillier, 2013; El-Awady et al., 2014). A similar finding was also observed in the present study with 48-h incubation in HG and in aorta of *db/db* mice. Moreover, treatment with HBN significantly reversed the dysfunction demonstrating the vascular protective effect of HBN. The improvement demonstrated by HBN is comparable to apocynin, an antioxidant, and glibenclamide, an antidiabetic agent. High glucose has been shown to induce ROS production, which ultimately may contribute to the endothelial dysfunction (Cho et al., 2013; Salisbury and Bronas, 2015). Similarly, the vascular ROS, especially superoxide anion was elevated in aorta of *db/db* mice and aorta exposed to high glucose and HBN decreased the superoxide production in the high-glucose exposed tissues, indicating HBN protects against endothelial dysfunction by inhibiting ROS production. This is in agreement with previous researches that showed edible bird's nest ameliorated oxidative stress by reducing production of ROS in SH-SY5Y cells and human keratinocytes (Yew et al., 2014; Hou et al., 2015; Lim et al., 2015).

In order to provide further insights into the mechanistic basis for the effects of HBN, the effect of HBN against high glucose-induced oxidative stress was investigated in aorta of *db/db* mice and HUVECs. Parallel to the finding with mice aorta, HUVECs exposed to high glucose also demonstrated an elevated level of ROS. This was accompanied by a decrease in NO level. ROS was mainly derived from NADPH oxidase which plays a role in the pathogenesis of vascular endothelial dysfunction in diabetes (Wong et al., 2010). High glucose-induced ROS elevation is mainly associated with increased expression of NADPH oxidase subunits such as NOX-2, which was also reduced by HBN. Basically, superoxide anions, the main species of ROS will react

with NO to produce peroxynitrite radicals which will later lower NO bioavailability (Maritim et al., 2003). The role of peroxynitrite in high glucose-stimulated HUVECs and aorta of *db/db* was confirmed by detecting an increased expression of nitrotyrosine due to the facilitation of tyrosine nitration by peroxynitrate radicals. However, following co-treatment with HBN, expression of nitrotyrosine was significantly reduced. This was accompanied with increased production of NO as observed with an increase in p-eNOS expression and total nitrate/nitrite level in HBN treated *db/db* mice. Thus, the ROS inhibiting effect of HBN possibly contributed to restoring hemostatic imbalance which augments NO level in high-glucose stimulated endothelial cells in order to improve endothelial function.

Overall evidence suggests that on one hand, hyperglycemia induces free radicals; on the other hand, it impairs the endogenous antioxidant defense system in patients with diabetes (Pitocco et al., 2010). Endogenous antioxidant defense mechanisms such as glutathione (GSH), superoxide dismutase (SOD), and catalase (CAT), protects against toxic ROS (Gupta et al., 2014). HBN treatment increased SOD-1 protein level against the reduction induced by HG in the HUVECs and in treated *db/db* aorta. Likewise, previous reports by Hou et al. (2015) demonstrated that treatment with edible bird's nest increased SOD activity and mRNA levels of SOD-1 in H₂O₂-induced oxidative stress in SH-SY5Y cells. Similarly, edible bird's nest reduced the production of ROS in human HaCat keratinocytes and SH-SY5Y human neuroblastoma cells (Kim et al., 2012; Yew et al., 2014). HBN (Yida et al., 2015) and sialic acid (Pawluczyk et al., 2014) has been previously demonstrated to upregulate antioxidant enzymes including SOD at transcriptional levels. Although in the present study, only protein level of SOD was measured, the increase in gene expression is most likely reflected in the protein expression.

Previous study found that the composition on edible bird nest consist of protein (56.47–60.63%), water (17.26–24.05%), ash (3.29–7.41%), carbohydrates (1.04–2.48%), crude fiber (12.162.59%), and fat (0.07–12.57%) (Daud et al., 2016). The monosaccharides composition of glycoprotein in edible bird's nest contains about 9% of sialic acid, 4.19–7.2% of galactosamine, about 5.3% of glucosamine, 5.03–16.9% of galactose, and about 0.7% of fructose (Kathan and Weeks, 1969). Wang and Brand-Miller (2003) reported that edible bird's nest contains a high amount of sialic acid and this may contribute to brain development and learning ability. This is further supported by a recent work by Oliveros et al. (2018), whereby they demonstrated supplementation of sialic acid and sialylated Oligosaccharide supplementation during lactation improved learning and memory in rats. Similarly, sialic acid has been shown to restore mitochondrial SOD mRNA expression and quench oxidative burst in puromycin aminonucleoside-induced desialylation and oxidative stress in human podocytes (Pawluczyk et al., 2014). In 2016, Guo et al. has demonstrated exogenous supplement of sialic acid ameliorated atherosclerosis in apolipoprotein E-deficient mice partly by elevating antioxidant activity by restoring the activity or improving protein expression of antioxidant enzymes, thus demonstrating the beneficial effect of sialic acid on cardiovascular disease (Guo et al., 2016). The efficacy of HBN against high glucose-induced oxidative stress and endothelial

dysfunction was comparable to the sialic acid, the main carbohydrate found in edible bird's nest. Therefore, sialic acid contained in edible bird's nest could be used as an important parameter for determining for their quality and their biological activities. The results suggest that sialic acid may represent the active compound in edible bird's nest which is responsible for the mechanism involves reducing oxidative stress.

CONCLUSION

In summary, both *in vitro*, *ex vivo*, and *in vivo* treatments with HBN significantly protect against high-glucose induced endothelial dysfunction by inhibiting oxidative stress and increasing NO bioavailability. These results provide further evidence for edible bird's nest to be used as a functional food for the prevention of cardiometabolic diseases by combating oxidative stress and thus subsequently protect endothelial function in hyperglycemic conditions.

DATA AVAILABILITY STATEMENT

The datasets generated for this study are available on request to the corresponding authors.

ETHICS STATEMENT

The study protocol involving the use of animals in the present study was approved by the University of Malaya Animal Care and Ethics Committee (Ethics Reference No: 2015-180709) and accredited by the Association for Assessment and Accreditation of Laboratory Animal Care International (AAALAC). The animal study was carried out in strict accordance with the established institutional guidelines and the NIH guidelines on the use of experimental animals. Consent to participate was not applicable.

AUTHOR CONTRIBUTIONS

MM, DM and KC participated in designing the study. ZZ and KC performed the *in-vitro*, *ex-vivo* and *in-vivo* experiments and analyzed the data. NZ, MC and YL performed the phytochemical analyses. DM and ZZ prepared the first manuscript draft. MM, KC and YL participated in editing and preparation of the final manuscript draft. All authors read and approved the final manuscript.

FUNDING

This study was funded by Government Agency grant GA001-2017. The funding agencies played no role in the design of the study and collection, analysis, and interpretation of data and in writing the manuscript, which are fully the responsibilities of the authors.

ACKNOWLEDGMENTS

Special thanks to Royal Bird's Nest Sdn Bhd (Kuala Lumpur, Malaysia) for providing raw bird's nest extract.

REFERENCES

- Cho, Y. E., Basu, A., Dai, A., Haldak, M., and Makino, A. (2013). Coronary endothelial dysfunction and mitochondrial reactive oxygen species in type 2 diabetic mice. *Am. J. Physiol.-Cell Physiol.* 305, C1033–C1040. doi: 10.1152/ajpcell.00234.2013
- Choy, K. W., Lau, Y. S., Murugan, D., and Mustafa, M. R. (2017). Chronic treatment with paeonol improves endothelial function in mice through inhibition of endoplasmic reticulum stress-mediated oxidative stress. *PLoS One* 12, e0178365. doi: 10.1371/journal.pone.0178365
- Daud, N. A., Ghassem, M., Fern, S. S., and Babji, A. S. (2016). Functional bioactive compounds from freshwater fish, edible birdnest, marine seaweed and phytochemical. *Am. J. Food Nutr.* 6, 33–38. doi: 10.5251/ajfn.2016.6.2.33.38
- El-Awady, M. S., El-Agamy, D. S., Suddek, G. M., and Nader, M. A. (2014). Propolis protects against high glucose-induced vascular endothelial dysfunction in isolated rat aorta. *J. Physiol. Biochem.* 70, 247–254. doi: 10.1007/s13105-013-0299-7
- Guo, C. T., Takahashi, T., Bukawa, W., Takahashi, N., Yagi, H., Kato, K., et al. (2006). Edible bird's nest extract inhibits influenza virus infection. *Antiviral Res.* 70, 140–146. doi: 10.1016/j.antiviral.2006.02.005
- Guo, S., Tian, H., Dong, R., Yang, N., Zhang, Y., Yao, S., et al. (2016). Exogenous supplement of N-acetylneuraminic acid ameliorates atherosclerosis in apolipoprotein E-deficient mice. *Atherosclerosis* 251, 183–191. doi: 10.1016/j.atherosclerosis.2016.05.032
- Gupta, R. K., Patel, A. K., Shah, N., Chaudhary, A., Jha, U., Yadav, U. C., et al. (2014). Oxidative stress and antioxidants in disease and cancer. *Asian Pac. Cancer Prev.* 15, 4405–4409. doi: DOI: 10.7314/apjcp.2014.15.11.4405
- Haghani, A., Mehrbod, P., Safi, N., Aminuddin, N. A., Bahadoran, A., Omar, A. R., et al. (2016). In vitro and in vivo mechanism of immunomodulatory and antiviral activity of Edible Bird's Nest (EBN) against influenza A virus (IAV) infection. *J. Ethnopharmacol.* 5, 327–340. doi: 10.1016/j.jep.2016.03.020
- Hou, Z., Imam, M. U., Ismail, M., Azmi, N., Ismail, N., Ideris, A., et al. (2015). Lactoferrin and ovotransferrin contribute toward antioxidative effects of Edible Bird's Nest against hydrogen peroxide-induced oxidative stress in human SH-SY5Y cells. *Biosci. Biotech. Biochem.* 79, 1570–1578. doi: 10.1080/09168451.2015.1050989
- Jay, D., Hitomi, H., and Griendling, K. K. (2006). Oxidative stress and diabetic cardiovascular complications. *Free Radical Biol. Med.* 40, 183–192. doi: 10.1016/j.freeradbiomed.2005.06.018
- Just, A., Whitten, C. L., and Arendshorst, W. J. (2008). Reactive oxygen species participate in acute renal vasoconstrictor responses induced by ETA and ETB receptors. *Am. J. Physiol.-Renal Physiol.* 294, F719–F728. doi: 10.1152/ajprenal.00506.2007
- Kathan, R. H., and Weeks, D. I. (1969). Structure studies of collocalia mucoid: I. Carbohydrate and amino acid composition. *Arch. Biochem. Biophys.* 134, 572–576. doi: 10.1016/0003-9861(69)90319-1
- Kim, K. C., Kang, K. A., Lim, C. M., Park, J. H., Jung, K. S., and Hyun, J. W. (2012). Water extract of edible bird's nest attenuated the oxidative stress-induced matrix metalloproteinase-1 by regulating the mitogen-activated protein kinase and activator protein-1 pathway in human keratinocytes. *J. Korean Soc. Appl. Biol. Chem.* 55, 347–354. doi: 10.1007/s13765-012-2030-8
- Kong, Y., Keung, W., Yip, T., Ko, K., Tsao, S., and Ng, M. (1987). Evidence that epidermal growth factor is present in swiftlet's (Collocalia) nest. *Comp. Biochem. Physiol. B Comp. Biochem.* 87, 221–226. doi: 10.1016/0305-0491(87)90133-7
- Lau, Y. S., Tian, X. Y., Mustafa, M. R., Murugan, D., Liu, J., Zhang, Y., et al. (2013). Boldine improves endothelial function in diabetic db/db mice through inhibition of angiotensin II-mediated BMP4-oxidative stress cascade. *Br. J. Pharmacol.* 170, 1190–1198. doi: 10.1111/bph.12350
- Lim, C. L., Koh, R. Y., Haw, T. Y., and Boudville, L. A. (2015). Antioxidant activity of the sea bird nest (*Eucheuma cottonii*) and its radical scavenging effect on human keratinocytes. *J. Med. Bioeng.* 4, 461–465. doi: 10.12720/jomb.4.6.461-465
- Loscalzo, J. (2013). The identification of nitric oxide as endothelium-derived relaxing factor. *Circ. Res.* 113, 100–103. doi: 10.1161/CIRCRESAHA.113.301577
- Ma, F., and Liu, D. (2012). Sketch of the edible bird's nest and its important bioactivities. *Food Res. Int.* 4, 559–567. doi: 10.1016/j.foodres.2012.06.001
- Mangipudi, R. K. C., and Hillier, C. (2013). Mechanisms mediating the protective effect of curcumin on vascular endothelial dysfunction induced by high glucose. *J. Physiol. Pharmacol. Adv.* 3, 85–93. doi: 10.5455/jppa.20130320024131
- Maritim, A., Sanders, A., and Watkins, J. (2003). Diabetes, oxidative stress, and antioxidants: a review. *J. Biochem. Mol. Toxicol.* 17, 24–38. doi: 10.1002/jbt.10058
- Marni, S., Marzura, M., Norzela, A., Khairunnisak, M., Bing, C., and Eddy, A. (2014). Preliminary study on free sialic acid content of edible bird nest from Johor and Kelantan. *EMalaysian J. Vet. Res.* 5, 9–14.
- Matough, F. A., Budin, S. B., Hamid, Z. A., Alwahabi, N., and Mohamed, J. (2012). The role of oxidative stress and antioxidants in diabetic complications. *Sultan Qaboos Univ. Med. J.* 12, 5–18. doi: 10.12816/0003082
- Matsukawa, N., Matsumoto, M., Bukawa, W., Chiji, H., Nakayama, K., Hara, H., et al. (2011). Improvement of bone strength and dermal thickness due to dietary edible bird's nest extract in ovariectomized rats. *Biosci. Biotech. Biochem.* 75, 590–592. doi: 10.1271/bbb.100705
- Namin, S. M., Nofallah, S., Joshi, M. S., Kavallieratos, K., and Tsoukias, N. M. (2013). Kinetic analysis of DAF-FM activation by NO: Toward calibration of a NO-sensitive fluorescent dye. *Nitric. Oxide* 28, 39–46. doi: 10.1016/j.niox.2012.10.001
- Oliveros, E., Vázquez, E., Barranco, A., Ramírez, M., Gruart, A., Delgado-García, J. M., et al. (2018). Sialic acid and sialylated oligosaccharide supplementation during lactation improves learning and memory in rats. *Nutrients* 10, pii: E1519. doi: 10.3390/nu10101519
- Pawluczky, I. Z., Najafabadi, M. G., Patel, S., Desai, P., Vashi, D., Saleem, M. A., et al. (2014). Sialic acid attenuates puromycin aminonucleoside-induced desialylation and oxidative stress in human podocytes. *Exp. Cell Res.* 320, 258–268. doi: 10.1016/j.yexcr.2013.10.017
- Pitocco, D., Zaccardi, F., Di Stasio, E., Romitelli, F., Santini, S. A., Zuppi, C., et al. (2010). Oxidative stress, nitric oxide, and diabetes. *Rev. Diabetes Stud.* 7, 15–25. doi: 10.1900/RDS.2010.7.15
- Rajendran, P., Rengarajan, T., Thangavel, J., Nishigaki, Y., Sakthisekaran, D., Sethi, G., et al. (2013). The vascular endothelium and human diseases. *Int. J. Biol. Sci.* 9, 1057–1069. doi: 10.7150/ijbs.7502
- Salisbury, D., and Bronas, D. (2015). Reactive oxygen and nitrogen species: impact on endothelial dysfunction. *Nurs. Res.* 64, 53–66. doi: 10.1097/NNR.0000000000000068
- Schulz, E., Jansen, T., Wenzel, I. P., Daiber, A., and Münzel, T. (2008). Nitric oxide, tetrahydrobiopterin, oxidative stress, and endothelial dysfunction in hypertension. *Antioxid. Redox Signal.* 10, 1115–1126.
- Sena, C. M., Pereira, A. M., and Seica, R. (2013). Endothelial dysfunction—a major mediator of diabetic vascular disease. *Biochim. Biophys. Acta (BBA)-Mol. Basis Dis.* 1832, 2216–2231. doi: 10.1016/j.bbadis.2013.08.006
- Vimala, B., Hussain, H., and Nazaimoon, W. W. (2012). Effects of edible bird's nest on tumour necrosis factor- α secretion, nitric oxide production and cell viability of lipopolysaccharide-stimulated RAW 264.7 macrophages. *Food Agric. Immunol.* 23, 303–314. doi: 10.1080/09540105.2011.625494
- Wang, B., and Brand-Miller, J. (2003). The role and potential of sialic acid in human nutrition. *Eur. J. Clin. Nutr.* 57, 1351–1369. doi: 10.1038/sj.ejcn.1601704
- Wong, W. T., Tian, X. Y., Xu, A., Ng, C. F., Lee, H. K., Chen, Z. Y., et al. (2010). Angiotensin II type 1 receptor-dependent oxidative stress mediates endothelial dysfunction in type 2 diabetic mice. *Antioxid. Redox Signal.* 13, 757–768. doi: 10.1089/ars.2009.2831
- Yew, M. Y., Koh, R. Y., Chye, S. M., Othman, I., and Ng, K. Y. (2014). Edible bird's nest ameliorates oxidative stress-induced apoptosis in SH-SY5Y human neuroblastoma cells. *BMC Complement Altern. Med.* 14, 391. doi: 10.1186/1472-6882-14-391
- Yida, Z., Imam, M. U., and Ismail, M. (2014). In vitro bioaccessibility and antioxidant properties of edible bird's nest following simulated human gastro-intestinal digestion. *BMC Complement Alter. Med.* 14, 468. doi: 10.1186/1472-6882-14-468
- Yida, Z., Imam, M. U., Ismail, M., Ooi, D. J., Sarega, N., Azmi, N. H., et al. (2015). Edible bird's nest prevents high fat diet-induced insulin resistance in rats. *J. Diabetes Res.* 2015, 760535. doi: 10.1155/2015/760535

Conflict of Interest: The authors declare that the research was conducted in the absence of any commercial or financial relationships that could be construed as a potential conflict of interest.

Copyright © 2020 Murugan, Md Zain, Choy, Zamakshshari, Choong, Lim and Mustafa. This is an open-access article distributed under the terms of the Creative Commons Attribution License (CC BY). The use, distribution or reproduction in other forums is permitted, provided the original author(s) and the copyright owner(s) are credited and that the original publication in this journal is cited, in accordance with accepted academic practice. No use, distribution or reproduction is permitted which does not comply with these terms.



Protective Effect of Stachydrine Against Cerebral Ischemia-Reperfusion Injury by Reducing Inflammation and Apoptosis Through P65 and JAK2/STAT3 Signaling Pathway

OPEN ACCESS

Edited by:

Zhang Yuefan,
Shanghai University,
China

Reviewed by:

Marong Fang,
Zhejiang University,
China
Junping Kou,
China Pharmaceutical
University, China

*Correspondence:

Junqin Mao
maojq204@163.com

[†]These authors have contributed
equally to this work

Specialty section:

This article was submitted to
Ethnopharmacology,
a section of the journal
Frontiers in Pharmacology

Received: 09 July 2019

Accepted: 22 January 2020

Published: 18 February 2020

Citation:

Li L, Sun L, Qiu Y, Zhu W, Hu K and
Mao J (2020) Protective Effect of
Stachydrine Against Cerebral
Ischemia-Reperfusion Injury by
Reducing Inflammation and Apoptosis
Through P65 and JAK2/STAT3
Signaling Pathway.
Front. Pharmacol. 11:64.
doi: 10.3389/fphar.2020.00064

Li Li^{1†}, Lili Sun^{2†}, Yan Qiu¹, Wenjun Zhu¹, Kangyuan Hu¹ and Junqin Mao^{1*}

¹ Department of Pharmacy, Shanghai Pudong New Area People's Hospital, Shanghai, China, ² Department of Pharmacy, Shanghai Pudan Hospital, Shanghai, China

Stachydrine, a constituent of *Leonurus japonicus* Houtt which also called Japanese motherwort has been shown to improve vascular microcirculation and ameliorate endothelial dysfunction. This study investigated the neuroprotective effect of stachydrine. Male Sprague-Dawley (SD) rats were randomly divided into sham, control, and stachydrine groups. The neurological deficit score was evaluated and the infarct size of the brain was measured using 2,3,5-triphenyltetra-zolium (TTC) chloride staining assay, and the pathological changes in the brain tissues were examined by HE staining. Nissl and terminal deoxynucleotidyl transferase deoxyuridine triphosphate nick end labeling (TUNEL) staining were performed to assess the numbers of Nissl bodies and the levels of apoptosis in the neurons. The activities of superoxide dismutase (SOD) and the levels of malondialdehyde (MDA) were also measured. The release of inflammatory factors IL-1 β and TNF- α were detected by Enzyme-linked immunosorbent assay (ELISA). Compared with the control group, the stachydrine group showed a significant prevention of neurological deficit, as indicated by the reduced infarct volume in the brain. Moreover, the stachydrine treatment reduced the activities of SOD, the levels of MDA and decreased the amount of IL-1 β , and TNF- α , indicating that it could function to decrease the level of inflammation, thus reducing brain damage. The ischemic stroke model of PC12 cells was prepared via oxygen-glucose deprivation (OGD) protocol for 6 h. The expression of P65 and JAK2/STAT3 signaling pathway related proteins was measured by western blot. The treatment group was found to have the survival rate of PC12 cells improved and the release of inflammatory factors reduced when compared with the OGD group. This study demonstrated that stachydrine could improve nerve function by inhibiting the phosphorylation of P65/JAK2 and STAT3.

Keywords: stachydrine, ischemia-reperfusion injury, PC12, oxygen-glucose deprivation, anti-inflammatory

INTRODUCTION

Stroke is the second leading cause of death in the industrialized countries and the leading cause of acquired adult disability (Go et al., 2013). Focal brain ischemia is usually caused by ischemic stroke, which account for around 80% of all stroke cases. It was estimated that there would be 1.5 million stroke patients in Europe each year till 2025 (Leech et al., 2019; A.K. Boehme et al., 2017). Currently, thrombolysis is well recognized to be the only effective therapy for stroke; however, approximately 5% of the patients treated this way are at a high risk of intracranial hemorrhagic transformation (Campos et al., 2013). Ischemic stroke was reported to show a complex pathophysiological course involving a plethora of distinct molecular and cellular pathways (Wang et al., 2014). Therefore, it is still imperative that we pursue a consistently effective therapy for stroke.

In the past few years, over one hundred traditional Chinese medicine (TCM) patents have been registered for ischemic stroke treatment in China (Chen et al., 2013), among which are the therapies for ischemic reperfusion injury (Moskowitz et al., 2010). Japanese motherwort has been traditionally used to treat some gynecological diseases with blood-circulation problems in East Asia for centuries, the cardio-cerebrovascular benefits of which have been reported from experimental and clinical studies (Zhang et al., 2018). Motherwort has antioxidant properties; leonurine as one of its important constituents has been reported to protect the brain in rats by exerting antioxidant and anti-apoptosis effects (Zhang et al., 2018). It has also been found to improve cerebral ischemia-reperfusion injury in rats (Loh et al., 2010). Stachydrine, a major constituent of motherwort, can exhibit protective effects on vascular endothelial cells (ECs), as indicated by a recent study which reported that stachydrine reversed the Hcy-induced endothelial dysfunction and prevented eNOS uncoupling by increasing the expression of GTPCH1 and dihydrofolate reductase (DHFR) (Servillo et al., 2013; Xie et al., 2018). The low doses of stachydrine could inhibit hydrogen peroxide and induce myometrial smooth muscle cell apoptosis by upregulating Bcl-2 expression (Liu Xin et al., 2012). In the hippocampus, it could improve pathological changes by inhibiting inflammatory reactions after ischemia (Miao et al., 2017). Additionally, stachydrine has been shown to exert antioxidant effects by reducing plasma lactate dehydrogenase (LDH) activity in the animal models of acute myocardial ischemia (Liu Xin et al., 2012; Zhao et al., 2017). However, there is a dearth of literature on whether stachydrine can function to treat stroke effectively.

In this study we focused on rats and PC12 cells, because stachydrine was reported to produce a protective effect on cerebral ischemic reperfusion damage in rats, thus enhancing the survival of PC12 cells after oxygen-glucose deprivation (OGD). The OGD cell model was prepared to explore the underlying molecular mechanism of stachydrine's effects; consequently, stachydrine was found to be capable of reducing the cell death rate and improving neuronal function recovery.

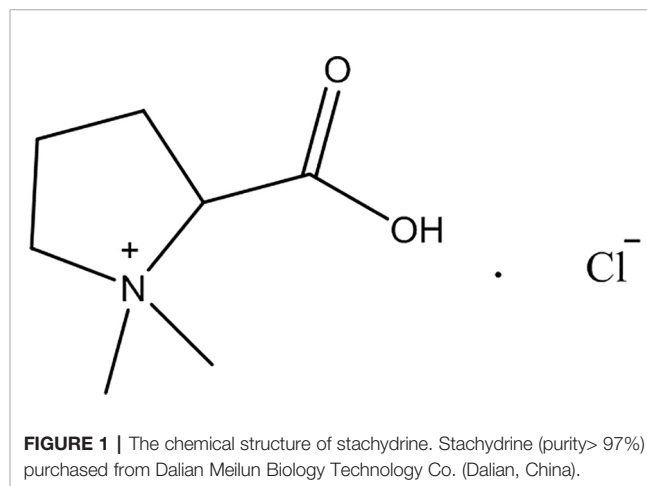
MATERIALS AND METHODS

Reagent

For this study were purchased stachydrine hydrochloric (purity > 97%; Dalian Meilun Biology Technology Company, Dalian, China); 2,3,5-triphenyltetrazolium chloride (Sigma, MO, USA); total RNA Kit (Takara, Shiga, Japan); ELISA Kit (R&D Systems, MN, USA); the antibodies of P65 (1:1,000), p-P65 (1:1,000), ikB (1:1,000), p-ikB (1:1,000), JAK2 (1:500), p-JAK2 (1:1,000), STAT3 (1:1,000), and p-STAT3 (1:1,000; Cell Signaling Technology Danvers, MA, USA); and goat anti-rabbit immunoglobulin G (IgG) (Cell Signaling Technology, Danvers, MA, USA). As illustrated in **Figure 1**, the structure of stachydrine was presented.

Animal Care and Experimental Protocol

Approved by Ethics Committee of Shanghai Pudong New Area People's Hospital, this study was carried out in accordance with the Basel Declaration's recommendations of the care and use of laboratory animals. Purchased from Shanghai Experimental Animal Center of Chinese Academy of Sciences (Shanghai, China), the rats were housed in the controlled environment under a 12 h light/dark cycle, and fed with standard rat chow and water. The male Sprague-Dawley rats weighing 260–280 g were housed in diurnal lighting condition, with free access to food and water. All rats were divided randomly into sham-operation group; control group, i.e., Middle Cerebral Artery Occlusion (MCAO) group injected with saline solution; and stachydrine groups, i.e., MCAO group injected once with stachydrine hydrochloric (Sta 27.93, Sta 55.87, Sta 111.73, Sta 167.60 mM) through the caudal vein 15 min after MCAO surgery. The neurobehavioral deficits were assessed and the brain of each rat was harvested 24 h after MCAO surgery. Those which received stachydrine 167.60 mM were treated, once daily (24 h), with stachydrine hydrochloric for 48 or 72 h through the caudal vein, while the sham and control groups received the same volume of normal saline.



Cell Culture

Obtained from the Cell Bank of Chinese Academy of Sciences (Shanghai, China), PC12 cells were cultured in Dulbecco's modified Eagle's medium (DMEM) (Hyclone, Logan, UT, USA) and 100 µg/ml penicillin-streptomycin solution (Thermo Scientific, Waltham, MA, USA), which were supplemented with 10% fetal bovine serum (Gibco, Carlsbad, CA, USA). The cells were cultured under the conditions of 37°C, 5% CO₂, and 95% humidified atmosphere.

Middle Cerebral Artery Occlusion Surgery

The male adult SD rats were anesthetized with 2% sodium pentobarbital (200 mM, i.p.), the neck shaved and cleaned with 75% ethanol. The left MCAO surgery was performed as previously described (Zhang et al., 2012). The left common carotid artery (CCA) was exposed through an incision in the middle of neck. The external carotid artery (ECA) was tied to prevent bleeding. A 4-0 poly-L-lysine filament (250–300 g) with a blunt end (Beijing Cinontech Co. Ltd, China) was inserted into the CCA to be advanced into the middle cerebral artery *via* the internal carotid artery (ICA) until a mild resistance was felt and the dark mark on the filament was in the vascular bifurcation position (18–20 mm), and then the blood of the middle cerebral artery was occluded. Two hours after the ischemia, the filament was slowly withdrawn until the dark mark was seen. Afterwards, the animals were returned to their cages to allow 24 h-reperfusion. Their body temperature was maintained at 37 ± 0.5°C with a heating lamp during the surgery. In the sham group, ECA was surgically prepared for filament insertion, but it was not inserted. After this surgery, the animals were sent to their cages to recover from anesthesia.

Neurological Deficit

After MCAO, neural dysfunction was evaluated based on the deficit grading system and according to the classic method introduced by Longa EZ and coworkers (Longa et al., 1989). A scale of 0 to 5 was used to assess the behavioral and motor changes in rats after MCAO surgery. When suspended by the tail, the rats extended both forelimbs toward on the floor, which represented a normal behavior corresponding to a score of 0. The rats were assigned a score of 1 when the contralateral forelimbs were on the side, without other abnormalities observed. The rats were placed on the ground to be allowed to move freely, their circling behavior observed. A score of 2 was assigned to those which moved spontaneously in all directions, but showed a monodirectional circling; a score of 3, to those which showed a consistent spontaneous contralateral circling (Loh et al., 2009); and a score of 4, to those which were very weak and collapsed.

Infarct Volume of Brain

To the infarct volume of brain was applied TTC staining (Sigma, MO, USA) for assessment. The brain specimens were harvested to be frozen at –20°C for 30 min, and the cerebellum was removed. The brain was sectioned into six pieces of 2 mm thick coronal slices using a new scalpel blade. The sections were stained with 1% TTC solution at 37°C for 20 min before

preserved in 4% formaldehyde at 4°C for at least 24 h. The brain infarct areas were analyzed with Image-Pro Plus 6.0 to estimate the infarct volume in the whole hemisphere.

Hematoxylin and Eosin Staining

When the animals were euthanized, the brain was carefully kept in 4% paraformaldehyde for 24 h. The slices were dyed with hematoxylin and then stained with eosin. The color changes were observed under a microscope to control the degree of dyeing. After dyed, those slices were washed with distilled water and dehydrated with gradient alcohol. Dried at room temperature, the histological changes were examined under an optical microscope.

Nissl Staining

The paraffinized brain samples were treated with Nissl staining solution (Sangon Biotech, Shanghai, China). Upon dyeing, a bluish-purple color was observed, which displayed the basic nervous structure of the brain. Large and numerous Nissl bodies were observed, indicating that the nerve cells had a high ability to synthesize proteins. When the nerve cells were damaged, however, the number of Nissl corpuscles decreased significantly. The number of stained cells was counted from the randomly selected fields and analyzed with Image-Pro Plus 6.0.

Terminal Deoxynucleotidyl Transferase Deoxyuridine Triphosphate Nick End Labeling Assay

The brain cells were treated with terminal deoxynucleotidyl transferase deoxyuridine triphosphate nick end labeling (Tunel) assay to determine the number of apoptotic cells. (In Situ Cell Death Detection Kit, Roche, Basle, Switzerland). The slides were heated to 60°C before washed with xylene and rehydrated through a series of concentration gradients of ethanol. The tissue sections were incubated in a working solution for about 20 min before put into the reaction mixture solution. The phosphate buffered saline (PBS) was used to wash the slides for analysis under a microscope. The apoptotic cells were those which had a brown-stained nucleus. The number of apoptotic cells was counted from the randomly selected fields.

Immunohistochemistry and Immunofluorescence

The brain slices were pretreated with 0.3% H₂O₂ and blocked in 0.1% bovine serum albumin for 30 min, before incubated overnight at 4°C with primary antibody P65. After rinsing, they were incubated with goat anti-rabbit IgG secondary antibody for 1 h at room temperature. After that, they were observed under a microscope. Methods double label immunofluorescence were observed with confocal laser microscope.

Oxygen-Glucose Deprivation

PC12 cells were subjected to the OGD procedure to mimic ischemic conditions *in vitro* as previously described (Zhu et al., 2016). Before OGD, the cells were washed thrice with PBS, and

then pretreated with stachydrine and glucose-free DMEM for 1 h. After that, they were incubated in a humidified modular hypoxia chamber (Billups-Rothenberg, Del Mar, USA) with 5% CO₂ and 95% N₂ for 6 h. The chamber was placed in an incubator set at 37°C. A normal normoxia medium served as the control.

Real-Time Polymerase Chain Reaction Assay

Total RNA was isolated from the cells subjected to OGD using Total RNA Kit (Takara, Shiga, Japan), and the complementary DNAs (cDNAs) were synthesized by 5×Primescript reverse transcription reagents (Takara, Shiga, Japan) following the manufacturer's instructions. Real-time (RT)-PCR was performed using SYBR Premix ExTaq™ (Tili RnaseH Plus; Takara, Shiga, Japan) on 7500 Real-Time PCR System (Applied Biosystems). The primers were used as follows:

Rat TNF- α	ForwardAAATGGGCTCCCTCTCATCAGTTC
	ReverseTCTGCTTGGTGGTTTGCTACGAC
Rat IL-1 β	ForwardAGGCTGACAGACCCCAAAAG
	ReverseCTCCACGGGCAAGACATAGG
Rat GAPDH	ForwardACCACAGTCCATGCCATCAC
	ReverseTCCACCACCTGTTGCTGTA

Enzyme-Linked Immunosorbent Assay

ELISA was employed to determine the release of inflammatory cytokines IL-1 β and TNF- α in serum and the supernatant of the rats and PC12 cells. The examination of IL-1 β and TNF- α was carried out according to the instructions of the kit (R&D Systems, MN, USA).

Western Blot Analysis

PC12 cells were kept at a density of 1.5×10^5 cells/ml in six-well plates for 24 h. After OGD, the protein was isolated from the whole cell lysate with M-PER Protein Extraction Reagent (Pierce, Rockford, IL) supplemented with protease inhibitor cocktail. The protein was resolved on sodium dodecyl sulfate polyacrylamide gel electrophoresis (SDS-PAGE) according to the molecular weight, and then transferred to the membranes, which were blocked for 2 h with 5% BSA before incubated with rabbit anti-P65 antibody (1:1,000), p-P65 (1:1,000), ikB (1:1,000), p-ikB (1:1,000), JAK2 (1:500), p-JAK2 (1:1,000), STAT3 (1:1,000), and p-STAT3 (1:1,000) overnight at 4°C. The immunoreactive proteins were detected using enhanced chemiluminescence (ECL) reagents western blotting substrate (Thermo Scientific, Waltham, MA, USA).

Statistical Analysis

All data was analyzed using SPSS19.0 software and expressed as the mean \pm SEM. The significant differences between the groups were examined by one-way analysis of variance (ANOVA). $P < 0.05$ was considered to be statistically significant.

RESULTS

The Neuroprotective Effect of Stachydrine on the Neurological Deficit and Infarct Volume

The classic method introduced by Longa EZ was used to assess the behavioral and motor changes in the rats after MCAO surgery. The sham group did not show any neurological deficit, but had a neurological score of 0. The control group presented the highest score after the surgery (Longa et al., 1989). The stachydrine group had the scores decrease significantly when compared with the control group. The scores of the control group increased significantly after reperfusion when compared with those of the sham group (2.50 ± 0.25 vs. 0.00 ± 0.00 ; $P < 0.01$). After 24 h-reperfusion, the administration of stachydrine significantly decreased the neurological deficit scores in the stachydrine group when compared with those in the control group (1.50 ± 0.23 [Sta 167.60 mM] vs. 2.50 ± 0.25 ; $P < 0.01$; **Figure 2D**). Moreover, the neurological deficit scores decreased over time (**Figure 2E**).

Since the sham group presented no neuronal injury, no infarct area was observed after TTC stained. Compared with that in the sham group, the cerebral infarct volume increased significantly in the control group. In contrast, the infarct area was significantly reduced in the stachydrine group when compared with that in the control group [$22.52 \pm 2.5\%$ (Sta 167.60 mM for 24 h) vs. $38.99 \pm 1.54\%$; $P < 0.01$; **Figures 2A, B**]. The infarcted area decreased over time (**Figure 2C**).

As indicated by the results of the histopathological changes examined in all groups by HE staining, the brain tissue structure was normal in the sham group. The nerve cells showed a clear outline with rounded nuclei and clear, visible nucleoli. In the hippocampus, the cells appeared orderly. The cerebral tissue in the control group showed edema on the half side of the ischemia-reperfusion injury. The HE staining revealed the presence of many vacuoles in different sizes in the brain tissue, the cells loosely arranged. The degree of cytoplasmic staining was uneven, while the cell nucleus was wrinkled and deformed.

The histopathological changes in the brain tissues were detected in the stachydrine group in comparison to the control group. The neuronal structure was found to be relatively regular, the nuclei visible and the vacuolization smaller without obvious damages both in cortex and hippocampus (**Figure 2F**).

Stachydrine Ameliorates Neurons Apoptosis

From Nissl staining used to examine the ischemia-reperfusion induced injury of neurons in the cerebral cortex, the results showed that the sham group had bluish-purple color Nissl bodies with orderly nuclei. Moreover, there were many and large neurons with normal structure. In the cortex of the control group, the cells were disorderly, the number of Nissl bodies significantly reduced, the cell gap increased and many vacuoles formed. The stachydrine group increased the number of Nissl bodies, thus leading to a clear nucleus when compared with the control group.

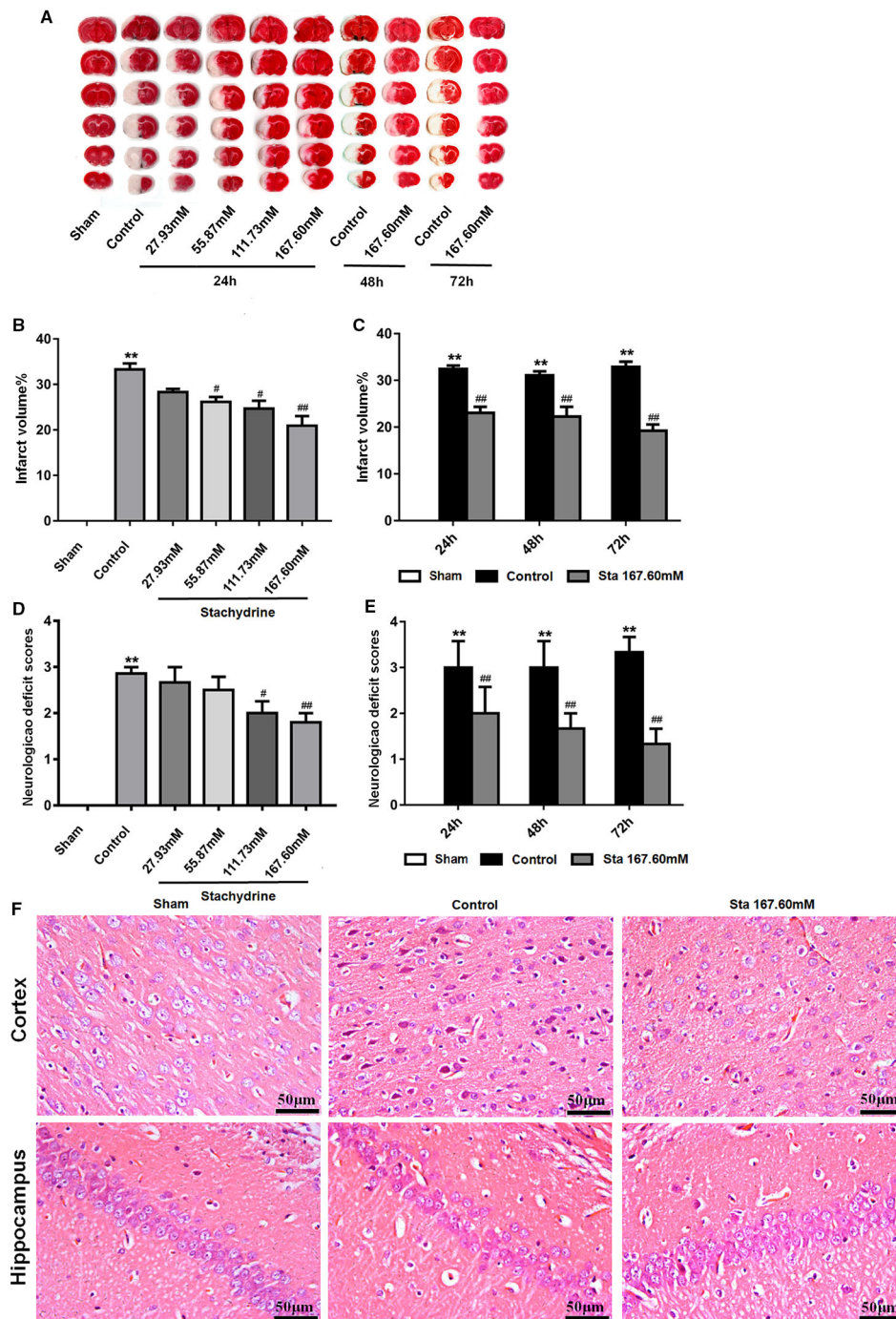


FIGURE 2 | The neuroprotective of stachydrine on neurological deficit and infarct volume. The neuroprotective effect of stachydrine on the neurological deficit and infarct volume of the brain was stained by tetrazolium chloride (TTC) and HE. **(A)** TTC staining used to assess the infarct areas of the brain. **(B)** The brain infarct areas analyzed with Image-Pro Plus 6.0 to estimate the infarct areas in the whole hemisphere after MCAO; ** $P < 0.01$, Sham group vs. Ccontrol group, # $P < 0.05$, ## $P < 0.01$ vs. control group, $n = 6$. **(C)** The infarct areas in the whole hemisphere of stachydrine (167.60 mM) treatment after MCAO 24, 48, and 72 h, analyzed; ** $P < 0.01$, Sham group vs. Ccontrol group, ### $P < 0.01$ vs. control group, $n = 6$. **(D)** Effect of stachydrine on the neurological scores after MCAO; ** $P < 0.01$, Sham group vs. Ccontrol group, # $P < 0.05$, ## $P < 0.01$ vs. control group, $n = 6$. **(E)** Effect of stachydrine (167.60 mM) on neurological scores after MCAO 24, 48, and 72 h, detected; ** $P < 0.01$, Sham group vs. Ccontrol group, ### $P < 0.01$ vs. control group; $n = 6$. **(F)** Pathological changes in cortex and hippocampus of brain evidenced by HE staining.

After Nissl staining, the cell number was 159 ± 8.18 cells/mm² in the sham group, but 70.83 ± 76.34 cells/mm² in the control group. The cell number was 115.3 ± 8.47 cells/mm² in the stachydrine group of 167.60 mM, which was significantly higher than that in the control group ($P < 0.01$; **Figure 3A**). Brown karyon staining cells were observed to be apoptotic under Olympus light microscope, which were counted in the groups. Additionally, the treatment of stachydrine decreased the number of apoptotic cells as compared with the control group ($P < 0.01$; **Figure 3B**).

Decreased Expression of P65 and p-STAT3 in Rat Brain

As revealed by immunohistochemistry staining assay, a decrease was observed in the rat brain section P65 protein levels after MCAO surgery (**Figure 4A**). According to the immunofluorescence staining to determine the expression of p-STAT3 protein in the rat brain section after ischemia reperfusion injury, the treatment of stachydrine decreased the protein expression of p-STAT3 (**Figure 4B**).

Superoxide Dismutase Activities Increased While Malondialdehyde, IL-1 β , and TNF- α Levels Decreased

Since oxidative stress plays an important role in ischemia-reperfusion injury, we investigated the effect of stachydrine on superoxide dismutase (SOD) activities and malondialdehyde (MDA) levels in the brain tissue and serum. The stachydrine group showed a decrease in the levels of MDA ($P < 0.05$; **Figure 5A**) as well as in the serum levels of MDA ($P < 0.01$, **Figure 5C**), when compared with the control group, respectively. Moreover, SOD activities were significantly lower in the control group than in the stachydrine group ($P < 0.05$; **Figure 5B**). The serum activities of SOD showed a similar trend ($P < 0.05$; **Figure 5D**).

To examine whether stachydrine treatment could induce an anti-inflammatory pattern, ELISA was employed to detect the levels of IL-1 β and TNF- α in serum after 24 h-reperfusion. The sham group had significantly lower levels of IL-1 β and TNF- α than the control group ($P < 0.01$). The stachydrine group showed a reduction in the levels of IL-1 β when compared with the control group ($P < 0.01$; **Figure 5E**). TNF- α expression was decreased after treatment with stachydrine compared with control group ($P < 0.05$; **Figure 5F**).

Viability Increased and IL-1 β and TNF- α Levels Decreased in PC12 Cells After Oxygen-Glucose Deprivation

When the cell viability was tested by MTT, it was found that the stachydrine group showed an increase in the survival rate of PC12 cells when compared with OGD group (**Figure 6A**). The results of the flow cytometry showed the OGD cells treated with 10 μ M stachydrine had a higher percentage of total apoptotic cells than the OGD group ($P < 0.01$; **Figure 6B**). Moreover, ROS was reduced in PC12 cells treated with 10 μ M stachydrine, as revealed by the flow cytometry ($P < 0.01$; **Figure 6C**).

As indicated by the measurement of IL-1 β and TNF- α levels in the supernatants of PC12 cells by ELISA, a decrease was observed in IL-1 β levels of OGD cells treated with 10 μ M stachydrine ($P < 0.05$; **Figure 7A**), and also in TNF- α levels ($P < 0.05$; **Figure 7B**). Real-time PCR assay showed that IL-1 β and TNF- α messenger RNA (mRNA) levels were up-regulated after OGD, which, however, were down-regulated after the treatment of stachydrine ($P < 0.05$; **Figures 7C, D**).

P65 and JAK2/STAT3 Signaling Pathway Suppressed in PC12 Cells After Oxygen-Glucose Deprivation

Since stachydrine was found to have an effect on anti-inflammatory factors of IL-1 β and TNF- α , we postulated that it could regulate P65. Indeed, our results showed that the phosphorylation of P65 and p-IkB were decreased in the stachydrine group in comparison with the OGD group ($P < 0.05$; **Figure 8A**). The expressions of p-STAT3 and p-JAK2 were increased in the OGD group in comparison with the control group, while stachydrine pretreatment suppressed the expressions of p-STAT3 and p-JAK2 proteins, as compared with the OGD group ($P < 0.05$; **Figure 8B**).

DISCUSSION

Over the years, a quite number of drugs have been used in treating stroke, some of them proved to be effectively neuroprotective. However, the currently used drugs are not satisfactory enough to control stroke. In this study, we tested whether stachydrine could inhibit excessive inflammation and oxidative stress *in vitro* and *in vivo*. The *in vivo* results showed that stachydrine improved the pathological changes in the hippocampus, thus preventing neuronal injury, which was similar to the previously reported finding (Miao et al., 2017). Although this finding is in agreement with our results in some ways, but the animal models were different. Another previous study demonstrated that stachydrine suppressed traumatic brain injury *via* anti-inflammatory mechanisms (Yu et al., 2018). The effects of stachydrine on immunity and inflammation have also been reported in recent studies (Cao et al., 2017; Meng et al., 2019).

In the present study, the infarcted areas were identified by TTC staining, and the neurological deficits scores were evaluated after 24 h-reperfusion injury. The treatment of 167.60 mM stachydrine significantly reduced the infarct volume and alleviated the neurological impairment, thereby resulting in lesser histological damage, as compared with the control group.

In view of which, we investigated the underlying therapeutic mechanism of stachydrine. It is well known that necrosis or apoptosis can aggravate ischemic damage. Ischemia-reperfusion injury is associated with inflammatory response and apoptosis, but the exact mechanism is unclear (Mestriner et al., 2013; Fluri et al., 2015; Hu et al., 2015). In the current study, the treatment of stachydrine significantly reduced the number of Tunel-positive cells after ischemia. Nissl staining suggested that the treatment

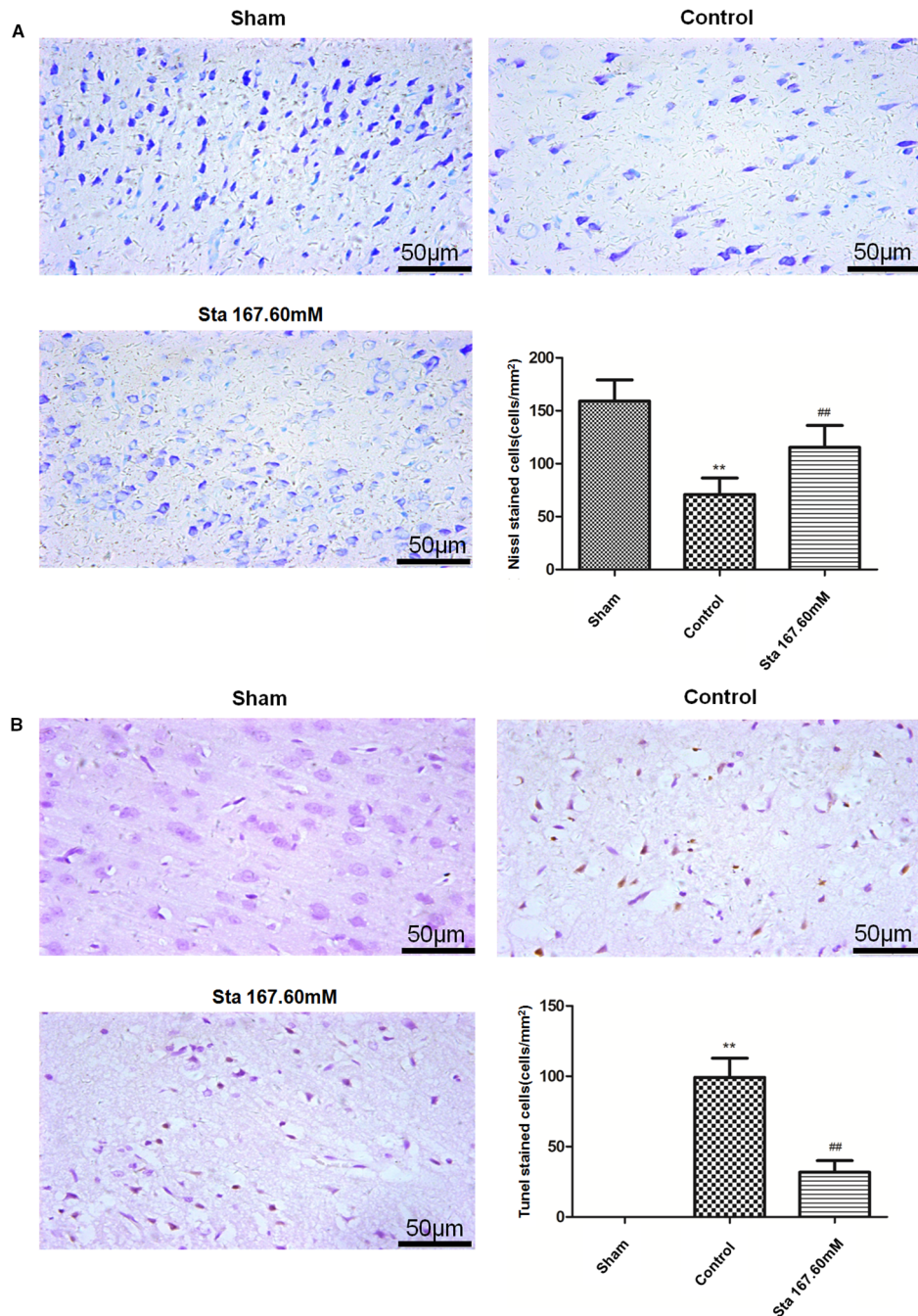


FIGURE 3 | Stachydrine ameliorates neurons apoptosis. Nissl staining and terminal deoxynucleotidyl transferase deoxyuridine triphosphate nick end labeling (TUNEL) staining used to examine the ischemia-reperfusion injury of neurons in cerebral cortex. **(A)** Pathological changes detected by Nissl staining, and the number of Nissl bodies counted; ** $P < 0.01$, sham group vs. control group; ## $P < 0.01$, stachydrine (167.60 mM) group vs. control group, $n = 4$. **(B)** TUNEL staining of apoptosis in brain and quantification of TUNEL-positive cells, examined; ** $P < 0.01$, sham group vs. control group, ## $P < 0.01$, stachydrine (167.60 mM) group vs. control group, $n = 3$.

alleviated neuronal injury and significantly increased the number of Nissl bodies. Although oxidative stress is characterized by imbalance between antioxidant defense mechanisms and free radicals, the mechanism of this imbalance is not clear in ischemic-induced apoptosis.

Under normal physiological conditions, the level of ROS is low in cells, and controlled by internal antioxidants without causing damage (Heiler et al., 2011; Wei et al., 2015; Momosaki et al., 2016; Andrienko et al., 2017). Since SOD and MDA are among the key biomarkers of oxidative stress, their levels directly

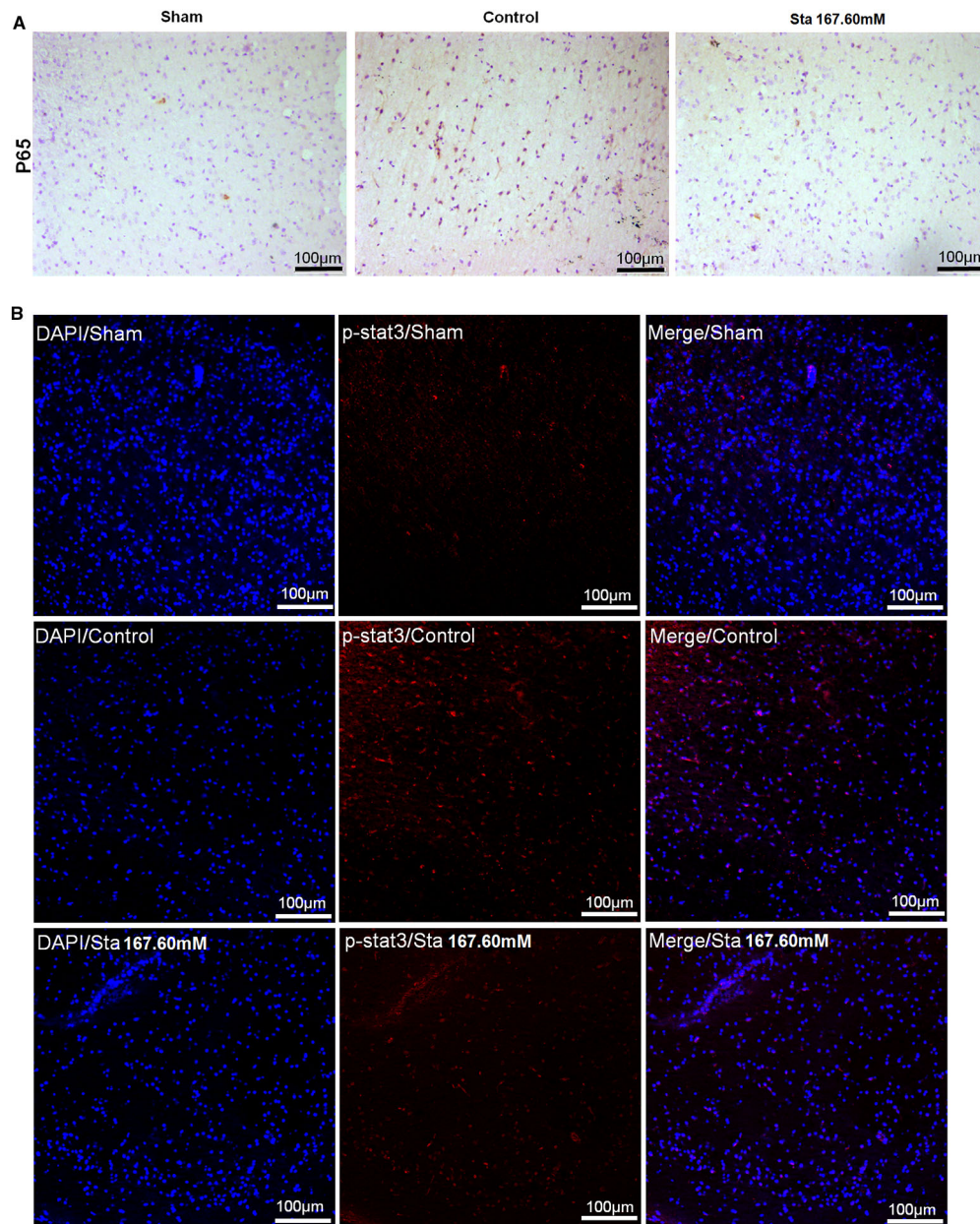


FIGURE 4 | Effect of stachydrine on P65 and p-STAT3 expression. **(A)** Immunohistochemistry staining used to analyze the expression of P65 protein levels after MCAO surgery in rat brain. **(B)** Immunofluorescence staining employed to observe the effect of p-STAT3 protein after ischemia reperfusion injury under confocal microscopy; stachydrine: 167.60 mM.

reflect the speed and degree of lipid peroxidation, and indirectly show the level of free radical scavengers (Krupinski et al., 2003; Yan et al., 2017). The reduced activity of SOD and enhanced production of MDA in brain tissue and serum of the control group implied that cerebral ischemia induced severe oxidative stress. In the current study, the effect of cerebral ischemia on the level of these oxidative biomarkers were reversed following the treatment of stachydrine. It therefore followed that the *in vivo*

therapeutic effect of stachydrine could be strongly related to the antioxidant effect. When compared with the OGD group, the stachydrine group showed a reduction in ROS levels of PC12 cells, as revealed by flow cytometry.

As one of the key factors involved in stroke development, tumor necrosis factor alpha (TNF- α) can interfere with the normal function of the brain, affecting the permeability of the blood-brain barrier, and impairing the transmission of glutamic

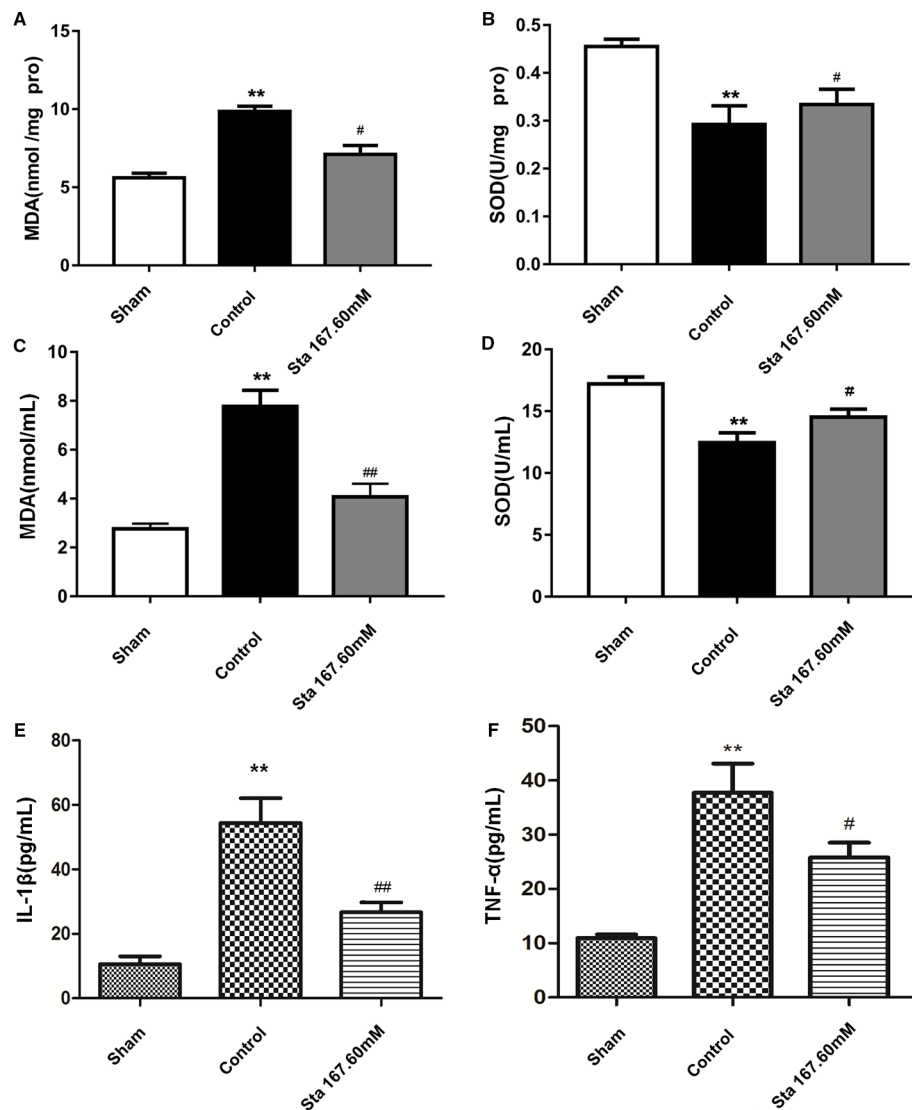


FIGURE 5 | Effect of stachydrine on the activities of superoxide dismutase (SOD) and the levels of malondialdehyde (MDA), interleukin (IL)-1 β , and TNF- α . MDA and SOD detection kits used to investigate the effect of stachydrine on the levels of malondialdehyde (MDA) and the activities of superoxide dismutase (SOD); ELISA used to detect the IL-1 β and TNF- α in serum collected at the time point of 24 h after reperfusion; effect of brain tissue (A) MDA, (B) SOD, effect of (C) MDA, (D) SOD, (E) IL-1 β , and (F) TNF- α in rat serum with stachydrine on cerebral ischemia reperfusion injury, examined; stachydrine: 167.60 mM; ** $P < 0.01$, sham group vs. control group, # $P < 0.05$, ## $P < 0.01$, stachydrine group vs. control group, $n = 3$.

acid as well as the plasticity of the synapse. Other studies have reported that TNF- α increased the density of the receptors associated with neurotoxicity (Stephenson et al., 2000; Gu et al., 2013). TNF- α could also be involved in the activation of multiple signaling pathways, such as P65 pathway and JAK2/STAT3 signaling pathway (Qi et al., 2012). IL-1 β regulating inflammatory responses as one of the cytokines involved in stroke development, the overexpression of IL-1 β could affect the functions of cognition and memory (Zhong et al., 2003). The current results showed that serum of TNF- α and IL-1 β was

decreased to varying degrees, indicating that the protective effect of stachydrine may be related to the suppression of overall inflammatory response.

JAK/STAT signaling was reported to play a key role in cerebral ischemia-reperfusion injury, remodeling ischemia reperfusion-induced brain dysfunction (Chang et al., 2014). JAK is a tyrosine kinase composed of four family members, JAK1, JAK2, JAK3, and JAK4; JAK1 and JAK2 are widely distributed in various tissues and cells (Kuang et al., 2014; Zhao et al., 2017). STAT could directly transmit signals into

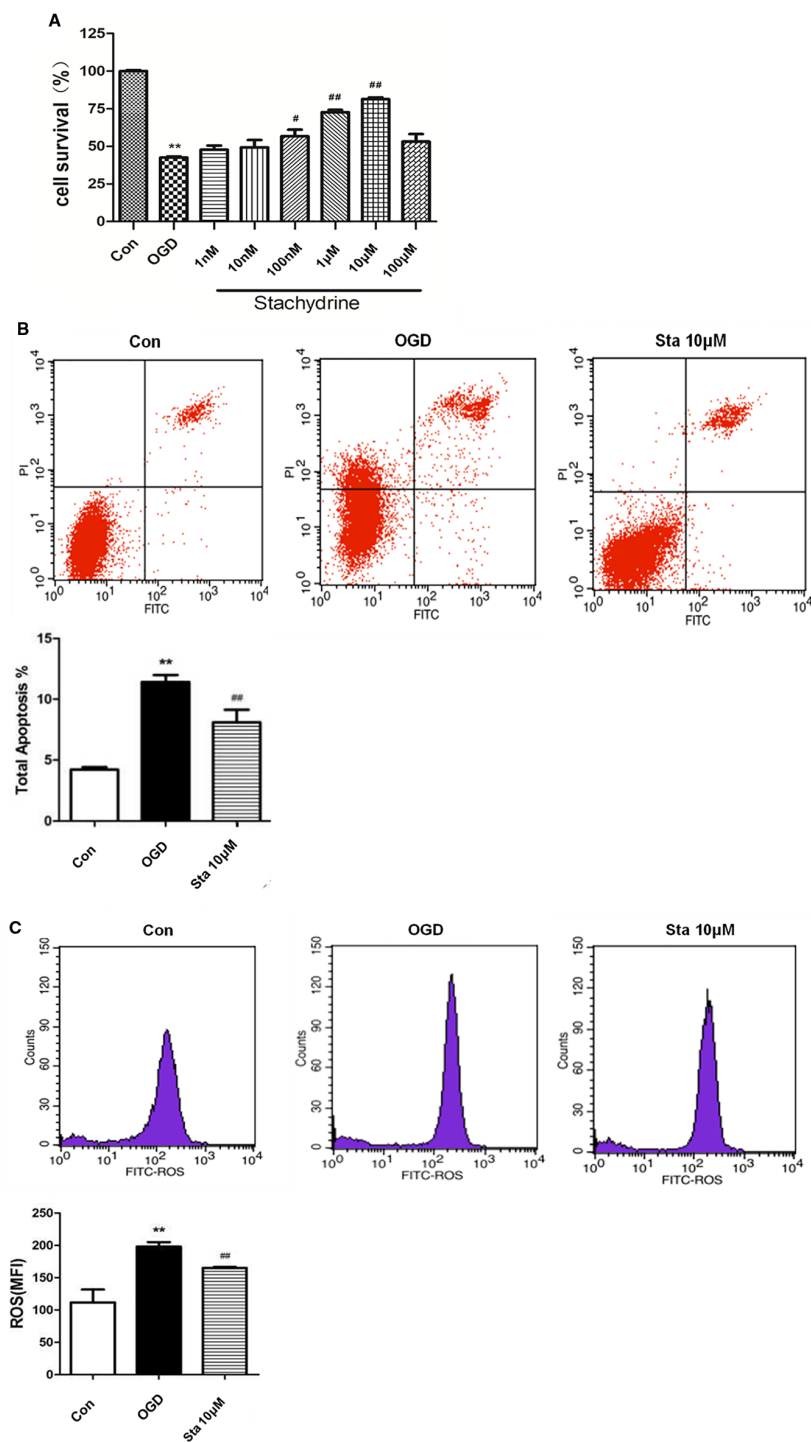


FIGURE 6 | Cell viability in PC12 cells after oxygen-glucose deprivation (OGD). **(A)** MTT used to test PC12 cells viability. **(B)** The flow cytometry results used to show the percentage of total apoptotic cells, as compared with OGD groups. **(C)** The flow cytometry results used to show the level of ROS in PC12 cells; stachydrine: 10 μ M; ** $P < 0.01$, control group vs. OGD group, # $P < 0.05$, ## $P < 0.01$, stachydrine group vs. OGD group, $n = 3$.

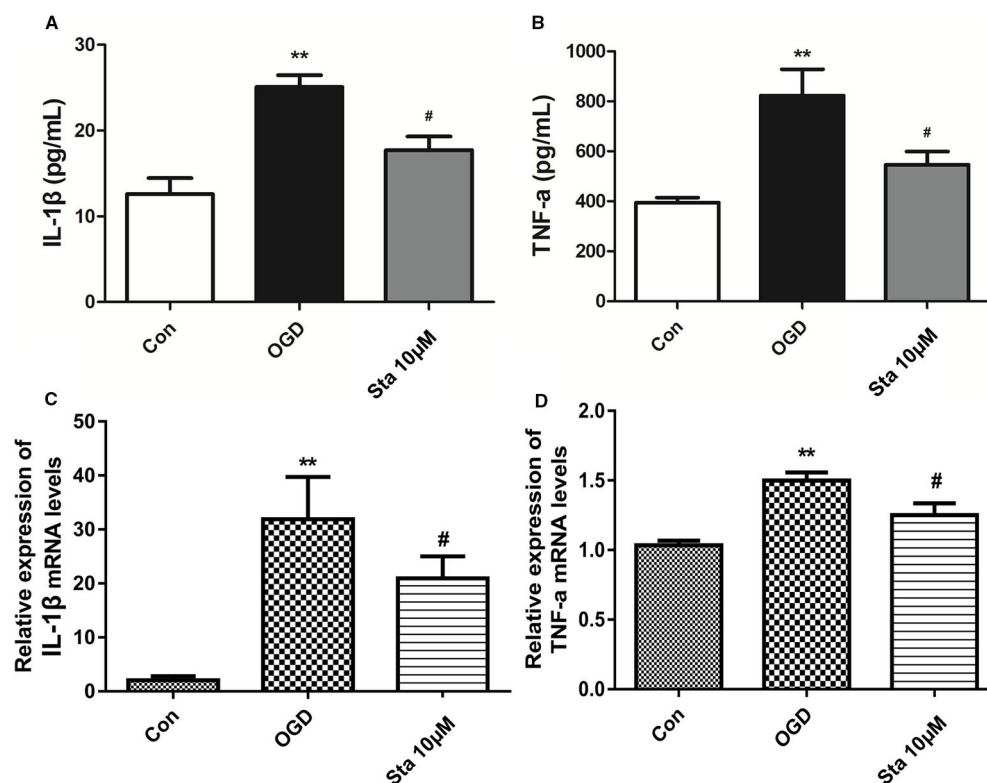


FIGURE 7 | Effect of stachydrine on interleukin (IL)-1 β and TNF- α levels in PC12 cells after oxygen-glucose deprivation (OGD). The level of IL-1 β and TNF- α in supernatants of PC12 cells measured by ELISA. **(A)** The IL-1 β and **(B)** TNF- α levels in supernatants from PC12 cells, examined. Real-time PCR used to evaluate the **(C)** IL-1 β and **(D)** TNF- α mRNA levels in PC12 cells; stachydrine: 10 μ M, ** P < 0.01, control group vs. OGD group, # P < 0.05, stachydrine group vs. OGD group, n = 3.

the nucleus (Alhadidi and Shah, 2017). STAT3 could regulate the expression of genes encoding proteins involved in inflammation (Murase et al., 2012). Some studies have shown that these proteins participate in disease mechanisms such as inflammation in neurodegenerative disorders, that the JAK2/STAT3 signaling pathway is activated after cerebral ischemia, which can increase the expression of HMGB1 and aggravate post-ischemic inflammatory responses (Saydmohammed et al., 2010; Wu et al., 2018; Zhou et al., 2019). The P65 pathway has been found to mediate the process of ischemic brain injury, hence a promising therapeutic target for ischemic stroke, and $\text{I}\kappa\text{B}$ as the master inhibitor of the P65 pathway, to have a degrading function during pathway activation (Hayden et al., 2008; Tu et al., 2014; Wang et al., 2017). A recent study has shown that linagliptin could suppress the expression of phosphorylated JAK2, phosphorylated STAT3 and P65 to confer neuroprotection (Marotta et al., 2011; Chang et al., 2018; Elbaz Eman et al., 2018). These results are similar to those which were found in the current study, which suggests the effects of inflammation reduction and neuroprotection.

In the current study, the treatment of stachydrine inhibited the P65 and JAK2/STAT3 signaling *in vitro*, as evidenced by the down-regulation of p-P65, p- $\text{I}\kappa\text{B}$, p-JAK2, and p-STAT3, which suggested that stachydrine could protect against OGD injury in PC12 cells.

In conclusion, the current study demonstrated that stachydrine reduced neurological dysfunction, neuronal injury and cerebral infarction in a rat model, which may be associated with the down-regulation of inflammatory processes. This indicates that the treatment of stachydrine could be beneficial to stroke patients, as it prevents reperfusion-induced injury due to its endogenous antioxidant capacity and anti-inflammatory effect.

The current study still had certain limitations. It was to study the protective effect of ischemia-reperfusion injury; thrombolysis was not involved as the main treatment; and stachydrine was mainly administered as an auxiliary treatment as part of the rehabilitation after thrombolysis. Further studies are advocated to design therapeutic agents based on stachydrine to control cerebral ischemia-reperfusion injury.

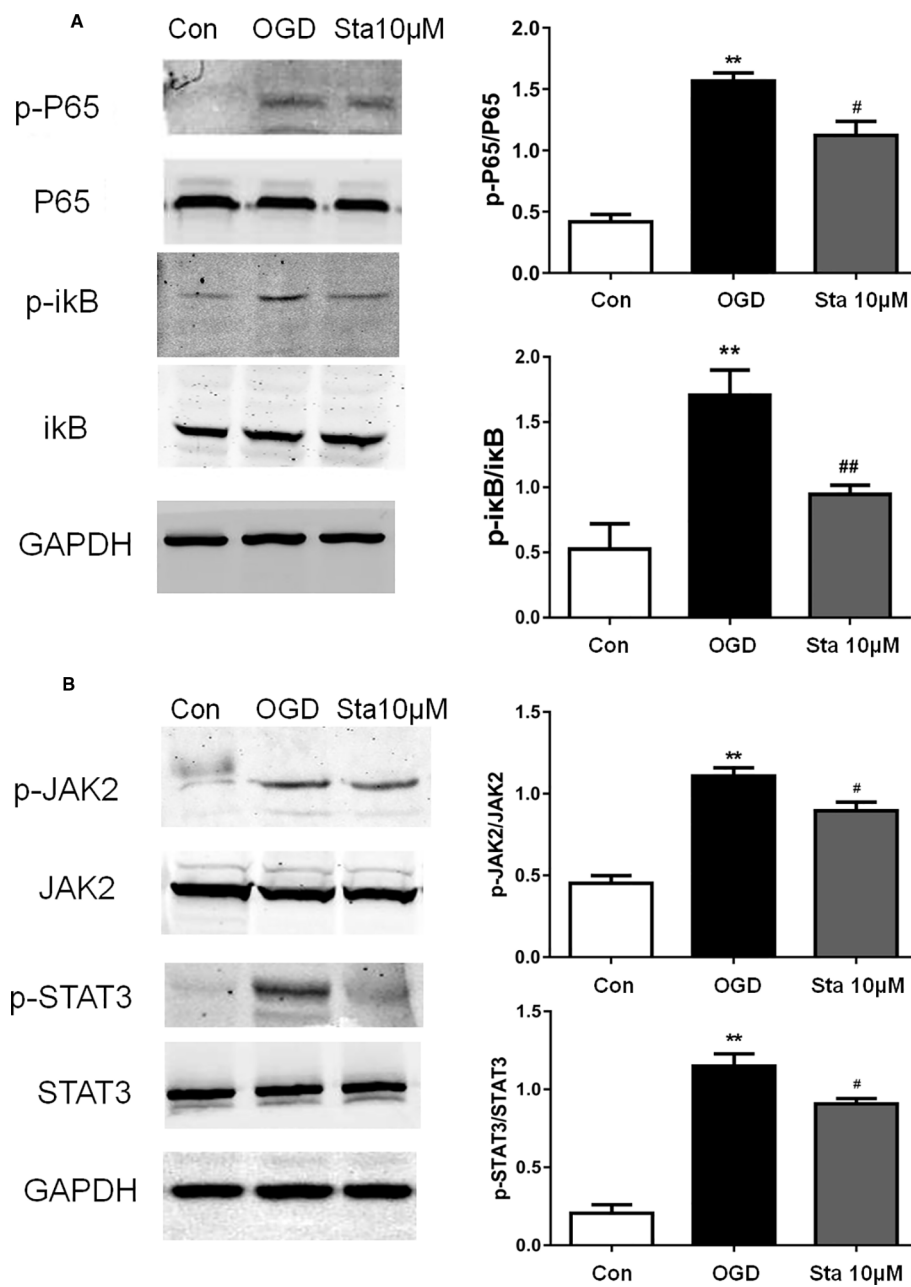


FIGURE 8 | Effect of stachydrine on P65 and JAK2/STAT3 signaling pathway in PC12 cells after oxygen-glucose deprivation (OGD). Western blot used to detect the protein levels in PC12 cells after OGD. **(A)** The expression of p-P65 and p-IkB levels in PC12 cells after oxygen and glucose deprivation, examined. **(B)** The expression of p-STAT3 and p-JAK2 levels in the OGD group, control group, and stachydrine group, examined; stachydrine: 10 µM; ** $P < 0.01$, control group vs. OGD group, # $P < 0.05$, ## $P < 0.01$, stachydrine group vs. OGD group, $n = 3$.

DATA AVAILABILITY STATEMENT

All datasets generated for this study are included in the article/**Supplementary Material**.

ETHICS STATEMENT

This study was carried out in accordance with the principles of the Basel Declaration and recommendations of the care and use of laboratory animals, Ethics Committee of Shanghai Pudong New Area People's Hospital. The protocol was approved by the Ethics Committee of Shanghai Pudong New Area People's Hospital.

AUTHOR CONTRIBUTIONS

JM conceived the study. LL and KH constructed the animal model. LS and WZ performed the cell experiments, LL analyzed the data and wrote the manuscript. JM and YQ revised the manuscript.

REFERENCES

- Alhadidi, Q., and Shah, Z. A. (2017). Cofilin Mediates LPS-induced microglial cell activation and associated neurotoxicity through activation of NF- κ B and JAK-STAT pathway. *Mol. Neurobiol.* 55, 1676–1691. doi: 10.1007/s12035-017-0432-7
- Andrienko, T. N., Pasdois, P., Pereira, G. C., Ovens, M. J., and Halestrap, A. P. (2017). The role of succinate and ROS in reperfusion injury-A critical appraisal. *J. Mol. Cell. Cardiol.* 110, 1–14. doi: 10.1016/j.yjmcc.2017.06.016
- Boehme, A. K., Esenwa, C., and Elkind, M. S. (2017). Stroke risk factors, genetics, and prevention. *Circ. Res.* 120 (3), 472–495. doi: 10.1161/CIRCRESAHA.116.308398
- Campos, F., Qin, T., Castillo, J., Seo, J. H., Arai, K., Lo, E. H., et al. (2013). Fingolimod reduces hemorrhagic transformation associated with delayed tissue plasminogen activator treatment in a mouse thromboembolic model. *Stroke* 44, 505–511. doi: 10.1161/STROKEAHA.112.679043
- Cao, T., Chen, H., Dong, Z., Xu, Y., Zhao, P., Guo, W., et al. (2017). Stachydrine protects against pressure overload-induced cardiac hypertrophy by suppressing autophagy. *Cell. Physiol. Biochem.* 42, 103–114. doi: 10.1159/000477119
- Chang, Y., Chen, K., Chen, C., Lin, M., Sun, Y., Lee, J., et al. (2014). SH2B1 β interacts with STAT3 and enhances fibroblast growth factor 1-induced gene expression during neuronal differentiation. *Mol. Cell Biol.* 34, 1003–1019. doi: 10.1128/MCB.00940-13
- Chang, R., Song, L., Xu, Y., Wu, Y., Dai, C., Wang, X., et al. (2018). Loss of Wwox drives metastasis in triple-negative breast cancer by JAK2/STAT3 axis. *Nat. Commun.* 9, 3486. doi: 10.1038/s41467-018-05852-8
- Chen, C. L. H., Young, S. H. Y., Gan, H. H., Singh, R., Lao, A. Y., Baroque, A. C., et al. (2013). Chinese medicine neuroaid efficacy on stroke recovery: a double-blind, placebo-controlled, randomized study. *Stroke* 44 (8), 2093–2100. doi: 10.1161/STROKEAHA.113.002055
- Elbaz Eman, M., Senousy Mahmoud, A., El-Tanbouly Dalia, M., and Sayed Rabab, H. (2018). Neuroprotective effect of linagliptin against cuprizone-induced demyelination and behavioural dysfunction in mice: a pivotal role of AMPK/SIRT1 and JAK2/STAT3/NF- κ B signalling pathway modulation. *Toxicol. Appl. Pharmacol.* 352, 153–161. doi: 10.1016/j.taap.2018.05.035
- Fluri, F., Schuhmann, M. K., and Kleinschnitz, C. (2015). Animal models of ischemic stroke and their application in clinical research. *Drug des. Dev. Ther.* 9, 3445–3454. doi: 10.2147/DDDT.S56071
- Go, A. S., Mozaffarian, D., Roger, V. L., Benjamin, E. J., Berry, J. D., Borden, W. B., et al. (2013). Executive summary: heart disease and stroke statistics-2013 update: a report from the American Heart Association. *Circulation* 127 (1), 143–152. doi: 10.1161/CIR.0b013e318282ab8f

FUNDING

This work was supported by the Project of Shanghai University of Medicine & Health Sciences Cooperative Innovation Project (Grant No. SPCI-18-13-001); Important Weak Subject Construction Project of Pudong Health and Family Planning Commission of Shanghai (Grant No. PWZbr2017-16).

SUPPLEMENTARY MATERIAL

The Supplementary Material for this article can be found online at: <https://www.frontiersin.org/articles/10.3389/fphar.2020.00064/full#supplementary-material>

FIGURE S1 | Western blot results of p65, p-p65, κ B, p- κ B and GAPDH.

FIGURE S2 | Western blot results of JAK2, p-JAK2, STAT3, p-STAT3 and GAPDH.

- Gu, L., Wu, G., Long, J., Su, L., Yan, Y., Chen, Q., et al. (2013). The role of TNF- α 308G > A polymorphism in the risk for ischemic stroke. *Am. J. Med. Sci.* 345 (3), 227–233. doi: 10.1097/MAJ.0b013e31825f92da
- Hayden, M. S., and Ghosh, S. (2008). Shared principles in NF- κ B signaling. *Cell* 132 (3), 344–362. doi: 10.1016/j.cell.2008.01.020
- Heiler, P. M., Langhauser, F. L., Wetterling, F., Ansar, S., Grudzinski, S., Konstandin, S., et al. (2011). Chemical shift sodium imaging in a mouse model of thromboembolic stroke at 9.4T. *J. Magn. Reson. Imaging.* 34, 935–940. doi: 10.1002/jmri.22700
- Hu, X., Leak, R. K., Shi, Y., Suenaga, J., Gao, Y., Zheng, P., et al. (2015). Microglial and macrophage polarization-new prospects for brain repair. *Nat. Rev. Neurol.* 11 (1), 56–64. doi: 10.1038/nrneurol.2014.207
- Krupinski, J., Slevin, M., Marti, E., Catena, E., Rubio, F., and Gaffney, J. (2003). Time-course phosphorylation of the mitogen activated protein (MAP) kinase group of signalling proteins and related molecules following middle cerebral artery occlusion (MCAO) in rats. *Neuropathol. Appl. Neurobiol.* 29 (2), 144–158. doi: 10.1046/j.1365-2990.2003.00454.x
- Kuang, X., Wang, L. F., Yu, L., Li, Y., Wang, Y., He, Q., et al. (2014). Ligustilide ameliorates neuroinflammation and brain injury in focal cerebral ischemia/reperfusion rats: involvement of inhibition of TLR4/peroxiredoxin 6 signaling. *Free Radic. Biol. Med.* 71, 165–175. doi: 10.1016/j.freeradbiomed.2014.03.028
- Leech, T., Chattipakorn, N., and Chattipakorn, S. C. (2019). The beneficial roles of metformin on the brain with cerebral ischaemia/reperfusion injury. *Pharmacol. Res.* 146, 104261. doi: 10.1016/j.phrs.2019.104261
- Liu Xin, H., Pan Li, L., and Zhu Yi, Z. (2012). Active chemical compounds of traditional Chinese medicine Herba Leonuri: implications for cardiovascular diseases. *Clin. Exp. Pharmacol. Physiol.* 39, 274–282. doi: 10.1111/j.1440-1681.2011.05630.x
- Loh, K. P., Huang, S. H., Tan, B. K., and Zhu, Y. Z. (2009). Cerebral protection of purified Herba Leonuri extract on middle cerebral artery occluded rats. *J. Ethnopharmacol.* 125, 337–343. doi: 10.1016/j.jep.2009.05.025
- Loh, K. P., Qi, J., Tan, B. K. H., Liu, X., Wei, B., and Zhu, Y. (2010). Leonurine protects middle cerebral artery occluded rats through antioxidant effect and regulation of mitochondrial function. *Stroke* 41 (11), 2661–2668. doi: 10.1161/STROKEAHA.110.589895
- Longa, E. Z., Weinstein, P. R., Carlson, S., and Cummins, R. (1989). Reversible middle cerebral artery occlusion without craniectomy in rats. *Stroke* 20 (1), 84–91. doi: 10.1161/01.STR.20.1.84
- Marotta, L. L. C., Almendro, V., Marusyk, A., Shipitsin, M., Schemme, J., Walker, S. R., et al. (2011). The JAK2/STAT3 signaling pathway is required for growth of CD44+CD24– stem cell-like breast cancer cells in human tumors. *J. Clin. Invest.* 121 (7), 2723–2735. doi: 10.1172/JCI44745

- Meng, J., Zhou, C., Zhang, W., Wang, W., He, B., Hu, B., et al. (2019). Stachydrine prevents LPS-induced bone loss by inhibiting osteoclastogenesis via NF- κ B and Akt signalling. *J. Cell. Mol. Med.* 23 (10), 6730–6743. doi: 10.1111/jcmm.14551
- Mestriner, R. G., Miguel, P. M., Bagatini, P. B., Saur, L., Boisserand, L. S. B., Baptista, P. P. A., et al. (2013). Behavior outcome after ischemic and hemorrhagic stroke, with similar brain damage, in rats. *Behav. Brain Res.* 244, 82–89. doi: 10.1016/j.bbr.2013.02.001
- Miao, M., Wang, T., Lou, X., Ming, B., Xi, P., Liu, B., et al. (2017). The influence of stachydrine hydrochloride on the reperfusion model of mice with repetitive cerebral ischemia. *Saudi. J. Biol. Sci.* 24 (3), 658–663. doi: 10.1016/j.sjbs.2017.01.039
- Momosaki, R., Yasunaga, H., Kakuda, W., Matsui, H., Fushimi, K., and Abo, M. (2016). Very early versus delayed rehabilitation for acute ischemic stroke patients with intravenous recombinant tissue plasminogen activator: a nationwide retrospective cohort study. *Cerebrovascular. Dis.* 42, 41–48. doi: 10.1159/000444720
- Moskowitz, M. A., Lo, E. H., and Iadecola, C. (2010). The Science of stroke: mechanisms in search of treatments. *Neuron* 67, 181–198. doi: 10.1016/j.neuron.2010.07.002
- Murase, S., Kim, E., Lin, L., Hoffman, D. A., and McKay, R. D. (2012). Loss of signal transducer and activator of transcription 3 (STAT3) signaling during elevated activity causes vulnerability in hippocampal neurons. *J. Neurosci.* 32, 15511–15520. doi: 10.1523/JNEUROSCI.2940-12.2012
- Qi, H., Han, Y., and Rong, J. (2012). Potential roles of PI3K/Akt and Nrf2-Keap1 pathways in regulating hormesis of Z-ligustilide in PC12 cells against oxygen and glucose deprivation. *Neuropharmacology* 62, 1659–1670. doi: 10.1016/j.neuropharm.2011.11.012
- Saydmohammed, M., Joseph, D., and Syed, V. (2010). Curcumin suppresses constitutive activation of STAT-3 by up-regulating protein inhibitor of activated STAT-3 (PIAS-3) in ovarian and endometrial cancer cells. *J. Cell Biochem.* 110, 447–456. doi: 10.1002/jcb.22558
- Servillo, L., D'Onofrio, N., Longobardi, L., Sirangelo, I., Giovane, A., Cautela, D., et al. (2013). Stachydrine ameliorates high-glucose induced endothelial cell senescence and SIRT1 downregulation. *J. Cell Biochem.* 114 (11), 2522–2530. doi: 10.1002/jcb.24598
- Stephenson, D., Yin, T., Smalstig, E. B., Hsu, M. A., Panetta, J., Little, S., et al. (2000). Transcription factor nuclear factor-kappa B is activated in neurons after focal cerebral ischemia. *J. Cereb. Blood Flow Metab.* 20 (3), 592–603. doi: 10.1097/00004647-200003000-00017
- Tu, X. K., Yang, W. Z., Chen, J. P., Chen, Y., Ouyang, L. Q., Xu, Y. C., et al. (2014). Curcumin inhibits TLR2/4-NF- κ B signaling pathway and attenuates brain damage in permanent focal cerebral ischemia in rats. *Inflammation* 37, 1544–1551. doi: 10.1007/s10753-014-9881-6
- Wang, M., Shu, Z. J., Wang, Y., and Peng, W. (2017). Stachydrine hydrochloride inhibits proliferation and induces apoptosis of breast cancer cells via inhibition of Akt and ERK pathways. *Am. J. Transl. Res.* 9, 1834–1844.
- Wang, G., Lan, R., Zhen, X., Zhang, W., Xiang, J., and Cai, D. (2014). An-Gong-Niu-Huang Wan protects against cerebral ischemia induced apoptosis in rats: up-regulation of Bcl-2 and down-regulation of Bax and caspase-3. *J. Ethnopharmacol.* 154 (1), 156–162. doi: 10.1016/j.jep.2014.03.057
- Wei, X., Qi, Y., Zhang, X., Gu, X., Cai, H., Yang, J., et al. (2015). ROS act as an upstream signal to mediate cadmium-induced mitophagy in mouse brain. *NeuroToxicology* 46, 19–24. doi: 10.1016/j.neuro.2014.11.007
- Wu, Y., Xu, J., Xu, J., Zheng, W., Chen, Q., and Jiao, D. (2018). Study on the mechanism of JAK2/STAT3 signaling pathway-mediated inflammatory reaction after cerebral ischemia. *Mol. Med. Rep.* 17 (4), 5007–5012. doi: 10.3892/mmr.2018.8477
- Xie, X., Zhang, Z., Wang, X., Luo, Z., Lai, B., Xiao, L., et al. (2018). Stachydrine protects eNOS uncoupling and ameliorates endothelial dysfunction induced by homocysteine. *Mol. Med.* 24, 10. doi: 10.1186/s10020-018-0010-0
- Yan, R., Wang, S. J., Yao, G. T., Liu, Z., and Xiao, N. (2017). The protective effect and its mechanism of 3-n-butylphthalide pretreatment on cerebral ischemia reperfusion injury in rats. *Eur. Rev. Med. Pharmacol. Sci.* 21 (22), 5275–5282. doi: 10.26355
- Yu, N., Hu, S., and Hao, Z. (2018). Beneficial effect of stachydrine on the traumatic brain injury induced neurodegeneration by attenuating the expressions of Akt/mTOR/PI3K and TLR4/NF- κ B pathway. *Transl. Neurosci.* 9, 175–182. doi: 10.1515/tnsci-2018-0026
- Zhang, Y., Chen, J., Li, F., Li, D., Xiong, Q., Lin, Y., et al. (2012). A pentapeptide monocyte locomotion inhibitory factor protects brain ischemia injury by targeting the eEF1A1/endothelial nitric oxide synthase pathway. *Stroke* 43 (10), 2764–2773. doi: 10.1161/STROKEAHA.112.657908
- Zhang, R., Liu, Z., Yang, D., Zhang, X., Sun, H., and Xiao, W. (2018). Phytochemistry and pharmacology of the genus Leonurus: the herb to benefit the mothers and more. *Phytochemistry* 147, 167–183. doi: 10.1016/j.phytochem.2017.12.016
- Zhao, L., Wu, D., Sang, M., Xu, Y., Liu, Z., and Wu, Q. (2017). Stachydrine ameliorates isoproterenol-induced cardiac hypertrophy and fibrosis by suppressing inflammation and oxidative stress through inhibiting NF- κ B and JAK/STAT signaling pathways in rats. *Int. Immunopharmacol.* 48, 102–109. doi: 10.1016/j.intimp.2017.05.002
- Zhong, Z., Li, G., Li, H., Zhao, W., Tian, Y., Li, D., et al. (2003). Expressions of TNF-alpha and IL-1beta in human ischemic brain tissues. *Xi Bao Yu Fen Zi Mian Yi Xue Za Zhi* 19 (4), 349–350.
- Zhou, K., Chen, J., Wu, J., Wu, Q., Jia, C., Xu, Y., et al. (2019). Atractylenolide III ameliorates cerebral ischemic injury and neuroinflammation associated with inhibiting JAK2/STAT3 Drp1-dependent mitochondrial fission in microglia. *Phytomedicine* 59, 152922. doi: 10.1016/j.phymed.2019.152922
- Zhu, Q., Zhang, Y., Liu, Y., Cheng, H., Wang, J., Zhang, Y., et al. (2016). MLIF Alleviates SH-SY5Y Neuroblastoma Injury Induced by Oxygen-Glucose Deprivation by Targeting Eukaryotic Translation Elongation Factor 1A2. *PloS One* 11, e0149965. doi: 10.1371/journal.pone.0149965

Conflict of Interest: The authors declare that the research was conducted in the absence of any commercial or financial relationships that could be construed as a potential conflict of interest.

Copyright © 2020 Li, Sun, Qiu, Zhu, Hu and Mao. This is an open-access article distributed under the terms of the Creative Commons Attribution License (CC BY). The use, distribution or reproduction in other forums is permitted, provided the original author(s) and the copyright owner(s) are credited and that the original publication in this journal is cited, in accordance with accepted academic practice. No use, distribution or reproduction is permitted which does not comply with these terms.



OPEN ACCESS

Edited by:

Ismail Laher,
University of British Columbia, Canada

Reviewed by:

Simone Carradori,
University "G. d'Annunzio" of
Chieti-Pescara, Italy
Hai Zhang,
Shanghai First Maternity and
Infant Hospital, China
Devin William McBride,
University of Texas Health Science
Center at Houston, United States
Siavash Parvardeh,
Shahid Beheshti University of
Medical Sciences, Iran

***Correspondence:**

Yongfang Yuan
nmxyyf@126.com

Specialty section:

This article was submitted to
Ethnopharmacology,
a section of the journal
Frontiers in Pharmacology

Received: 14 May 2019

Accepted: 19 March 2020

Published: 15 April 2020

Citation:

Wang J, Mao J, Wang R, Li S, Wu B
and Yuan Y (2020) Kaempferol
Protects Against Cerebral Ischemia
Reperfusion Injury Through Intervening
Oxidative and Inflammatory
Stress Induced Apoptosis.
Front. Pharmacol. 11:424.
doi: 10.3389/fphar.2020.00424

Kaempferol Protects Against Cerebral Ischemia Reperfusion Injury Through Intervening Oxidative and Inflammatory Stress Induced Apoptosis

Jing Wang¹, Junqin Mao², Rong Wang¹, Shengnan Li¹, Bin Wu¹ and Yongfang Yuan^{1*}

¹ Department of Pharmacy, Shanghai 9th People's Hospital, Shanghai Jiao Tong University School of Medicine, Shanghai, China, ² Department of Pharmacy, Shanghai Pudong New Area People's Hospital, Shanghai, China

The aim of this research is to investigate the potential neuro-protective effect of kaempferol which with anti-oxidant, anti-inflammatory, and immune modulatory properties, and understand the effect of kaempferol on reducing cerebral ischemia reperfusion (I/R) injury *in vivo*. Male adult Sprague Dawley (SD) rats were pretreated with kaempferol for one week *via* gavage before cerebral I/R injury operation. We found that kaempferol treatment can reduce the cerebral infarct volume and neurological score after cerebral I/R. Rats were sacrificed after 24 h reperfusion. We observed that kaempferol improved the arrangement, distribution, and morphological structure of neurons, as well as attenuated cell apoptosis in brain tissue *via* hematoxylin and eosin (H&E) staining, Nissl staining and TUNEL staining. Superoxide dismutase (SOD), malondialdehyde (MDA), and glutathione peroxidase (GSH) kit analysis, enzyme-linked immunosorbent (ELISA) assay, real-time PCR, Western blot, and immunohistochemical examination indicated that kaempferol mitigated oxidative and inflammatory stress *via* regulating the expression of proteins, p-Akt, p-GSK-3 β , nuclear factor erythroid2-related factor 2 (Nrf-2), and p-NF- κ B during cerebral I/R, thus increasing the activity of SOD and GSH, meanwhile decreasing the content of MDA in serum and brain tissue, as well as restoring the expression levels of tumor necrosis factor alpha (TNF- α), interleukin-1 β (IL-1 β), and IL-6 *in vivo*. Taken together, this study suggested that kaempferol protects against cerebral I/R induced brain damage. The possible mechanism is related with inhibiting oxidative and inflammatory stress induced apoptosis.

Keywords: kaempferol, cerebral ischemia reperfusion, oxidative stress, inflammation, Nrf-2, NF- κ B

INTRODUCTION

Ischemia and hemorrhagic stroke are common cerebrovascular sicknesses, with proportion of 87 and 13%, respectively (Broussalis et al., 2012; Xue et al., 2017). A long period of ischemia results in the shortage of oxygen and glucose which destroy the cellular homeostasis. Theoretically, restoring blood flow is necessary. However, reperfusion can aggravate brain damage (Zhang et al., 2013). Cerebral ischemia reperfusion (I/R) leads to the imbalance of brain energy, which is characterized by an insufficient oxygen supply and restoration of blood flow, meanwhile involves complex and multi-factorial mechanism, and further causes cerebral injury including neuro-inflammation, neuronal damage, and cerebral edema (Zhou et al., 2017). Due to narrow therapeutic time window, the options for acute ischemia remain very limited, and few neuroprotective treatments have been successfully developed to prevent ischemic injury (Li Q. et al., 2019). I/R results in irreversible damage to brain tissue as well as subsequent disability and a high morbidity to patients. Thus, finding more safe and effective therapeutic agent is becoming more pressing (Ma et al., 2015; Yu et al., 2016). During I/R injury, the excessive production of reactive oxygen species and reactive nitrogen species, excitatory amino acid toxicity, and inflammatory reaction are implicated in the neuronal damage (Li Z. et al., 2019).

During I/R injury, oxidative stress and a mediator of the secondary injury process that involving inflammation and apoptosis are considered as crucial roles (Xie et al., 2017; Fu et al., 2018). Thus, improving the expression of the endogenous antioxidant proteins may be an effective approach to reduce cell and brain tissue injury. Research evidence indicates that there is a close relationship between endogenous antioxidant systems and nuclear factor erythroid2-related factor 2 (Nrf-2) (Danilov et al., 2009). Nrf-2 is regarded as an important transcription factor that through binding to antioxidant response elements (AREs) induces the transcription of phase II detoxifying anti-oxidant genes (Wang R. et al., 2018). Present studies demonstrate that GSK, a serine/threonine protein kinase, plays an important role in regulating and degrading Nrf-2 in a Keap1-independent manner (Rada et al., 2011). Moreover, activation of AKT stimulates phosphorylation of GSK-3 β which is involved in neuroprotective effect against transient forebrain ischemia. Nuclear factor-kappa B (NF- κ B) is a significant transcription factor that regulates inflammation (Qi et al., 2012). A large number of inflammatory factors, including tumor necrosis factor alpha (TNF- α), interleukin-1 β (IL-1 β), and IL-6, can be regulated by the activation of NF- κ B (Umesalma and Sudhandiran, 2010).

Recent study showed that NF- κ B is activated in cerebral vascular endothelial cells after cerebral ischemia, which triggers a dramatically increasing production of inflammatory cytokines, leading to an inflammatory cascade reaction and aggravating brain damage (Shi et al., 2014).

Kaempferol (3,4',5,7-tetrahydroxyflavone) is one of the widest distributed flavonoids, and abundant in many kinds of

traditional Chinese medicine, foods, and nutraceuticals. It has reported that kaempferol can have beneficial and/or protective effects against several diseases, due to its anti-oxidant, anti-inflammatory, and immune modulatory properties *in vitro* and *in vivo* (Wang J. et al., 2018). Previous studies exhibited that kaempferole quips with various beneficial pharmacology effects, such as alleviating gamma radiation induced injury by inhibiting oxidative stress and modulating apoptotic molecules cytochrome c, Prx-5, caspase 9, and caspase 3 expression, attenuating the anoxia/reoxygenation-induced cardiomyocyte apoptosis through SIRT1 mediated mitochondrial pathway (Guo et al., 2015) and inhibiting pancreatic cancer cell growth and migration *via* blocking EGFR-related pathway (Lee and Ki, 2016). Except that, kaempferol was reported can selectively inhibit human monoamine oxidases-A (MAO-A) in brain mitochondrial. The role of MAOs is to catalyze the α -carbon two-electron oxidation of amine substrates in the peripheral tissues and brain (Gidaro et al., 2016). So far, there are still lack of reports about the neuroprotective effect and possible mechanisms of kaempferol on I/R *in vivo*. Therefore, the present study aims to investigate whether kaempferol with neuroprotective effect and understand the potential mechanisms.

METHODS AND MATERIALS

Animals and Reagents

Male adult Sprague Dawley (SD) rats (body weight, 240–260g) were all purchased from Changzhou Cavens Experimental Animal Co. (Jiangsu, China). All rats were managed under specific-pathogen-free (SPF) conditions and used according to the Guidelines of National Institutes of Health on the Care and Use of Laboratory Animals. This research was approved by the Scientific Investigation Board of the Second Military Medical University (Number: SYXK2017-0004). Kaempferol (purity \geq 98%) was purchased from Dalian Meilun Biology Technology Co. (Dalian, China). Kaempferol was diluted with 0.5% sodium carboxymethylcellulose (CMC-Na) to different concentrations. 2,3,5-triphenyltetrazolium chloride (TTC) was purchased from Sigma-Aldrich Co. (St. Louis, MO, USA); The superoxide dismutase (SOD), malondialdehyde (MDA), and glutathione peroxidase (GSH) assay kit were purchased from Nanjing Jiancheng Bioengineering Institute (Nanjing, China).

Experimental Group and Drug Administration

Firstly, in order to observe the protective effect of kaempferol in rat I/R injury, rats were randomly divided into five groups and drug was administrated continuously one week before operation: Sham group (5 rats; 0.5% CMC-Na; intragastrically administrated; dosing one time per day for one week; expose left common, external and internal artery, but no blockage), I/R group (5 rats; 0.5% CMC-Na; intragastrically administrated; dosing one time per day for one week; ischemia for 2 h and

reperfusion for 24 h), three Kaempferol treatment groups (each group 5 rats; 1.75, 3.49, 6.99 mM, respectively; intragastrically administrated; 1 ml/kg weight; dosing one time per day for one week; ischemia for 2 h and reperfusion for 24h).

Secondly, to understand kaempferol neuroprotective effect, rats were randomly divided into three groups and 10 rats in each groups: Sham group, I/R group and 6.99 mM kaempferol treatment group. The 6.99 mM kaempferol treatment group was intragastrically administrated 1 ml/kg weight, continuous one week, prior to ischemia 2 h and reperfusion 24 h operation. The Sham group and I/R group were administrated with equal volume of 0.5% CMC-Na solution. After operation, there was one rat mortality in 6.99 mM kaempferol treatment group. 5 rats brain tissues in sham group and I/R group, 4 rats brain tissues in kaempferol treatment group were fixed with 4% formaldehyde, meanwhile 5 rats brain tissues in each groups were homogenized. Whole blood samples were collected from rat aortaventrals without anticoagulant except mortality rat. H&E stain, Nissl stain, TUNEL stain, and immunohistochemical examination were share the same tissue samples which were fixed.

Cerebral I/R Model and Neurological Score

I/R rat model was operated according to Longa's methods with minor revisable (Bösel et al., 2005). Rats were anesthetized with 4% isoflurane (4% for anesthesia induction; 2% for anesthesia maintenance, 3 ml/kg). Then carefully exposed the left common carotid artery (CCA), internal carotid artery (ICA), and external carotid artery (ECA). The left CCA and the ECA were blocked with micro-vascular aneurysm clips, followed by occluding the middle cerebral artery (MCA) by inserting a nylon filament (Product No:2634-100; Beijing Sunbio Biotech, Beijing, China) coated through the ICA. Finally, the filament was slowly removed from ICA to achieve reperfusion 2 h after occlusion. Then rats continued to be monitored in the same SPF conditions. Rats in Sham group received the same procedures except filament inserted to the MCA. Neurological score was tested when rats revived after 2 h ischemia and removed filament. 1–3 score considered successful operation and included in the following experiment.

After 24 h reperfusion, the neurological score of each rat was evaluated by Longa's method (Longa et al., 1989) of a 5-point scale: 0, no neurological deficit; 1, the contralateral torso and forelimb may not be thoroughly stretched; 2, when the tail was held, the animal may be turned to the ipsilateral side; 3, no spontaneous motor activity or falling to the left; 4, unable to walk or loss of consciousness. Researcher was blinded to the different treatments.

Assessment of Cerebral Infarct Volume

Followed the neurological score evaluation, the rats were sacrificed, and the brains were carefully collected, sliced into five coronal sections, with each 2 mm thick. The slices were placed in 2% TTC solution, and incubated at room temperature for 15 min. Then the brain slices were fixed in 4% formaldehyde at 4°C for 24 h. Slices images were captured. The infarct volumes were calculated *via* image analysis software (Image-Pro Plus, Version 6.0). Normal brain section was stained to red and the infarct section was stained to white. The infarct volume percentage was measured by the following equation:

$$\text{Infarct volume (\%)} = [(\text{normal hemisphere volume} - \text{non-infarct volume of the infarct side}) / \text{normal hemisphere volume}] \times 100\%$$

Biochemical Parameters Analysis

Rats were anesthetized after 24 h reperfusion, and whole blood samples were collected from rat aortaventrals without anticoagulant. Whole blood samples were stored at room temperature for 1 h, then centrifuged at 1,000×g for 30 min. Brain tissues were dissected, penumbra to the ischemia core area was collected (Figure S3), and 10% tissue homogenates were prepared. The supernatant was used to determine the level of SOD, MDA, and GSH, according to the protocols provided by the manufacturer (Nanjing Jiancheng Bioengineering Institute, Nanjing, China).

Enzyme-Linked Immunosorbent Assay (ELISA)

Rats were anesthetized, whole blood sample was obtained from rat aortaventrals, then centrifuged at 1,000×g for 30min. After centrifugal operation, serum supernatant samples were collected. Meanwhile, brain tissues were dissected and homogenized. The expression levels of TNF- α , IL-1 β , and IL-6 in the serum and brain tissue were determined according to TNF- α , IL-1 β , and IL-6 ELISA kit (R&D Systems, Minneapolis, USA) instructions, respectively.

Real-Time PCR Assay

Brain tissues were dissected and homogenized using a TL2010 grinding instrument (DHS Life Science& Technology, Beijing, China). Total RNA was extracted using the TRIzol reagent (Invitrogen, Carlsbad, CA, USA) and determined the concentration and purity through Nanodrop 2000 spectrophotometer (Thermo Fisher Scientific, Gene Company Limited, Shanghai, China). Then, the total RNA was reverse transcribed by the PrimeScript™ RT Master Mix reagent kit (Takara, Shiga, Japan). TNF- α , IL-1 β , IL-6, and GAPDH mRNA

TABLE 1 | Gene primers sequences for mRNA amplification.

Gene name	Forward(5'-3')	Reverse(5'-3')	Product length
TNF- α	TCAGCCTCTTCTCATTCTGC	TTGGTGGTTTGCTACGACGTG	179
IL-1 β	CAGCAATGGTCGGGAC	TAGGTAAGTGGTTGCCT	118
IL-6	CCGGAGAGGAGACTTCAGA	GGTCTGGGCCATAGAAGCTGA	232
GAPDH	CCAGCCAGCAAGGATACTG	GGTATTCGAGAAGGGAGGGC	256

expression level were detected by the SYBR Premix Ex Taq™ kit (Takara, Japan). cDNA was amplified using a three-step program. Ct values were used to calculate the mRNA expression level. The primers were synthesized by Sangon Biotech Co. Ltd (Shanghai, China) and are listed in **Table 1**.

Histopathological and Immunohistochemical Examination

The rats were sacrificed after 24 h reperfusion, and brain tissues were fixed with 4% formaldehyde. The brain tissues were dehydrated with different concentration gradients alcohol and embedded in paraffin and cut into 5 mm sections. To detect morphological changes in neurons, the sections were stained with hematoxylin and eosin (H&E) according to the standard procedure, and subjected to Nissl staining using 0.1% cresyl violet acetate. The number of intact cells in the penumbra of the ischemic cortex by Nissl staining was counted through five lesion regions randomly.

The sections were used for immunohistochemical examination. Briefly, these slices were dewaxed, dehydrated, and operated antigen retrieval. Furthermore, slices were blocked by 0.1% bovine serum albumin in PBS for 30 min; NF- κ B and Nrf-2 primary antibodies (Cell Signaling Technology) were used to incubate slices at 4°C overnight. The goat anti-rabbit IgG (Cell Signaling Technology) was used as the secondary antibody. Afterwards, positive areas were checked with a light microscope (Olympus, Tokyo, Japan) and analyzed using Image J software.

TUNEL Assay

To test the DNA fragmentation associated with apoptosis, the TUNEL assay was performed. The brain slices in each group were prepared and In situ Cell Death Detecting Kit (Roche Diagnostics FmbH, Penzberg, Germany) was used for achieving TUNEL staining. TUNEL staining was performed according to the routine method of kit. Apoptotic cells were identified as those with a brown-stained nucleus. Cell counting was using five randomly selected fields, and the apoptosis index was calculated as the percentage of positive cells to total cells. Samples were analyzed under a microscope and researchers were blinded to different groups.

Western Blot Assay

The brain tissues were dissected after I/R model. The total protein was extracted from fresh brain tissues on the ice and appropriate volumes of Protein Extraction Regent (Pierce, Rockford, USA) were added. Bradford protein assay was used to measure the concentration of total protein and bicinchoninic acid (BCA) protein assay kit was performed. Western blot was performed to separate and analyze the expression levels of several target proteins. Subsequently, the membranes were incubated at 4°C overnight with corresponding primary antibodies, Akt (1:500), p-Akt (Ser473, 1:250), GSK-3 β (1:500), p-GSK-3 β (Ser9, 1:250), Nrf-2 (1:500), p-NF- κ B (Ser536, 1:100), and GAPDH (1:1,000) (Cell signaling technology. Co) included. Then, membranes were washed with Tris-buffered saline with 0.05% Tween-20 (TBST) for 5 min \times 3 times. Followed

incubating appropriate secondary antibodies (Kangchen, Shanghai, China) at room temperature respectively, and detected with chemiluminescence plus detection system (Fusion FX7 Spectra; VilberLourmat, Eberhardzell, Germany). The intensities of each protein bands were measured with Quantity One software.

Statistical Analysis

All the results are shown as the Mean \pm SEM; the differences among multiple independent comparisons were analyzed by one-way analysis of variance test, followed by Student-Newman-Keuls *post hoc* test. Nonparametric test followed by Kruskal-Wallis H test was used to analyze the results of neurological score. $P \leq 0.05$ was considered statistically significant differences.

RESULTS

Kaempferol Ameliorated Neurological Scores and Reduced Infarct Volume

To confirm the protective effect of kaempferol on cerebral I/R injury, cerebral infarct areas and neurological scores in each group were evaluated by TTC staining and Longa's way, respectively. Firstly, we confirmed that the CMC-Na solution didn't interfere the results of MCAO operation (**Figure S2**). From **Figures 1A, B**, we can find infarct volume in I/R group compared to Sham group ($P < 0.05$, Sham group vs. I/R group). The cerebral infarct area in Kaempferol treatment groups (1.75, 3.49, 6.99 mM) are all smaller than I/R group, especially Kaempferol 3.49 and 6.99 mM treatment groups ($P < 0.05$, $P < 0.05$; Kaempferol 3.49 mM treatment group vs. I/R group, Kaempferol 6.99 mM treatment group vs. I/R group). Meanwhile, infarct volume in kaempferol 6.99 mM treatment group is smaller than kaempferol 1.75 mM treatment group ($P < 0.05$, Kaempferol 6.99 mM treatment group vs. Kaempferol 1.75 mM treatment group). Kaempferol also can increase cell viabilities in vitro after oxygen and glucose deprivation (**Figure S1**). From **Figure 1C**, rats subjected to I/R showed apparent severe neurological deficits ($P < 0.05$, I/R group vs. Sham group). Meanwhile, Kaempferol treatment groups (1.75, 3.49, 6.99 mM) can reduce neurological deficit scores compared with I/R group, especially kaempferol 6.99 mM treatment group ($P < 0.05$; Kaempferol 6.99 mM treatment group vs. I/R group).

Kaempferol Protected Against I/R-Induced Brain Tissue Injury and Weakened the Brain Tissue Apoptosis

We thus observed the protective effects of kaempferol on cell injury in the rat brain tissues after I/R injury. We used H&E staining to check the morphological changes. As shown in **Figure 2A**, in the cerebral cortex, the cells with abundant cytoplasm and clear nuclei were all arranged orderly in the Sham group. However, most neurons in the ischemic penumbra of cerebral cortex presented shrunken and deep stained in I/R group. Contrary to I/R group, residual neuron structures were

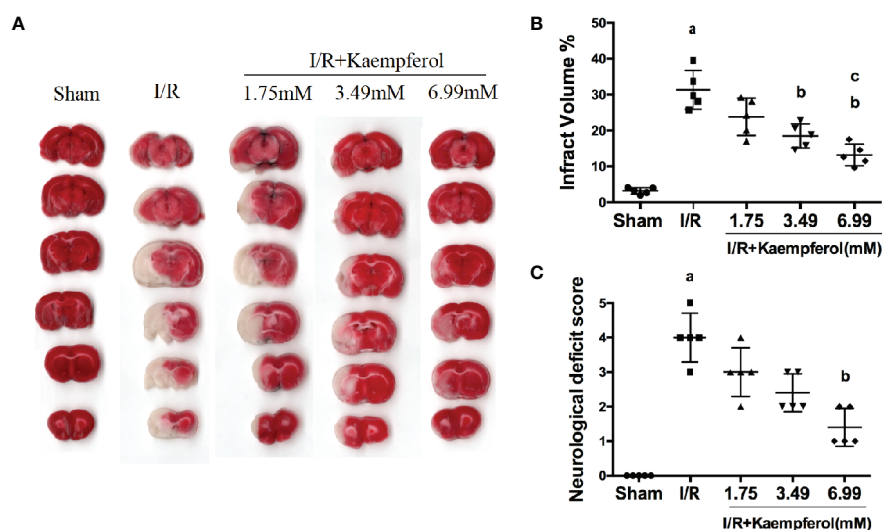


FIGURE 1 | Kaempferol ameliorated neurological scores and infarct volume. Rats were administrated with 1.75mM, 3.49mM and 6.99mM kaempferol for 7 days before I/R operation. Infarct volumes were assessed by TTC staining. **(A)** Representative TTC staining results of brain slices in different groups. **(B)** Quantitative analysis of brain infarct volumes. **(C)** Neurological scores in different groups. $n=5$, ^a $p < 0.05$, compared with the sham group; ^b $p < 0.05$, compared with the I/R model group; ^c $p < 0.05$, compared with the I/R+kaempferol1.75mM group.

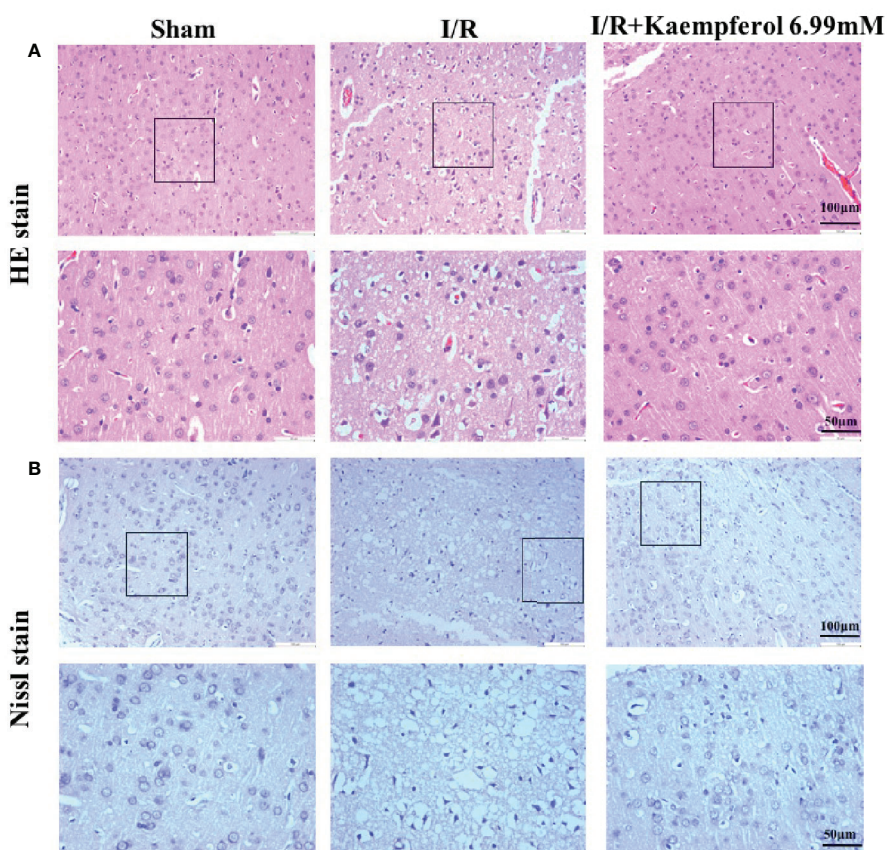


FIGURE 2 | Kaempferol inhibited I/R-induced brain tissues injury. **(A)** H&E staining results. **(B)** Nissl staining results. $n=4$, Original magnification 200x and 400x, respectively. The area in box was presented as magnification 400x.

improved in the kaempferol treatment group. Visible membranes and nuclei and more intact neurons were observed in the kaempferol treatment group. Nissl staining (**Figure 2B**) indicated that the large number of cells were shrunk with an enlarged intercellular space and more dark color staining in the I/R group relative to Sham group. Meanwhile, these characteristic changes were all improved in kaempferol treatment group. Furthermore, to determine the effect of kaempferol on neurons apoptosis TUNEL staining was used. **Figures 3A–C** demonstrated that kaempferol can significantly ameliorated I/R induced neurons apoptosis ($P < 0.05$, I/R group vs. Kaempferol treatment group). These results suggested that kaempferol relieves the damage caused by cerebral I/R

Effect of Kaempferol on the Expression Levels of SOD, MDA, and GSH in the Serum and Brain Tissue

To understand the protective effect of kaempferol on cerebral I/R, the activity level of SOD, MDA, and the content of GSH in the serum and brain tissues were determined. We observed that, compared with Sham group, the activities of SOD and GSH in serum and brain tissues were significantly decreased in I/R group ($P < 0.05$; $P < 0.05$; $P < 0.05$; $P < 0.05$; Sham group vs. I/R group). At the same time the content of MDA in serum and brain tissue were increased in I/R group ($P < 0.05$; $P < 0.05$; Sham group vs. I/R group). Surprisingly, kaempferol treatment not only significantly increased the activities of SOD (**Figures 4A, D**; $P < 0.05$; $P < 0.05$; Kaempferol 6.99 mM treatment group vs. I/R

group) and GSH (**Figures 4C, F**; $P < 0.05$; $P < 0.05$; Kaempferol 6.99 mM treatment group vs. I/R group), but also the content of MDA was decreased (**Figures 4B, E**; $P < 0.05$; $P < 0.05$; Kaempferol 6.99 mM treatment group vs. I/R group) relative to I/R group in serum and brain tissues. According to this results we believed that the beneficial effects of kaempferol administration under cerebral I/R are associated with anti-oxidative function.

Effect of Kaempferol on the Expression of Inflammatory Factors TNF- α , IL-1 β , and IL-6

To detect the expression level of inflammatory factors TNF- α , IL-1 β , and IL-6 after kaempferol treatment under cerebral I/R, ELISA and real-time PCR assay were used. **Figure 5A** indicates that I/R resulted in the high expression level of TNF- α , IL-1 β , and IL-6 ($P < 0.05$; $P < 0.05$; $P < 0.05$; I/R group vs. Sham group) in serum compared with Sham group. However, the expression levels of TNF- α , IL-1 β , and IL-6 in serum showed a significant decrease after kaempferol treatment ($P < 0.05$; $P < 0.05$; $P < 0.05$; I/R group vs. Kaempferol treatment group). In **Figure 5B**, we found that after I/R injury the expression levels of TNF- α , IL-1 β , and IL-6 in brain tissues are all significantly increased ($P < 0.05$; $P < 0.05$; $P < 0.05$; I/R group vs. Sham group). Kaempferol treatment can decreased TNF- α , IL-1 β , and IL-6 expression levels in brain tissue ($P < 0.05$; $P < 0.05$; $P < 0.05$; I/R group vs. Kaempferol treatment group). Further analysis is shown in **Figure 5C**, we found that the mRNA level of TNF- α , IL-1 β , and

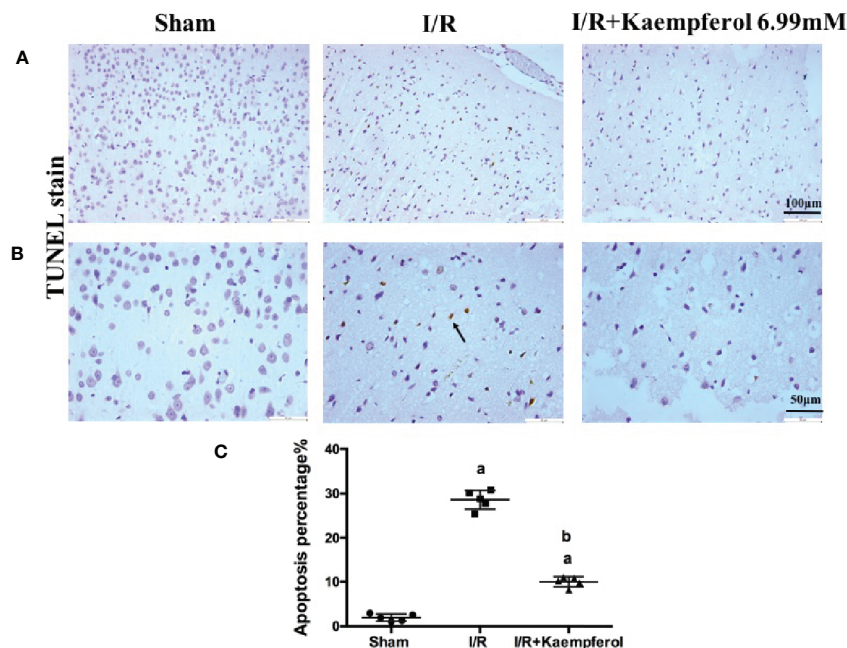


FIGURE 3 | Kaempferol protected against I/R-induced neurons apoptosis in brain tissues. TUNEL staining results were showed in original magnification 200 \times (**A**) and 400 \times (**B**), respectively. Quantification of TUNEL-positive cells in cerebral cortex (**C**). $n=4$, ^a $p < 0.05$, compared with the sham group; ^b $p < 0.05$, compared with the I/R model group. Black arrow points the apoptotic cell.

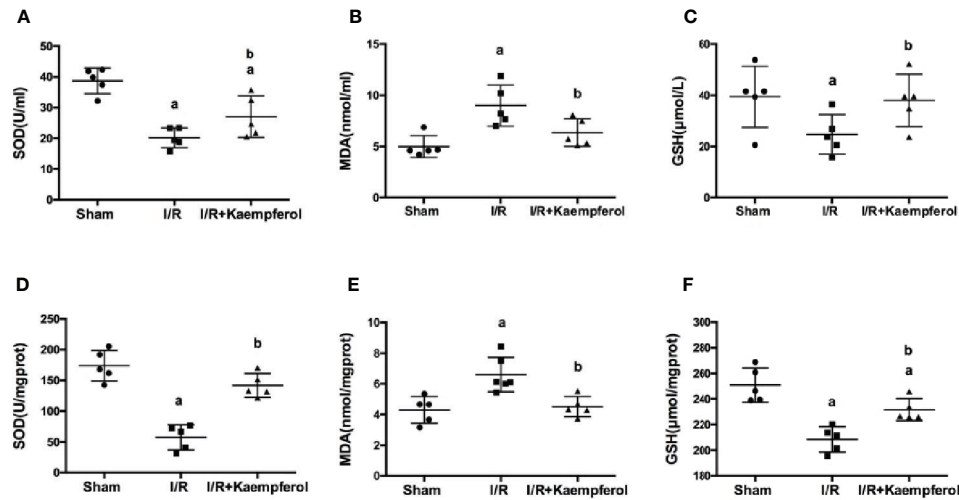


FIGURE 4 | Effect of kaempferol on the expression levels of SOD (A, D), MDA (B, E) and GSH (C, F) in serum (n=9) and brain tissues (n=5) after ischemia/reperfusion injury. ^a*p* < 0.05, compared with the sham group; ^b*p* < 0.05, compared with the I/R model group.

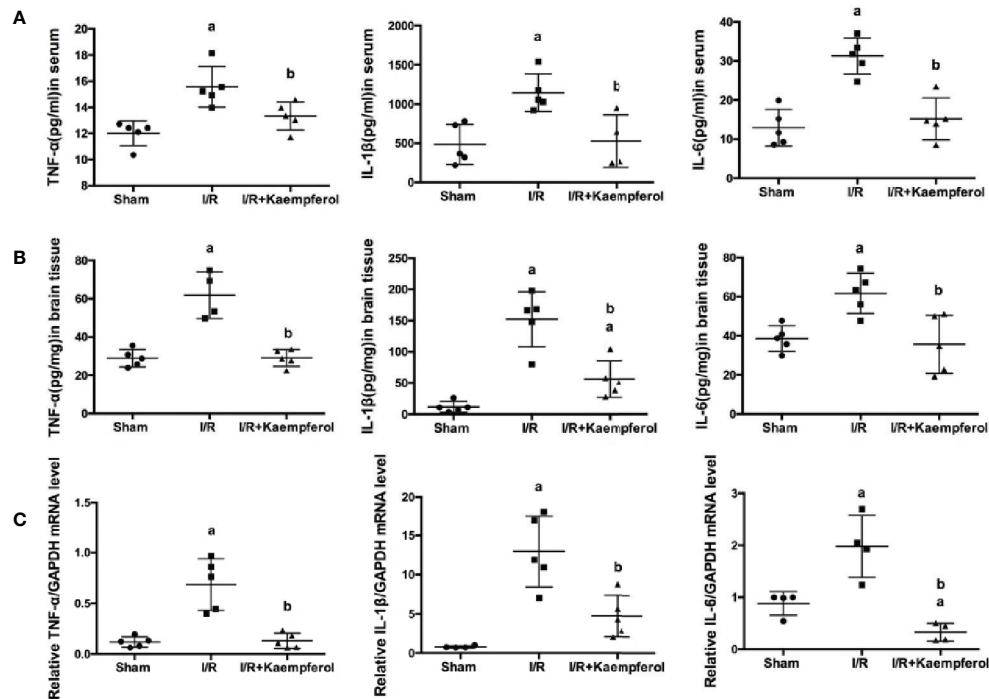


FIGURE 5 | ELISA assay was performed to detect the effect of kaempferol on inflammatory factors (TNF-α, IL-1β and IL-6) expression level in serum (n=5) (A) and brain tissues (n=5) (B) after ischemia/reperfusion injury. TNF-α, IL-1β and IL-6 mRNA expression levels in brain tissues were tested by real-time PCR (C). ^a*p* < 0.05, compared with the sham group; ^b*p* < 0.05, compared with the I/R model group.

IL-6 in brain tissues were all markedly increased after I/R ($P < 0.05$; $P < 0.05$; $P < 0.05$; I/R group vs. Sham group). These inflammatory factors' mRNA expression levels were remarkably down-regulated after kaempferol treatment ($P < 0.05$; $P < 0.05$; $P < 0.05$; I/R group vs. Kaempferol treatment group). According to the above description, we assumed that kaempferol administration under cerebral I/R are associated with anti-inflammatory effect.

Kaempferol Regulated the Expression Levels of Akt, p-Akt, p-GSK-3 β , Nrf-2, NF- κ B, and p-NF- κ B in Rat Brain Tissues

To observe the effect of kaempferol on protecting the neurons after I/R and according to the previous research results described above, the expression levels of Akt, p-Akt, p-GSK-3 β , Nrf-2, NF- κ B, and p-NF- κ B in rat brain tissues were performed *via* western blot and immunohistochemical staining. We observed that the I/R injury increased expression of proteins NF- κ B and p-NF- κ B (Figures 6B, 7C), p-GSK-3 β (Figure 7B), and Nrf-2 (Figures 6A, 7D), and decreased expression of protein p-Akt (Figure 7A) compared with Sham group. What is surprising is that the expression levels of proteins NF- κ B, p-NF- κ B, and p-GSK-3 β

were down-regulated after kaempferol treatment, and the expression levels of proteins Nrf-2, p-Akt were up-regulated in comparison with I/R group.

DISCUSSION

Cerebral ischemia with high morbidity and mortality, however, the complicated pathological mechanisms lead to identify a novel neuroprotective pharmacological drug becoming difficult. Accumulated evidences indicate that numerous factors are included in ischemia brain injury, involving apoptosis, excitotoxicity, oxidative stress, per-infarct depolarization, nutritive stress, reactive oxygen species (ROS), and inflammation (Xu et al., 2016; Zerna et al., 2016; Xing et al., 2018). Moreover, during the ischemia damage stage, the cell metabolism abnormalities may be resulted from the shortage of blood, oxygen, and glucose supply, which commonly led to neuronal death or apoptosis. Thus, anti-oxidant and anti-inflammation treatment strategies are being developed to treat cerebral I/R injury. Traditional Chinese medicine with characteristics of multi-function and multi-mechanism. A

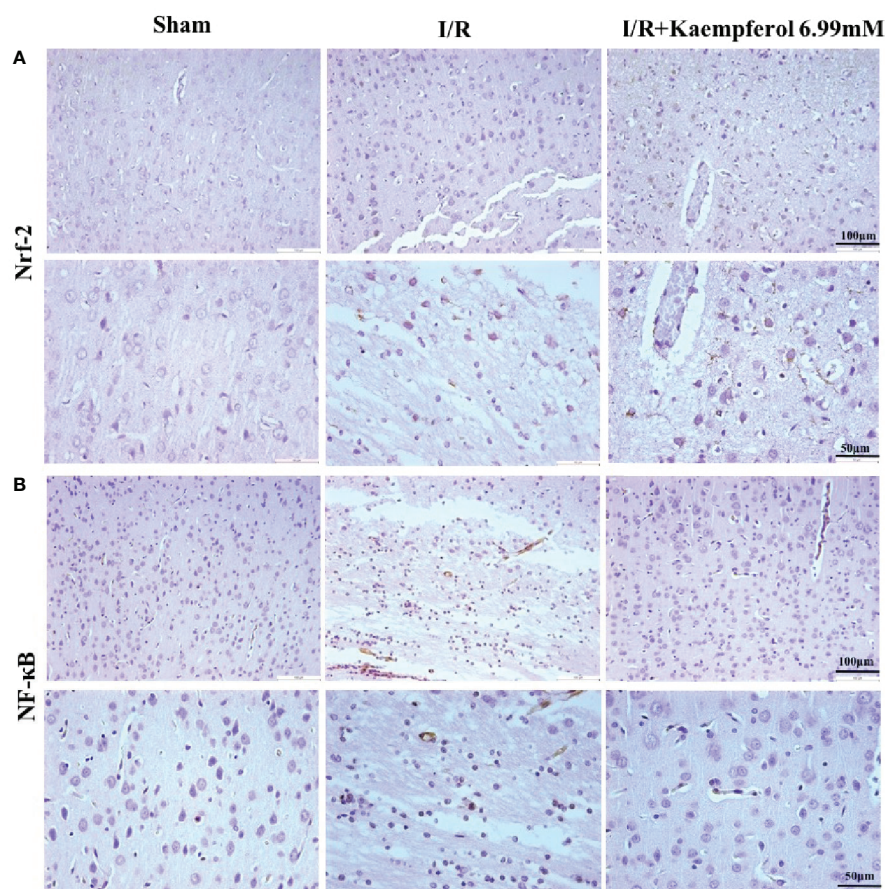


FIGURE 6 | Kaempferol affected expression levels of Nrf-2 and NF- κ B in cerebral cortex after ischemia and reperfusion injury. Immunohistochemical staining was used to examine the expression of Nrf-2 (A) and NF- κ B (B). $n=4$, Original magnification 200 \times and 400 \times .

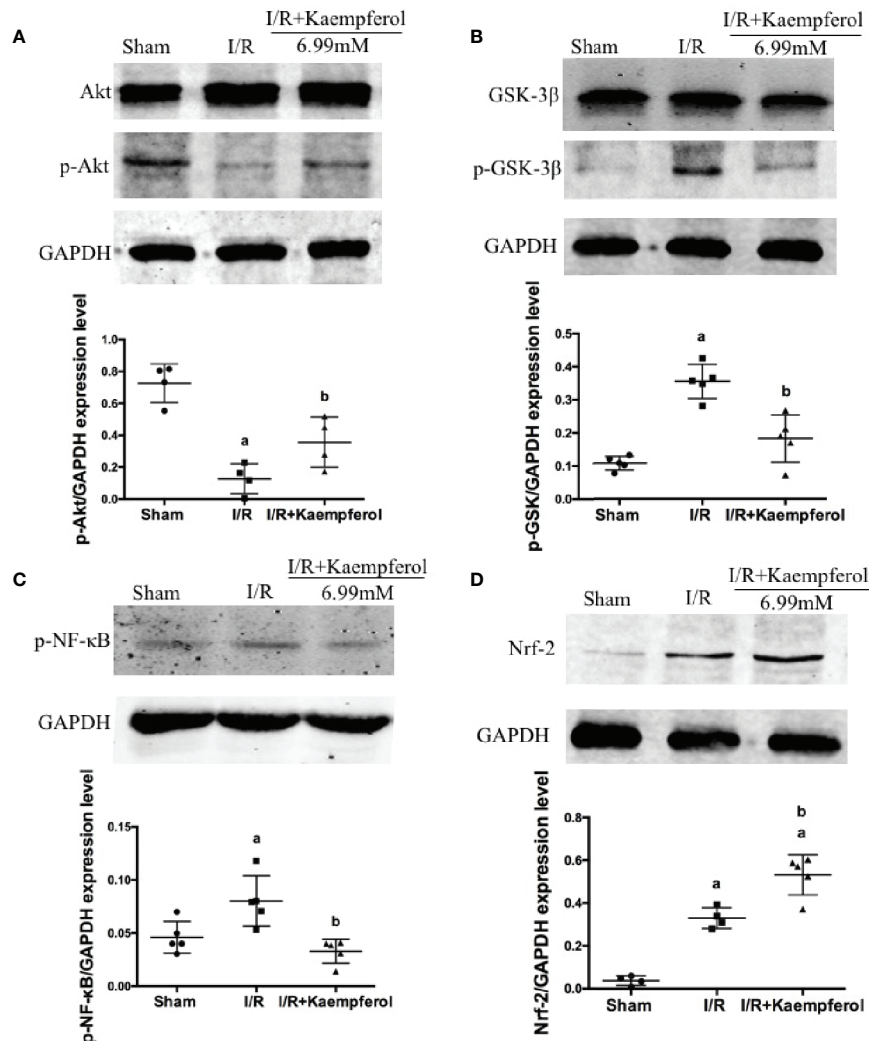


FIGURE 7 | Kaempferol affected expression levels of proteins Akt, p-Akt, GSK-3 β , p-GSK-3 β , p-NF- κ B and Nrf-2 in brain tissues after ischemia reperfusion injury. Western blot assay and Quantity One software were used to investigate and calculate the expression levels of proteins Akt and p-Akt (A), GSK-3 β and p-GSK-3 β (B), p-NF- κ B (C) and Nrf-2 (D). $n=5$, ^a $p < 0.05$, compared with the sham group; ^b $p < 0.05$, compared with the I/R model group.

previous report showed kaempferol with anti-oxidant and anti-inflammation properties *in vivo* and *in vitro* because of its phenolic and hydroxyl group structure (Wang et al., 2018). Due to the complex pathological process of I/R, it is promising that kaempferol could play a powerful anti-oxidant and anti-inflammation role in brain tissue during cerebral I/R.

Firstly, detecting the cerebral infarct volume in brain tissue by TTC staining to observe the protective effect of kaempferol on cerebral I/R injury (Li et al., 2019). The results showed that kaempferol can significantly decrease the cerebral infarct volumes after I/R injury in rat model. Besides, kaempferol treatment greatly improved neurobehavioral defects. In our experiment, the rat brain tissues were detected by H&E staining and Nissl staining. The results, both in H&E stain and Nissl stain, indicated that kaempferol treatment improved the arrangement, distribution, and morphological structure of

neurons. These results suggested that kaempferol relieves the damage caused by cerebral I/R.

The mechanisms of brain injury during cerebral I/R are comprehensive. ROS are believed to be a key factor of nerve damage post cerebral I/R (Granger and Kvietys, 2015). During ischemia physiological condition, few free radicals are present; thus, the absorbance of oxygen radicals decreases (Valko et al., 2007). Afterwards, on the stage of recovery, known as reperfusion, the blood supply of the tissue triggers the “explosion” of oxygen free radicals; therefore, the accumulated ROS attacks the cells and lead to injury (Droge, 2002). Following, the antioxidant enzymes, such as SOD, GSH are involved, in the defensive system for protecting against oxidative stress. MDA is an oxidative stress marker, which is also a product of lipid peroxidation reaction. These play an important role in neurons against ROS-induced cell injury (Ren et al., 2017). Hence, the

anti-oxidative activities of kaempferol on neuroprotective role were investigated. Increasing SOD and GSH activities and decreasing MDA content have been observed after kaempferol treatment. Additionally, an inflammatory response develops within several hours after damage and is characterized by the activation of pro-inflammatory cytokines and infiltration of neutrophils (Fu et al., 2018). The inflammatory response makes neurological injury in a worse situation and promotes neural cells apoptosis (Anusha et al., 2017). A large number of evidences showed that the pro-inflammatory cytokines released in the periphery and neuronal apoptosis induced by cerebral I/R may occur potential injury to the hippocampal cells, which are associated with memory and learning functions (Chen et al., 2015). TNF- α , IL-1 β , and IL-6 are reported as major mediators in several central nervous systems, and increased level of them related to pathological mechanisms of secondary damage, including neuronal cells apoptosis or death (Fan et al., 2014). In this study, we observed that kaempferol treatment can decreased the expression levels of TNF- α , IL-1 β , and IL-6 in blood and brain tissue, meanwhile a reduction of neurons apoptosis was presented by TUNEL stain assay. According to the above description we believed that the beneficial effects of kaempferol administration under cerebral I/R are associated with anti-oxidative and anti-inflammatory, as well as reduction of neural cells apoptosis.

There are various signaling pathways involved in the cerebral I/R injury to regulate pathological mechanisms (Kisoh et al., 2019). Nrf-2 is a transcription factor implicated in mediating protection against electrophiles and oxidants and enhances cell survival in many tissues, including brain tissue (Baird and Dinkova-Kostova, 2011). Nrf-2 binds to the AREs and stimulates transcription of antioxidant proteins, which associated with scavenging ROS and glutathione (GSH) biosynthesis and regeneration (Motohashi and Yamamoto, 2004). NF- κ B, a transcription factor, is a key regulator of many genes (such as TNF- α and IL-6) involved in inflammation. Activation of NF- κ B stimulated by ROS and several inflammatory mediators, leads to neuron death and irreversible brain damage in cerebral I/R (Ridder and Schwaninger, 2009). Additionally, it has been reported that Nrf-2 is involved in the inflammatory response and can inhibit the activation of NF- κ B (Lee et al., 2012). To assess the effect of kaempferol on molecular changes undergo cerebral I/R, we evaluated the proteins expression of Nrf-2 and NF- κ B in brain tissues. We found that kaempferol treatment significantly increased the Nrf-2 expression and inhibited NF- κ B expression.

Recent reports indicated that GSK-3 β is a negative regulator of Nrf-2 transcription activity and participates in the distribution of Nrf-2 inside or outside of the nucleus (Chowdhry et al., 2013). GSK-3 is a component in the glycogen metabolism pathway and a crucial regulator in multiple intracellular contexts. GSK-3 β is famous to be involved in a number of human disorders, including diabetes, cancer, oxidative stress, and Alzheimer's disease at

all (Juhászová et al., 2009). GSK-3 α and GSK-3 β are two members of GSK-3 family, which are all predominantly expressed in the brain (Kim and Snider, 2011). Numerous reports have declared that GSK-3 β , involved in the regulation of differentiation, survival, activation, or over-expression are related to ischemia neuronal death during transient cerebral ischemia (Chen et al., 2017). GSK-3 β acts in memory function and cerebral ischemia-induced neurogenesis (Kim et al., 2015) depending on the site of phosphorylation. Moreover, GSK-3 β is an important downstream protein in the Phosphoinositide-3-kinase/Akt (PI3K/Akt) pathway and activated Akt stimulates phosphorylation of GSK-3 β . It is known that PI3K/Akt signal pathway can promote cell growth and survival in response to extracellular stimulations (Wang et al., 2010). This pathway is associated with neuroprotective function against ischemia damage (Chen et al., 2017).

To further understand protective effect of kaempferol on I/R injury, the proteins expression level of p-GSK-3 β , Akt, p-Akt in brain tissues after cerebral I/R injury were tested. Surprisingly, kaempferol treatment increased the expression of p-Akt and decreased the expression of p-GSK-3 β . Based on previous results and findings, we found that kaempferol with neuroprotective effect under cerebral I/R injury. The neuroprotective effect is related to anti-oxidative and anti-inflammation stresses, as well as alleviation of neurons apoptosis, which are potentially associated with up regulation of p-Akt and Nrf-2, meanwhile down regulation of p-NF- κ B and p-GSK-3 β . This research still exists limitations, which including we need more experiments to verify detailed molecular mechanism and modify available pharmaceutical form to further investigate kaempferol treatment effect on I/R except prophylaxis. Even though Kaempferol had a benefit on oxidative stress, inflammation, and apoptosis, it is not known which of these pathological events is more important for kaempferol's benefit.

CONCLUSION

In conclusion, the present study confirms the neuroprotective effect of kaempferol on cerebral ischemia and reperfusion injury *in vivo*. Kaempferol protects against cerebral I/R-induced oxidative stress, inflammation, and apoptosis, which are potentially associated with up regulation of p-Akt and Nrf-2, meanwhile down regulation of p-NF- κ B and p-GSK-3 β .

DATA AVAILABILITY STATEMENT

The datasets analyzed in this article are publicly available. Requests to access the datasets also can be directed to wangjing93wj@126.com.

ETHICS STATEMENT

The animal study was reviewed and approved by the Animal Ethics Committee of Shanghai 9th People's Hospital, Shanghai Jiao Tong University School of Medicine.

AUTHOR CONTRIBUTIONS

JW offered substantial contributions to the conception, design of the work, and drafted the work. JM, RW, SL, and BW analyzed data for the work. YY revised manuscript critically for important intellectual content and provided approval for publication of the content.

FUNDING

This project was financially supported by the National Natural Science Foundation of China (No.81803815 and No.81703779).

REFERENCES

- Anusha, C., Sumathi, T., and Joseph, L. D. (2017). Protective role of apigenin on rotenone induced rat model of Parkinson's disease: Suppression of neuroinflammation and oxidative stress mediated apoptosis. *Chem. Biol. Interact.* 269, 67–79. doi: 10.1016/j.cbi.2017.03.016
- Bösel, J., Ruscher, K., Ploner, C. J., and Valdeuza, J. M. (2005). Delayed neurological deterioration in a stroke patient with postoperative acute anemia. *Eur. Neurol.* 53, 36–38. doi: 10.1159/000084261
- Baird, L., and Dinkova-Kostova, A. T. (2011). The cytoprotective role of the Keap1-Nrf2 pathway. *Arch. Toxicol.* 85 (4), 241–272. doi: 10.1007/s00204-011-0674-5
- Broussalis, E., Killer, M., McCoy, M., Harrer, A., Trinka, E., and Kraus, J. (2012). Current therapies in ischemic stroke. Part A. Recent developments in acute stroke treatment and in stroke prevention. *Drug Discovery Today* 17 (7–8), 296–309. doi: 10.1016/j.drudis.2011.11.005
- Chen, B., Wu, Z., Xu, J., and Xu, Y. (2015). Calreticulin Binds to Fas Ligand and Inhibits Neuronal Cell Apoptosis Induced by Ischemia-Reperfusion Injury. *BioMed. Res. Int.* 2015, 895284. doi: 10.1155/2015/895284
- Chen, B. H., Ahn, J. H., Park, J. H., Shin, B. N., Lee, Y. L., Kang, I. J., et al. (2017). Transient Cerebral Ischemia Alters GSK-3 β and p-GSK-3 β Immunoreactivity in Pyramidal Neurons and Induces p-GSK-3 β Expression in Astrocytes in the Gerbil Hippocampal CA1 Area. *Neurochem. Res.* 42 (8), 2305–2313. doi: 10.1007/s11064-017-2245-5
- Chowdhry, S., Zhang, Y., McMahon, M., Sutherland, C., Cuadrado, A., and Hayes, J. D. (2013). Nrf2 is controlled by two distinct beta-TrCP recognition motifs in its Neh6 domain, one of which can be modulated by GSK-3 activity. *Oncogene* 32 (32), 3765–3781. doi: 10.1038/ncr.2012.388
- Danilov, C. A., Chandrasekaran, K., Racz, J., Soane, L., Zielke, C., and Fiskum, G. (2009). Sulforaphane protects astrocytes against oxidative stress and delayed death caused by oxygen and glucose deprivation. *Glia* 57 (6), 645–656. doi: 10.1002/glia.20793
- Droge, W. (2002). Free radicals in the physiological control of cell function. *Physiol. Rev.* 82 (1), 47–95. doi: 10.1152/physrev.00018.2001
- Fan, J., Zhang, Z., Chao, X., Gu, J., Cai, W., Zhou, W., et al. (2014). Ischemic preconditioning enhances autophagy but suppresses autophagic cell death in rat spinal neurons following ischemia-reperfusion. *Brain Res.* 1562, 76–86. doi: 10.1016/j.brainres.2014.03.019
- Fu, J., Sun, H., Zhang, Y., Xu, W., Wang, C., Fang, Y., et al. (2018). Neuroprotective Effects of Luteolin Against Spinal Cord Ischemia-Reperfusion Injury by Attenuation of Oxidative Stress, Inflammation, and Apoptosis. *J. Med. Food.* 21 (1), 13–20. doi: 10.1089/jmf.2017.4021

The work was funded by the Clinical Pharmacy Innovation Research Institute of Shanghai Jiao Tong University School of Medicine, the project number are CXYJY2019MS002 and CXYJY2019QN002.

SUPPLEMENTARY MATERIAL

The Supplementary Material for this article can be found online at: <https://www.frontiersin.org/articles/10.3389/fphar.2020.00424/full#supplementary-material>

FIGURE S1 | Kaempferol increased the cell viability under OGD/R. $^{##}P < 0.01$, Con group vs. OGD/R group; $^{**}P < 0.01$, OGD/R group vs. OGD/R + Kaempferol 10 μ M treatment group.

FIGURE S2 | The infarct volume in I/R only group and I/R+vehicle treatment group. To investigate the effect of 0.5% CMC-Na intragastrically per day for one week on ischemia reperfusion injury.

FIGURE S3 | Schematic diagram for ischemia hemisphere.

- Gidaro, M. C., Astorino, C., Petzer, A., Carradori, S., Alcaro, F., Costa, G., et al. (2016). Kaempferol as Selective Human MAO-A Inhibitor: Analytical Detection in Calabrian Red Wines, Biological and Molecular Modeling Studies. *J. Agric. Food Chem.* 64 (6), 1394–1400. doi: 10.1021/acs.jafc.5b06043
- Granger, D. N., and Kvietys, P. R. (2015). Reperfusion injury and reactive oxygen species: The evolution of a concept. *Redox Biol.* 6, 524–551. doi: 10.1016/j.redox.2015.08.020
- Guo, Z., Liao, Z., Huang, L., Liu, D., Yin, D., and He, M. (2015). Kaempferol protects cardiomyocytes against anoxia/reoxygenation injury via mitochondrial pathway mediated by SIRT1. *Eur. J. Pharmacol.* 761, 245–253. doi: 10.1016/j.ejphar.2015.05.056
- Juhászová, M., Zorov, D. B., Yaniv, Y., Nuss, H. B., Wang, S., and Sollott, S. J. (2009). Role of glycogen synthase kinase-3 β in cardioprotection. *Circ. Res.* 104 (11), 1240–1252. doi: 10.1161/CIRCRESAHA.109.197996
- Kim, W. Y., and Snider, W. D. (2011). Functions of GSK-3 Signaling in Development of the Nervous System. *Front. Mol. Neurosci.* 4, 44. doi: 10.3389/fnmol.2011.00044
- Kim, D. H., Lee, H. E., Kwon, K. J., Park, S. J., Heo, H., Lee, Y., et al. (2015). Early immature neuronal death initiates cerebral ischemia-induced neurogenesis in the dentate gyrus. *Neuroscience* 284, 42–54. doi: 10.1016/j.neuroscience.2014.09.074
- Kisoh, K., Hayashi, H., Arai, M., Orita, M., Yuan, B., and Takagi, N. (2019). Possible Involvement of PI3-K/Akt-Dependent GSK-3 β Signaling in Proliferation of Neural Progenitor Cells After Hypoxic Exposure. *Mol. Neurobiol.* 56 (3), 1946–1956. doi: 10.1007/s12035-018-1216-4
- Lee, J., and Ki, J. H. (2016). Kaempferol Inhibits Pancreatic Cancer Cell Growth and Migration through the Blockade of EGFR-Related Pathway In Vitro. *PLoS One* 11 (5), e0155264. doi: 10.1371/journal.pone.0155264
- Lee, E., Yin, Z., Sidoryk-Węgrzynowicz, M., Jiang, H., and Aschner, M. (2012). 15-Deoxy-Delta12,14-prostaglandin J(2) modulates manganese-induced activation of the NF-kappaB, Nrf2, and PI3K pathways in astrocytes. *Free Radic. Biol. Med.* 52 (6), 1067–1074. doi: 10.1016/j.freeradbiomed.2011.12.016
- Li, Q., Tian, Z., Wang, M., Kou, J., Wang, C., Rong, X., et al. (2019). Luteolide attenuates neuroinflammation in focal cerebral ischemia in rats via regulation of the PPARgamma/Nrf2/NF-kappaB signaling pathway. *Int. Immunopharmacol.* 66, 309–316. doi: 10.1016/j.intimp.2018.11.044
- Li, Z., Yulei, J., Yaqing, J., Jinmin, Z., Xinyong, L., Jing, G., et al. (2019). Protective effects of tetramethylpyrazine analogue Z-11 on cerebral ischemia reperfusion injury. *Eur. J. Pharmacol.* 844, 156–164. doi: 10.1016/j.ejphar.2018.11.031
- Longa, E. Z., Weinstein, P. R., Carlson, S., and Cummins, R. (1989). Reversible middle cerebral artery occlusion without craniectomy in rats. *Stroke* 20, 84–91. doi: 10.1161/01.STR.20.1.84

- Ma, X. H., Gao, Q., Jia, Z., and Zhang, Z. W. (2015). Neuroprotective capabilities of TSA against cerebral ischemia/reperfusion injury via PI3K/Akt signaling pathway in rats. *Int. J. Neurosci.* 125 (2), 140–146. doi: 10.3109/00207454.2014.912217
- Motohashi, H., and Yamamoto, M. (2004). Nrf2-Keap1 defines a physiologically important stress response mechanism. *Trends Mol. Med.* 10 (11), 549–557. doi: 10.1016/j.molmed.2004.09.003
- Qi, S., Xin, Y., Guo, Y., Diao, Y., Kou, X., Luo, L., et al. (2012). Ampelopsin reduces endotoxin inflammation via repressing ROS-mediated activation of PI3K/Akt/NF-kappaB signaling pathways. *Int. Immunopharmacol.* 12 (1), 278–287. doi: 10.1016/j.intimp.2011.12.001
- Rada, P., Rojo, A. I., Chowdhry, S., McMahon, M., Hayes, J. D., and Cuadrado, A. (2011). SCF/ β -TrCP promotes glycogen synthase kinase 3-dependent degradation of the Nrf2 transcription factor in a Keap1-independent manner. *Mol. Cell Biol.* 31 (6), 1121–1133. doi: 10.1128/MCB.01204-10
- Ren, Z., Zhang, R., Li, Y., Li, Y., Yang, Z., and Yang, H. (2017). Ferulic acid exerts neuroprotective effects against cerebral ischemia/reperfusion-induced injury via antioxidant and anti-apoptotic mechanisms in vitro and in vivo. *Int. J. Mol. Med.* 40 (5), 1444–1456. doi: 10.3892/ijmm.2017.3127
- Ridder, D. A., and Schwanninger, M. (2009). NF-kappaB signaling in cerebral ischemia. *Neuroscience* 158 (3), 995–1006. doi: 10.1016/j
- Shi, S. S., Yang, W. Z., Chen, Y., Chen, J. P., and Tu, X. K. (2014). Propofol reduces inflammatory reaction and ischemic brain damage in cerebral ischemia in rats. *Neurochem. Res.* 39 (5), 793–799. doi: 10.1007/s11064-014-1272-8
- Umesalma, S., and Sudhandiran, G. (2010). Differential inhibitory effects of the polyphenol ellagic acid on inflammatory mediators NF-kappaB, iNOS, COX-2, TNF-alpha, and IL-6 in 1,2-dimethylhydrazine-induced rat colon carcinogenesis. *Basic Clin. Pharmacol. Toxicol.* 107 (2), 650–655. doi: 10.1111/j.1742-7843.2010.00565.x
- Valko, M., Leibfritz, D., Moncol, J., Cronin, M. T., Mazur, M., and Telser, J. (2007). Free radicals and antioxidants in normal physiological functions and human disease. *Int. J. Biochem. Cell Biol.* 39 (1), 44–84. doi: 10.1016/j.biocel.2006.07.001
- Wang, J. K., Yu, L. N., Zhang, F. J., Yang, M. J., Yu, J., Yan, M., et al. (2010). Postconditioning with sevoflurane protects against focal cerebral ischemia and reperfusion injury via PI3K/Akt pathway. *Brain Res.* 1357, 142–151. doi: 10.1016/j.brainres.2010.08.009
- Wang, J., Li, T., Feng, J., Li, L., Wang, R., Cheng, H., et al. (2018). Kaempferol protects against gamma radiation-induced mortality and damage via inhibiting oxidative stress and modulating apoptotic molecules in vivo and vitro. *Environ. Toxicol. Pharmacol.* 60, 128–137. doi: 10.1016/j.etap.2018.04.014
- Wang, R., Wang, J., Song, F., Li, S., and Yuan, Y. (2018). Tanshinol ameliorates CCl4-induced liver fibrosis in rats through the regulation of Nrf2/HO-1 and NF-kappaB/IkappaBalpha signaling pathway. *Drug Des. Devel. Ther.* 12, 1281–1292. doi: 10.2147/DDDT.S159546
- Xie, L., Wang, Z., Li, C., Yang, K., and Liang, Y. (2017). Protective effect of nicotinamide adenine dinucleotide (NAD⁺) against spinal cord ischemia-reperfusion injury via reducing oxidative stress-induced neuronal apoptosis. *J. Clin. Neurosci.* 36, 114–119. doi: 10.1016/j.jocn.2016.10.038
- Xing, P., Ma, K., Wu, J., Long, W., and Wang, D. (2018). Protective effect of polysaccharide peptide on cerebral ischemiareperfusion injury in rats. *Mol. Med. Rep.* 18 (6), 5371–5378. doi: 10.3892/mmr.2018.9579
- Xu, M., Wang, H. F., Zhang, Y. Y., and Zhuang, H. W. (2016). Protection of rats spinal cord ischemia-reperfusion injury by inhibition of MiR-497 on inflammation and apoptosis: Possible role in pediatrics. *Biomed. Pharmacother.* 81, 337–344. doi: 10.1016/j.biopha.2016.04.028
- Xue, T. F., Ding, X., Ji, J., Yan, H., Huang, J. Y., Guo, X. D., et al. (2017). PD149163 induces hypothermia to protect against brain injury in acute cerebral ischemic rats. *J. Pharmacol. Sci.* 135 (3), 105–113. doi: 10.1016/j.jphs.2017.10.004
- Yu, Z. H., Cai, M., Xiang, J., Zhang, Z. N., Zhang, J. S., Song, X. L., et al. (2016). “PI3K/Akt pathway contributes to neuroprotective effect of Tongxinluo against focal cerebral ischemia and reperfusion injury in rats. *J. Ethnopharmacol.* 181, 8–19. doi: 10.1016/j.jep.2016.01.028
- Zerna, C., Assis, Z., d’Este, C. D., Menon, B. K., and Goyal, M. (2016). Imaging, Intervention, and Workflow in Acute Ischemic Stroke: The Calgary Approach. *AJNR Am. J. Neuroradiol.* 37 (6), 978–984. doi: 10.3174/ajnr.A4610
- Zhang, S., Qi, Y., Xu, Y., Han, X., Peng, J., Liu, K., et al. (2013). Protective effect of flavonoid-rich extract from *Rosa laevigata* Michx on cerebral ischemia-reperfusion injury through suppression of apoptosis and inflammation. *Neurochem. Int.* 63 (5), 522–532. doi: 10.1016/j.neuint.2013.08.008
- Zhou, X., Wang, H. Y., Wu, B., Cheng, C. Y., Xiao, W., Wang, Z. Z., et al. (2017). Ginkgolide K attenuates neuronal injury after ischemic stroke by inhibiting mitochondrial fission and GSK-3beta-dependent increases in mitochondrial membrane permeability. *Oncotarget* 8 (27), 44682–44693. doi: 10.18632/oncotarget.17967

Conflict of Interest: The authors declare that the research was conducted in the absence of any commercial or financial relationships that could be construed as a potential conflict of interest.

Copyright © 2020 Wang, Mao, Wang, Li, Wu and Yuan. This is an open-access article distributed under the terms of the Creative Commons Attribution License (CC BY). The use, distribution or reproduction in other forums is permitted, provided the original author(s) and the copyright owner(s) are credited and that the original publication in this journal is cited, in accordance with accepted academic practice. No use, distribution or reproduction is permitted which does not comply with these terms.



OPEN ACCESS

Edited by:

Zhang Yuefan,
Shanghai University, China

Reviewed by:

Qingchun Zeng,
Southern Medical University, China

Rui Song,
Loma Linda University,
United States

Anna Malashicheva,
Saint Petersburg State University,
Russia

***Correspondence:**

Nianguo Dong
dongnianguo@hotmail.com
Kang Xu
kangxu@hust.edu.cn

[†]These authors have contributed
equally to this work

Specialty section:

This article was submitted to
Ethnopharmacology,
a section of the journal
Frontiers in Pharmacology

Received: 03 November 2019

Accepted: 19 May 2020

Published: 07 July 2020

Citation:

Liu M, Li F, Huang Y, Zhou T, Chen S,
Li G, Shi J, Dong N and Xu K (2020)
Caffeic Acid Phenethyl Ester
Ameliorates Calcification by Inhibiting
Activation of the AKT/NF- κ B/NLRP3
Inflammasome Pathway in Human
Aortic Valve Interstitial Cells.
Front. Pharmacol. 11:826.
doi: 10.3389/fphar.2020.00826

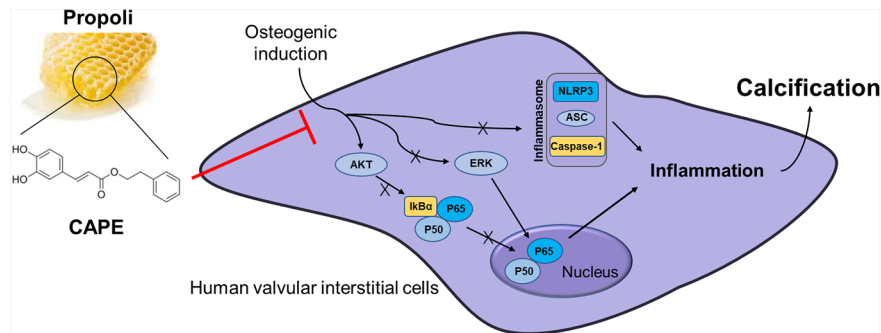
Caffeic Acid Phenethyl Ester Ameliorates Calcification by Inhibiting Activation of the AKT/NF- κ B/NLRP3 Inflammasome Pathway in Human Aortic Valve Interstitial Cells

Ming Liu[†], Fei Li[†], Yuming Huang[†], Tingwen Zhou, Si Chen, Geng Li, Jiawei Shi,
Nianguo Dong* and Kang Xu*

Department of Cardiovascular Surgery, Union Hospital, Tongji Medical College, Huazhong University of Science and Technology, Wuhan, China

Calcific aortic valve disease (CAVD) occurs via a pathophysiological process that includes inflammation-induced osteoblastic differentiation of aortic valvular interstitial cells (AVICs). Here, we investigated the role of the anti-inflammatory compound caffeic acid phenethyl ester (CAPE) in inhibiting CAVD. Human AVICs were isolated and cultured in osteogenic induction medium (OM) with or without 10 μ M CAPE. Cell viability was assessed using CCK8 assays and calcified transformation of AVICs was evaluated by Alizarin Red staining and osteogenic gene/protein expression. RNA-sequencing was conducted to identify differentially expressed genes (DEGs) and enrichment in associated pathways, as potential molecular targets through which CAPE inhibits osteogenic induction. The regulatory effects of CAPE on activation of the AKT/NF- κ B and NLRP3 inflammasome were evaluated by Western blot analysis and immunofluorescent staining. CAPE slowed the growth of AVICs cultured in OM but did not show significant cytotoxicity. In addition, CAPE markedly suppressed calcified nodule formation and decreased gene/protein expression of RUNX2 and ALP in AVICs. Gene expression profiles of OM-induced AVICs cultured with or without CAPE revealed 518 common DEGs, which were highly enriched in the NOD-like receptor, PI3K-AKT, and NF- κ B signaling pathways. Furthermore, CAPE inhibited phosphorylation of AKT, ERK1/2, and NF- κ B, and suppressed NLRP3 inflammasome activation in AVICs cultured in OM. Thus, CAPE is implicated as a potent natural product for the prevention of CAVD by inhibiting activation of the AKT/NF- κ B pathway and NLRP3 inflammasome.

Keywords: human aortic valve disease, natural product, polyphenolic compound, NF- κ B pathway, inflammasome



GRAPHICAL ABSTRACT | CAPE significantly inhibits OM-induced calcification and phenotypic transformation of AVICs *via* signaling pathways including AKT, ERK1/2, NF- κ B/NLRP3 inflammasome.

INTRODUCTION

Calcified aortic valve disease (CAVD), the most common Cardiac valvular disease worldwide, is characterized by valvular calcification, leading to aortic stenosis and subsequent heart failure (Nkomo et al., 2006). Increasing evidence obtained over the past decade suggests that CAVD is not simply a passive degenerative process, but an active pathological condition similar to that associated with atherosclerosis, including processes such as lipoprotein deposition, chronic inflammation, and osteoblastic differentiation of aortic valve interstitial cells (AVICs) (Li et al., 2013; P et al., 2014; Rutkovskiy et al., 2017). Currently, there is no effective pharmacological therapy for CAVD other than surgical or interventional aortic valve replacement (Da et al., 2015).

Both *in vitro* and clinical studies have suggested that a sequence of active osteogenic processes contribute to CAVD, and that osteogenic activity is initiated by inflammation (Nadra et al., 2005; Marincheva-Savcheva et al., 2011; New and Aikawa, 2011; Pawade et al., 2015). AVICs are the principle cell type found within aortic valve leaflets and participate in the process of CAVD primarily by inducing both inflammation and osteoblastic differentiation (Rutkovskiy et al., 2017). This inflammatory damage is a critical factor that causes CAVD. Therefore, the search for effective treatment modalities for valvular calcification, such as the use of medication to regulate inflammatory responses, has important clinical value and significance, and may effectively delay the onset of aortic valve calcification.

Caffeic acid phenethyl ester (CAPE), a natural polyphenolic compound, is mainly found in the bark of conifer trees, but is also present in propolis from honeybee hives (Wu et al., 2011). Previous studies have shown that CAPE is effective against various pathologies such as infections, oxidative stress, inflammation, cancer, diabetes, neurodegeneration, and anxiety (Parlakpınar et al., 2005; Celik and Erdogan, 2008; Tolba et al., 2016; Nie et al., 2017). Moreover, CAPE has been demonstrated to inhibit NF- κ B and to contribute to anti-inflammatory processes (Celik and Erdogan, 2008; Nie et al., 2017). In our previous studies, we confirmed that inflammatory responses accelerate the formation of valvular calcification (Xu et al.,

2018; Huang et al., 2019; Xu et al., 2019a). Therefore, we investigated the anti-calcification effect of CAPE.

In this study, we found that CAPE significantly inhibited osteogenic medium (OM)-induced calcification in human AVICs. To further clarify the mechanism by which CAPE inhibits AVIC calcification, we conducted high-throughput RNA-sequencing quantification to analyze global changes in gene expression induced in AVICs cultured in OM with or without CAPE. Finally, we confirmed the involvement of inhibition of the AKT/NF- κ B signaling pathway and NLRP3 inflammasome in the mechanism by which CAPE inhibits AVIC calcification.

MATERIALS AND METHODS

Cell Culture and Treatments

This human study was approved by the ethics committee of the Union Hospital, Tongji Medical College, Huazhong University of Science and Technology (China). Human specimens were obtained from the Department of Cardiovascular Surgery, Union Hospital, Tongji Medical College, Huazhong University of Science and Technology. All participants provided written informed consent according to the Declaration of Helsinki. From October 2018 to April 2019, aortic valve leaflets were obtained intra-operatively from patients (**Table 1**) undergoing the Bentall operation due to acute type I aortic dissection. Patients with a history of infective endocarditis, rheumatic heart disease, or a genetic syndrome were excluded. The degree of calcification of the aortic valve samples was determined as previously described (Li et al., 2017). Briefly, isolated leaflets were digested in medium containing 1 mg/mL collagenase I at 37°C for 30 min. After vortexing, the leaflets were further digested with a fresh solution of 1 mg/mL collagenase medium at 37°C for 8–10 h. After repeated aspiration to break up the tissue mass, the suspension was centrifuged at 300 \times g for 10 min. Subsequently, the cells were resuspended and cultured in M199 growth medium, supplemented with 100 U/mL penicillin, 100 μ g/mL streptomycin and 10% fetal bovine serum at 37°C under 5% CO₂.

TABLE 1 | Sample information.

Sample type	Degree	Sex	Age
Health	0	Male	36
Health	0	Male	53
Health	0	Female	42

Cells were used in experiments at passage 3. For the osteogenic differentiation model, hVICs were cultured in osteogenic induction medium (OM) (Cyagen Biosciences, HUXMA-90021) to stimulate osteogenic differentiation according to previously described protocols (Huang et al., 2020; Zhou et al., 2020). CAPE was purchased from Selleck (Cat. No. S7414) and dissolved in DMSO to yield a 10 mM stock solution. The treatment groups were as follows: Control group (without OM and CAPE), OM-treated group (OM alone) and OM + CAPE-treated group.

Cell Viability Analysis

The cells were seeded on the 48-well plates at the cell density of 5×10^3 cells/well and cultured in 10% FBS-DMEM medium for 24 h. Subsequently, the medium was changed into serum-free medium for starvation for 12 h. Then, the cells were treated with different final concentrations of CAPE (0–25 μ M) for 72 h, and IC50 was calculated. In addition, the cells were also treated with 10 μ M CAPE for 5 days. Cell viability in the experiments was detected with a CCK-8 assay (Bimake, Houston, TX). Briefly, at the end of each time interval, cell samples were washed with PBS and incubated with serum free medium containing 10% CCK-8 reagent. After 3 h of incubation at 37°C under 5% CO₂, aliquots were pipetted into a 96-well plates and measured at 490 nm using an enzyme labeling instrument.

Calcification Analysis

Cells were seeded into 12-well plates and cultured for 2–3 days to reach confluence. Cells were then cultured in either OM with or without 10 μ M CAPE for 21 days. The degree of cell calcification was measured by Alizarin Red S (Sciencell, 0223) staining according to the manufacturer's instructions. In brief, after 21 days of treatment, the cells were fixed with 4% paraformaldehyde (PFA) and then incubated with 2% Alizarin Red S solution for 30 min at room temperature. After washing twice with distilled water, images were captured for evaluation of the degree of calcification. For quantitative analysis, cells were incubated in a 10% aqueous solution of cetylpyridinium chloride and the amount of Alizarin Red S dye released from the extracellular matrix was quantified by spectrophotometry at a wavelength of 550 nm.

qRT-PCR Assay

Cells were harvested using a Trizol reagent (Invitrogen, Carlsbad, CA), followed by RNA isolation. Each sample cDNA was reverse transcribed using the Revert Aid First Strand cDNA Synthesis Kit (Thermo Fisher Scientific, Waltham, MA). Then, the reverse transcription product was used as a template to perform real-time polymerase chain reaction (PCR) on a Step One Plus

thermal cycler (Applied Biosystems, Foster City, CA) using a PowerUpTM SYBRTM Green Master Mix (Applied Biosystems) following the manufacturer's guide. All the primers were referenced from the previous study, and synthesized by Invitrogen; primer sequences are shown in **Supplementary Table 1**. The final data were analyzed by the 2- $\Delta\Delta$ ct method.

Western Blot Analysis

After culture for 48 h or 7 days, cells were harvested, lysed in the RIPA buffer containing protease and further boiled. The protein samples were resolved by SDS-PAGE (4%–20% gels) and then transferred to PVDF membranes using a wet-transfer system. After blocking with 5% (wt/vol) skimmed milk in TBS-T solution (50 mM Tris/HCL, pH 7.6, 150 mM NaCl and 0.1% (vol/vol) Tween-20) at room temperature for 1 h, membranes were incubated at 4°C overnight with primary detection antibodies for RUNX2 (CST, 8486s), ALP (Zenbio, 220678), GAPDH (Proteintech, 60004-1-Ig), AKT (CST, 4685s), p-AKT (CST, 9614), I κ B α (CST, 4814s), p-I κ B α (CST, 2859s), p-ERK (Zenbio, 310065), ERK (Zenbio, 340373), NLRP3 (CST, D4D8T), ASC (CST, E1E3I), and P20 (ag-0042). The membranes were then incubated for 1 h at room temperature with the appropriate horseradish peroxidase (HRP)-conjugated secondary detection antibodies diluted in 5% (wt/vol) skimmed milk in TBS-T solution. Finally, the immunoreactive bands were developed using SuperSignal West Femto Maximum Sensitivity Substrate (Thermo Fisher Scientific), and the images were analyzed using Image J software.

Detection of mRNA Profiles

RNA-sequencing (RNA-seq) quantification was utilized to investigate changes in cell mRNA profiles among the different treatments performed. Cells were harvested using a Trizol reagent (Invitrogen, Carlsbad, CA), followed by RNA isolation. Isolated RNA was sent to BGI Co., LTD (Wuhan, China) for RNA-seq performed on BGISEQ-500. Sequencing results were further analyzed using the “R (version 3.5.1)” to identify differential expression genes (DEGs) and then a Kyoto Encyclopedia of Genes and Genomes (KEGG) pathway enrichment analysis was performed.

Cell Immunostaining Assays

The AVICs were cultured with different treatments for 48 h. The cell immuno-staining was performed according to the previous protocols. The primary antibodies RUNX2 (Abcam, ab23981), ALP (Zenbio, 220678), and P65 (Cell Signaling Technology: 8242) were used. After secondary antibody incubation, the cell nucleus was stained with DAPI (Roche) for 15 min, then the samples were observed and captured by fluorescent microscopy (Zeiss).

Statistical Analysis

All data were expressed as the mean \pm standard deviation (SD). All semiquantitative measurements were captured using Image J software. Differences between groups were evaluated by analysis of variance (ANOVA). *P*-values less than (<) 0.05 were considered to indicate statistical significance.

RESULTS

Effect of CAPE on Cell Viability and Morphology

To assess the toxic effects of CAPE on AVICs, we determined the half-maximal inhibitory concentration (IC₅₀). CAPE was found to exhibit overt signs of toxicity when the concentration in the culture medium exceeded 10 μ M (**Figure 1C**). Therefore, 10 μ M CAPE was used for further experiments. The viability of AVICs cultured in the presence of CAPE was then evaluated in CCK-8 assays (**Figure 1B**: molecular structure). As shown in **Figure 1A**, compared with the control group, the viability of cells cultured in the presence of CAPE declined on day 5; however, no cytotoxicity was observed, even after 21 days of treatment (**Supplementary Figure 1**). Furthermore, there was no visible difference in the morphology of AVICs cultured with or without 10 μ M CAPE for 5 days (**Figure 1D**).

CAPE Inhibits OM-Induced Osteogenic Differentiation of AVICs

Compared with the control group, significantly more AVICs were positively stained with Alizarin Red S staining after culture in OM for 21 days (* $P < 0.05$; **Figure 1E**). CAPE treatment resulted in a gradual decrease in Alizarin Red S positive staining compared with that of the OM group (* $P < 0.05$; **Figure 1E**) (**Supplementary Figure 2**). Subsequently, we analyzed the expression of the osteogenic differentiation-related genes

RUNX2 and ALP in AVICs cultured in OM with or without CAPE for 24 h, 48 h, and 7 days (**Figure 2A**). Compared with the control group, OM significantly upregulated the expression of ALP and RUNX2 (* $P < 0.05$). With the addition of CAPE to the OM culture medium, ALP and RUNX2 were both significantly downregulated (# $P < 0.05$). Immunofluorescent staining of AVICs cultured in OM with and without CAPE for 48 h, revealed a similar pattern of ALP and RUNX2 protein expression (**Figure 2B**). Furthermore, following treatment with OM and CAPE for 48 h (**Figure 2C**) and 7 days (**Figure 2D**), the expression of RUNX2 and ALP at the protein level was significantly increased (* $P < 0.05$) compared with those detected in the control group (without OM and CAPE treatment), while the expression of these proteins was decreased compared to the levels detected in AVICs cultured in OM alone (# $P < 0.05$).

Identification of DEGs and KEGG Pathway Analysis

Compared with the control group, we observed marked differential gene expression (982 upregulated and 933 downregulated) in AVICs cultured in OM (**Figure 3A**). Furthermore, we observed marked differences in the global gene expression profiles of AVICs cultured in OM with and without CAPE (**Figure 3B**), with 1,069 DEGs (613 upregulated and 456 downregulated) detected in the presence of CAPE. Based on Venn diagrams of DEGs identified by comparison of the gene expression profiles in the OM versus control

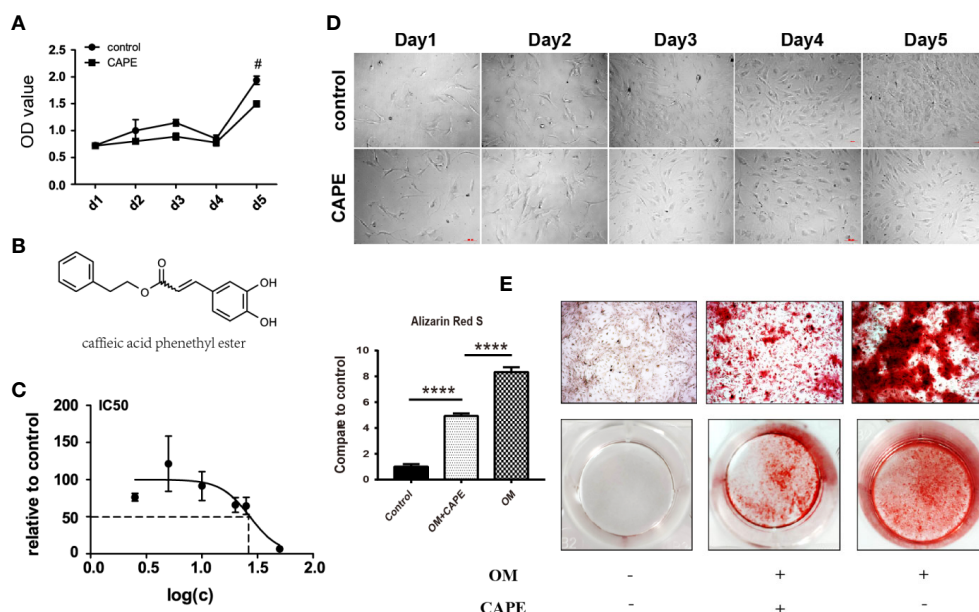


FIGURE 1 | Viability and calcification of AVICs with treatment of CAPE. **(A)** Cell proliferation curve with or without CAPE treatment (10 μ M) for 5 days, **(B)** Molecular structure of CAPE. **(C)** IC₅₀ of CAPE on AVICs, concentrations were transferred to Log(c); $n = 5$. **(D)** Cell morphology of AVICs with or without CAPE treatment (10 μ M) for 5 days. **(E)** Alizarin Red S staining of the cells with different conditioned coloring: control (normal culture medium), OM (osteogenic medium), OM+CAPE (osteoblastic medium plus CAPE treatment); # $p < 0.05$ and **** $p < 0.01$ were accepted as significant difference, $n=3$.

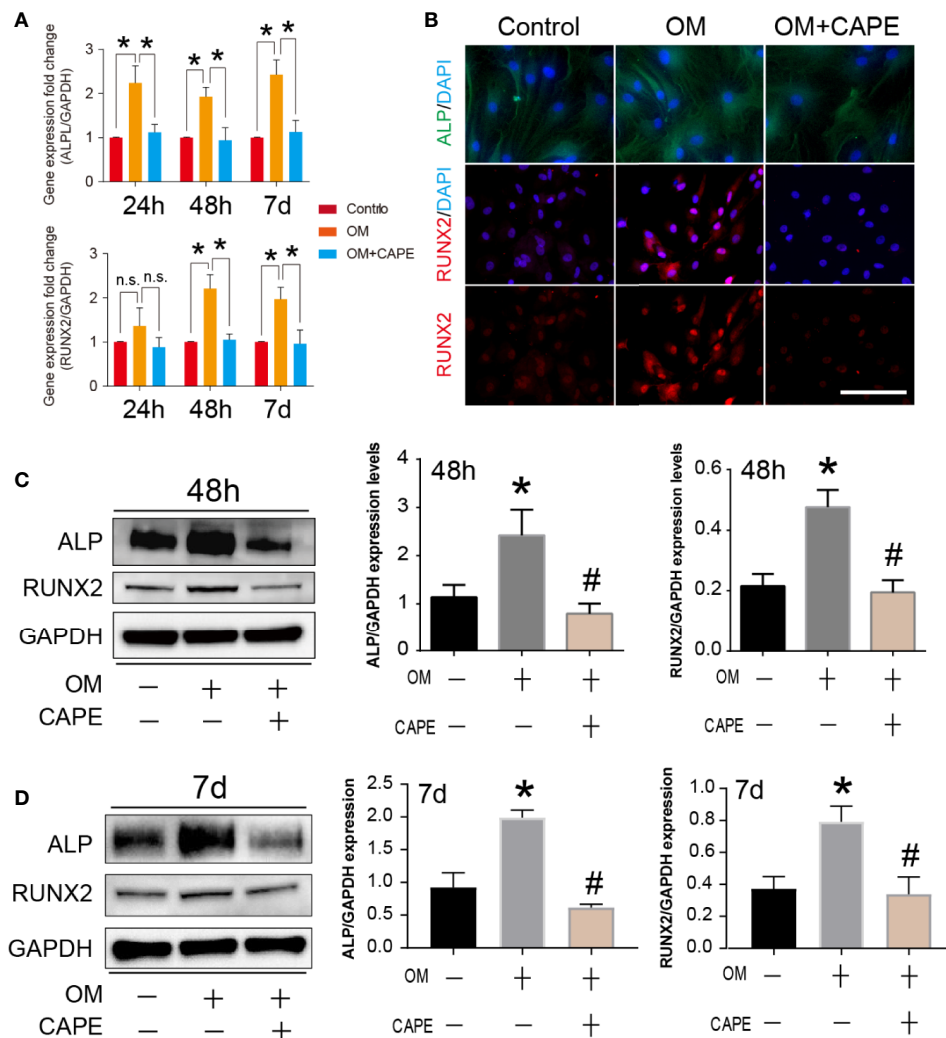


FIGURE 2 | Effect of CAPE on OM induced calcific-related gene/protein expression in AVICs. **(A)** AVICs were stimulated with OM and then treated or not treated with 10 μ M CAPE for 24 h, 48 h and 7 days, the mRNA expression levels of RUNX2, ALP were detected by qRT-PCR. **(B)** The immunofluorescent staining of ALP, RUNX2 on AVICs with above conditioned culturing for 48 h, **(C, D)** The protein expression levels of the above genes were determined by Western blot and quantification analysis for 48 h **(C)** and 7 days **(D)** treatment with CAPE. * $p < 0.05$ compared with control, # $p < 0.05$ compared with OM.

groups and the OM plus CAPE versus OM groups, we identified 518 common DEGs for further analysis (**Figures 3C, D**). KEGG signaling pathway enrichment analysis showed that these DEGs were highly enriched in functions related to the NOD-like receptor, TNF, PI3K-AKT, mTOR, NF- κ B, and Toll-like receptor signaling pathways (**Figure 3E**).

CAPE Inhibits Calcification of AVICs by Inhibiting NF- κ B Activation

Based on the results of RNA-seq analysis, we selected the NF- κ B and PI3K-AKT pathway signaling for further studies. Compared with the control group, the protein levels of phospho-Erk, phospho-I κ B α , and phospho-AKT were markedly increased in

the OM group, and CAPE treatment decreased their expression, although the total levels of these proteins were unaffected (**Figures 4A, C**). In addition, CAPE inhibited nuclear translocation of NF- κ B p65 in AVICs (**Figure 4D**). These findings indicated that activation of AKT, ERK1/2, and NF- κ B was restrained in AVICs by the addition of CAPE to OM.

CAPE Suppresses NLRP3 Inflammasome Activation in AVICs

The NLRP3 inflammasome is a novel target that regulates cell differentiation and inflammation (Sun et al., 2017). NF- κ B is well-known to be a prerequisite for NLRP3 inflammasome activation (Afonina et al., 2017). Western blot analysis showed

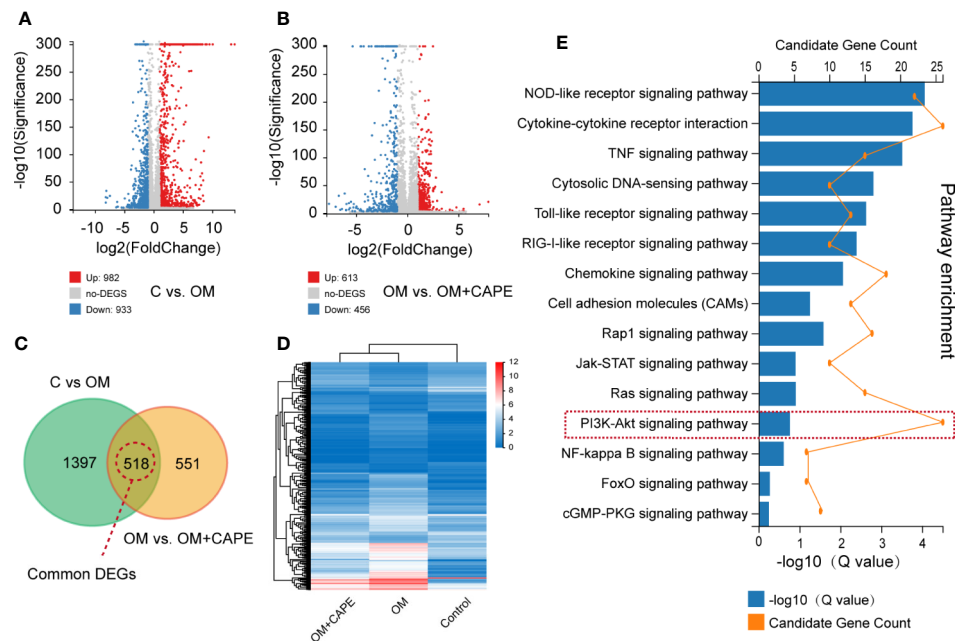


FIGURE 3 | Gene expression profiles with RNA-sequencing under the OM (osteogenic medium) conditioned culturing with or without Caffeic Acid Phenethyl Ester (CAPE). **(A, B)** Volcano map of differentially expressed genes (DEGs) in C versus OM ($\log_2(\text{OM}/\text{C})$); **(A)**, up-regulation: 982 and down-regulation: 933; and OM versus OM + CAPE ($\log_2(\text{OM} + \text{CAPE}/\text{OM})$); **(B)**, up-regulation: 613 and down-regulation: 456, FC (fold change) > 1 was accepted as positive DEGs, **(C)** Venn interaction of DEGs of C versus OM ($\log_2(\text{OM}/\text{C})$) and OM versus OM + CAPE ($\log_2(\text{OM} + \text{CAPE}/\text{OM})$), **(D)** Heatmap for common DEGs gene expression with group clusters, **(E)** KEGG pathway enrichment, orange dots indicate the degree of enrichment (Q value ($-\log_{10}$)), histogram indicates gene counts matched the pathway enrichment.

that protein expression levels of NLRP3, ASC, cleaved caspase-1 (P20) in AVICs were markedly increased in AVICs cultured in OM for 3 days, and that this effect was inhibited in the presence of CAPE (**Figures 4B, C**).

DISCUSSION

Many studies support the concept that CAVD is an active process involving multiple mechanisms, including abnormal calcium or phosphate metabolism, valvular inflammation, and pro-osteogenic reprogramming of AVICs (Aikawa and Libby, 2017). Our previous studies showed that many natural compounds with anti-inflammatory properties significantly inhibit valve calcification (Huang et al., 2020; Zhou et al., 2020). In this study, for the first time, we demonstrate that CAPE functions as an efficient inflammation inhibitor to suppress OM-induced calcification of human AVICs. Thus, our findings confirm the potential of anti-inflammatory interventions against CAVD.

In the current study, we first determined that 10 μM CAPE had no significant cytotoxic effects on AVICs but slowed cell proliferation over time. It has been widely reported that CAPE inhibits cell proliferation (Chang et al., 2017), and proliferation of AVICs has been linked with development of aortic valve

calcification (Paradis et al., 2014). Thus, it is possible that CAPE prevents aortic valve calcification by suppressing cell growth.

Previous studies showed that AVICs from calcified aortic valves produce higher levels of pro-osteogenic biomarkers, including Runx2 and ALP (Rutkovskiy et al., 2017). In the present study, we demonstrated that OM induced increased expression of Runx2 and ALP, an effect that was inhibited by CAPE. To investigate the mechanism by which CAPE inhibited OM-induced calcification of AVICs, we performed a high-throughput gene expression analysis to rapidly and accurately identify the relevant molecular signaling pathways. DEGs selected by transcriptome sequencing were highly enriched in the TNF, PI3K-AKT, mTOR, NF- κ B, Toll-like receptor, and NOD-like receptor signaling pathways. Of these, the NF- κ B and NOD-like receptor signaling pathways are the most common inflammatory response-mediated signaling pathways.

The NLRP3 inflammasome, which is the core factor in NOD-like receptor signaling pathway, is a cytosolic complex involved in early inflammatory responses. It has been demonstrated that the NLRP3 inflammasome contributes to vascular smooth muscle cell phenotype switching, proliferation, and vascular remodeling in hypertension (Sun et al., 2017). NF- κ B is a necessary prerequisite for NLRP3 inflammasome activation (Boaru et al., 2015). Following activation, NLRP3 forms a complex with its adaptor ASC, which facilitates the conversion

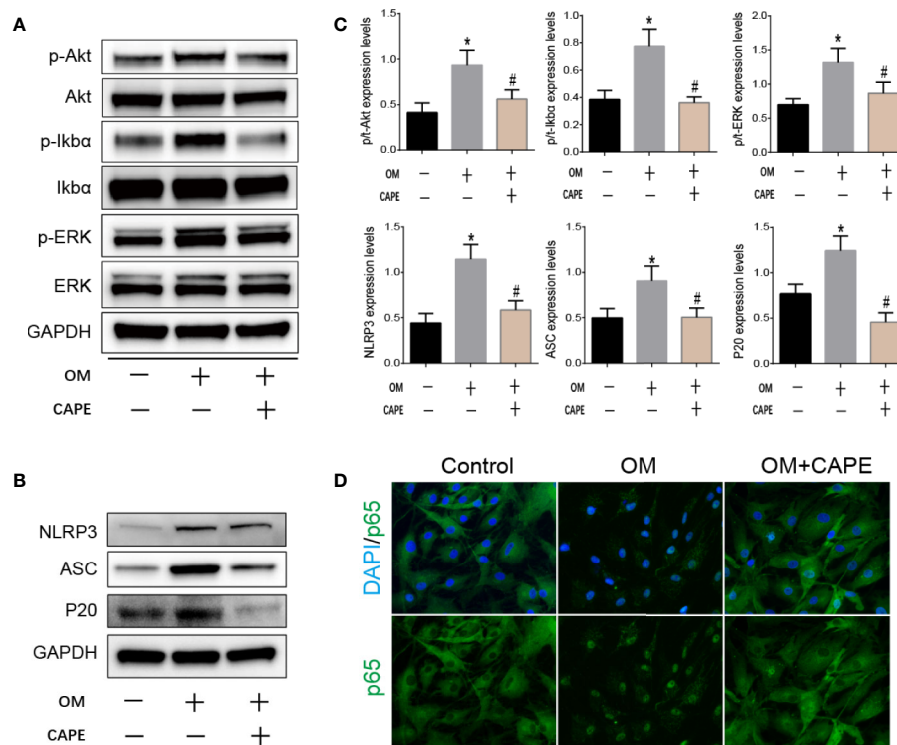


FIGURE 4 | CAPE inhibits calcification of AVICs *via* interfering AKT, ERK1/2, NF- κ B, and NLRP3 inflammasome activation. **(A)** Protein expression profiles of phosphorylated ERK, I κ B α and AKT under the OM (osteogenic medium) conditioned culturing with or without CAPE, **(B)** The protein expression levels of NLRP3, ASC, P20 were determined by Western blot **(C)** Statistical analysis of p/t-ERK (phospho-ERK/total ERK), p/t-I κ B α (phospho-I κ B α /total-I κ B α), p/t-AKT (phospho-AKT/total-AKT), and NLRP3, ASC, P20 were collected according to the gray semi-quantification. **(D)** Immunofluorescent staining for verifying that CAPE represses OM induced cell nucleus translocation of P65. * $p < 0.05$ compared with control and # $p < 0.05$ compared with OM showed significant difference.

of pro-caspase-1 to the active caspase-1 p10/p20 tetramer, leading to maturation of proinflammatory cytokines, such as IL-1 β and IL-18 (F et al., 2002). In this study, we found that CAPE inhibited nuclear translocation of NF- κ B p65 in AVICs and decreased the phosphorylated levels of I κ B α . These results confirm that CAPE has a significant inhibitory effect on NF- κ B activation. Furthermore, Western blot analysis of the protein expression of NLRP3, ASC, and P20 protein in AVICs cultured in OM in the presence of CAPE confirmed that CAPE effectively inhibited the activation of NLRP3, ASC, P20. These results indicate that the anti-calcification effect of CAPE depends on inhibition of the NF- κ B/NLRP3 pathway. Moreover, it was shown that CAPE treatment markedly impaired the phosphorylation of AKT and ERK required to promote cell proliferation (Wang et al., 2019; Xu et al., 2019b). Thus, our findings confirm that mechanistically, CAPE inhibits the growth of AVICs by inhibiting the phosphorylation of AKT and ERK.

Therefore, CAPE reverses osteoblastic differentiation of aortic valve interstitial cells by regulating cell proliferation, inhibiting inflammation *via* AKT, ERK, NF- κ B/NLRP3 pathways. Thus, our findings provide important clarification of the mechanism underlying the anti-calcification effects of CAPE.

CONCLUSION

Our results suggest that CAPE significantly inhibits OM-induced calcification and phenotypic transformation of AVICs *via* signaling pathways including PI3K-AKT, ERK1/2, and NF- κ B/NLRP3 inflammasome. Thus, CAPE represents a potential medical supplement to prevent the occurrence of CAVD.

DATA AVAILABILITY STATEMENT

The datasets analyzed in this article have been deposited in the Sequence Read Archive (SRA) database of NCBI under accession code PRJNA643215.

ETHICS STATEMENT

The studies involving human participants were reviewed and approved by Ethics committee of Union Hospital, Tongji Medical College, Huazhong University of Science and Technology. The patients/participants provided their written informed consent to participate in this study.

AUTHOR CONTRIBUTIONS

KX, ML, and YH designed the project, collected the data, and wrote the manuscript. KX, TZ, YH, and FL analyzed the data, wrote and revised the manuscript. SC and GL revised the manuscript. ND and JS designed the project, gave financial support, and wrote the manuscript, and KX revised the manuscript. All authors contributed to the article and approved the submitted version.

FUNDING

This work was supported by the National Key R&D Program of China (2016YFA0101100); the National Natural Science Foundation of China (81770387, 30371414, 30571839, 81700339, 81974034, 81670351; the Hubei Provincial Natural Science

Foundation of China (2017CFB647); and the China Postdoctoral Science Foundation (Grant Number: 2018M630867).

SUPPLEMENTARY MATERIAL

The Supplementary Material for this article can be found online at: <https://www.frontiersin.org/articles/10.3389/fphar.2020.00826/full#supplementary-material>

SUPPLEMENTARY FIGURE 1 | Cell viability of CAPE treatment for 21 days.

SUPPLEMENTARY FIGURE 2 | Two more repeats of **Figure 1E**, Alizarin Red S staining of the cells with different conditioned culturing: control (normal culture medium), OM (osteogenic medium), OM+CAPE (osteoblastic medium plus CAPE treatment).

SUPPLEMENTARY TABLE 1 | List of qPCR primers.

REFERENCES

- Afonina, I. S., Zhong, Z., Karin, M., and Beyaert, R. (2017). Limiting inflammation-the negative regulation of NF-kappaB and the NLRP3 inflammasome. *Nat. Immunol.* 18, 861–869. doi: 10.1038/ni.3772
- Aikawa, E., and Libby, P. (2017). A Rock and a Hard Place: Chiseling Away at the Multiple Mechanisms of Aortic Stenosis. *Circulation* 135, 1951–1955. doi: 10.1161/CIRCULATIONAHA.117.027776
- Boaru, S. G., Borkham-Kamphorst, E., Van De Leur, E., Lehnen, E., Liedtke, C., and Weiskirchen, R. (2015). NLRP3 inflammasome expression is driven by NF-kappaB in cultured hepatocytes. *Biochem. Biophys. Res. Commun.* 458, 700–706. doi: 10.1016/j.bbrc.2015.02.029
- Celik, S., and Erdogan, S. (2008). Caffeic acid phenethyl ester (CAPE) protects brain against oxidative stress and inflammation induced by diabetes in rats. *Mol. Cell Biochem.* 312, 39–46. doi: 10.1007/s11010-008-9719-3
- Chang, H., Wang, Y., Yin, X., Liu, X., and Xuan, H. (2017). Ethanol extract of propolis and its constituent caffeic acid phenethyl ester inhibit breast cancer cells proliferation in inflammatory microenvironment by inhibiting TLR4 signal pathway and inducing apoptosis and autophagy. *BMC Complement. Altern. Med.* 17, 471. doi: 10.1186/s12906-017-1984-9
- Da, L., S. P., and N. A. (2015). Calcific Aortic Valve Disease: Molecular Mechanisms and Therapeutic Approaches. *Eur. Cardiol.* 10 (2), 108–112. doi: 10.15420/ecr.2015.10.2.108
- F, M., K. B., and J. T. (2002). The inflammasome: a molecular platform triggering activation of inflammatory caspases and processing of proIL-beta. *Mol. Cell* 10 (2), 417–426. doi: 10.1016/s1097-2765(02)00599-3
- Huang, Y., Xu, K., Zhou, T., Zhu, P., Dong, N., and Shi, J. (2019). Comparison of Rapidly Proliferating, Multipotent Aortic Valve-Derived Stromal Cells and Valve Interstitial Cells in the Human Aortic Valve. *Stem Cells Int.* 2019, 7671638. doi: 10.1155/2019/7671638
- Huang, Y., Zhou, X., Liu, M., Zhou, T., Shi, J., Dong, N., et al. (2020). The natural compound andrographolide inhibits human aortic valve interstitial cell calcification via the NF-kappa B/Akt/ERK pathway. *BioMed. Pharmacother.* 125, 109985. doi: 10.1016/j.biopha.2020.109985
- Li, C., Xu, S., and Gottlieb, A. I. (2013). The progression of calcific aortic valve disease through injury, cell dysfunction, and disruptive biologic and physical force feedback loops. *Cardiovasc. Pathol.* 22, 1–8. doi: 10.1016/j.carpath.2012.06.005
- Li, G., Qiao, W., Zhang, W., Li, F., Shi, J., and Dong, N. (2017). The shift of macrophages toward M1 phenotype promotes aortic valvular calcification. *J. Thorac. Cardiovasc. Surg.* 153, 1318–1327. e1311. doi: 10.1016/j.jtcvs.2017.01.052
- Marincheva-Savcheva, G., Subramanian, S., Qadir, S., Figueroa, A., Truong, Q., Vijayakumar, J., et al. (2011). Imaging of the aortic valve using fluorodeoxyglucose positron emission tomography increased valvular fluorodeoxyglucose uptake in aortic stenosis. *J. Am. Coll. Cardiol.* 57, 2507–2515. doi: 10.1016/j.jacc.2010.12.046
- Nadra, I., Mason, J. C., Philippidis, P., Florey, O., Smythe, C. D., McCarthy, G. M., et al. (2005). Proinflammatory activation of macrophages by basic calcium phosphate crystals via protein kinase C and MAP kinase pathways: a vicious cycle of inflammation and arterial calcification? *Circ. Res.* 96, 1248–1256. doi: 10.1161/01.RES.0000171451.88616.c2
- New, S. E., and Aikawa, E. (2011). Molecular imaging insights into early inflammatory stages of arterial and aortic valve calcification. *Circ. Res.* 108, 1381–1391. doi: 10.1161/CIRCRESAHA.110.234146
- Nie, J., Chang, Y., Li, Y., Zhou, Y., Qin, J., Sun, Z., et al. (2017). Caffeic Acid Phenethyl Ester (Propolis Extract) Ameliorates Insulin Resistance by Inhibiting JNK and NF-kappaB Inflammatory Pathways in Diabetic Mice and HepG2 Cell Models. *J. Agric. Food Chem.* 65, 9041–9053. doi: 10.1021/acs.jafc.7b02880
- Nkomo, V. T., Gardin, J. M., Skelton, T. N., Gottdiener, J. S., Scott, C. G., and Enriquez-Sarano, M. (2006). Burden of valvular heart diseases: a population-based study. *Lancet* 368, 1005–1011. doi: 10.1016/S0140-6736(06)69208-8
- P, M., Mc, B., and R, B. (2014). Molecular biology of calcific aortic valve disease: towards new pharmacological therapies. *Expert Rev. Cardiovasc. Ther* 12 (7), 851–862. doi: 10.1586/14779072.2014.923756
- Paradis, J. M., Fried, J., Nazif, T., Kirtane, A., Harjai, K., Khalique, O., et al. (2014). Aortic stenosis and coronary artery disease: what do we know? What don't we know? A comprehensive review of the literature with proposed treatment algorithms. *Eur. Heart J.* 35, 2069–2082. doi: 10.1093/eurheartj/ehu247
- Parlakpınar, H., Sahná, E., Acet, A., Mizrak, B., and Polat, A. (2005). Protective effect of caffeic acid phenethyl ester (CAPE) on myocardial ischemia-reperfusion-induced apoptotic cell death. *Toxicology* 209, 1–14. doi: 10.1016/j.tox.2004.10.017
- Pawade, T. A., Newby, D. E., and Dweck, M. R. (2015). Calcification in Aortic Stenosis: The Skeleton Key. *J. Am. Coll. Cardiol.* 66, 561–577. doi: 10.1016/j.jacc.2015.05.066
- Rutkovskiy, A., Malashicheva, A., Sullivan, G., Bogdanova, M., Kostareva, A., Stenslokken, K. O., et al. (2017). Valve Interstitial Cells: The Key to Understanding the Pathophysiology of Heart Valve Calcification. *J. Am. Heart Assoc.* 6 (9). doi: 10.1161/JAHA.117.006339
- Sun, H. J., Ren, X. S., Xiong, X. Q., Chen, Y. Z., Zhao, M. X., Wang, J. J., et al. (2017). NLRP3 inflammasome activation contributes to VSMC phenotypic transformation and proliferation in hypertension. *Cell Death Dis.* 8, e3074. doi: 10.1038/cddis.2017.470
- Tolba, M. F., Omar, H. A., Azab, S. S., Khalifa, A. E., Abdel-Naim, A. B., and Abdel-Rahman, S. Z. (2016). Caffeic Acid Phenethyl Ester: A Review of Its Antioxidant Activity, Protective Effects against Ischemia-reperfusion Injury and Drug Adverse Reactions. *Crit. Rev. Food Sci. Nutr.* 56, 2183–2190. doi: 10.1080/10408398.2013.821967

- Wang, G., Yin, L., Peng, Y., Gao, Y., Gao, H., Zhang, J., et al. (2019). Insulin promotes invasion and migration of KRAS(G12D) mutant HPNE cells by upregulating MMP-2 gelatinolytic activity via ERK- and PI3K-dependent signalling. *Cell Prolif.* 52, e12575. doi: 10.1111/cpr.12575
- Wu, J., Omene, C., Karkoszka, J., Bosland, M., Eckard, J., Klein, C. B., et al. (2011). Caffeic acid phenethyl ester (CAPE), derived from a honeybee product propolis, exhibits a diversity of anti-tumor effects in pre-clinical models of human breast cancer. *Cancer Lett.* 308, 43–53. doi: 10.1016/j.canlet.2011.04.012
- Xu, K., Zhou, T., Huang, Y., Chi, Q., Shi, J., Zhu, P., et al. (2018). Anthraquinone Emodin Inhibits Tumor Necrosis Factor Alpha-Induced Calcification of Human Aortic Valve Interstitial Cells via the NF-kappaB Pathway. *Front. Pharmacol.* 9, 1328. doi: 10.3389/fphar.2018.01328
- Xu, K., Huang, Y., Zhou, T., Wang, C., Chi, Q., Shi, J., et al. (2019a). Nobiletin exhibits potent inhibition on tumor necrosis factor alpha-induced calcification of human aortic valve interstitial cells via targeting ABCG2 and AKR1B1. *Phytother. Res.* 33, 1717–1725. doi: 10.1002/ptr.6360
- Xu, K., Sha, Y., Wang, S., Chi, Q., Liu, Y., Wang, C., et al. (2019b). Effects of Bakuchiol on chondrocyte proliferation via the PI3K-Akt and ERK1/2 pathways mediated by the estrogen receptor for promotion of the regeneration of knee articular cartilage defects. *Cell Prolif.* 52, e12666. doi: 10.1111/cpr.12666
- Zhou, T., Wang, Y., Liu, M., Huang, Y., Shi, J., Dong, N., et al. (2020). Curcumin inhibits calcification of human aortic valve interstitial cells by interfering NF-kappaB, AKT, and ERK pathways. *Phytother. Res.* doi: 10.1002/ptr.6674

Conflict of Interest: The authors declare that the research was conducted in the absence of any commercial or financial relationships that could be construed as a potential conflict of interest.

Copyright © 2020 Liu, Li, Huang, Zhou, Chen, Li, Shi, Dong and Xu. This is an open-access article distributed under the terms of the Creative Commons Attribution License (CC BY). The use, distribution or reproduction in other forums is permitted, provided the original author(s) and the copyright owner(s) are credited and that the original publication in this journal is cited, in accordance with accepted academic practice. No use, distribution or reproduction is permitted which does not comply with these terms.

Advantages of publishing in Frontiers



OPEN ACCESS

Articles are free to read
for greatest visibility
and readership



FAST PUBLICATION

Around 90 days
from submission
to decision



HIGH QUALITY PEER-REVIEW

Rigorous, collaborative,
and constructive
peer-review



TRANSPARENT PEER-REVIEW

Editors and reviewers
acknowledged by name
on published articles

Frontiers

Avenue du Tribunal-Fédéral 34
1005 Lausanne | Switzerland

Visit us: www.frontiersin.org

Contact us: frontiersin.org/about/contact



REPRODUCIBILITY OF RESEARCH

Support open data
and methods to enhance
research reproducibility



DIGITAL PUBLISHING

Articles designed
for optimal readership
across devices



FOLLOW US

@frontiersin



IMPACT METRICS

Advanced article metrics
track visibility across
digital media



EXTENSIVE PROMOTION

Marketing
and promotion
of impactful research



LOOP RESEARCH NETWORK

Our network
increases your
article's readership